# AUTOPARAMETRIC INTERACTION IN A STRUCTURE CONTAINING A LIQUID

RAOUF ATTIA IBRAHIM

Thesis Submitted for the Degree of
Doctor of Philosophy

University of Edinburgh

February 1974

CONTENTS

ACKNOWLEDGEMENTS

I would like to express my deepest gratitude to the many people who have helped me during the course of this research. In particular I would like to thank my supervisors Professor A.D.S. Barr, Professor of Mechanical Engineering at the University of Dundee, and Dr. G.T.S. Done of this University.

Special thanks are also due to Professor J.L. King, Regius Professor of Mechanical Engineering at this University, for his encouragement throughout my stay in Edinburgh, Dr. J.A. Linnett for his assistance in helping me overcome the language problem and Dr. D.A. Boffey for his help in designing the air bearing.

I am also very grateful to Messrs. G. Smith and H. McKeating for their help in the design and construction of the experimental apparatus, to the staff of the Edinburgh Regional Computing Centre for their help in programming, to Mr. R. MacKenzie for photography and to Miss Avril Myles for her typing.

The award of a studentship by the University of Edinburgh, which made all this work possible is gratefully acknowledged.

## SYNOPSIS

An elastic structure carrying a rigid tank containing a liquid with a free surface is considered. Autoparametric interaction between the vibrating structure modes and the liquid sloshing modes is investigated theoretically and experimentally when the system possesses two, three and four degrees of freedom.

The mathematical model for two structure modes interacting with the liquid free surface modes inside the tank is formulated. The resulting governing equations are coupled through inertial nonlinear terms. This coupling is significant since it determines the behaviour of the system under internal resonance conditions. The asymptotic expansion method due to Struble has been used to give an approximate solution of the governing equations. The method predicts the autoparametric conditions (under which the response of the system has been examined). The response of the system is obtained analytically and numerically in the neighbourhood of the internal resonance conditions. Under the principal internal resonance condition (i.e. when one of the normal mode frequencies is twice one of the other mode frequencies), the system possesses a steady-state solution. Under the summed or difference internal resonance conditions (i.e. one of the normal mode frequencies equals the sum or difference of another two mode frequency) the system does not achieve a constant amplitude steady-state response.

Experimental investigations confirm the possible existence of most of the internal resonance conditions considered in the analytical study, however theoretical amplitude-frequency response curves are rather higher than the experimental results. Experiments showed that other kinds of instabilities occur when the liquid free surface exhibits

rotational flow at a forcing frequency just above twice the liquid antisymmetric sloshing frequency. Under autoparametric resonance conditions of four mode interaction experimental observations showed that the system is severely unstable and structure failure could occur if the excitation were not prevented.

# CHAPTER I

## HISTORICAL REVIEW

Containers partially filled with liquid and supported by an elastic structure constitute a complex dynamic system and the analysis of their response to various types of excitations is rather complicated. These types of structure are found in many practical applications such as elevated water tanks, fuel or cargo tanks of automotive vehicles and liquid propellent space vehicles. The dynamic behaviour of the fluids and their influence upon the surrounding structures have received a wide range of theoretical and experimental investigation, and in the following sections the main outline of the results of these studies are reviewed.

### I.1 Liquid Dynamics in Stationary Structures:

Liquid sloshing and its interaction with its structural system have interested civil engineers and seismologists studying the performance of oil tanks, water reservoirs and elevated water tanks during earthquakes. Steinbrugge and Moran[S12]* showed that the damage that occurred to water tanks and reservoirs in Sacramento, California, in 1954 was a result of resonance occurrence between the oscillations of the ground motion - caused by the earthquake - and the natural frequency of the water.

During the Chilean earthquakes of May 1960, a number of elevated water tanks were badly damaged but others survived without

---

*Numbers in brackets [ ] refer to references in the Bibliography.

damage. Housner[H8], in treating the dynamic analysis of these tanks, took into account the motion of the water relative to the tank as well as the motion of the tank relative to the ground. He showed that the forces exerted on the tank by the water as a result of a horizontal ground acceleration are of two kinds: one is the inertia force of a mass $M_r$ attached rigidly to the tank wall, and the other called the sloshing force resulting from the free water oscillations. The latter force is the same as would be exerted by a mass $M_{s1}$ oscillating horizontally against a restraining spring as shown in Fig. (I.1). The mass $M_{s1}$ and its associated spring are equivalent to the fundamental mode of water free surface oscillation, which is the important mode for most earthquake problems.

The technique of equivalent mechanical models is a very useful mathematical tool in solving the complete dynamic problem of a system containing liquid. Graham[G4], in 1951, developed an equivalent pendulum to represent the free surface oscillations of a fluid in a stationary tank. At the same time Graham and Rodrigues[G3] established another model consisting of a sloshing point mass, attached with springs to the tank wall at a specified depth, and a fixed rigid mass. The principles of constructing a mechanical model are taken in the sense that the masses, damping constants, moments of inertia, centre of gravity, modes of oscillations, forces and moments are completely equivalent to the physical system. Other modified equivalent models are found in details in reference [A2].

For a time civil engineers indicated in several analyses[C5,N2] that ground motions might be idealised ordinarily as horizontal, i.e. the vertical component could be neglected for the calculation of

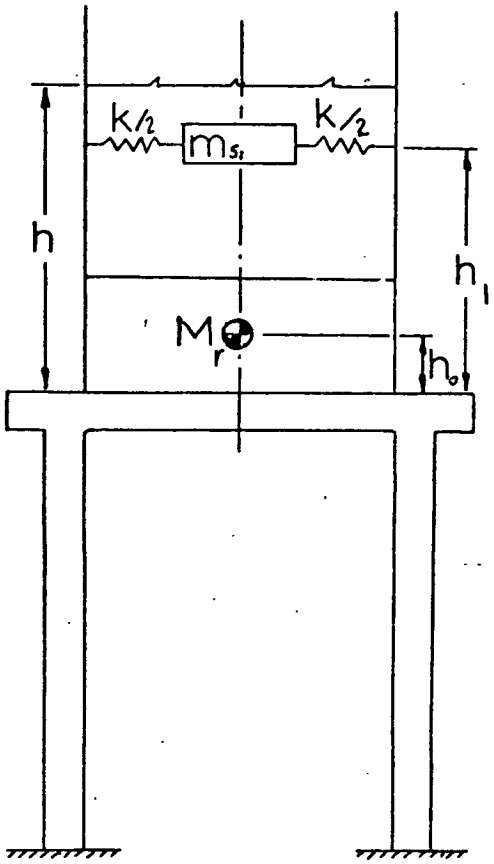


Fig(I.1)Housner Equivalent Mechanical System For an Elevated Water Tank.

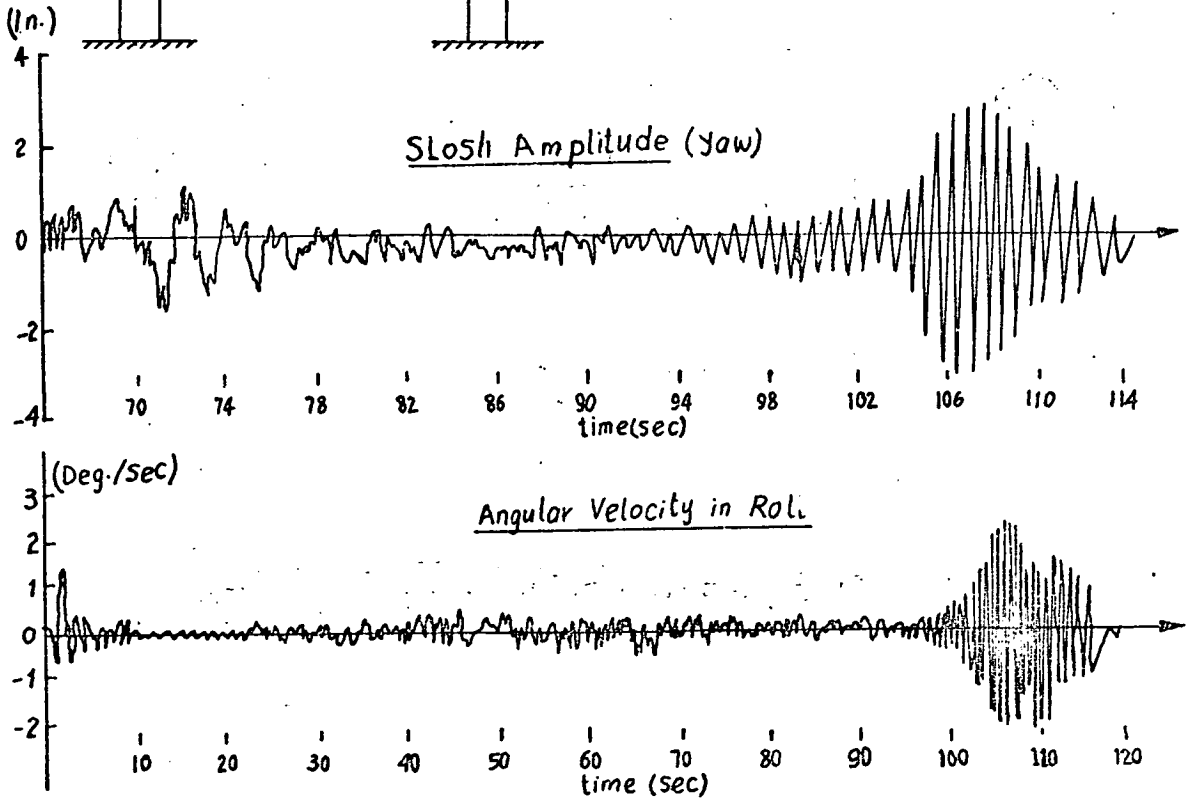


Fig.(I.2) Saturn-I Fuel Slosh Instability (ref. A2)

hydrodynamic pressures without introducing undue errors. Yet, a recent paper by Chopra[C8] has yielded surprisingly high values of the hydrodynamic pressures due to vertical ground acceleration. Another analysis[N2] indicates the decisive influence of the direction of travel of earth waves relative to the dam. When the ground motion travels towards the structure, pressures may reach several times the values predicted under the assumption that the motion reaches the bottom simultaneously. They are many times smaller when the earth waves travel away from the dam.

More recently, Newmark and Rosenblueth[N2] have shown that earthquake disturbances cause essentially two types of hydrodynamic response: compression waves and surface waves. The influence of each type on the behaviour of a structure is governed by the range of frequencies involved. They found that in most cases one type of phenomena is significant and the other can be ignored. However, practically the entire hydrodynamic phenomenon in tanks is associated with surface waves which occur at low frequencies.

## I.2 Liquid Behaviour in Moving Tanks

More recently, with the advent of the jet age, the effects of fuel motion in tanks of some high speed aircraft and large space vehicles have been included in the dynamic stability studies. Since the 1950's an active technical interest has been devoted to this subject and the exponential increase in the number of reports and papers on this problem is a reflection of this trend[A2,C10].

The tendency in modern space technology is towards a continuous increase in the size of space vehicles, consequently both the fundamental bending frequencies and the natural frequencies of the liquid

propellent become lower. The liquid sloshing is mainly a problem during the launch stage since the fuel and oxidizer of the liquid propellent boosters represents at least 90% of the total mass of the vehicle. The oscillations of the free surface of the propellent exert forces and moments on the missile and may couple with the control system dynamics or the structure system dynamics. Such coupling may cause dynamic instabilities or structural failure. Severe oscillations occur when the excitation frequency lies in the neighbourhood of the lower mode of the fluid oscillation. Abramson[A2] reported an actual example taken from telemetry records of an early Saturn-I, Configuration: A, flight. Figure (I.2) shows the liquid propellent slosh amplitude in one of the outer LOX tanks against the vehicle angular velocity in roll. The cause of the observed oscillations (at t = 100 sec) was attributed to a phase lag in the filter network of the roll control loop that exhibited itself near the frequency of the first rotational mode of that vehicle.

The cancellation or reduction of the deleterious effects of liquid sloshing is the main target of design engineers in the preliminary design stage. The engineering solution consists of building into the fuel and oxident tanks a system of mechanical baffles or subdividing the tank[A2]. Bisplinghoff and Douglass[B9] gave an account showing the influence of tank compartmentation on the fuel sloshing frequency and the first bending mode frequency of its structure. This relationship is resketched in Fig. (I.3).

The liquid sloshing characteristics of various tank geometries, in different orientations and excitations have been the subject of a wide range of studies. The following are the classifications of the kinds of liquid motion which can occur in large liquid propellent tanks[A1,2];

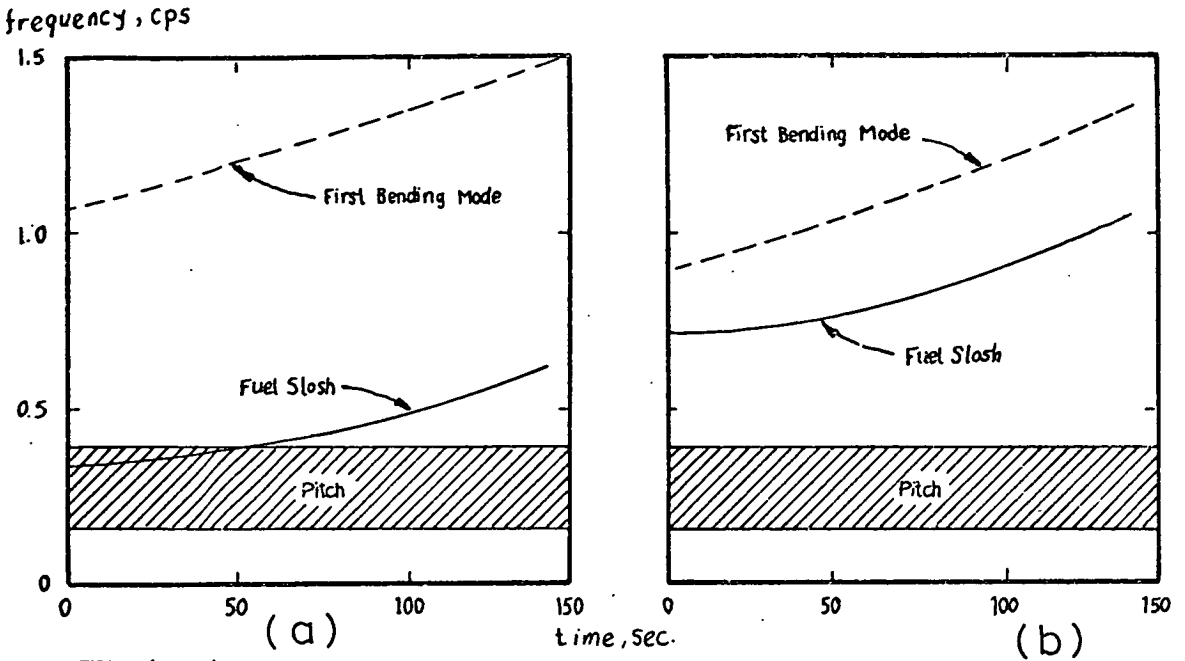


Fig(I.3) Variation of Vehicle Frequencies with Flight Time for: a) Cylindrical Tank
b) Scalloped Tank

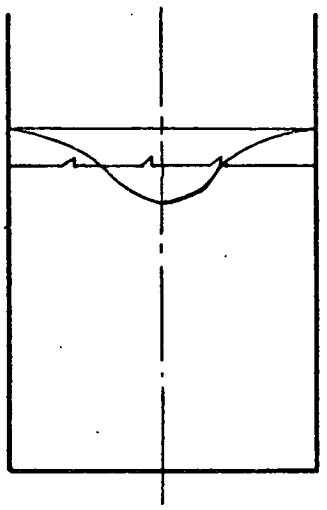

Fig.(I.4b)
Symmetric Mode

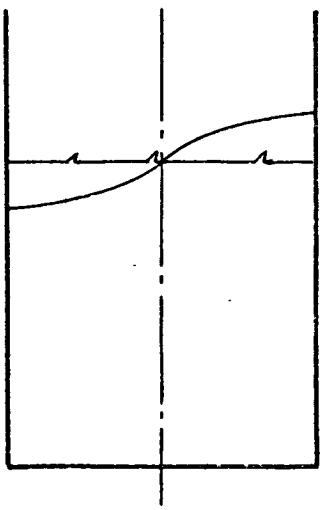

Fig.(I.4a)
Antisymmetric Mode

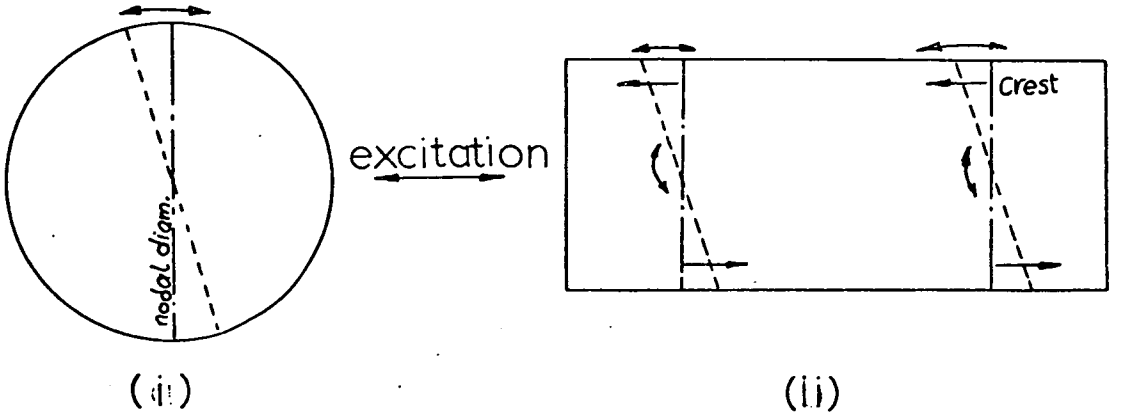


Fig(I.4c) Production of Rotational Flow under Lateral Excitation in;
(i) Circular tank.
(ii) Rectangular tank.

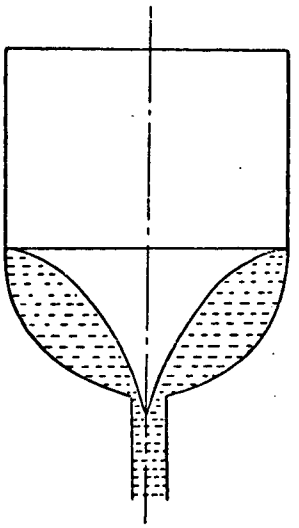

Fig(I.4d)
Vortex Formation
During Draining

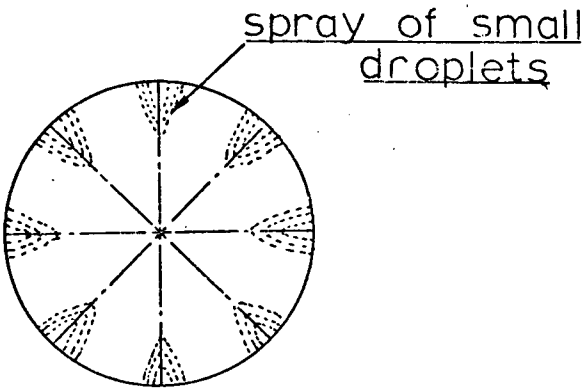


Fig(I.4e)
Spatial Resonance

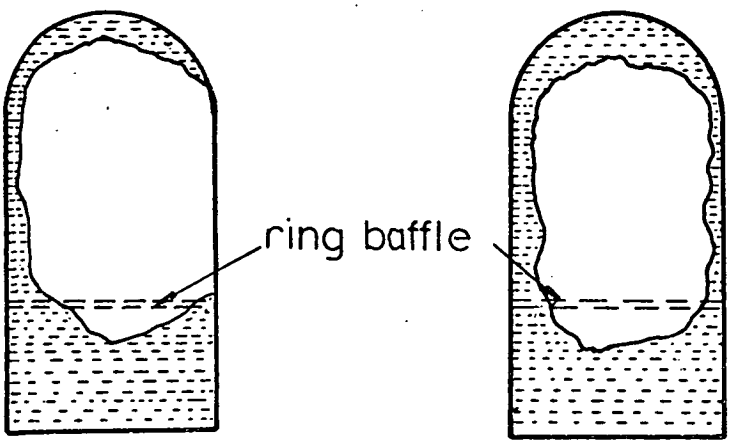


Fig(I.4f)

Liquid Orientation Under Low Gravity
(ref.G5)

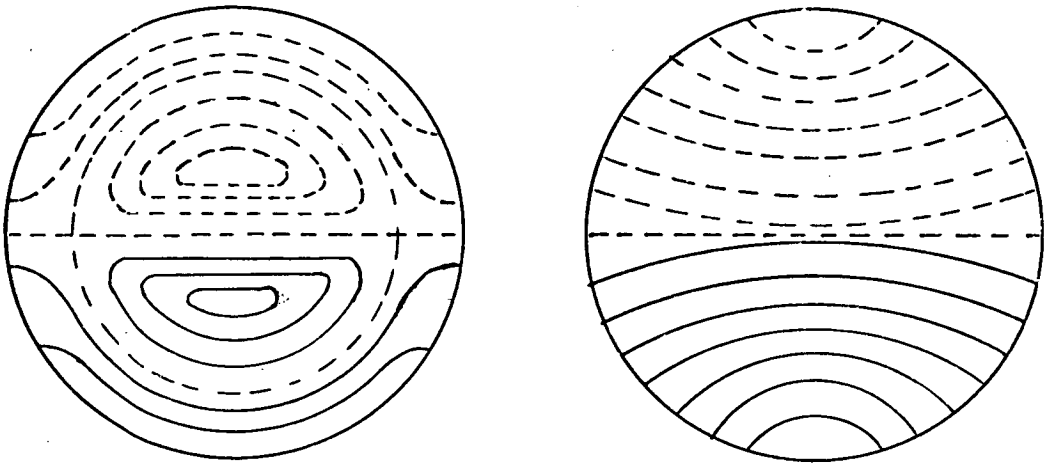


Fig(I.5)

Liquid Free Surface Contour Lines
a) First Mode b) Second Mode

1) Lateral Sloshing (or Normal Sloshing): resulting from translational or pitching excitation of the tank. The most important mode of this kind is the first antisymmetric, Fig. (I.4a).

2) Parametric (or Vertical) Sloshing: is the response of the liquid free surface when its container vibrates vertically. Such motion is characterised primarily by symmetric modes, Fig. (I.4b).

3) Rotational (Swirl) Sloshing: During translational excitation of a partially filled tank at a frequency near the natural frequency of the first antisymmetric mode the liquid exhibits a rotational motion (as a type of beating about the tank logitudinal axis). The mechanism that causes rotary fluid motion is a nonlinear coupling of fluid motions parallel with and perpendicular to the excitation plane, Fig. (I.4c).

4) Vortex Formation: occurs during the draining of propellant from the tank. The vortex or rotational flow surrounds a hollow core and consequently causes a remarkable decrease in the flow rate by reducing the effective cross-sectional area of the drain outlet, Fig. (I.4d).

5) Surface Spray (Spatial Resonance): a development of a dense spray of small droplets at the liquid-free surface as a result of high frequency rigid body excitation or elastic spatial vibration, Fig. (I.4e).

6) Dome Impact: under the conditions of abrupt thrust cut-off while the rocket is in flight, impact of liquid propellant against the opposing tank bulkhead can occur.

7) Low Gravity Phenomena: under conditions of nearly zero gravity- in orbital or interplanetary flight - the liquid behaviour is governed primarily by surface tension (and viscous) forces rather than by inertial forces and may be orientated randomly within the tank depending essentially upon wetting characteristics on the tank wall, Fig. (I.4f).

8) Docking Impact: liquid impact upon a tank bulkhead arising from docking or other manoeuvres in space flight, when the liquid is initially controlled by low gravity conditions.

The first two types of fluid motion are the most significant for the subject of the present thesis, therefore, the main dynamic characteristics involved are reviewed in some detail.

## I.3 Dynamics of Lateral Slosh:

Mathematical models for describing the free surface oscillations of the fluid under lateral excitation have been quite well developed so that there is now a relatively complete body of theoretical work available, well-supported by experimental results[A2]. The linear theory has been developed on the assumption of irrotational flow in an incompressible and inviscid fluid. These assumptions led to the representation of the velocity vector as a gradient of velocity potential. The velocity potential is consequently obtained by solving Laplace's equation - i.e. the equation of continuity for incompressible flow - and satisfying the boundary conditions. Having obtained the velocity potential function the fluid dynamic characteristics such as pressure distribution, forces, and moments can be easily determined.

Confining our attention to a circular cylindrical tank with a flat bottom, the natural frequencies and mode shapes of the free surface of the liquid are found to be[H12]:

$$\omega_{mn}^2 = \frac{\xi_{mn} g}{a} \tanh(\xi_{mn} h/a) \qquad (I.1)$$

$$\eta_{mn} = \frac{1}{g} \sum_{m=0}^{\infty} \sum_{n=1}^{\infty} \omega_{mn} A_{mn} . \sin(m\theta) . \cosh(\xi_{mn} h/a) . J_m(\xi_{mn} r/a) \cos\omega_{mn} t \qquad (I.2)$$

where

$a$ = radius of the tank

$h$ = fluid depth

$g$ = gravitational acceleration

$\xi_{mn}$ = zeros of the first derivative of the Bessel function of the first kind $J'_m(\xi_{mn}) = 0$

$A$ = constant depending on the initial conditions of the free surface of the fluid.

It is clear from Fig. (III.2) that most of the change in frequency $\omega_{mn}$ occurs for shallow liquid depths. Fig. (I.5) shows the contour lines of the free surface for the first and second modes as given by Lamb[L1]. These lines meet the boundary at right angles and the simple harmonic oscillations of the fluid particles take place in straight lines perpendicular to the plane of the contour lines.

In forced sinusoidal excitation $\delta_o \cos\Omega t$, the velocity potential function $\Phi$ is given by the expression[A4],

$$\Phi = -\Omega\delta_o \cos(\Omega t).\cos\theta\left\{ r + \sum_{n=1}^{\infty} \left(\frac{2a}{\xi_{1n}^2 - 1}\right)\left(\frac{\Omega^2}{\omega_{1n}^2 - \Omega^2}\right)\left[\frac{J_1(\xi_{1n} r/a)}{J_1(\xi_{1n})}\right]\left[\frac{\cosh[\xi_{1n}(z+h)/a]}{\cosh(\xi_{1n} h/a)}\right]\right\}$$

.....(I.3)

The surface wave height is obtained by substituting (I.3) in the Bernoulli equation[A4]

$$\frac{\partial \Phi}{\partial t} - gZ - \frac{P}{\rho} = C(t) \qquad (I.4)$$

where $C(t)$ is an arbitrary function of time.

With $P = 0$, $Z = \eta$. Incorporating $C(t)$ in $\Phi$, takes the form:

$$\eta = \frac{\delta_o \Omega^2}{g} \sin(\Omega t).\cos\theta\left\{ r + \sum_{n=1}^{\infty} \left(\frac{2a}{\xi_{1n}^2 - 1}\right)\left(\frac{\Omega^2}{\omega_{1n}^2 - \Omega^2}\right)\left[\frac{J_1(\xi_{1n} r/a)}{J_1(\xi_{1n})}\right]\right\} \qquad (I.5)$$

The total force exerted by the fluid onto the walls can be determined by the integration $\oint P.dA$ where P is expressed in terms of $\Phi$, using (I.3) and (I.4). Along $\theta = 0$ the force is found to be [A4];

$$F_X = M_F \delta_o \Omega^2 \sin\Omega t\left\{ 1 + \sum_{n=1}^{\infty} \frac{(a/h)}{\xi_{1n}} \left(\frac{\Omega^2}{\omega_{1n}^2 - \Omega^2}\right) \frac{2}{(\xi_{1n}^2 - 1)} \cdot \tanh(\xi_{1n} h/a)\right\}$$

.....(I.6)

where $\delta_o$ = amplitude of excitation.

$\Omega$ = forced frequency.

$M_F$ = total mass of the fluid.

Equation (I.5) indicates that when the driving frequency $\Omega$ approaches any sloshing frequency $\omega_{1n}$, $\eta$ becomes arbitrary large. In such a case, these solutions are not valid due to the neglect of fluid damping and other nonlinear effects. Fig. (I.6) is a typical

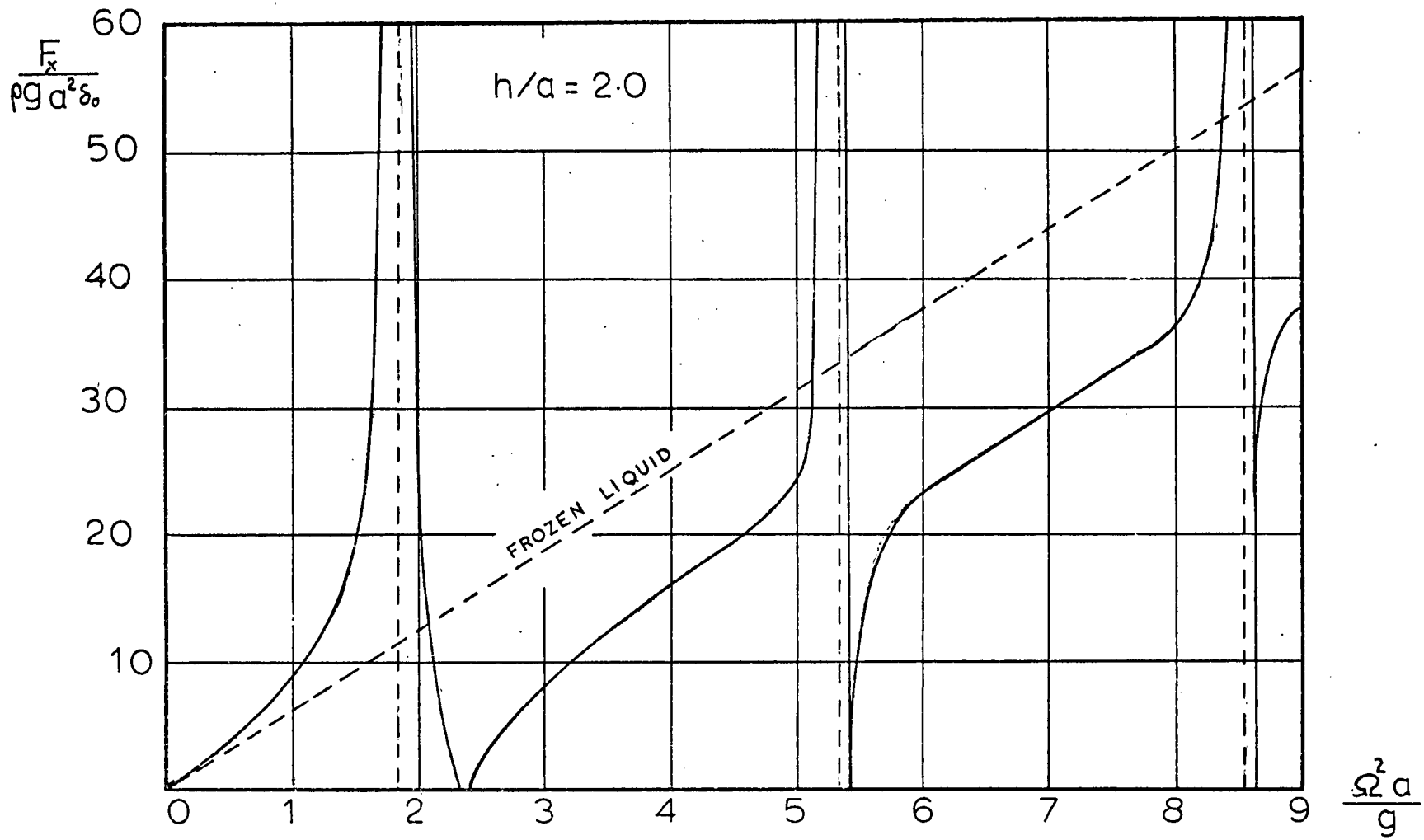


Fig.(1.6) Sloshing Force of a Liquid in a Circular Tank.

plot of the sloshing force as a function of the forcing frequency for $h/a = 2$.

## I.4 Behaviour of Fluid/Structure Systems Under Longitudinal Excitation:

The response of systems subjected to longitudinal excitation can exhibit some form of the following instabilities depending on excitation characteristics and the system configuration:

i) POGO Type Instability.

ii) Parametric Resonance.

iii) Internal Resonance.

The last two types belong to one class of problems which is quite different from the first one. The nature and conditions of occurrence of these phenomena will be discussed in the following sections, in some detail for types (ii) and (iii).

### I.4.1 POGO Type Instability

POGO oscillation is a nickname given to self-excited longitudinal oscillation. This phenomenon was observed in 1962 on the Titan-II structure in the first stage flight. The vibration was apparently caused by a regenerative feedback interaction between the vehicle's propulsion system and structure. The occurrence of this oscillation is not desirable in the carrier vehicles for it would seriously degrade the astronaut's ability to perform his functions and could lead to physical injury. The prevention or reduction of the POGO oscillations could be achieved by suppressing the propagation of pressure pulses in the liquid propellent feedlines which coupled the vehicle's structure with its propulsion system.

In the oxidiser and fuel feedlines the pressure propagation is amplified by the occurrence of resonances. It was found in Gemini[G2] that the feedline resonance were too close to the vehicle's lowest longitudinal structural frequency during the later part of the first stage flight. Among the various methods[A2] for eliminating the pressure resonances, the hydraulic resonators system connected to the feedlines was found to be most effective.

I.4.2 Parametric Resonance

The well known phenomenon of normal resonance in forced vibration systems occurs when the disturbing frequency $\Omega$ is near or equal to one of the natural frequencies $\omega_n$ of the system. In this type the excitation function appears on its own on the right hand side of the equation of motion. However, in parametric excitation, the situation is altered and we are concerned with the so called "Parametric resonance" which occurs when the forced excitation frequency is equal to twice (or any integer multiple of) the natural frequency of the system, i.e. $\Omega = 2\omega_n$ (or $\Omega = m\omega_n$). This type of resonance is found to occur when the loads are parametric with respect to their perpendicular direction. The term "Parametric Loads"[E2] stems from the fact that such loads appear as a parameter in a perturbed equilibrium equation.

Parametric vibration can easily be illustrated by three examples shown in Fig. (I.7). The beam shown in Fig. (I.7c) is subjected to a periodic longitudinal load and can respond with either longitudinal vibrations or transverse (parametric) vibrations. The fluid in the container, Fig. (I.7a), can experience sloshing motion as a result of parametric excitation. The third example in

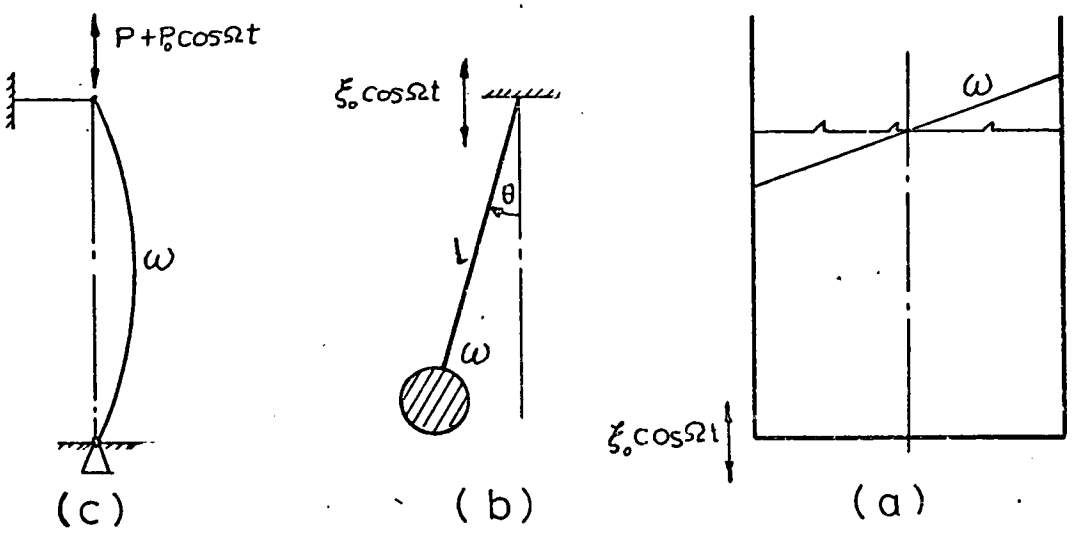


Fig(I.7) Examples of Systems Under Parametric Excitation ($\Omega = 2\omega$)

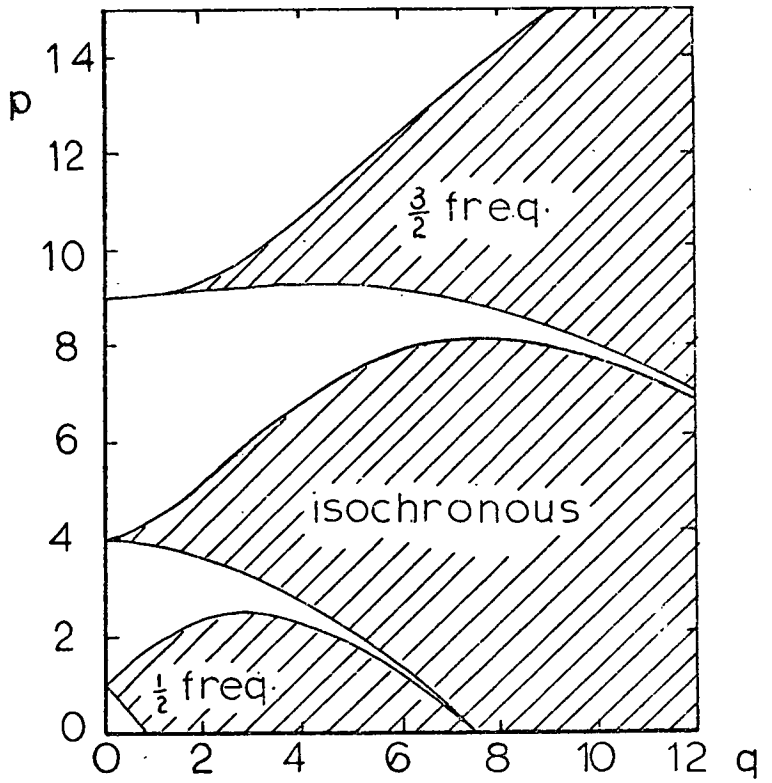


Fig.(I.8) Stability Chart for the Solutions of Mathieu's Equation (ref. B6)

Fig. (I.7b) is the motion of a pendulum resulting from vertical oscillation of its support. Under that class of systems the motion is governed by a differential equation whose stiffness coefficient is function of the parametric load as;

$$\frac{d^2a_m}{dT^2} + (P_m - 2q_m \cos 2T)a_m = 0 \qquad (I.7)$$

Equation (I.7) is the standard form of Mathieu's equation[M3].

Before discussing the properties of equation (I.7), it is useful to review the historical development of parametric resonance. In 1831 Faraday[F1] noticed that the fluid inside a glass container oscillated at one half of the external vertical excitation frequency. Another similar series of experiments conducted by Matthiessen[M2,2a] 1868, 1870 showed that the fluid vibrations were synchronous. The contradiction of the two observations led Lord Rayleigh[R1-2] to make a further series of experiments with improved equipment, and his observations supported Faraday's view. During that time, Mathieu, 1868, formulated his equations which helped Rayleigh to explain this phenomenon mathematically. Ince (1915-1941)[M3] extended the work on Mathieu functions, and introduced the stability chart in 1925. The problem was investigated again by Benjamin and Ursell[B6] who explained mathematically the descrepancy between Faraday's and Rayleigh's observations on the one hand and Matthiessen's findings on the other hand. Their analysis led to a system of Mathieu equations in the form (I.7) where:

$a_m$ = nondimensional wave height parameter

$P_m = 4\omega_m^2/\Omega^2$

$q_m = 2(\xi_m/a)X_o \tanh(\xi_m h/a)$

$T = \omega_m t$

$X_o$ = amplitude of vertical excitation

Depending on the values of the characteristic numbers $P_m$ and $q_m$ the solutions of (I.7) can be stable or unstable. The boundaries of stability are usually given in a chart such as shown in Fig. (I.8). Mathematical expressions for these boundaries are well documented[A6,M3]. The shaded regions in that chart correspond to unstable solutions of (I.7), i.e. if the point (p,q) lies in one of these areas the fluid amplitude increases until eventually it is restrained by nonlinear or damping effects, which are not considered in that theory, or until the free surface disintegrates. If (p,q) lies in the unshaded areas then the solution of (I.7) will be bounded. Benjamin and Ursell also showed that if the plane free surface were unstable, the resulting motion could have frequency (N/2) times the excitation frequency where N is an integer. Since the motion might be a half frequency subharmonic, harmonic or superharmonic, both Faraday and Matthiessen could be correct, however, the experimental results of Benjamin and Ursell only showed the half frequency subharmonic. These results also showed that damping prevents the unstable regions from extending to the p-axis. Woodward[W1] suggested that in most real fluids there is sufficient damping such that the unstable regions - except the first several unstable ones - will be located completely above the line $q_m = X_o\Omega^2 P_m/2g$, and consideration need only be given to those modes in the lower frequency range.

Bolotin[B11], and Sorokin[S11] found that the domains of instability could be reduced somewhat if linear damping due to viscosity was introduced in the Mathieu equation as;

$$\ddot{a} + 2C\dot{a} + (\omega_n^2 - \Omega^2 X_o \lambda \cos\Omega t)a = 0 \qquad (I.8)$$

where

$C = 2\nu\lambda^2$ the damping coefficient as assumed by Sorokin, see Lamb[L1]

$\lambda$ = Wave number

$\nu$ = Kinematic viscosity

The regions of instability according to Sorokin are determined by the inequality

$$1 - \sqrt{(2X_o\lambda)^2 - 4(\frac{2C}{\Omega})^2} < (\frac{2\omega_n}{\Omega})^2 < 1 + \sqrt{(2X_o\lambda)^2 - 4(\frac{2C}{\Omega})^2} \qquad (I.9)$$

c.f. the undamped case[D2];

$$1 - 2X_o\lambda < (\frac{2\omega_n}{\Omega})^2 < 1 + 2X_o\lambda \qquad (I.10)$$

(I.9) determines the critical excitation amplitude ($X_c$) under which the fluid would remain plain. This amplitude is determined by equating the expression under the radical sign to zero at $\frac{\Omega}{2\omega_n} = 1$ as;

$$X_c = 2C/\lambda\Omega$$

For $X_o > X_c$ the free surface amplitude increases at an exponential rate $e^{(\zeta-c)t}$ where $\zeta = \frac{1}{2}\Omega X_o\lambda$ and $(\zeta-c)$ is positive. Brand and Nyborg[B13] carried out a series of experiments to measure $X_c$, i.e. the minimum values of X required for excitation of half frequency surface waves. The measured values of $X_c$ were found to be much greater than those predicted by the theory. They attributed this difference to the lack of development in the previous theories of the

free surface damping coefficient. Considerable efforts have been given in the last few years by Miles[M8], and Mei and Liu[M4] to improve the damping theories taking into account the most possible sources of energy dissipation.

Owing to the mathematical difficulties involved in analysing tanks of various geometrical configurations, Kana[K1] conducted an experimental investigation of liquid surface oscillations in $90^{\circ}$ sector cylindrical and spherical tanks. The liquid response in both containers was found to be essentially similar to its behaviour in a cylindrical tank, especially the half frequency subharmonic response. The free surface modes in a spherical tank are dependent on the fluid depth. It was anticipated in that study that the motion of the liquid in the first mode of the $90^{\circ}$ sector tank could exert a net torque about the longitudinal axis, if the proper phase relationships exist in the motion. Such a torque cannot occur in a non-sectored tank, or even in a sectored tank under lateral translational input.

The influence of parametric excitation on the discharge of liquid propellent from tanks of space vehicles has been determined experimentally by Schoenhalls, Winter and Griggs[S3]. It was found to be a remarkable flow retardation as the amplitude of the acceleration level increases, on the other hand the flow retardation decreases as the frequency of excitation increases for a fixed acceleration amplitude.

In a recent field, the parametric response of the interface between two dielectric liquids under an alternating electrostrictive force has been studied by Reynolds[R5], Devitt and Melcher[D1] and Briskman and Shaidurov[B14]. Their studies showed that, for stability of the interface, the applied voltage must be high enough to suppress surface tension effects and lower than a certain analytically determined

critical value. For voltages greater than this critical value, experiments[R5] indicated that the interface is unstable. The critical voltage $V_c$ in this case is analogous to the critical onset exciting amplitude $X_c$, and the stability criteria follows the boundaries of the Mathieu Chart.

Mathieu's equation (I.7) is adequate to predict the stability of fluid motion, however it fails to give a unique bounded solution for the liquid response amplitude. This fact led Skalak and Yarymovych[S10] to utilise the nonlinear mathematical model of free oscillations of wave motion developed by Penny and Price[P1] to investigate theoretically the finite amplitude surface motion for an infinitly deep rectangular tank subjected to longitudinal excitations. While agreeing theoretically with Benjamin and Ursell, their experiments yielded only one-half subharmonic response. They suggested that damping was a secondary effect on the one-half subharmonic motion.

Dodge, Kana, and Abramson[D2] used the same method of attack for the case of a circular cylinder subjected to the same type of excitation. They found that the symmetric liquid modes appear as prominently as antisymmetric modes. In their experiments, both half frequency subharmonic and harmonic liquid motion were observed, but the latter was less common.

Chu[C9] followed another line of attack based on Moiseev perturbation theory[M10] to investigate the subharmonic liquid response. Moiseev theory however, is dependent on the accuracy of the numerical construction of the Neumann function and the characteristic function. Nevertheless this method has not received any more applications in this field.

The influence of the tank geometry was studied theoretically by Woodward and Bauer[W2] who considered an annular sector cross-section partially filled with liquid. They showed that stability considerations would make the occurrence of harmonic and super-harmonic responses very difficult. They concluded that a response at frequency ($N\Omega/2$) could be maintained if the disturbance, resulting from equipment imperfections, etc. was less than the order of $(X_o/a)^N$ where N is integer.

Chang[C4] and Bauer, Chang and Wang[B5] extended these studies to determine the effect of the tank bottom elasticity on the liquid motion in a circular tank under longitudinal excitations. They found that the influence of the elastic bottom upon the liquid response is more significant as the tank diameter increases and as the bottom thickness and height decrease.

Fluids, structure elements and mechanisms (as pendulums) exhibit the same characteristics of instability according to the linear theory. However, it has been found[W1] that the nonlinear formulation of the free surface dynamics is governed by an equation (for one mode) similar to a certain extent to the nonlinear differential equation of motion of a parametrically excited pinned-end beam, Fig. (I.7c). Bolotin[B12] discussed the latter case in detail and found that for a beam oscillating in the first mode with a deflection expressed in the form;

$$W(x,t) = f(t)\ \sin(\pi x/\ell)$$

the time function is governed by the nonlinear differential equation

$$\ddot{f} + 2c\dot{f} + \omega_1^2(1 - 2\mu\ \cos\Omega t)f + \Psi_1(f) + \Psi_2(f,\dot{f},\ddot{f}\ ) = 0$$

.....(I.11)

where

$\Psi_1(f) = \gamma f^3$ is a nonlinear function of displacements characterising the nonlinear stiffness of the system.

$\Psi_2(f,\dot{f},\ddot{f}) = 2Kf[f\ddot{f} + (\dot{f})^2]$ is a nonlinear function determining the nonlinear inertia.

$\gamma$ = coefficient of nonlinear elasticity

K = coefficient of nonlinear inertia

$\omega_1 = \sqrt{[\frac{\pi^4 EJ}{m\ell^4}]}$ natural frequency of the first mode

$\ell$ = length of the beam

EJ = bending stiffness

m = mass per unit length of the beam

$\mu = \frac{P_t}{2(P_1^* - P_o)}$ excitation parameter

$P_1^*$ = Euler buckling load of the first mode ( $= \pi^2 EJ/\ell^2$)

C = Damping coefficient

Depending on the values $\gamma$ and K the characteristic of the system response can be determined. Bolotin gave a typical picture for the influence of nonlinear inertia, Fig. (I.9b), and nonlinear stiffness Fig. (I.9a), where dotted lines indicate an unstable solution. The response curve in Fig. (I.9a) is given for hard system, $\gamma > 0$. In most liquids the free surface response exhibits soft characteristics, i.e. the amplitude increases in the direction of decreasing forcing frequency.

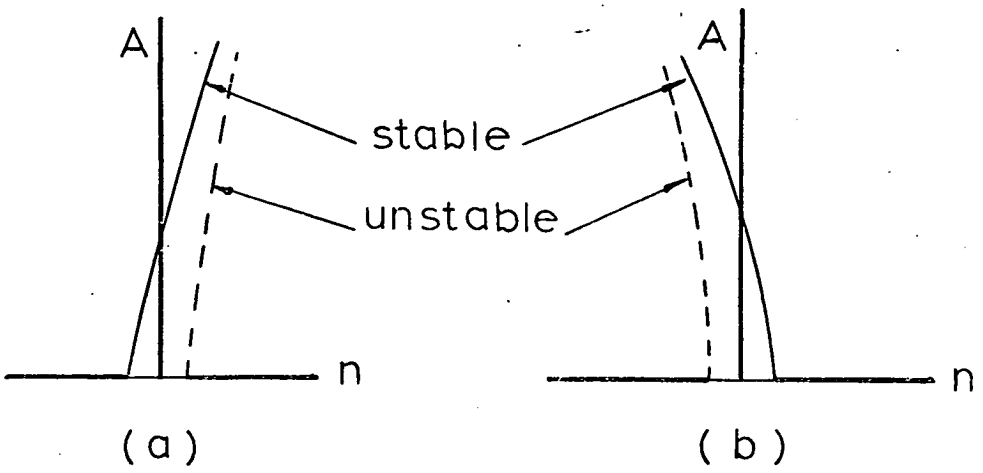


Fig(1.9) Amplitude Response of a System with a)Nonlinear Elasticity. b)Nonlinear Inertia. (ref.B12)

$n = \frac{\Omega}{2\omega}$

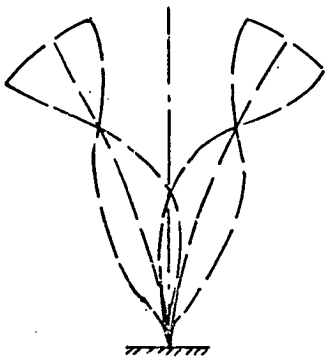

Fig.(1.10) Combination Modes of a beam under Combination Resonance $\Omega = \omega_1 + \omega_2$ (ref. J1)

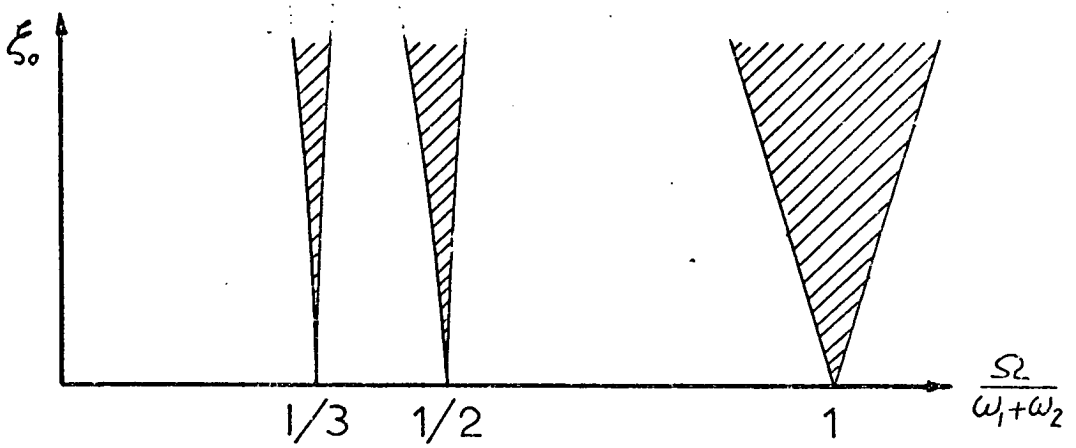


Fig.(1.11) Stability Boundary Chart of Combination Resonance (ref.M 7)

Nonlinear analytical solutions of parametric resonance problems can be obtained by perturbation methods[S13] or by the averaging techniques devised by Bogoliubov and Mitropolskii[B10], Evan-Iwanowski[E2] presented a survey of the parametric response of structure elements, such as columns, arches, plates and members of aircraft structures and listed the various techniques used for the determination of the stability boundaries and the amplitude-frequency response.

The previous discussion covers the phenomenon of parametric resonance assuming that the excitation is sinusoidal which is an ideal case. In practical applications such as the motion generated by earthquakes, the excitation consists of many harmonics and sometimes appears as a beating type motion. This latter was considered by Barr and McWhannell[B1] who studied the stability behaviour of a single-degree-of-freedom system subjected to a vertical ground motion consisting of two inputs of equal acceleration amplitudes but with different frequencies $\Omega$ and $k\Omega$, where $k>1$ is a real number. Their analysis predicted two regions of instability near the following resonance condition

$$\omega = \tfrac{1}{2}\,\Omega\,(k+1) \qquad \text{(a)}$$

$$\omega = \tfrac{1}{2}\,\Omega\,(k-1) \qquad \text{(b)} \qquad \text{(I.12)}$$

Where $\omega$ is the natural frequency of the system. The first relation (I.12a) was found to be of small influence because of its relatively narrow instability region. Relation (I.12b) gave a considerably wider instability region when k was not far from unity.

A similar problem was treated by Yamamoto and Saito[Y1] but, instead of applying two parametric excitations, they considered one parametric load with frequency $k\Omega$ and a disturbing force with frequency $\Omega$ acting laterally. They found that instability occurs at;

$$\omega = \Omega(k + 1) \qquad \text{(a)}$$
$$\omega = \Omega(k - 1) \qquad \text{(b)} \qquad \text{(I.12*)}$$

Again the difference type (I.12*b) was more significant in causing instability than the solution of the sum type (I.12*a).

Combination Resonance: Systems with several degrees-of-freedom can exhibit instability of a resonance type when the exciting frequency and two or more natural frequencies satisfy a linear relation with integral coefficients. Under such circumstances the system vibrates simultaneously in several normal modes. This phenomenon is a special type of parametric resonance and the approach to it is by the theory of linear differential equations with periodic coefficients. It is due to Cesari[C2] who deduced mathematically the two regions of instability at;

$$\Omega = \frac{1}{n}\left|\omega_k + \omega_\ell\right| \qquad \text{(a)}$$
$$\Omega = \frac{1}{n}\left|\omega_k - \omega_\ell\right| \qquad \text{(b)} \qquad \text{(I.13)}$$

where $\Omega$ is the frequency of excitation , $\omega_k$ and $\omega_\ell$ are two natural frequencies of the system, and n is a positive integer number. When $k \neq \ell$ the instability is referred to as a "combination resonance of the

second kind[M6,7]. It is of the first kind if k = $\ell$, the case which was discussed in the previous section. Furthermore, Bolotin[B12] referred to relation (I.13a) as the combination resonance for canonical systems while (I.13b) is for non-canonical systems. The subsequent motion of the system under resonance conditions (I.13) can be described as two normal mode oscillations, with indices k and $\ell$, which are simultaneously excited. Typical mode shapes for a simple vertical cantilever subjected to vertical excitation were observed by Jaeger and Barr[J1] and are resketched in Fig. (I.10).

Mettler[M7] presented a survey containing most of the important mathematical methods, results and various problems relating to the combination resonance. Investigations have been extended to many applications. In aircraft structures, Barr and Done[B2] found that for small fuselage excitation the substructures can exhibit instability regions of the summed type (I.13a). At the same school, Barr and McWhannell[B1] showed that the combination resonance is one of the remarkable sources of instability in multistorey building structures subjected to vertical ground excitation.

Stability under conditions (I.13) has been investigated by Gelfand and Lidskii[G1] and Hahn[H2]. They showed that under certain circumstances the system is unstable under the summed type relation (I.13a) while it is stable in the difference type (I.13b). In the first case the amplitude increases exponentially with time, and thus introduces nonlinearities in inertia, stiffnesses and damping and these factors alter the problem[B12] as we shall see in the next section. In the second case the solutions are still oscillatory. Sen Gupta[S4] indicated that the transition from oscillatory or stable solutions to those of unstable ones should be continuous with respect to the parameters of the equations of motion.

Typical stability boundaries of a straight bar subjected to an axial pulsating load are delineated by Mettler[M7] and presented in Fig. (I.11) for the first three regions of instability (n = 1,2,3). In a comprehensive paper, however, Yamamoto and Saito[Y1] showed that to the first approximation there is no unstable vibration of summed and differential types of higher order (n = 2,3,....). Their conclusion was confirmed experimentally. For higher orders however, vibrations of type (I.13) can appear at the nth approximation, and there are unstable vibrations of higher order only of the summed type.

As the damping was not considered in the Mettler example, Fig. (I.11), the onset excitation amplitude is zero at $\omega = \Omega$. However, contrary to the results for a single degree-of-freedom, the damping forces do not always decrease the width of the unstable regions in which two unstable vibrations of frequencies $\omega_k$ and $\omega_\ell$ build up simultaneously. This destabilising effect of the damping forces was found by Massa[M1], Hagedorn[H1] and Fu and Nemat-Nasser[F2]. The effect is similar to that found by Ziegler[Z1], Bolotin[B12] and Herrmann[H6] for nonconservative elastic systems with two-degrees-of-freedom.

With three mode interaction, the system can exhibit instability of the third kind as;

$$\Omega = \omega_1 + \omega_2 + \omega_3 \tag{I.14}$$

Some remarks on this type are found in ref. [M7].

## I.4.3 Autoparametric/Internal (Nonlinear) Resonance

Within the scope of the classical theory of small oscillations in multi-degrees-of-freedom systems, it is possible to perform a linear transformation into the principal co-ordinates which results in an uncoupled set of n equations of motion. The corrresponding solutions are harmonic and quite adequate to describe the response of the system as long as the corresponding motions are not far from the stable static equilibrium configuration. However, for some systems it is not always possible to get a response to remain near that stable configuration and unexpected types of motion can occur. The response of systems in such situations can be determined by considering the nonlinear terms which couple the different normal modes. This fact has been realised by many authors[H9-10, S5,6 K2, B3,4] and can be illustrated by the example given by Kane and Kahn[K2], of a spring mass system free to oscillate about a horizontal axis. They showed that, if the spring is given an initial elongation with a small angle $\theta$, then under certain circumstances the value of $\theta$ grow with successive oscillations. The motion eventually becomes almost pendulum-like, the angular oscillations then decrease with a corresponding increase in the spring elongation and the process repeats itself periodically. This energy flow between the two modes cannot be predicted by the linear theory. Sethna[S10] and Barr[B4] showed that the nonlinearities in such systems appear as a product of the different modes. Barr's paper gave the equation;

$$\ddot{P}_r + \omega_r^2 P_r = \epsilon \left\{ \sum_j \sum_i \ell_{rij} P_i \ddot{P}_j - m_{rij} \dot{P}_i \dot{P}_j - K_{rj}(t) P_j - \omega_r d_{rr} \dot{P}_r - F_r(t) \right\} \quad \ldots\ldots(I.15)$$

Equation (I.15) in fact represents n equations ($r = 1,2,\ldots n$) in the nondimensional normal co-ordinates $P_r$. The first two terms on the right hand side are the inertial nonlinearities, the third term is the parametric excitation, the fourth is the damping and the last is the forcing term. $\epsilon$ is a small parameter, $\ell_{rij}$, $m_{rij}$ and $d_{rr}$ are constants for a given structure.

The nonlinear inertia terms have an important influence upon the behaviour of the system, especially under the condition of internal (or nonlinear) resonance. Internal resonance indicates the presence of a linear relationship between the natural frequencies of the different modes. For a two degree of freedom system with quadratic nonlinearities internal resonance occurs when the natural frequency of one mode equals twice the natural frequency of the other mode. For three degrees of freedom system with quadratic nonlinearities the natural frequency of one mode equals the sum or difference of the natural frequencies of the two other modes, viz.

$$\omega_r = 2\omega_j \qquad \text{(a)}$$

$$\omega_r = \omega_j \pm \omega_i \qquad \text{(b)} \qquad \text{(I.16)}$$

With a cubic nonlinearity Tomáš[T2] showed that internal resonance can occur at one of the two conditions;

$$\omega_r = \frac{2}{3}\omega_j \qquad \text{(a)}$$

$$\omega_r = \frac{1}{3}\omega_j \qquad \text{(b)} \qquad \text{(I.17)}$$

The motion arising due to the nonlinear coupling of the different modes is similar to the energy exchange between different modes as observed in free vibration test[K2]. In forced oscillation systems one mode may act as a vibration absorber to another. This property led Sevin[S8], Struble and Heinbockel[S18,19] and Haxton and Barr[H5] to study the characteristics of systems named by the latter authors, as autoparametric vibration absorbers. It was Minorsky[M9] who gave the term "autoparametric" to a vibrating elastic pendulum with nonlinear inertia interaction between the modes. The autoparametric coupling can be distinguished from the parametric case by the presence of nonlinear terms linking two different modes such as $P_i\ddot{P}_j$. Here $P_j$ - an implicit function of time - acts as a parametric load with the stiffness $P_i$. In parametric problems the external periodic excitation - an explicit function of time - appears as a coefficient of $P_i$. The coefficient $P_j$ "is not, however, an infinite energy source independent of $P_i$ but is linked to it through the equation of motion[B4]".

With autoparametric coupling there is a corresponding "autoparametric resonance" which occurs when the conditions of internal resonance (I.16 or 17) and external resonance (when $\omega_r$ nearly equals the external frequency $\Omega$) are met simultaneously. Under these conditions it is found[B4] that the modes related by the internal resonance can interact in such a way that, for example, ordinary forced excitation of one mode will result in exponential growth of another.

As a recent topic, these class of problems have been treated by a few authors[A5, B1-4, S5,6] considering some applications to vibrating systems. Asmis and Tso[A5] studied the effect of internal

resonance on the combination resonant response in a two degrees-of-freedom system. They found that the internal resonance tends to reinforce the combination resonance, resulting in a larger steady-state dynamic response than that with the combination resonance alone. However, the effect of the internal detuning was found to cause desynchronisation of the system, which means that the system may not be able to reach a steady state and beating results, due to the continuous exchange of energy between the two modes.

Barr and McWhannell[B1] realised the importance of autoparametric resonance on the instability of multi-storey building structures. A qualitative analytical study, accompanied by an experiment illustrated the interaction of two normal modes of a frame arranged to have an internal resonance condition (I.16a). Barr and Done[B2] demonstrated the possibility of the occurrence of autoparametric instability in an aeroelastic model wing (with a typical store). Hermann and Hauger[H7] found that divergence and flutter emerge formally as special cases of autoparametric resonance. The dynamic response of a thin-walled column subjected to parametric excitation has been obtained by Popelar[P2] through a numerically integrated solution of the nonlinear differential equations. The results showed that a cyclic interchange of energy occurs between the axial and torsional motion.

That field is still open for many investigations of different systems; however, the mathematical tools for tackling such kinds of problems are well documented. Among these tools the averaging method by Bogoliuboff and Mitropolski [B10] has been used by Sethna [S5-S7] and others [M5]. Another powerful and straightforward technique, the asymptotic method devised by Struble [S14], found applications to

this type of problem [C7, H5, S15, S17]. Kane and Kahn [K2] presented two methods based on the Floquet Theory [C3] and the Hamilton-Jacobi Theory [O1] to obtain conditions of nonlinear resonance. These different techniques and many others have been well compiled more recently in a book by Nayfeh [N1].

## I.5 Scope of the Presented Research

The present problem is an application of the theory of autoparametric coupling in a structure containing a liquid. The dynamic interaction of the structure modes with the fluid sloshing modes are investigated theoretically and experimentally. A general mathematical model is formulated from which three cases of study have been investigated, namely two, three and four modes interaction. The theory of asymptotic expansion due to Struble [S14] has been used in solving the coupled nonlinear differential equations in the neighbourhood of the critical regions of autoparametric resonance. In Chapters (III, IV) the Struble method shows that the autoparametric condition consists of one external and another internal resonance condition while in Chapter (V) it consists of one external and two simultaneous internal resonance conditions. For two mode interaction a solution is obtained by considering cubic nonlinear terms in the governing equations of motion. A FORTRAN CDPOLR subroutine has been used to solve a polynomial of eighth order. For higher modes, analysis is confined to second order terms. Use has been made of the Continuous System Modelling Program (CSMP) to solve a system of six simultaneous nonlinear differential equations. In some other cases the IMP Davden routines are used to solve a system of nonlinear algebraic equations.

# CHAPTER II

## GENERAL FORMULATION OF THE PROBLEM

An elevated water tower structure or a liquid propellent space vehicle are examples of complicated structure systems. The analysis of these systems, when subjected to various loads, can be greatly simplified by representing the system components by an appropriate mechanical system. Figure (II.1) is a typical representation of a structure system consisting of the three sub-systems;

a) The fluid which is contained in the top tank.

b) The spring-mass system carrying the fluid container.

c) A damped spring-mass system carrying the other two systems.

The interaction of the fluid dyanmics with the dynamics of the structure systems will be studied when the base is subjected to a vertical sinusoidal excitation $\xi_0 \cos\Omega t$. Under this type of excitation the fluid container moves up and down and, under certain conditions (to be shown in Chapter IV), moves laterally as well. Accordingly, the free surface of the fluid exhibits normal sloshing and hydrodynamic forces are fed back to the structure.

The mathematical model of the dynamics of the system will be derived by studying the derivation of the fluid governing equations and the equations of motion of the mechanical system.

### II.1 Fluid Field Equations

The general equations of motion of fluids have been documented in books on theoretical hydrodynamics[L1, T1]. Using these equations in

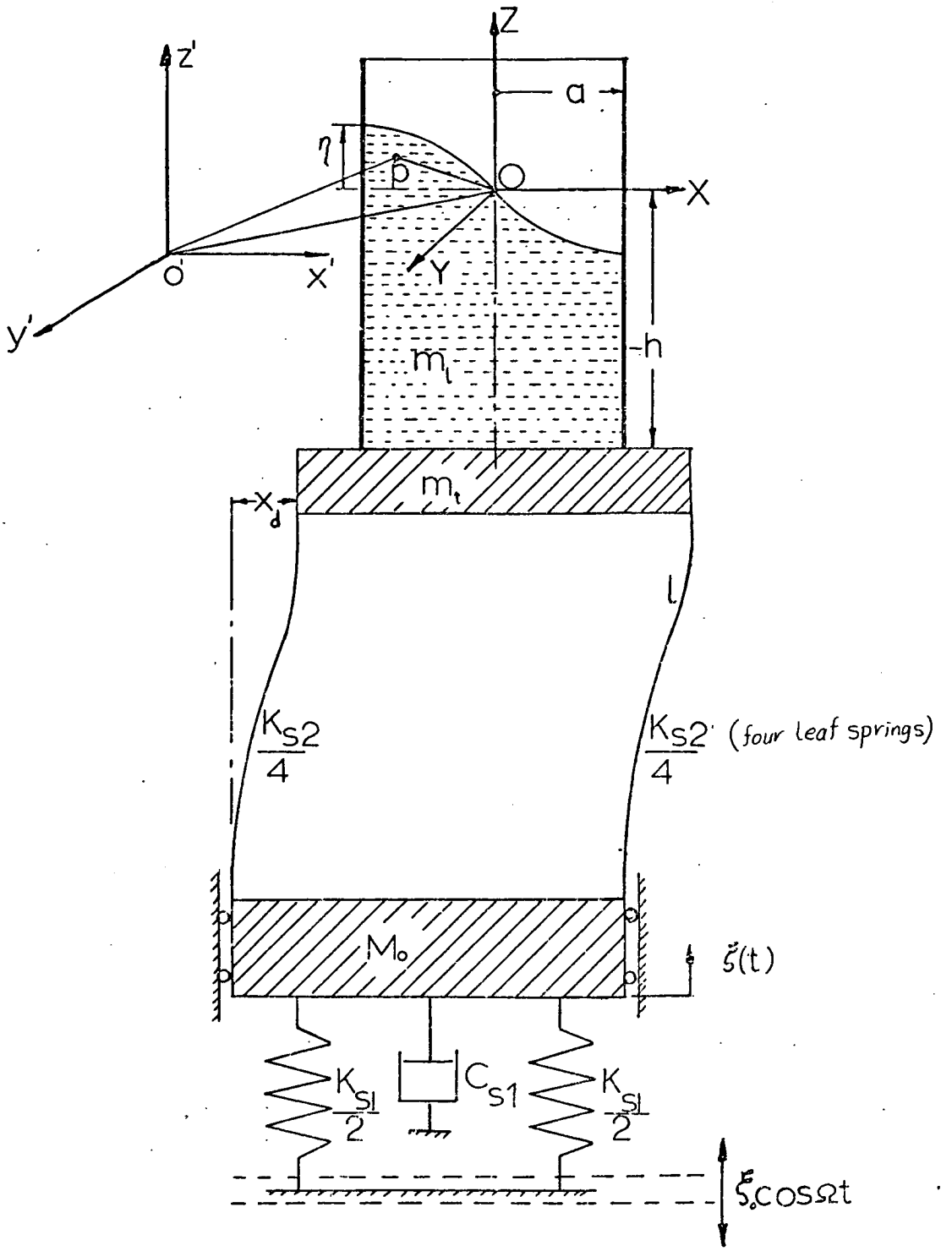


Fig(II·1) Schematic Diagram of the System and Coordinate Systems.

in their exact form seems to be rather difficult, hence the problem will be simplified by introducing the following assumptions;

i) The container is rigid and impermeable

ii) The fluid will be assumed inviscid* and incompressible and initially irrotational

iii) Capillary or surface tension effects on the liquid surface waves are neglected.

The tank will be displaced along some trajectory in space. It is convenient to refer the fluid motion to a moving co-ordinate system as the variables are to be measured by a measuring device which is moving relative to the inertial system.

However, it will be useful to write the fluid equation of motion with reference to both stationary and moving co-ordinates.

II.1.1 Fixed Co-ordinate System

Let $O\acute{}\ X\acute{}\ Y\acute{}\ Z\acute{}$ be the stationary Cartesian co-ordinates (an inertial reference frame) in which the plane $O\acute{}\ X\acute{}\ Y\acute{}$ coincides with the undisturbed free fluid surface. The Euler equations of motion of the fluid are[T1];

$$\frac{\partial \underline{q}}{\partial t} + (\underline{q}.\underline{\nabla})\underline{q} = -\frac{1}{\rho}\underline{\nabla}P - \underline{\nabla}(gZ\acute{}) \qquad (II.1)$$

---

*This assumption is applied only through the derivation of the fluid equations. Damping term will be inserted after the formulation of fluid equations.

where

$\underline{q}$ = fluid vector velocity

$\frac{\partial \underline{q}}{\partial t}$ = local acceleration of the flow at a point whose co-ordinates are not allowed to vary. This acceleration is measured by a fixed observer.

$(\underline{q}.\underline{\nabla})\underline{q}$ = the convective acceleration for a particle drifting with the stream at a velocity q in the flow direction. This acceleration is measured by an observer moving with the particle.

P = fluid pressure at the point in question

$\rho$ = fluid density

$g\acute{Z}$ = the gravitational potential field

for irrotational motion there exists a velocity potential function whose negative gradient gives the fluid velocity, i.e.

$$\underline{q} = -\underline{\nabla}\Phi \tag{II.2}$$

Introducing this relation in equation (II.1) gives;

$$\underline{\nabla}\left(\frac{P}{\rho} + \tfrac{1}{2}\, q^2 + g\acute{Z} - \frac{\partial \Phi}{\partial t}\right) = 0 \tag{II.3}$$

after integration (II.3) becomes;

$$\frac{P}{\rho} + \tfrac{1}{2}\, q^2 + g\acute{Z} - \frac{\partial \Phi}{\partial t} = C(t) \tag{II.4}$$

where C(t) is an arbitrary function of time.

Equation (II.4) is the general form of Kelvin's equation for an unsteady fluid. In this equation the potential function $\Phi$ is a function of space and time, and its derivative with respect to time measures the unsteadness of the flow. However, $\frac{\partial \Phi}{\partial t}$ is interpreted as the work done on a unit mass of fluid whose co-ordinates are (X, Y, Z ), due to local acceleration.

Equation (II.4) is valid only for incompressible flow, in which the velocity potential function $\Phi$ should satisfy Laplace's equation of continuity;

$$\nabla^2 \Phi = 0 \qquad \text{(II.5)}$$

II.1.2 Moving Co-ordinate System

Let OXYZ be another co-ordinate system fixed to the tank such that the OXY plane coincides with the undisturbed free surface. The moving frame OXYZ coincides with the inertial frame $\acute{O}\,\acute{X}\,\acute{Y}\,\acute{Z}$ when the container is at rest. Let $V_o$ be the velocity of the origin O relative to the fixed origin $\acute{O}$, where;

$$\underline{V}_o = \dot{X}_o\,\underline{i} + \dot{y}_o\,\underline{j} + \dot{Z}_o\,\underline{k}$$

$$= (\dot{X}_o\cos\theta + \dot{y}_o\sin\theta)\underline{i}_r + (\dot{y}_o\cos\theta - \dot{X}_o\sin\theta)\underline{i}_\theta + \dot{Z}_o\underline{i}_Z$$

the second expression gives the velocity components in cylindrical co-ordinates. The fluid particle velocity $q_{rel}$ relative to the moving co-ordinates is given by;

$$\underline{q}_{rel} = \underline{q} - \underline{V}_o = -\underline{\nabla}\,\Phi - \underline{V}_o \qquad \text{(II.6)}$$

The velocity potential function $\Phi$ can now be split into two functions, a disturbance potential function $\tilde{\Phi}$ which accounts for the fluid motion relative to the tank, and a potential function $\Phi_o$ which defines the tank motion. Thus $\Phi$ is written as;

$$\Phi = \tilde{\Phi} + \Phi_o \tag{II.7}$$

Both $\tilde{\Phi}$ and $\Phi_o$ should satisfy Laplace's equation (II.5). Since the tank will oscillate in the plane OXZ, $V_o$ becomes

$$\underline{V}_o = (\dot{X}_o \cos\theta)\underline{i}_r - (\dot{X}_o \sin\theta)\underline{i}_\theta + \dot{Z}_o \underline{i}_Z \tag{II.8}$$

Therefore $\Phi_o$ can be determined by integrating (II.8) as;

$$\Phi_o = - \dot{X}_o r \cos\theta - \dot{Z}_o z - \tfrac{1}{2} \int(\dot{X}_o^2 + \dot{Z}_o^2)\, dt \tag{II.9}$$

introducing (II.6 - II.9) in (II.4) we write

$$\frac{P}{\rho} + \tfrac{1}{2}(\underline{\nabla}\tilde{\Phi}.\underline{\nabla}\tilde{\Phi}) + (g + \ddot{Z}_o)Z + \ddot{X}_o r\cos\theta - \tilde{\Phi}_t = C(t) \tag{II.10}$$

Equation (II.10) is the fluid field equation referred to the moving co-ordinate system which is moving with accelerations $\ddot{X}_o$ and $\ddot{Z}_o$.

The complete solution of equation (II.5) must satisfy the relevant boundary conditions of the problem which are;

i) At the wetted rigid wall and bottom the velocity component normal to the boundaries must vanish, i.e.,

$$\left.\frac{\partial\tilde{\Phi}}{\partial r}\right|_{r=a} = 0$$

$$\left.\frac{\partial\tilde{\Phi}}{\partial z}\right|_{z=-h} = 0 \qquad \text{(II.11)}$$

ii) At the free surface we have two unknowns, the shape of the free surface and the value of the velocity potential, therefore, two conditions are required. These are:

a) Dynamic Free Surface Condition

The dynamic condition is obtained from equation (II.10) by setting P equal to zero on the free surface $Z = \eta(r,\theta,t)$ as;

$$\left.\frac{\partial\tilde{\Phi}}{\partial t} - \tfrac{1}{2}(\underline{\nabla}\tilde{\Phi}.\underline{\nabla}\tilde{\Phi}) - (g + \ddot{Z}_o)\eta - r\ddot{X}_o\cos\theta = 0\right|_{z=\eta} \qquad \text{(II.12)}$$

where the function $C(t)$ has been absorbed in the potential function $\tilde{\Phi}$ and $\eta$ denotes the free surface waveheight of the liquid.

b) Kinematic Free Surface Condition

The kinematic condition requires that the vertical velocity of a fluid particle located on the free surface should equal the vertical velocity of the free surface itself. For zero surface tension, the equation of the free surface is given by

$$Z = \eta(r,\theta,t) \qquad \text{(II.13)}$$

or

$$\left. -\tilde{\Phi}_z = \frac{\partial\eta}{\partial t} - \tilde{\Phi}_r\eta_r - \frac{1}{r^2}\tilde{\Phi}_\theta\eta_\theta \right|_{\text{on } Z=\eta} \qquad \text{(II.14)}$$

Where letter subscript $(r, \theta, z)$ denotes differentiation w.r.t. the subscripted variable.

It is evident that equation (II.14) has been obtained from the geometrical considerations of the free surface. The left hand side of (II.14) is simply the velocity in the Z-direction of a fluid particle on the free surface while the right hand side is a statement that the same particle has the velocity of the free surface $\eta_t$ plus the algebraic sum of the vertical components of the velocity relative to the free surface.

The complete formulation of the boundary value problem in terms of the disturbance potential function is summarised as follows;

$$\left.\begin{aligned}
&1)\ \nabla^2\tilde{\Phi} = 0 && \text{inside the fluid domain} && \text{(a)}\\
&2)\ \frac{\partial\tilde{\Phi}}{\partial r} = 0 && \text{at } r=a && \text{(b)}\\
&3)\ \frac{\partial\tilde{\Phi}}{\partial Z} = 0 && \text{at } Z=-h && \text{(c)}\\
&4)\ \frac{\partial\tilde{\Phi}}{\partial t} - \tfrac{1}{2}(\underline{\nabla}\tilde{\Phi}.\underline{\nabla}\tilde{\Phi}) - (g+\ddot{Z}_o)\eta - r\ddot{X}_o\cos\theta = 0 && \text{at } Z=\eta && \text{(d)}\\
&5)\ \frac{\partial\tilde{\Phi}}{\partial t} - \tilde{\Phi}_r\eta_r - \frac{1}{r^2}\tilde{\Phi}_\theta\eta_\theta + \tilde{\Phi}_Z = 0 && \text{at } Z=\eta && \text{(e)}
\end{aligned}\right\} \quad \text{(II.15)}$$

A solution of equation (II.15a) that satisfies conditions (II.15b,c) is*)

$$\Phi(r,\theta,Z,t) = \sum_{m=o}^{\infty}\sum_{n=1}^{\infty} \alpha_{mn}(t)\, J_m(\lambda_{mn} r).\cos m\theta.\frac{\cosh[\lambda_{mn}(Z+h)]}{\cosh\lambda_{mn} h} \qquad \text{(II.16)}$$

where $\lambda_{mn}$ are the roots of $J'_m(\lambda_{mn} a) = 0$.

Alternatively an expression for the free surface elevation $\eta$ can be written

$$\eta(r,\theta,t) = \sum_{m=o}^{\infty}\sum_{n=1}^{\infty} a_{mn}(t)\, J_m(\lambda_{mn} r)\cos m\theta \qquad \text{(II.17)}$$

---

*this form of solution can easily be derived and is given in [D2] and elsewhere.

The coefficients $\alpha_{mn}$ and $a_{mn}$ (generalised co-ordinates of the mn modes) are time dependent and obtained through satisfying the free surface conditions (II.15d,e). The acceleration terms $\ddot{Z}_o$ and $\ddot{X}_o$ in (II.15d) are dependent upon the excitation of the system and the mechanical characteristics of the system. Their values as well as $\alpha_{mn}$ and $a_{mn}$ are not known since they are coupled with the equations of motion of the system.

## II.2 System Equations of Motion

The equations of motion of the system will be derived by applying Lagrange's equation

$$\frac{d}{dt}\left(\frac{\partial L}{\partial \dot{q}_i}\right) - \frac{\partial L}{\partial q_i} + \frac{\partial D}{\partial \dot{q}_i} = Q_i \qquad \text{(II.18)}$$

where

$L$ = T-V, the Lagrangian

$T$ = Kinetic energy of the system

$V$ = Potential energy

$Q_i$ = Generalised forces, corresponding to those external forces which cannot be derived from a potential

$D$ = Dissipation function

$q_i$ = Generalised co-ordinates which are independent of each other and satisfy the configuration of the system at any time, their number corresponds to the number of degrees of freedom of the system, in this case they are;

$\xi$ = Vertical displacement of the main mass

$X_d$ = Lateral displacement of the tank.

$a_{mn}$ = Fluid free surface displacement of the mode (mn)

The fluid forces will be considered as external forces. Regarding the dissipation function D there are two sources of energy dissipation;

a) The structural damping which is proportional to the amplitude of the elastic members and in phase with their velocities. Unfortunately, this will lead to complex elements which would complicate the analysis considerably. So for simplicity, Bauer[A2] assumed that the dissipation function will be equivalent to linear viscous damping. This is justifiable as long as the damping forces are small and only of importance in the neighbourhood of the bending frequencies. Making this assumption the dissipation function of the structure is given by;

$$D_i = \tfrac{1}{2} \sum_{i=1}^{i=2} C_i \dot{q}_i^2 \qquad \text{(II.19a)}$$

where $C_i$ is the structural damping coefficient of the ith mode.

b) The liquid and any dashpots. Their dissipation function is equivalent to linear viscous damping. This takes the form;

$$D_n = \tfrac{1}{2} \sum_{n=1}^{2} C_n \dot{a}_n^2 \qquad \text{(II.19b)}$$

where $C_n$ is the damping coefficient of the nth mode.

The relationship of the displacements of the system members in terms of the main mass displacement are still needed. For the given configuration, Figure (II.2), with a beam fixed at both ends, the horizontal displacement $X_d$ due to a lateral unit load acting upon one end equals $(\ell^3/12EI)$. This lateral displacement is

equivalent to twice the displacement produced by a cantilever whose length is $(\ell/2)$. Accordingly it can be assumed without loss of generality that the corresponding longitudinal displacement $\Delta$ of the end is twice the vertical drop $\acute{\Delta}$ of the end of the cantilever of length $(L/2)$

$$\acute{\Delta} = \tfrac{1}{2} \int_0^{\ell/2} \left(\frac{dX}{dZ}\right)^2 dZ \qquad \text{(II.20)}$$

Let the deflection curve be given by;

$$X = \frac{\acute{X}_d}{2(\ell/2)^3} [3(\ell/2)Z^2 - Z^3] \qquad \text{(II.21)}$$

where $\acute{X}_d$ is the end lateral deflection (at $\ell/2$).

Introducing (II.21) in (II.20) gives

$$\acute{\Delta} = \frac{6}{5\ell}(\acute{X}_d^2)$$

But for the beam of length $\ell$: $X_d = 2\acute{X}_d$ and $\Delta = 2\acute{\Delta}$, therefore

$$\Delta = \frac{3}{5}\frac{X_d^2}{\ell} \qquad \text{(II.22)}$$

which is the same form as that for the cantilever[H5], the only difference being in the value of $X_d$ which depends on end conditions.

The actual vertical displacement of the tank is, $= \xi - \Delta$

$$= \xi - \frac{3}{5\ell} X_d^2$$

and its velocity $= \dot{\xi} - \frac{6}{5\ell} X_d \dot{X}_d$

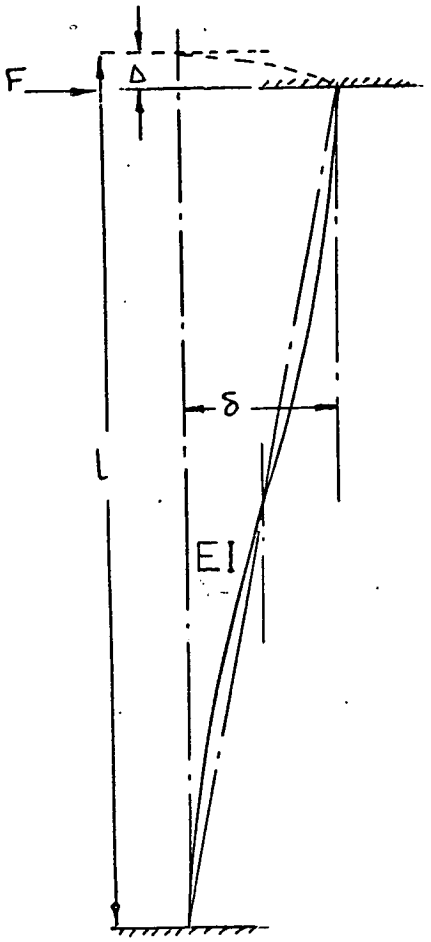


(a)

$$\frac{\delta}{F} = \frac{l^3}{12EI}$$

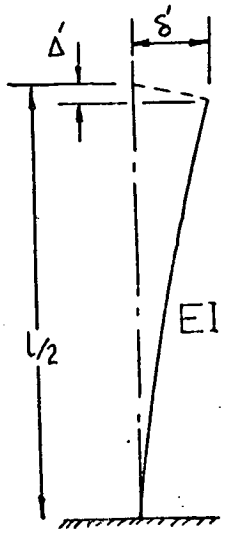


(b)

$$\delta' = \frac{(l/2)^3}{3EI}$$

Fig.(II.2)

The kinetic and potential energies are therefore:

$$T = \tfrac{1}{2} M_o \dot{\xi}^2 + \tfrac{1}{2} m_t(\dot{X}_d^2 + \dot{\xi}^2 - \frac{12}{5\ell}\dot{\xi}\dot{X}_d X_d + \frac{36}{25\ell^2} X_d^2 \dot{X}_d^2)$$

$$V = \tfrac{1}{2} K_{s1}\xi^2 + \tfrac{1}{2} K_{s2} X_d^2 + Mg\xi + mg(\xi - \frac{3}{5\ell} X_d^2) \qquad \text{(II.23)}$$

Applying equation (II.18) gives;

System equation of Motion in the vertical direction:

$$M_o\ddot{\xi} + C_1\dot{\xi} + K_{s1}\xi + m_t[\ddot{\xi} - \frac{6}{5\ell}\dot{X}_d^2 - \frac{6}{5\ell} X_d\ddot{X}_d] = -\int_o^a\int_o^{2\pi} Prdrd\theta + K_{s1}\xi_o \cos\Omega t \qquad \text{.....(II.24)}$$

System equation of Motion in the horizontal direction:

$$m_t\ddot{X}_d + C_2\dot{X}_d + K_{s2}X_d - \frac{6}{5\ell} m_t\ddot{\xi} X_d + \frac{36m_t}{25\ell^2} X_d[X_d\ddot{X}_d + \dot{X}_d^2] = -\int_h^o\int_o^{2\pi} P\cos\theta.ad\theta dZ \qquad \text{.....(II.25)}$$

*where $K_{s1}$ and $K_{s2}$ are the spring stiffnesses shown in fig (II·1)*

In equation (II.24) the origin of co-ordinate $\xi$ has been chosen at the position of static equilibrium where the gravitational forces $\sum_i m_i g$ are balanced by the spring force $K_{s1}\delta$ (where $\delta$ is the static deflection of the spring due to the weight $\sum_i m_i g$). Therefore only forces due to displacement from this position are included.

The acceleration expressions $\ddot{Z}$ and $\ddot{X}$ in equation (II.12) are now easily written as;

$$\left.\begin{aligned} \ddot{Z} &= \ddot{\xi} - \frac{6}{5\ell}(\dot{X}_d^2 + X_d\ddot{X}_d) \\ \ddot{X} &= \ddot{X}_d - \frac{6}{5\ell}\ddot{\xi} X_d + \frac{36}{25\ell^2} X_d(X_d\ddot{X}_d + \dot{X}_d^2) \end{aligned}\right\} \qquad \text{(II.26)}$$

Introducing the expressions (II.16,17) in the nonlinear fluid free surface boundary conditions (II.15d,e) produces a major difficulty because of the high degree of nonlinearity of the different modes and equations (II.15d,e) apply on a surface which is not known beforehand. In order to get any quantitative information, it appears essential to introduce approximation in the free surface equations. The previous literature has shown that methods have been developed for treating the large liquid surface amplitudes in rectangular and circular cylindrical containers. Three of the main theories will be summarised briefly;

a) Moiseev's Theory[M10]; this theory is based on constructing characteristic functions - normal mode functions - and characteristic numbers expressed by integral equations in terms of Green's function of the second kind. Moiseev's theory did not indicate how the characteristic function could be obtained. Chu[C9] generalised it by employing a perturbation method using the characteristic functions to determine the subharmonic response to an oscillatory axial excitation, however, the computations involved in its applications appear to be rather difficult.

b) Penney and Price Theory[P1]: this theory is dependent upon successive approximation. The potential function is expressed as a Fourier series in space with coefficients as functions of time. These coefficients are approximated by Fourier Series in time using the method of perturbation. The resulting solution is in the form of a double Fourier Series in space and time. This method has been applied by Skalak and Yarymovich[S8], and Dodge et al[D2].

c) Hutton's Theory[H12]: this theory is simply based on expanding the dynamic and kinematic free surface fluid equations in Taylor series about a stationary free surface position. The order of approximation could be obtained more easily and in a straightforward way. This method has been used recently by Woodward and Bauer[W2] in the case of parametric excitation of a circular cylindrical tank with sector-annular cross-section.

Using the last of these theories up to the third order approximation by inserting (II.26) in (II.15d,e) and expanding about $\eta=0$ gives;

$$\left\{\tilde{\Phi}_t - \tfrac{1}{2}(\tilde{\Phi}_r^2 + \tfrac{1}{r^2}\tilde{\Phi}_\theta^2 + \tilde{\Phi}_z^2) - r[\ddot{X}_d - \tfrac{6}{5\ell}\ddot{\xi}X_d + \tfrac{36}{25\ell^2}X_d(X_d\ddot{X}_d + \dot{X}_d^2)]\cos\theta\right\}_{\eta=0} +$$

$$+\left\{\tilde{\Phi}_{tz} - \tilde{\Phi}_r\tilde{\Phi}_{rz} - \tfrac{1}{r^2}\tilde{\Phi}_\theta\tilde{\Phi}_{\theta z} - \tilde{\Phi}_z\tilde{\Phi}_{zz} - [g + \ddot{\xi} - \tfrac{6}{5\ell}(\dot{X}_d^2 + X_d\ddot{X}_d)]\right\}_{\eta=0}\cdot\eta +$$

$$+\left\{\tilde{\Phi}_{tzz} - \tilde{\Phi}_{rz}^2 - \tilde{\Phi}_r\tilde{\Phi}_{rzz} - \tfrac{1}{r^2}\tilde{\Phi}_{\theta z}^2 - \tfrac{1}{r^2}\tilde{\Phi}_\theta\tilde{\Phi}_{\theta zz} - \tilde{\Phi}_{zz}^2 - \tilde{\Phi}_z\tilde{\Phi}_{zzz}\right\}_{\eta=0}\cdot\frac{\eta^2}{2} + \ldots = 0$$

.....(II.27)

and

$$\left\{\eta_t - \eta_r\tilde{\Phi}_r - \tfrac{1}{r^2}\eta_\theta\tilde{\Phi}_\theta + \tilde{\Phi}_z\right\}_{\eta=0} + \left\{\tilde{\Phi}_{zz} - \eta_r\tilde{\Phi}_{rz} - \tfrac{1}{r^2}\eta_\theta\tilde{\Phi}_{\theta z}\right\}_{\eta=0}\cdot\eta +$$

$$\left\{\tilde{\Phi}_{zzz} - \eta_r\tilde{\Phi}_{rzz} - \tfrac{1}{r^2}\eta_\theta\tilde{\Phi}_{\theta zz}\right\}_{\eta=0}\cdot\eta^2/2 + \ldots = 0 \qquad \text{(II.28)}$$

Substituting (II.16) and (II.17) in (II.27) and (II.28) gives;

$$- r[\ddot{X}_d - \frac{6}{5\ell}\ddot{\xi} X_d + \frac{36}{25\ell^2} X_d(X_d\ddot{X}_d + \dot{X}_d^2)]\cos\theta$$

$$+ \sum_{m=o}^{\infty}\sum_{n=1}^{\infty}\left\{\dot{\alpha}_{mn} - [g + \ddot{\xi} - \frac{6}{5\ell}(\dot{X}_d^2 + X_d\ddot{X}_d)]a_{mn}\right\}\cos m\theta . J_m(\lambda_{mn} r)$$

$$- \tfrac{1}{2}\sum_{m=o}^{\infty}\sum_{n=1}^{\infty}\sum_{p=o}^{\infty}\sum_{q=1}^{\infty}\Big\{\alpha_{mn}\alpha_{pq}\cos m\theta.\cos p\theta.\lambda_{mn}\lambda_{pq}.J_m(\lambda_{mn} r)J_p(\lambda_{pq} r)$$

$$+ \frac{1}{r^2}\alpha_{mn}\alpha_{pq}\, mp.\sin m\theta.\sin p\theta.J_m(\lambda_{mn} r).J_p(\lambda_{pq} r)$$

$$+ \alpha_{mn}\alpha_{pq}\cos m\theta.\cos p\theta J_m(\lambda_{mn} r)J_p(\lambda_{pq} r).\lambda_{mn}\lambda_{pq}.\tanh(\lambda_{mn} h).\tanh(\lambda_{pq} h)$$

$$- 2\dot{\alpha}_{mn} a_{pq}\cos m\theta.\cos p\theta.J_m(\lambda_{mn} r).J_p(\lambda_{pq} r)\lambda_{mn}\tanh(\lambda_{mn} h)\Big\}$$

$$- \sum_{m=o}^{\infty}\sum_{n=1}^{\infty}\sum_{p=o}^{\infty}\sum_{q=1}^{\infty}\sum_{k=o}^{\infty}\sum_{\ell=1}^{\infty}\Big\{\alpha_{mn}\alpha_{pq}a_{k1}\cos m\theta.\cos p\theta.\cos k\theta.\lambda_{mn}\lambda_{pq}^2 J_m(\lambda_{mn} r)\cdot$$

$$J_p(\lambda_{pq} r)\, J_k(\lambda_{k1} r)\tanh(\lambda_{pq} h)$$

$$+ \frac{1}{r^2}\alpha_{mn}\alpha_{pq}a_{k1}\, mp.\sin m\theta.\sin p\theta.\cos k\theta.\lambda_{pq}.J_m(\lambda_{mn} r)J_p(\lambda_{pq} r)J_k(\lambda_{k1} r)\tanh(\lambda_{pq} h)$$

$$+ \alpha_{mn}\alpha_{pq}a_{k1}\cos m\theta.\cos p\theta.\cos k\theta.\lambda_{mn}\lambda_{pq}^2 J_m(\lambda_{mn} r)J_p(\lambda_{pq} r).J_k(\lambda_{k1} r)\tanh(\lambda_{mn} h)$$

$$- \tfrac{1}{2}\dot{\alpha}_{mn} a_{pq}a_{k1}\cos m\theta.\cos p\theta\cos k\theta.\lambda_{mn}^2 J_m(\lambda_{mn} r)J_p(\lambda_{pq} r)J_k(\lambda_{k1} r)\Big\} + \ldots\ldots = 0$$

.....(II.29)

and;

$$\sum_{m=o}^{\infty}\sum_{n=1}^{\infty}\left\{\dot{a}_{mn}+\lambda_{mn}\tanh\lambda_{mn}h.\alpha_{mn}\right\}\cos m\theta.J_m(\lambda_{mn}r)-$$

$$-\sum_{m=o}^{\infty}\sum_{n=1}^{\infty}\sum_{p=o}^{\infty}\sum_{q=1}^{\infty}\left\{\alpha_{mn}a_{pq}.\cos m\theta.\cos p\theta.\lambda_{mn}\lambda_{pq}J'_m(\lambda_{mn}r)J'_p(\lambda_{pq}r)\right.$$

$$-\alpha_{mn}a_{pq}J_m(\lambda_{mn}r)J_p(\lambda_{pq}r)\left[\frac{1}{r^2}\,mp\sin m\theta.\sin p\theta\right.$$

$$\left.\left.+\lambda_{mn}^2\cos m\theta.\cos p\theta\right]\right\}$$

$$-\sum_{m=o}^{\infty}\sum_{n=1}^{\infty}\sum_{p=1}^{\infty}\sum_{q=1}^{\infty}\sum_{k=o}^{\infty}\sum_{l=1}^{\infty}\left\{\alpha_{mn}a_{pq}a_{kl}\lambda_{mn}^2\lambda_{pq}\cos m\theta\cos p\theta\cos k\theta.J'_m(\lambda_{mn}r)\right.$$

$$J'_p(\lambda_{pq}r)\,J_k(\lambda_{kl}r)\tanh\lambda_{mn}h$$

$$+\frac{1}{r^2}\alpha_{mn}a_{pq}a_{kl}mp\lambda_{mn}\sin m\theta.\sin p\theta.\cos k\theta.J_m(\lambda_{mn}r)J_p(\lambda_{pq}r)J_k(\lambda_{kl}r)\tanh\lambda_{mn}h$$

$$\left.-\tfrac{1}{2}\alpha_{mn}a_{pq}a_{kl}\cos m\theta\cos p\theta\cos k\theta.\lambda_{mn}^3J_m(\lambda_{mn}r)J_p(\lambda_{pq}r)J_k(\lambda_{kl}r)\tanh\lambda_{mn}h\right\}$$

$$+\ldots\ldots\qquad=0\ldots\ldots\quad(II.30)$$

The radial component r in equation (II.29) could be expanded in Dini series as

$$r=\sum_{n=1}^{\infty}F_n\,J_1(\lambda_{1n}r)$$

Pre multiplying both sides by $rJ_1(\lambda_{1n}r)$ and integrating from r=o to r=a, the value of $F_n$ is obtained as

$$F_n=\frac{2a}{(\lambda_{1n}^2a^2-1)\,J_1(\lambda_{1n}a)}$$

$$=1.4386\,a\qquad\text{for } n=1$$

Equations (II.29) and (II.30) can be re-written in another form of $J_m(\lambda_{mn}r)\cos m\theta$ terms as follows

The dynamic free surface equation (II.29)

$$-\left\{\left[\ddot{X}_d - \frac{6}{5\ell}\ddot{\xi}X_d + \frac{36}{25\ell^2}X_d(X_d\ddot{X}_d + \dot{X}_d^2)\right]\frac{2a}{(\lambda_{1n}^2a^2-1)J_1(\lambda_{1n}a)}\right\}\cos\theta J_1(\lambda_{1n}r)$$

$$+\sum_{m=o}^{\infty}\sum_{n=1}^{\infty}\left\{\dot{\alpha}_{mn} - \left[g + \ddot{\xi} - \frac{6}{5\ell}(\dot{X}_d^2 + X_d\ddot{X}_d)\right]a_{mn}\right\}\cos m\theta J_m(\lambda_{mn}\theta)$$

$$+ S(r,\theta,\alpha_{o1},\alpha_{11},\ldots,\dot{\alpha}_{o1},\dot{\alpha}_{11},\ldots,a_{o1},\ a_{11},\ldots) \quad = \quad 0 \ . \qquad \text{(II.31)}$$

Where S represents all the other nonlinear terms in equation (II.29). Consider $\alpha_{mn}$, $a_{mn}$ and their time derivatives in S as parameters and expand S in a Fourier-Bessel series:

$$S = \sum_{m=o}^{\infty}\sum_{n=1}^{\infty} S_{mn}(\alpha_{o1},\alpha_{11},\ldots\dot{\alpha}_{o1},\dot{\alpha}_{11},\ldots,a_{o1},a_{11},\ldots)\cos m\theta.J_m(\lambda_{mn}r)$$

$$\ldots\ldots \text{(II.32)}$$

where

$$S_{mn} = \frac{{}_o\int^a{}_o\int^{2\pi} S.r.\cos m\theta.J_m(\lambda_{mn}r)\,d\theta dr}{{}_o\int^a{}_o\int^{2\pi} r\cos^2 m\theta.J_m^2(\lambda_{mn}r)\,d\theta dr} \qquad \text{(II.33)}$$

substituting (II.32) in (II.31) gives

$$-\left\{\left[\ddot{X}_d - \frac{6}{5l}\ddot{\xi}X_d + \frac{36}{25l^2}X_d(X_d\ddot{X}_d + \dot{X}_d^2)\right]\frac{2a}{(\lambda_{1n}^2a^2-1)J_1(\lambda_{1n}a)}\right\}\cos\theta.J_1(\lambda_{1n}r)$$

$$+\sum_{m=o}^{\infty}\sum_{n=1}^{\infty}\left\{\dot{\alpha}_{mn} - \left[g + \ddot{\xi} - \frac{6}{5\ell}(\dot{X}_d^2 + X_d\ddot{X}_d)\right]a_{mn} + S_{mn}\right\}\cos m\theta.J_m(\lambda_{mn}r) = 0$$

$$\ldots\ldots \text{(II.34)}$$

Similarly, for equation (II.30)

$$\sum_{m=o}^{\infty}\sum_{n=1}^{\infty}\left\{\dot{a}_{mn} + (\lambda_{mn}\tanh\lambda_{mn}h)\alpha_{mn}\right\}\cos m\theta.J_m(\lambda_{mn}r)$$

$$+ H(r,\theta,\alpha_{o1},\alpha_{11},\ldots,a_{o1},a_{11},\ldots,\dot{a}_{o1},\dot{a}_{11},\ldots) = 0 \qquad \text{(II.35)}$$

Expanding H as;

$$H = \sum_{m=o}^{\infty}\sum_{n=1}^{\infty} h_{mn}(\alpha_{o1},\alpha_{11},\ldots,a_{o1},a_{11},\ldots,\dot{a}_{o1},\dot{a}_{11},\ldots)\cos m\theta.J_m(\lambda_{mn}r)$$

$$\ldots\ldots\text{(II.36)}$$

where;

$$h_{mn} = \frac{{}_o\int^a {}_o\int^{2\pi} Hr\cos m\theta.J_m(\lambda_{mn}r)d\theta dr}{{}_o\int^a {}_o\int^{2\pi} r\cos^2 m\theta.J_m^2(\lambda_{mn}r)d\theta dr} \qquad \text{(II.37)}$$

Introducing (II.36) in (II.35) results

$$\sum_{m=o}^{\infty}\sum_{n=1}^{\infty}\left\{\dot{a}_{mn} + (\lambda_{mn}\tanh\lambda_{mn}h)\alpha_{mn} + h_{mn}\right\}\cos m\theta.J_m(\lambda_{mn}\theta) = 0 \qquad \text{(II.38)}$$

The functions $\cos m\theta\, J_m(\lambda_{mn}\theta)$ in (II.34, 38) form an orthogonal set, such that their coefficients for every mode m and n constitute an equation in $\alpha_{mn}$ and $a_{mn}$. The coupling of modes appears if nonlinear terms in $\alpha_{mn}$ and $a_{mn}$ are considered.

By virtue of (II.10) the hydrodynamic pressure can be expressed in terms of the potential function in the system equations of motion as;

$$[M_o + m_{t1}]\ddot{\xi} + C_{s1}\dot{\xi} + K_{s1}\xi - \frac{6}{51}m_{t1}(X_d\ddot{X}_d + \dot{X}_d^2)$$

$$+ \rho_o{}_o\int^a {}_o\int^{2\pi}\left[\tilde{\Phi}_t - \tfrac{1}{2}\tilde{\Phi}_r^2 + \frac{1}{r^2}\tilde{\Phi}_\theta^2 + \tilde{\Phi}_z^2\right)\Big]_{z=-h} r\,d\theta.dr = K_{s1}\xi_o\cos\Omega t \qquad \text{(II.39)}$$

$$m_{t1}\ddot{X}_d + C_{s2}\dot{X}_d + K_{s2}X_d - \frac{6}{5\ell} m_{t1}\ddot{\xi} X_d + \frac{36}{25\ell^2} m_{t1} X_d(X_d\ddot{X}_d + \dot{X}_d^2)$$

$$- \rho \int_{-h}^{0}\int_{0}^{2\pi}[\tilde{\Phi}_t - \tfrac{1}{2}\tilde{\Phi}_r^2 + \frac{1}{r^2}\tilde{\Phi}_\theta^2 + \tilde{\Phi}_z^2)]_{r=a} \, a\cos\theta \, d\theta \, dz = 0 \qquad \text{(II.40)}$$

where $m_{t1}$ is the mass of the top structure with its Liquid

Considerable simplification is possible in the evaluation of the integrals in equations (II.34, 38, 39 and 40) by using the orthogonal and recurrence relations given in Appendix (A).

The problem is now described mathematically by the four equations (II.34,38,39,40) which are coupled through nonlinear terms. However, the fluid free surface equations (II.34,38) are still unbounded due to the presence of an infinite number of modes, and consequently an infinite number of equations. The order of magnitude of $\alpha_{mn}$ and $a_{mn}$ have to be known in order to decide the appropriate number of significant modes. This will limit the problem to a finite number of equations corresponding to the number of modes. In their studies of free standing waves, Penney and Price[P1] assumed that the forced waves are very nearly free waves. Skalak and Yarymovich[S8] showed the validity of that assumption and found that large amplitude surface waves can be maintained by small values of the excitation amplitude. They also developed an analysis of the orders of magnitude of $a_{mn}$ and $\alpha_{mn}$ for forced waves. In experiments performed with a circular cross section tank, Dodge, Kana and Abramson[D2] found that the (0,1) and(2,1) modes appeared as the secondary modes when the primary was the first antisymmetric mode (1,1). The mode (0,2) appeared as the secondary mode when the primary was the first symmetric mode (0,1), and so on for the other modes.

These relations can be expressed as follows.

1) Taking the first antisymmetric mode as the predominant:

$$a_{11} = O(a) \qquad \alpha_{11} = O(a)$$

$$a_{o1} = O(a^2) \qquad \alpha_{o1} = O(a^2)$$

$$a_{21} = O(a^2) \qquad \alpha_{21} = O(a^2)$$

$$a_{mn} = O(a^m) \qquad \alpha_{mn} = O(a^m)$$

2) Taking the first symmetric mode as the primary:

$$a_{o1} = O(a) \qquad \alpha_{o1} = O(a)$$

$$a_{o2} = O(a) \qquad \alpha_{o2} = O(a^2)$$

$$a_{on} = O(a^n) \qquad \alpha_{on} = O(a^n)$$

By induction the orders of magnitude of the other higher modes can be written.

## APPENDIX (A)

$$\int_0^{2\pi} \sin(m\theta).\sin(n\theta)\,d\theta = \begin{cases} \pi\,\delta_{mn} & \text{if } m \neq 0,\ n \neq 0 \\ 0 & \text{if } m \text{ or } n = 0 \end{cases} \qquad (A.1)$$

$$\int_0^{2\pi} \cos(m\theta).\cos(n\theta)\,d\theta = \begin{cases} \pi\,\delta_{mn} & \text{if } m \neq 0,\ n \neq 0 \\ 2\pi & \text{if } m = n = 0 \end{cases} \qquad (A.2)$$

where the Kroneker $\delta_{mn} = 1$ if $m = n$ or $\delta_{mn} = 0$ if $m \neq n$

$$\int_0^{2\pi} \left\{\cos\theta,\ \sin\theta,\ \cos\theta\cos\theta,\ \cos^2\theta\sin\theta,\ \sin^2\theta\cos\theta,\ \cos^3\theta,\ \sin^3\theta\right\} d\theta = 0 \qquad \ldots\ldots(A.3)$$

$$\int_0^a r\,J_o(\lambda_{om}r)\,J_o(\lambda_{on}r)\,dr = \begin{cases} 0 & m \neq n \\ \frac{a^2}{2}\,J_o^2(\lambda_{on}a) & m = n \end{cases} \qquad (A.4)$$

$$\int_0^a rJ_2(\lambda_{2m}r)\,J_2(\lambda_{2n}r)\,dr = \begin{cases} 0 & m \neq n \\ \dfrac{\lambda_{2n}^2a^2-4}{2\lambda_{2n}^2}\,J_2^2(\lambda_{2n}a) & m = n \end{cases} \qquad (A.5)$$

$$\int_0^a rJ_1(\lambda_{1m}r)J_1(\lambda_{1m}r)\,dr = \begin{cases} 0 & m \neq n \\ \dfrac{\lambda_{1n}^2a^2-1}{2\lambda_{1n}^2}\,J_1^2(\lambda_{1n}a) & m = n \end{cases} \qquad (A.6)$$

$$\int_0^a r^{m+1}\,J_m(\lambda_{mn}r)\,dr = \frac{a^{m+1}}{\lambda_{mn}}\,J_{m+1}(\lambda_{mn}a) \qquad (A.7)$$

$$\frac{d}{dX}\left\{J_m(X)/X^m\right\} = -J_{m+1}(X)/X^m \qquad (A.8)$$

$$\text{for } m = 0,\ J_o'(r) = -J_1(r)$$

$$nJ_n(r) + XJ_n'(r) = X\,J_{n-1}(r) \qquad (A.9)$$

$$J_{n-1}(r) + J_{n+1}(r) = \frac{2n}{r}\,J_n(r) \qquad (A.10)$$

$$nJ_n(r) - rJ_n'(r) = rJ_{n+1}(r) \qquad (A.11)$$

$$J_n'(r) = \tfrac{1}{2}[J_{n-1}(r) - J_{n+1}(r)] \qquad (A.12)$$

# CHAPTER III

## FLUID-STRUCTURE INTERACTION IN PURELY VERTICAL OSCILLATIONS

III.1

By assuming the container to oscillate only in the vertical direction, as shown schematically in Fig. (III.1), the governing equations of motion (II.34, 38, 39) will be considered and take the following form;

$$\dot{\alpha}_{mn} - (g + \ddot{\xi})a_{mn} + s_{mn} = 0 \qquad \text{(III.1)}$$

$$\dot{a}_{mn} + (\lambda_{mn} \tanh \lambda_{mn} h) + h_{mn} = 0 \qquad \text{(III.2)}$$

$$[M_o + m_{t1}]\ddot{\xi} + C_{s1}\dot{\xi} + K_{s1}\xi + \rho \int_0^{a} \int_0^{2\pi} [\tilde{\Phi} - \tfrac{1}{2}(\tilde{\Phi}_r^2 + \frac{1}{r^2}\tilde{\Phi}_\theta^2 + \tilde{\Phi}_z^2)] r d\theta dr$$

$$= K_{s1}\xi_o \cos\Omega t \qquad \text{(III.3)}$$

where dots refer to differentiation with respect to time, and a letter subscript (r, θ, z) denotes the partial differentiation with respect to the subscripted variable.

Only the first antisymmetric sloshing mode (m = 1, n = 1) will be considered. The functions S in equation (II.32), and H in equation (II.36) are;

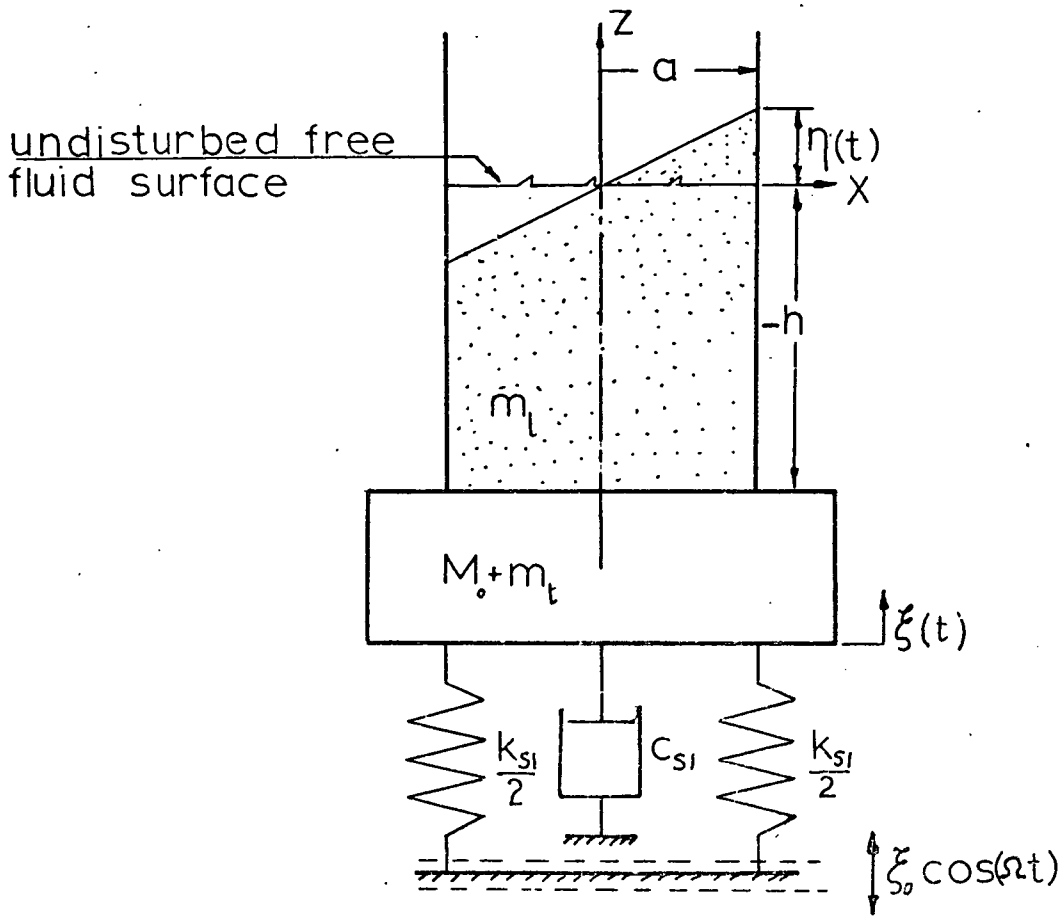


Fig(III·1) Schematic Diagram of Two Degree-of Freedom Autoparametric System.

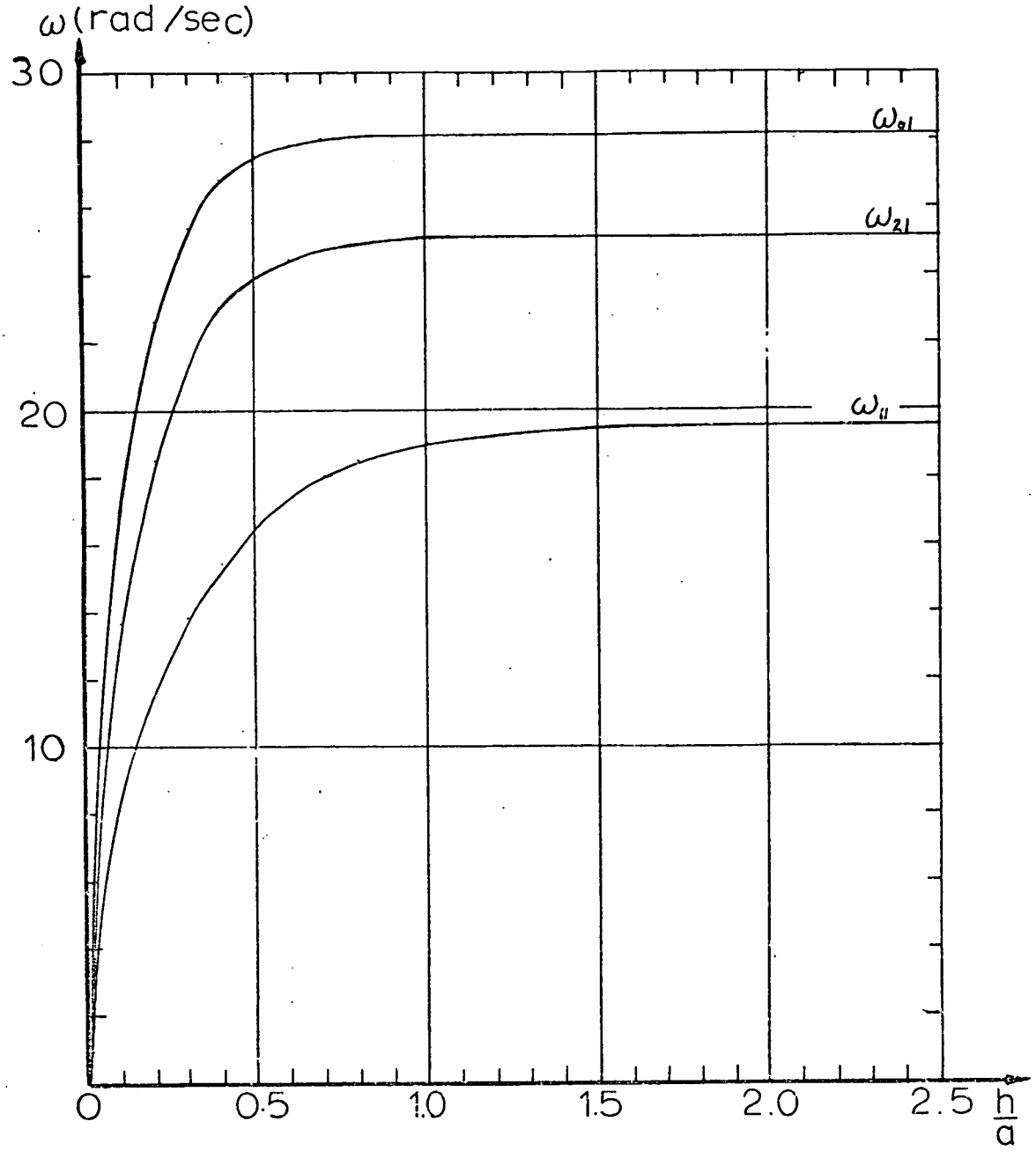


Fig.(III.2) Natural Frequencies of the Free Fluid Surface for the First Three Modes.

$$S_{11} = -\tfrac{1}{2}\alpha_{11}^2 \lambda_{11}^2 \tilde{J}_1^2(\lambda_{11}r)\cos^2\theta - \frac{1}{2r^2}\alpha_{11}^2 J_1^2(\lambda_{11}r)\sin^2\theta$$

$$-\tfrac{1}{2}\alpha_{11}^2 J_1^2(\lambda_{11}r)\cos^2\theta \tanh^2\lambda_{11}h$$

$$+\dot{\alpha}_{11} a_{11} \lambda_{11} J_1^2(\lambda_{11}r)\cos^2\theta \tanh\lambda_{11}h$$

$$-\alpha_{11}^2 a_{11}\lambda_{11}^3 J_1(\lambda_{11}r) J_1^2(\lambda_{11}r)\cos^2\theta \cdot \tanh\lambda_{11}h$$

$$-\frac{1}{r^2}\alpha_{11}^2 a_{11} \lambda_{11} J_1^3(\lambda_{11}r)\cos\theta \sin^2\theta \tanh\lambda_{11}h$$

$$-\alpha_{11}^2 a_{11}\lambda_{11}^3 J_1^3(\lambda_{11}r)\cos^3\theta \tanh\lambda_{11}h$$

$$+\tfrac{1}{2}\dot{\alpha}_{11} a_{11}^2\lambda_{11}^2 J_1^3(\lambda_{11}r)\cos^3\theta \qquad \text{(III.4)}$$

$$H_{11} = -\alpha_{11} a_{11} \lambda_{11}^2 \tilde{J}_1^2(\lambda_{11}r)\cos^2\theta - \frac{1}{r^2}\alpha_{11} a_{11} J_1^2(\lambda_{11}r)\sin^2\theta$$

$$+\alpha_{11} a_{11} \lambda_{11}^2 J_1^2(\lambda_{11}r)\cos^2\theta$$

$$-\alpha_{11} a_{11}^2 \lambda_{11}^3 J_1(\lambda_{11}r) \tilde{J}_1^2(\lambda_{11}r)\cos^3\theta \tanh\lambda_{11} h$$

$$-\frac{1}{r^2}\alpha_{11} a_{11}^2 \lambda_{11} J_1^3(\lambda_{11}r)\sin^2\theta \cos\theta \tanh\lambda_{11}h$$

$$+\tfrac{1}{2}\alpha_{11} a_{11}^2 \lambda_{11}^3 J_1^3(\lambda_{11}r)\cos^3\theta \tanh\lambda_{11}h \qquad \text{(III.5)}$$

where a prime denotes partial differentiation with respect to r.

Introducing (III.4) and (III.5) in (II.33) and (II.36) respectively and evaluating the Bessel integrals up to seven decimal figures by using the digital computer leads to,

$$s_{11} = 0.1045682\,\lambda_{11}^2\,\dot{\alpha}_{11}a_{11}^2 - 0.2810256\,\lambda_{11}^3\alpha_{11}^2 a_{11}\tanh\lambda_{11}h \qquad \text{(III.6)}$$

$$h_{11} = -\,0.122515\lambda_{11}^3\alpha_{11}a_{11}^2\,\tanh\lambda_{11}h \qquad \text{(III.7)}$$

The numerical integration of the hydrodynamic pressure in (III.3) gives;

$$F_s = -\frac{0.2020\pi\rho\alpha_{11}^2}{\cosh^2\lambda_{11}h} \qquad \text{(III.8)}$$

This means that the linear theory gives zero net force at the tank bottom. The nonlinear term of the sloshing force $F_s$ decreases rapidly as h/a increases due to the presence of $(1/\cosh^2\lambda_{11}h)$. For small fluid depths*, the fluid motion is governed by the shallow water theory in which the pressure variations are hydrostatic and hence no vertical acceleration of fluid particles takes place.

Introducing (III.6, 7) and the sloshing force term (III.8) in equations (III.1, 2, 3) gives;

$$\dot{\alpha}_{11} - (g+\ddot{\xi})a_{11} + 0.1045682\,\lambda_{11}^2\dot{\alpha}_{11}a_{11}^2 - 0.2810256\lambda_{11}^2\alpha_{11}^2 a_{11}\tanh\lambda_{11}h = 0 \qquad \text{....(III.9)}$$

$$\dot{a}_{11} + (\lambda_{11}\tanh\lambda_{11}h)\alpha_{11} - 0.122515\,\lambda_{11}^3\alpha_{11}a_{11}\tanh\lambda_{11}h = 0 \qquad \text{(III.10)}$$

$$[M_o+m_{t1}]\ddot{\xi} + C_{s1}\dot{\xi} + K_{s1}\xi - \frac{0.202\pi\rho\alpha_{11}^2}{\cosh^2\lambda_{11}h} = K_{s1}\xi_o\cos\Omega t \qquad \text{(III.11)}$$

---

* In private communication, Professor F.T. Dodge mentioned also that the term $(\dot{a}_{11})^2$ in equation (III.13) is identically zero if the forcing frequency is not in one of the critical ranges. For $\dot{a}_{11} \neq 0$ the forcing frequency must obey the relation;

$$\frac{(\lambda_{11}\tanh\lambda_{11}h)^2}{1+2\epsilon} \leqslant \Omega^2 \leqslant \frac{(\lambda_{11}\tanh\lambda_{11}h)^2}{1-2\epsilon}$$

as $h/a \to 0$ then it can be seen that $\Omega$ must approach zero like $\lambda_{11}\tanh\lambda_{11}h$. Since $\dot{a}_{11} = A\Omega\cos\Omega t$ then $(\dot{a}_{11})^2$ approaches zero like $(\lambda_{11}\tanh\lambda_{11}h)^2$ and $F_s$ approaches a finite limit rather than infinity.

Eliminating $\alpha_{11}$ and $\dot{\alpha}_{11}$ gives;

$$\ddot{a}_{11} + 2\omega_{11}\bar{\zeta}_{\ell}\dot{a}_{11} + \omega_{11}^2(1 + \frac{\ddot{\xi}}{g})a_{11} + \lambda_{11}^2 a_{11}(0.2270832a_{11}\ddot{a}_{11} + 0.5260556\dot{a}_{11}^2) = 0 \qquad \text{(III.12)}$$

$$\ddot{\xi} + 2\omega_{s1}\bar{\zeta}_{s1}\dot{\xi} + \omega_{s1}^2\xi - \frac{0.202\pi\rho}{[M_o+m_{t1}]\lambda_{11}^2 \sinh(\lambda_{11}h)}\dot{a}_{11}^2 = \omega_{s1}^2\xi_o\cos\Omega t \qquad \text{(III.13)}$$

where $\omega_{11} = \sqrt{g\lambda_{11}\tanh\lambda_{11}h}$ the first antisymmetric sloshing frequency Fig. (III.2)

$\omega_{s1} = \sqrt{\frac{K_{s1}}{[M_o+m_{t\ell}]}}$ the structure natural frequency .

$\bar{\zeta}_{\ell}$ = Damping ratio of the fluid (a damping term has been introduced in the fluid equation since it was rather difficult to consider the viscosity terms in Bernoulli's equation)

$\bar{\zeta}_{s1}$ = Damping ratio of the structure.

Equations (III.12) and (III.13) represent an autoparametric coupling case in which the term $\ddot{\xi}a_{11}$ arises linking the coordinates $\xi$ and $a_{11}$ and $\ddot{\xi}$ is an implicit function of time. If $\xi$ is directly expressed as a function of time, the two equations are reduced to (I .11 ) with $\ddot{\xi} = f(t)$ and the problem reduces to the case of liquid oscillations under parametric excitation [D2]. The present problem, however, is similar to a certain extent to the autoparametric vibration absorber studied by Haxton and Barr [H5]. The difference lies in the nature of the nonlinear term in equation (III.13) and the sign of the autoparametric term in (III.12). This similarity is of considerable help in anticipating the results of the present analysis.

It is convenient to write equations (III.12, 13) in a non-dimensional form. Referring to Struble's Analysis [S16, 17] of the simple pendulum motion under parametric excitation and to the analysis of the liquid surface oscillations under the same excitation by Dodge et al [D2], non-dimensional parameters that suit our problem can be derived;

$$\tau = \omega_{11} t \qquad \mu_1 = \frac{m_1}{M_o + m_{tl}}$$

$$\epsilon = \xi_o / a \qquad m_1 = \pi \rho a^2 h \quad \text{mass of the fluid} \qquad \text{(III.14)}$$

$$\sigma = \Omega / \omega_{11} \qquad \bar{\zeta}_i = \epsilon \zeta_i$$

$$r_{s1} = \omega_{s1} / \omega_{11}$$

$$\begin{bmatrix} a_{11} \\ \xi \end{bmatrix} = \frac{\epsilon}{\lambda_{11} \tanh \lambda_{11} h} \begin{bmatrix} A_{11} \\ Z \end{bmatrix}$$

Using (III.14) in (III.12, 13) gives;

$$\acute{A}_{11} + 2\epsilon\zeta_\ell \acute{A}_{11} + (1 + \epsilon Z'') A_{11} + \epsilon^2 A_{11} (C_1 A_{11} \acute{A}_{11} + C_2 \acute{A}_{11}^3) = 0 \qquad \text{(III.15)}$$

$$Z'' + 2\epsilon r_{s1} \zeta_{s1} Z' + r_{s1}^2 Z - \epsilon L_1 \acute{A}_{11}^2 = \epsilon f \cos \sigma \tau \qquad \text{(III.16)}$$

where:

$$C_1 = \frac{0.2270832}{\tanh^2 \lambda_{11} h}$$

$$C_2 = \frac{0.5260556}{\tanh^2 \lambda_{11} h}$$

$$L_1 = \frac{0.202\ \mu_1}{(h/a) \xi_{11}^2 . \tanh \lambda_{11} h . \sinh^2 \lambda_{11} h}$$

$$f = \frac{r_{s1}^2 \xi_{11} \tanh \lambda_{11} h}{\epsilon}$$

and prime denotes differentiation with respect to the non-dimensional time parameter $\tau$ .

In order to study the behaviour of the system at multiple sub-harmonic frequencies, it is convenient to re-write equations (III.15, 16) in the standard form devised by Bogoliuboff and Mitropolski. [B10]

$$Z'' + S_1^2\nu^2 Z = \epsilon\left\{ \epsilon^{-1}(S_1^2\nu^2 - r_{s1}^2)Z - 2r_{s1}\zeta_{s1}Z' + L_1 A_{11}'^2 + f\cos n\nu\tau \right\} \qquad \text{(III.17)}$$

$$A_{11}'' + S_2^2\nu^2 A_{11} = \epsilon\left\{ \epsilon^{-1}(S_2^2\nu^2 - 1)A_{11} - 2\zeta_\ell A_{11}' - A_{11}Z'' - \epsilon A_{11}(C_1 A_{11}A_{11}'' + C_2 A_{11}'^2) \right\} \qquad \text{....(III.18)}$$

The forcing frequency parameter $\sigma$ has been replaced by $n\nu$ where n is a number and $\nu$ is in the neighbourhood of the lowest frequency of the liquid mode, i.e. $\nu \approx 1$, $S_1 = P_1/q_1$ and $S_2 = P_2/q_2$ where $P_i$ and $q_i$ are integer numbers, $S_1$ and $S_2$ are introduced such that $\left| S_1^2\nu^2 - r_{s1}^2 \right| < \epsilon$ and $\left| S_2^2\nu^2 - 1 \right| < \epsilon$.

The solution of equations (III.17, 18) can be obtained by using the approximate asymptotic method outlined by Struble [S15]. Let the solution take the form;

$$\begin{aligned} Z &= B(\tau)\cos[r_{s1}\tau + \varphi(\tau)] + \epsilon Z_1(\tau) + \epsilon^2 Z_2(\tau) + \ldots \\ A_{11} &= A(\tau)\cos[\tau + \theta(\tau)] + \epsilon a_1(\tau) + \epsilon^2 a_2(\tau) + \ldots \end{aligned} \qquad \text{(III.19)}$$

where A, B, $\varphi$, and $\theta$ are slowly varying functions of the time parameter $\tau$, and exhibit only long period perturbations, while the additive perturbations $Z_1$, $Z_2$,.. and $a_1$, $a_2$,... depict higher harmonics of motion and are referred to as short period perturbations ( a designation borrowed from celestial mechanics [S16]). However, the

Struble method of asymptotic expansion (III.19) is carried out by the familiar process of successive approximations with certain innovations. For $\epsilon = 0$, equations (III.17, 18) will be decoupled and possess the elementary general solutions $Z = b\cos(r_{s1}\tau + \varphi)$, and $A_{11} = a\cos(\tau+\theta)$ where the amplitudes b and a are constants. For $\epsilon \neq 0$, the method is to permit slow variations in each of the amplitudes a, b and the phases $\varphi$ and $\theta$, and this determines these variations successively to increasing orders of powers of $\epsilon$ together with the additive corrections $Z_1, Z_1, \ldots$, and $a_1, a_2, \ldots$.

Substituting the expansions (III.19) in (III.17, 18) results in the equations;

$$[B'' - B(r_{s1} + \varphi')^2]\cos(r_{s1}\tau + \varphi) - [B\varphi'' + 2B'(r_{s1} + \varphi')]\sin(r_{s1}\tau + \varphi) + \epsilon Z_1'' + \ldots$$

$$+ S_1^2\nu^2 B\cos(r_{s1}\tau + \varphi) + \epsilon S_1^2\nu^2 Z_1 + \ldots$$

$$= \epsilon\left\{\epsilon^{-1}(S_1^2\nu^2 - r_{s1}^2)[B\cos(r_{s1}\tau + \varphi) + \epsilon Z_1 + \ldots]\right\}$$

$$- 2\epsilon r_{s1}\zeta_{s1}[B'\cos(r_{s1}\tau + \varphi) - B(r_{s1} + \varphi')\sin(r_{s1}\tau + \varphi) + \epsilon Z_1' + \ldots]$$

$$+ \epsilon L_1[A'^2\cos^2(\tau + \theta) - 2AA'(1 + \theta')\sin(\tau + \theta)\cos(\tau + \theta)$$

$$+ A^2(1 + \theta')^2 \sin^2(\tau + \theta)]$$

$$+ 2\epsilon^2 a_1 L_1[A' \cos(\tau + \theta) - A(1 + \theta') \sin(\tau + \theta)] + \ldots$$

$$+ \epsilon f \cos(n\nu\tau) \qquad \text{(III.20)}$$

$$[\acute{A} - A(1 + \acute{\theta})^2]\cos(\tau + \theta) - [A\acute{\theta} + 2\acute{A}(1 + \acute{\theta})]\sin(\tau + \theta) + \epsilon a_1' + \ldots$$

$$+ S_2^2 \nu^2 A\cos(\tau + \theta) + S_2^2 \nu^2 \epsilon a_1 + \ldots$$

$$= \epsilon\left\{ \epsilon^{-1}(S_2^2\nu^2 - 1)[A\cos(\tau + \theta) + \epsilon a_1 + \ldots.]\right\}$$

$$- 2\epsilon\zeta_1[\acute{A}\cos(\tau + \theta) - A(1 + \acute{\theta})\sin(\tau + \theta) + \epsilon a_1' + \ldots]$$

$$-\epsilon\left\{ A[\acute{B} - B(r_{s1} + \acute{\varphi})^2]\cos(r_{s1}\tau + \varphi)\cos(\tau + \theta)\right.$$

$$\left. - A[B\acute{\varphi} + 2\acute{B}(r_{s1} + \acute{\varphi})]\sin(r_{s1}\tau + \varphi)\cos(\tau + \theta)\right\}$$

$$-\epsilon^2\left\{ a_1[\acute{B} - B(r_{s1} + \acute{\varphi})^2]\cos(r_{s1}\tau + \varphi) - a_1[B\acute{\varphi} + 2\acute{B}(r_{s1} + \acute{\varphi})]\sin(r_{s1}\tau + \varphi)\right.$$

$$\left. + z_1' A\cos(\tau + \theta)\right\}$$

$$-\epsilon^2 C_1\left\{ A^2[\acute{A} - A(1 + \acute{\theta})^2]\cos^3(\tau + \theta) - A^2[A\acute{\theta} + 2\acute{A}(1 + \acute{\theta})]\sin(\tau + \theta)\cos^2(\tau + \theta)\right\}$$

$$-\epsilon^2 C_2\left\{ A\acute{A}^2\cos^3(\tau + \theta) - 2A^2\acute{A}(1 + \acute{\theta})\sin(\tau + \theta)\cos^2(\tau + \theta)\right.$$

$$\left. + A^3(1 + \acute{\theta})^2\cos(\tau + \theta)\sin^2(\tau + \theta)\right\} + \ldots \qquad \text{(III.21)}$$

The process is carried on by equating the coefficients of equal powers in $\epsilon$. The first equations that will be generated from the terms of order zero in $\epsilon$ are called variational equations while the other equations that come from coefficients of $\epsilon, \epsilon^2, \ldots$ are referred to as perturbational equations. At each step of the iteration process the variational equations are associated with the fundamental harmonic terms $\left\{\begin{matrix}\cos \\ \sin\end{matrix}(r_{s1}\tau + \varphi)\right\}$ and $\left\{\begin{matrix}\cos \\ \sin\end{matrix}(\tau + \theta)\right\}$ and the perturbational equations with the remaining nonresonant terms. Should a term appear which is "nearly" resonant, such as $\cos[(r_{s1} - 1)\tau + \varphi - \theta]$ for

$r_{s1} \approx 2 \pm \epsilon$, this is transferred to the variational equations. In this way all potentially resonant or nearly resonant terms which would lead to either secular terms or small divisors in the additive perturbations $Z_1$, $Z_2$,... and $a_1$, $a_2$,... are treated in the variational equations.

Since A, B, $\theta$ and $\varphi$ are slowly varying functions of time, terms involving $\acute{A}$, $\acute{B}$, $\acute{\varphi}$, $\acute{\theta}$, $\acute{A}\acute{\theta}$, and $\acute{B}\acute{\varphi}$ can be neglected. At the same time terms such as $\acute{A}$, $\acute{B}$, $\acute{\theta}$ and $\acute{\varphi}$ on the right hand side will also be ignored since they are of order $\epsilon$.

Terms of zero order of $\epsilon$ give the fundamental variational equations;

$$\left.\begin{aligned} -2r_{s1}B\acute{\varphi} &= \epsilon\left\{\epsilon^{-1}(S_1^2\nu^2 - r_{s1}^2)B\right\} \\ -2r_{s1}\acute{B} &= \epsilon\left\{2r_{s1}^2\zeta_{s1}B\right\} \\ -2A\acute{\theta} &= \epsilon\left\{\epsilon^{-1}(S_2^2\nu^2 - 1)A\right\} \\ -2\acute{A} &= \epsilon\left\{2\zeta_1 A\right\} \end{aligned}\right\} \qquad \text{(III.22)}$$

Terms of first order of $\epsilon$ give the first order perturbation equations;

$$Z_1'' + r_{s1}^2 Z_1 = 2r_{s1}^2\zeta_{s1}B\sin(r_{s1}\tau + \varphi) + \tfrac{1}{2}L_1A^2 - \tfrac{1}{2}L_1A^2\cos(2\tau + 2\theta)$$

$$+ f\cos(n\nu\tau) \qquad \text{(III.23)}$$

$$a_1'' + a_1 = 2\zeta_1 A\sin(\tau + \theta) + \tfrac{1}{2}ABr_{s1}^2\left\{\cos[(r_{s1} - 1)\tau + \varphi - \theta]\right.$$

$$\left. + \cos[(r_{s1} + 1)\tau + \varphi + \theta]\right\} \qquad \text{(III.24)}$$

In (III.23, 24) use has been made of the elementary identities;

$$\sin^2(\tau + \theta) = \tfrac{1}{2}[1 - \cos(2\tau + 2\theta)]$$

$$\cos(r_{s1}\tau + \varphi)\cos(\tau + \theta) = \tfrac{1}{2}\Big\{\cos[(r_{s1} - 1)\tau + \varphi - \theta] + \cos[(r_{s1} + 1)\tau + \varphi + \theta]\Big\}$$

The damping terms are secular terms; also some other terms give resonance at;

$$\left.\begin{aligned} r_{s1} &= 2 \text{ internal resonance} \\ n\,\nu &= r_{s1} \text{ external resonance} \end{aligned}\right\} \qquad \text{(III.25)}$$

An internal resonance condition occurs if the structure frequency is equal (or approximately equal) to twice the fluid frequency. If this condition holds, then the system will lie in the region of parametric instability if the external forcing frequency approaches $r_{s1}$ (or 2). This implies $n = 2$, $s_1 = 2$, and $s_2 = 1$.

Removing all secular terms in (III.23,24) to (III.22) and keeping non-resonant terms results in

$$\left.\begin{aligned} Z_1'' + r_{s1}^2 Z_1 &= \tfrac{1}{2} L_1 A^2 \\ a_1'' + a_1 &= \tfrac{1}{2} ABr_{s1}^2 \cos[(r_{s1}+1)\tau + \varphi + \theta] \end{aligned}\right\} \qquad \text{(III.26)}$$

The steady state solutions of these equations are;

$$\left.\begin{aligned} Z_1 &= \frac{L_1}{8} A^2 \\ a_1 &= \frac{AB}{4} \cos(3\tau + \varphi + \theta) \end{aligned}\right\} \qquad \text{(III.27)}$$

Now introducing the removed terms from (III.23, 24) to (III.22) the variational equations take the form;

$$\left.\begin{aligned}
-4B\dot{\varphi} &= \epsilon\left\{\bar{\epsilon}^{-1}(S_1^2\nu^2 - r_{s1}^2)B - \tfrac{1}{2}L_1A^2\cos(2\theta-\varphi) + f\cos\varphi\right\}\\
-4\dot{B} &= \epsilon\left\{8\zeta_{s1}B + \tfrac{1}{2}L_1A^2\sin(2\theta-\varphi) + f\sin\varphi\right\}\\
-2A\dot{\theta} &= \epsilon\left\{\bar{\epsilon}^{-1}(S_2^2\nu^2 - 1)A + 2AB\cos(2\theta-\varphi)\right\}\\
-2\dot{A} &= \epsilon\left\{2\zeta_\ell A + 2AB\sin(2\theta-\varphi)\right\}
\end{aligned}\right\} \qquad \text{(III.28)}$$

In order to write (III.28) in a more concise form, the following parameters will be introduced;

$$\left.\begin{aligned}
&\tau = 4T/\epsilon\sqrt{f} \qquad && \gamma = (1-\nu^2)/\epsilon\sqrt{f}\\
&\begin{Bmatrix}A\\B\end{Bmatrix} = \sqrt{f}\begin{Bmatrix}b_1\\b_2\end{Bmatrix} && \eta_{s1} = \frac{8\zeta_{s1}}{\sqrt{f}}\\
&S_1 = 2 && \eta_\ell = \frac{2\zeta_\ell}{\sqrt{f}}\\
&S_2 = 1
\end{aligned}\right\} \qquad \text{(III.29)}$$

Equations (III.28) become;

$$\left.\begin{aligned}
b_2\dot{\varphi} &= 4\gamma b_2 + \tfrac{1}{2}L_1b_1^2\cos(2\theta-\varphi) - \cos\varphi\\
\dot{b}_2 &= -\eta_{s1}b_2 - \tfrac{1}{2}L_1b_1^2\sin(2\theta-\varphi) - \sin\varphi\\
b_1\dot{\theta} &= 2\gamma b_1 - 4b_1b_2\cos(2\theta-\varphi)\\
\dot{b}_1 &= -2\eta_\ell b_1 - 4b_1b_2\sin(2\theta-\varphi)
\end{aligned}\right\} \qquad \text{(III.30)}$$

where a dot refers to differentiation with respect to T.

The steady state solution of (III.30) can be obtained by setting the left hand side to zero. The solution of the resulting algebraic equations is,

$$|b_2| = \tfrac{1}{2}\sqrt{\gamma^2 + \eta_\ell^2} \tag{III.31}$$

$$b_1^2 = \frac{1}{L_1}\left\{ -4\gamma^2 + \eta_\ell \eta_{s1} \pm \sqrt{4 - \gamma^2(\eta_{s1} + 4\eta_\ell)^2} \right\} \tag{III.32}$$

There is another solution given by $b_1 = 0$ and

$$b_2 = \frac{1}{\sqrt{16\gamma^2 + \eta_{s1}^2}} \tag{III.33}$$

Solution (III.31) exhibits the characteristics of the auto-parametric vibration absorber [H5] while the fluid response given by (III.32) is different from the absorber mass response of reference [H5], the difference lies in the sign of the first two terms. This difference changes the picture of the response curves as shown in Figs. (III.3, 4). Examining these results shows unrealistic values for the fluid amplitude especially at n = 1. This means that the second order solution is not adequate enough to predict the response of the system, and recourse must be made to consider third order terms in $\epsilon^2$.

## III.2 Third Order Solution

Considering terms of second order in $\epsilon^2$ in (III.20, 21) gives the second order perturbation equations,

$$\left.\begin{aligned} z_2'' + r_{s1}^2 z_2 &= -2r_{s1}\zeta_{s1} z_1' - 2a_1 L_1 A_1 \sin(\tau + \theta) \\ a_2'' + a_2 &= -2\zeta_\ell a_1' + a_1 B r_{s1} \cos(r_{s1}\tau + \varphi) + C_1 A^3 \cos^3(\tau + \theta) \\ &\quad - C_2 A^3 \cos(\tau + \theta)\sin^2(\tau + \theta) \end{aligned}\right\} \tag{III.34}$$

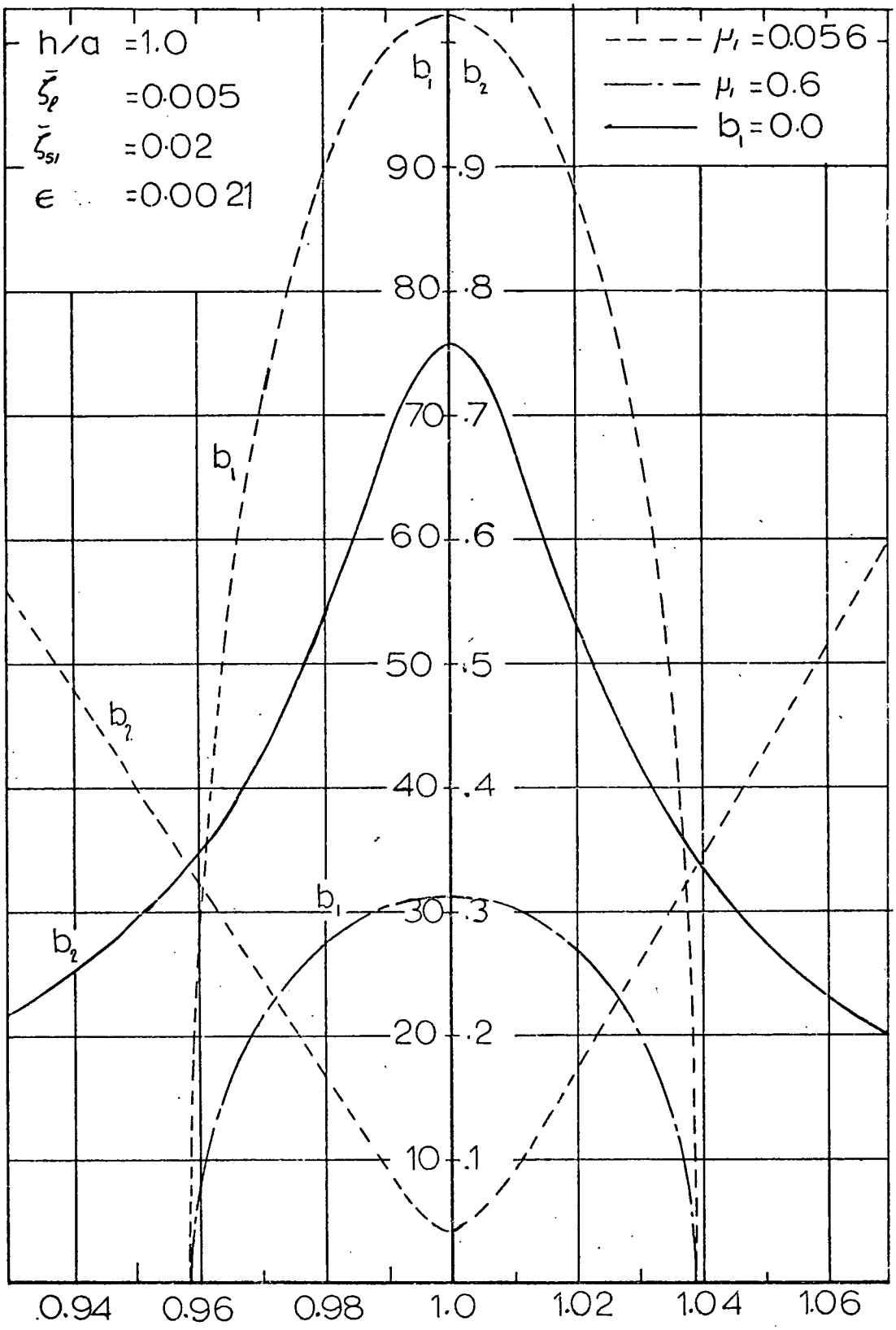


Fig.(III.3) Fluid and Structure Amplitude Responses Under Parametric Excitation, 2nd order solution

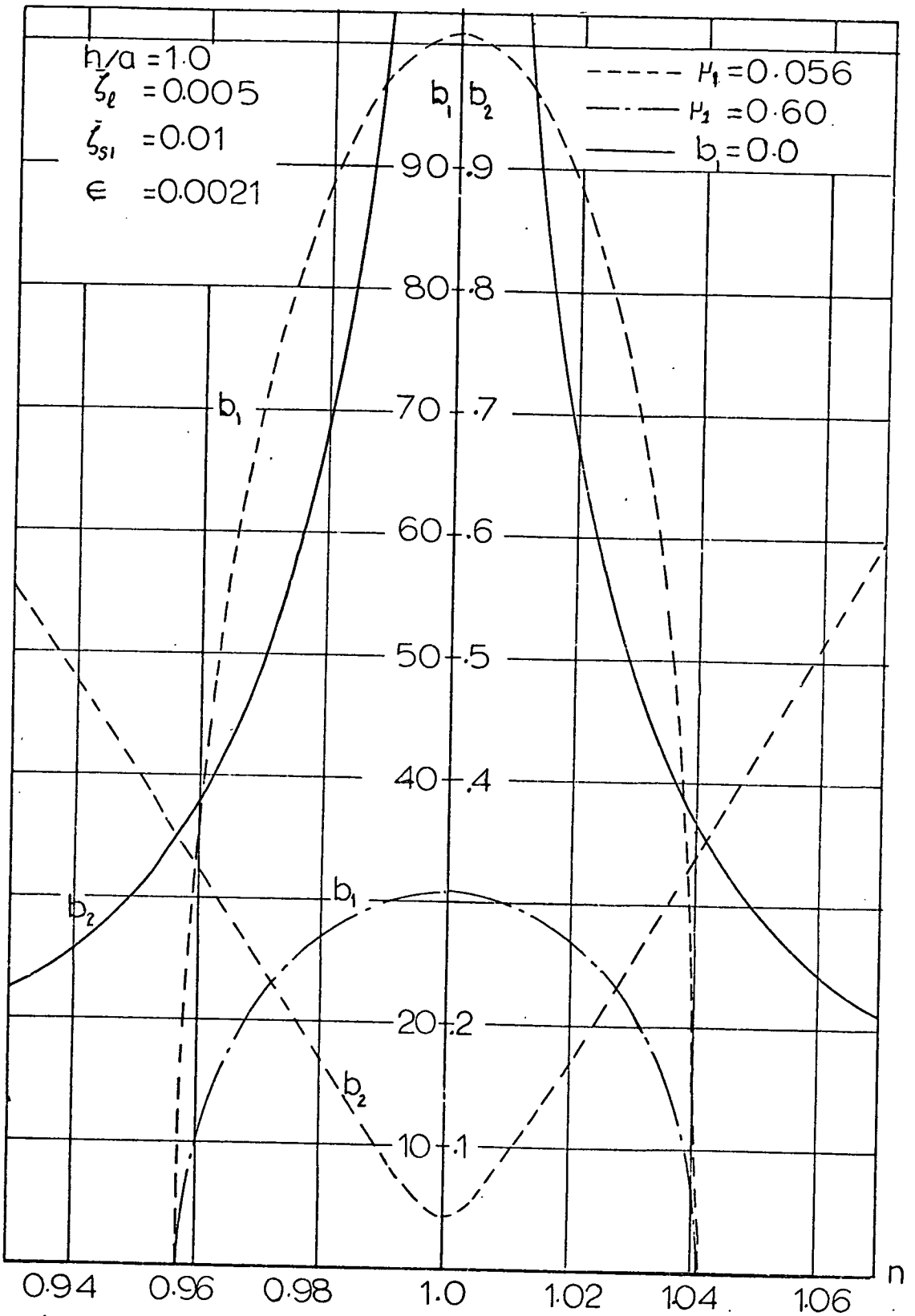


Fig(III.4) Fluid and Structure Amplitude Responses Under Pure Vertical Excitation.

Invoking the solutions of $a_1$ and $Z_1$ (III.27), the equations (III.29) take the form;

$$Z_2'' + r_{s1}^2 Z_2 = -\frac{L_1 A^2 B}{4}\left[\sin(4\tau + \varphi - 2\theta) - \sin(2\tau + \varphi)\right]$$

$$a_2'' + a_2 = \frac{3}{2}\zeta_\ell AB\sin(2\tau + \varphi + \theta) + \frac{r_{s1}}{8} AB^2\left\{\cos[(r_{s1} + 3)\tau + \theta + 2\varphi]\right.$$
$$\left. + \cos[(3 - r_{s1})\tau + \theta]\right\} + \frac{A^3}{4}\left\{C_1[\cos(2\tau + 3\theta) + 3\cos(t + \theta)]\right.$$
$$\left. - C_2[\cos(\tau + \theta) - \cos(3\tau + 3\theta)]\right\} \qquad .....(III.35)$$

The following relations have been used in (III.30)

$$\sin(\tau + \theta)\cos(3\tau + \varphi + \theta) = \tfrac{1}{2}\left\{\sin(4\tau + \varphi + 2\theta) - \sin(2\tau + \varphi)\right\}$$

$$\cos^3(\tau + \theta) = \tfrac{1}{4}[\cos(3\tau + 3\theta) + 3\cos(\tau + \theta)]$$

Equations (III.30) show that resonance occurs if;

$$r_{s1} = 2, \quad \text{or } r_{s1} = 4$$

Removing all resonance terms corresponding to $r_{s1} = 2$ in (III.35) and adding them to the variational equations (III.28) results in the following equations;

$$-4B\dot{\varphi} = \epsilon\left\{\epsilon^{-1}(S_1^2\nu^2 - r_{s1}^2)B - \tfrac{1}{2}L_1A^2\cos(2\theta - \varphi) + f\cos\varphi\right\}$$

$$-4\dot{B} = \epsilon\left\{8\zeta_{s1}B + \tfrac{1}{2}L_1A^2\sin(2\theta - \varphi) + f\sin\varphi\right\}$$
$$+ \epsilon^2\frac{L_1}{4}A^2B$$

$$
\begin{aligned}
-2A\dot{\theta} &= \epsilon\left\{\epsilon^{-1}(S_2^2\nu^2 - 1)A + 2AB\cos(2\theta - \varphi)\right\} \\
&\quad + \epsilon^2\left\{\tfrac{1}{4}AB^2 + \tfrac{1}{4}(3C_1 - C_2)A^3\right\} \qquad \text{(III.36)} \\
-2\dot{A} &= \epsilon\left\{2\zeta_\ell A + 2AB\sin(2\theta - \varphi)\right\}
\end{aligned}
$$

Using the same parameters of (III.29), equations (III.36) become;

$$
\left.
\begin{aligned}
b_2\dot{\varphi} &= 4\gamma b_2 + \tfrac{1}{2}L_1 b_1^2\cos(2\theta - \varphi) - \cos\varphi \\
\dot{b}_2 &= -\eta_{s1}b_2 - \tfrac{1}{2}L_1 b_1^2\sin(2\theta - \varphi) - \sin\varphi \\
&\quad - \delta_2 b_1^2 b_2 \\
b_1\dot{\theta} &= 2\gamma b_1 - 4b_1 b_2\cos(2\theta - \varphi) - \delta_1 b_1 b_2^2 - C_{12}b_1^3 \\
\dot{b}_1 &= -2\eta_\ell b_1 - 4b_1 b_2\sin(2\theta - \varphi)
\end{aligned}
\right\} \qquad \text{(III.37)}
$$

where

$$
\delta_1 = \frac{\epsilon\sqrt{f}}{4}
$$

$$
\delta_2 = \frac{\epsilon L_1\sqrt{f}}{4}
$$

$$
C_{12} = \frac{(3C_1 - C_2)}{4}\epsilon\sqrt{f}
$$

It seems rather laborious to obtain an analytic steady-state solution for (III.37) due to the presence of cubic terms. However, the term $\delta_2 b_1^2 b_2$ can be dropped since $\delta_2$ is very small. Moreover an attempt was made to investigate the influence of $\delta_1 b_1 b_2^2$ without considering $C_{12}b_1^3$, and it was found that that term has a negligible effect since the resulting solution was nearly similar to the solution (III.30, 31). Previous theories [D2, S10] showed that the fluid

amplitude can be obtained more accurately by considering third order terms in $b_1^3$. Accordingly the term $C_{12}b_1^3$ will be considered.

The steady state solution is given in the form;

$$b_2^2 = \frac{1}{16}\left[4(\gamma^2 + \eta_\ell^2) - 4C_{12}\gamma b_1^2 + C_{12}^2 b_1^4\right] \tag{III.38}$$

and $b_1$ is given by solving the quartic equation in $b_1^2$

$$A_5 b_1^8 + A_4 b_1^6 + A_3 b_1^4 + A_2 b_1^2 + A_1 = 0 \tag{III.39}$$

where

$$A_5 = 0.0625\ C_{12}^4(16\gamma^2 + \eta_{s1}^2) - \gamma L_1 C_{12}^3 + 0.25 L_1^2 C_{12}^2$$

$$A_4 = -\ 0.5\gamma C_1^3(16\gamma^2 + \eta_{s1}^2) + L_1 C_{12}^2(6\gamma^2 - 0.5\,\eta_\ell \eta_{s1}) - \gamma C_{12} L_1^2$$

$$A_3 = \tfrac{1}{2}\ C_{12}^2(16\gamma^2 + \eta_{s1}^2)(3\gamma^2 + \eta_\ell^2) - 4L_1 C_{12}\gamma(3\gamma^2 + \eta_\ell^2) + 2\eta_\ell \eta_{s1} L_1 C_{12}\gamma$$

$$+ L_1^2(\gamma^2 + \eta_\ell^2) - C_{12}^2$$

$$A_2 = -\ 2C_{12}\gamma(\gamma^2 + \eta_\ell^2)(16\gamma^2 + \eta_{s1}^2) + 2L_1(\gamma^2 + \eta_\ell^2)(4\gamma^2 - \eta_\ell \eta_{s1})$$

$$+ 4C_{12}\gamma$$

$$A_1 = (\gamma^2 + \eta_\ell^2)\left[16\gamma^2 + \eta_{s1}^2)(\gamma^2 + \eta_\ell^2) - 4\right]$$

Numerical solution of (III.39) are obtained by using the IBM Fortran Subroutine CDPOLR (Roots of a Polynomial with Complex Coefficients). Shown in Figs. (III.5 - 10) are the steady-state solutions for two fluid depth ratios h/a = 1 and 2, different values

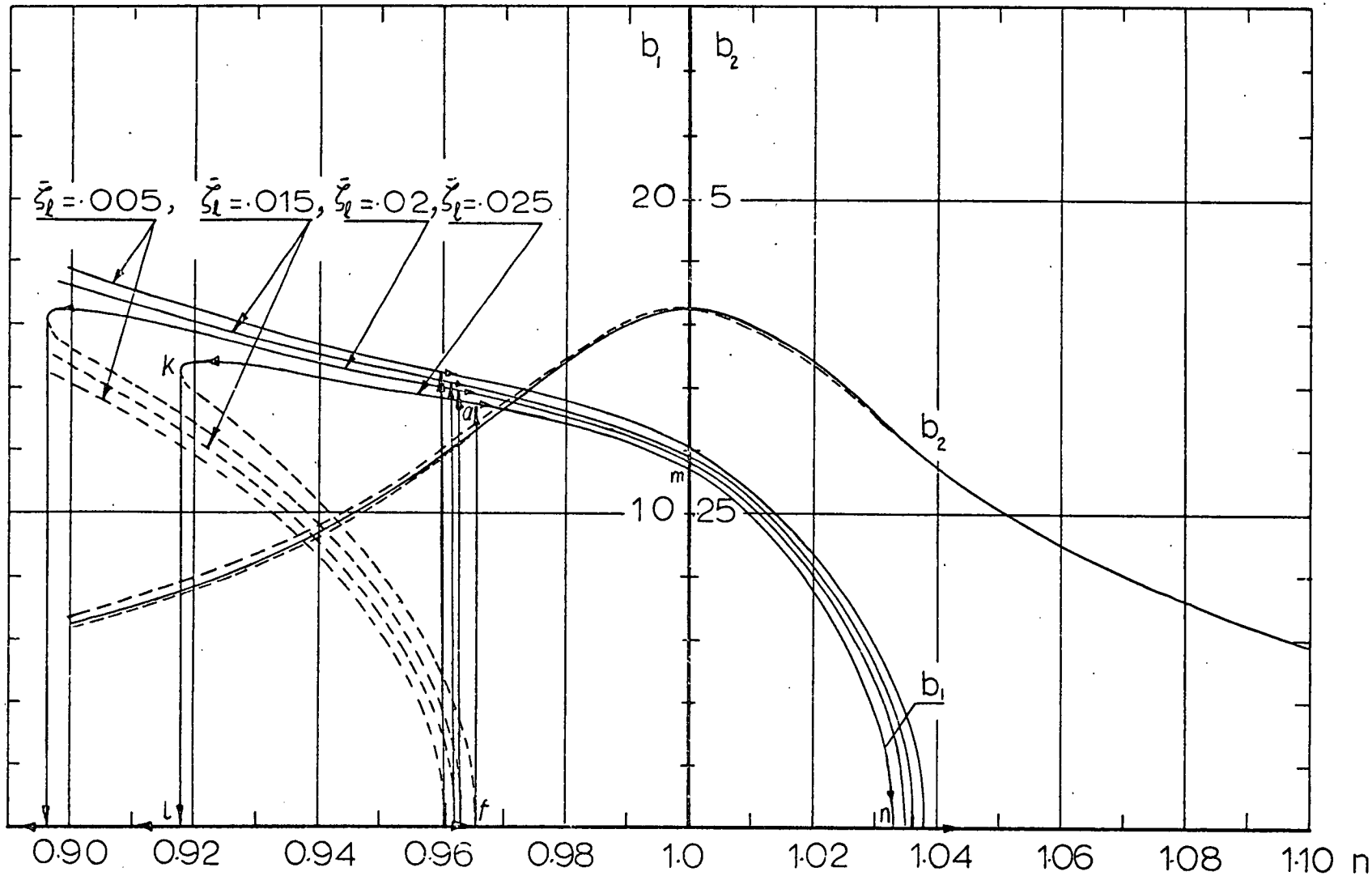


Fig.(III. 5) Response of Two Mode Interaction Under Parametric Excitation, $r_{s1} = 2.0$, $h/a = 1.0$, $\epsilon = .0025$, $\bar{\zeta}_{s1} = .04$

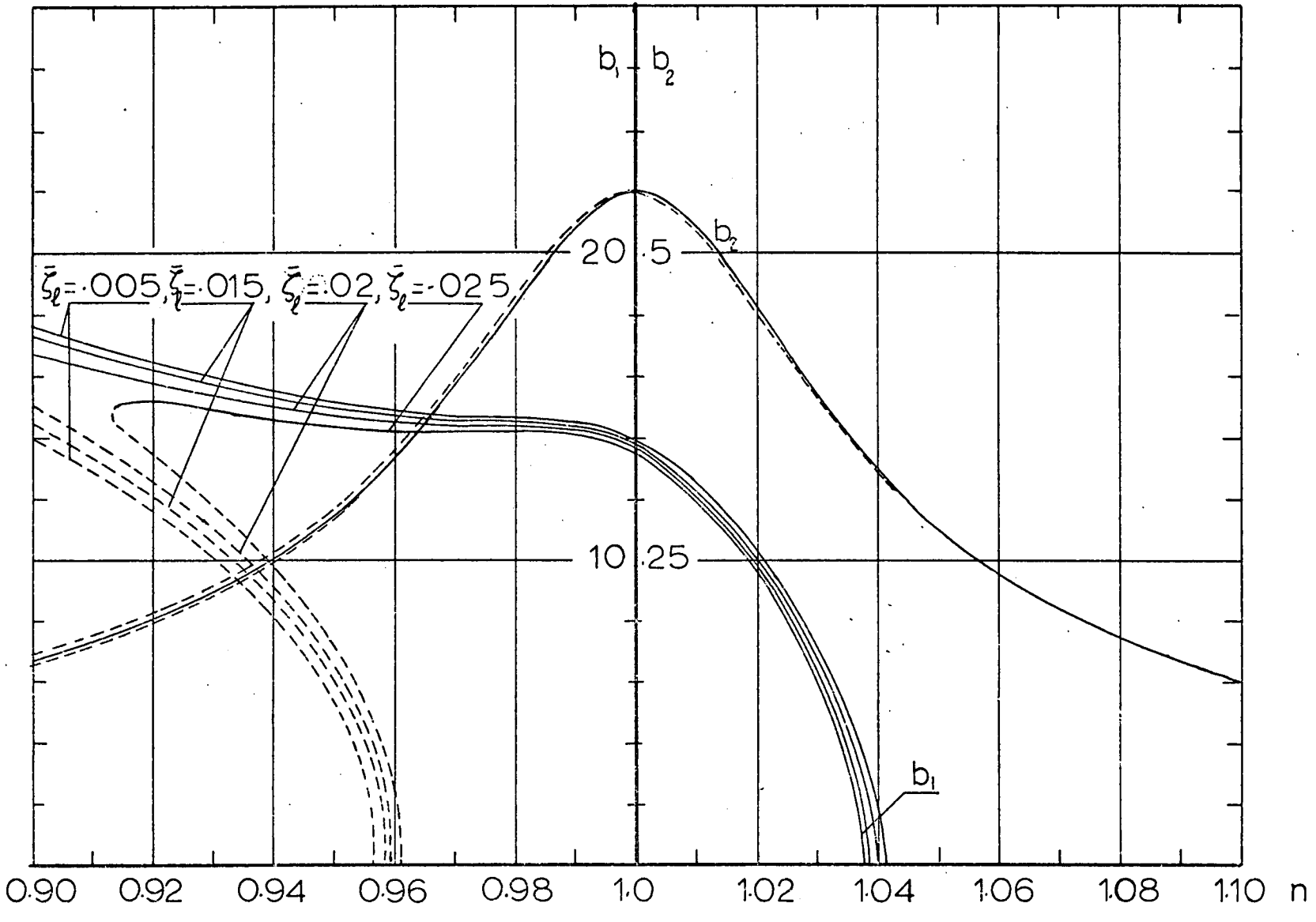


Fig.(III·6) Response of Two Mode Interaction under Parametric Excitation, r=2., h/a=1·0, e=·0025, $\bar{\zeta}_{s1}$=·03

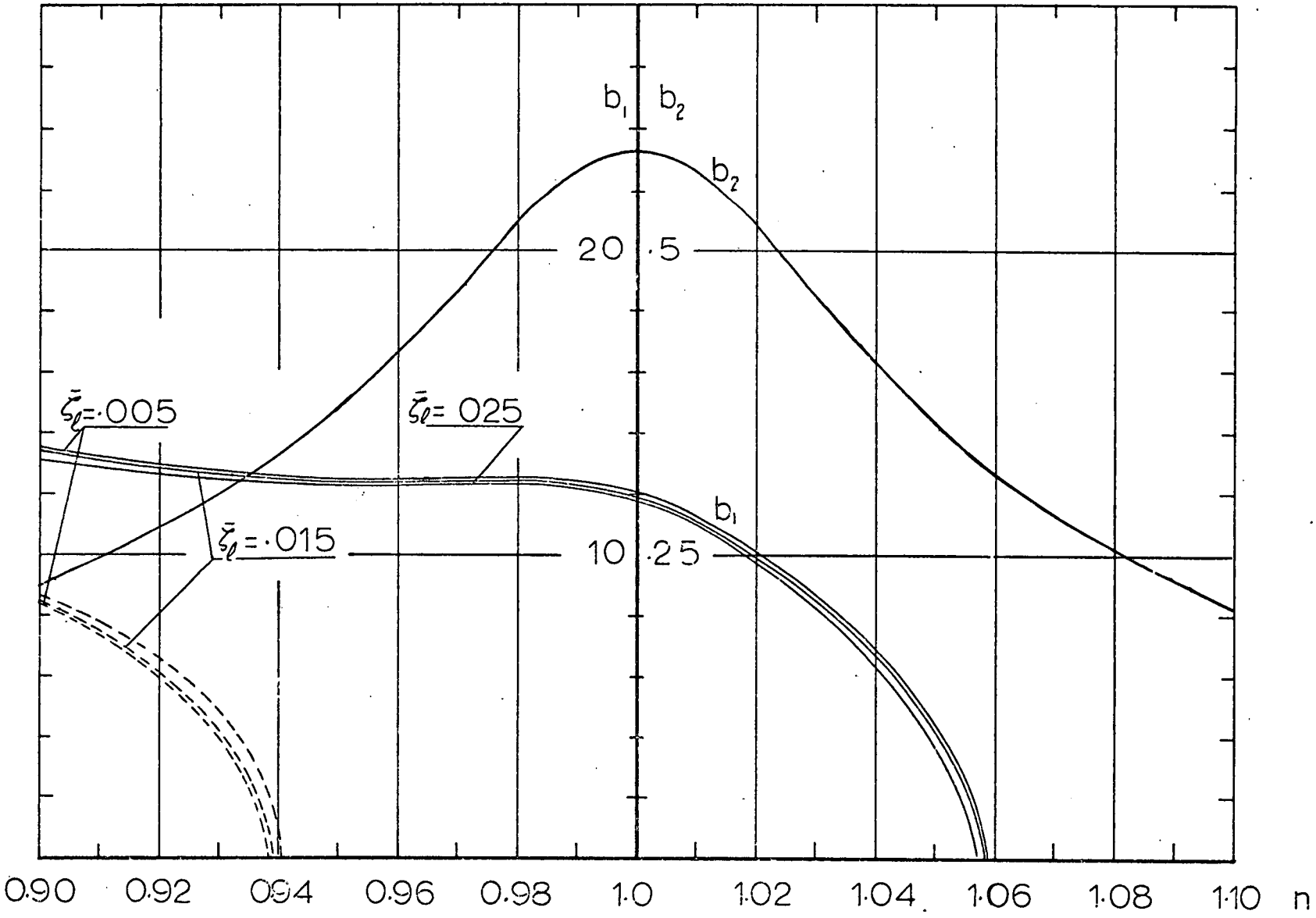


Fig(III·7) Response of Two Mode Interaction under Parametric Excitation, $r_{s1}$ = 2·0, h/a = 1·0, $\epsilon$ = ·005, $\bar{\zeta}_{s1}$ = ·04

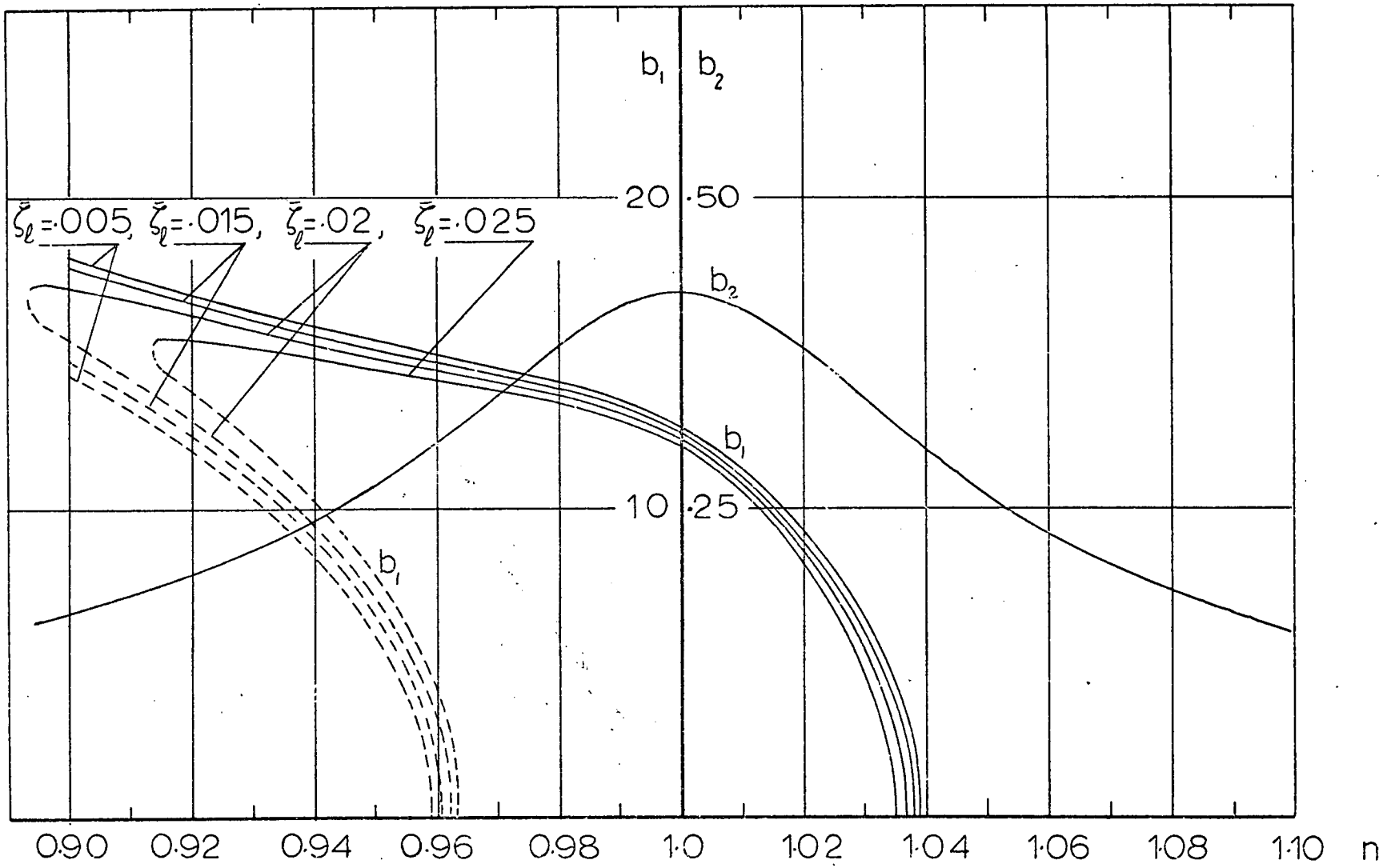


Fig(III. 8 ) Response of Two Mode Interaction under Parametric Excitation, $r_{s1} = 2.0$, $h/a = 2.0$, $\epsilon = .0025$, $\bar{\zeta}_{s1} = .04$

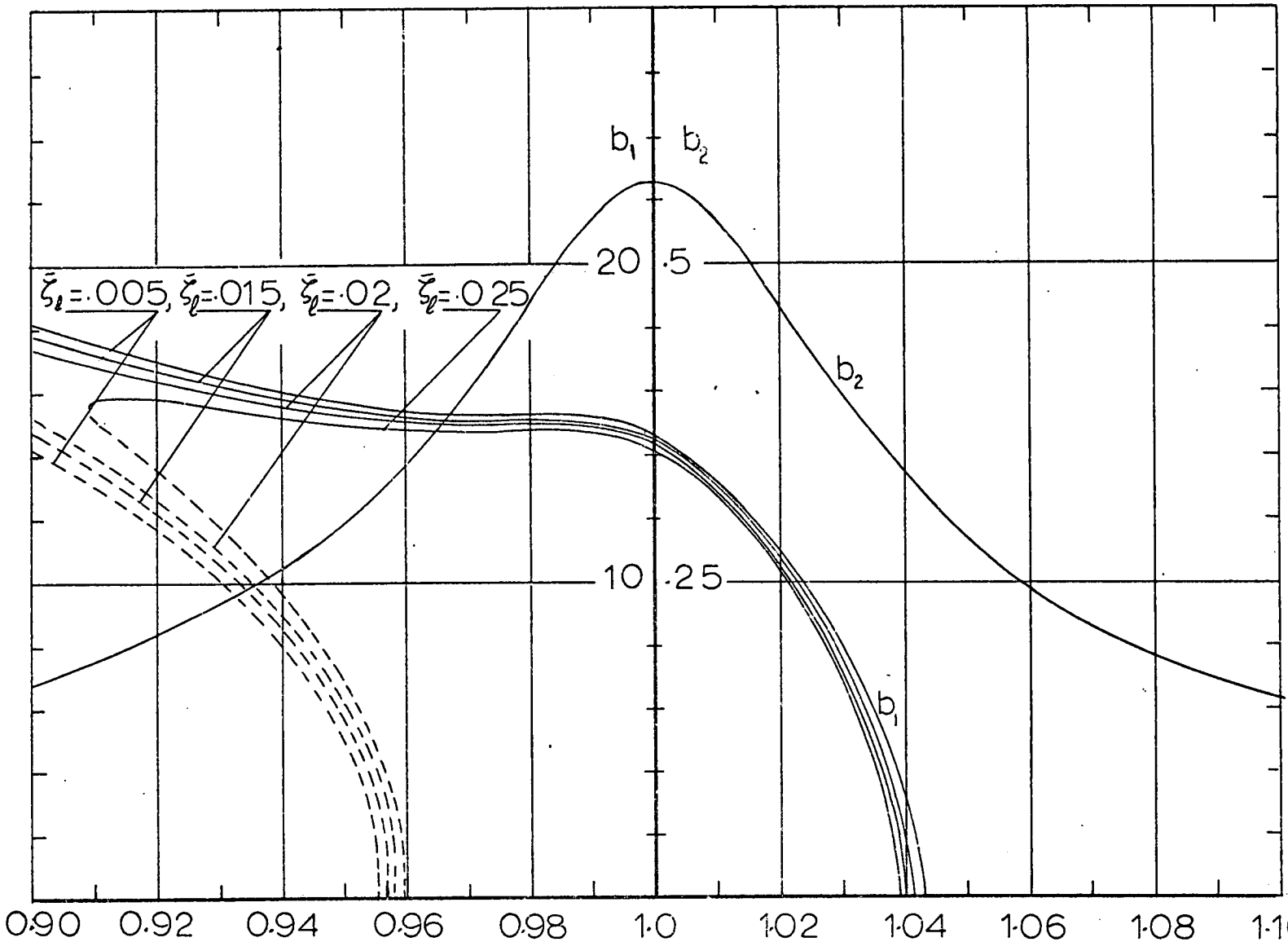


Fig.(III·9) Response of Two Mode Interaction under Parametric Excitation, r = 2·0, h/a = 2·0, ϵ = ·0025, $\bar{\zeta}_{s1}$ = ·03

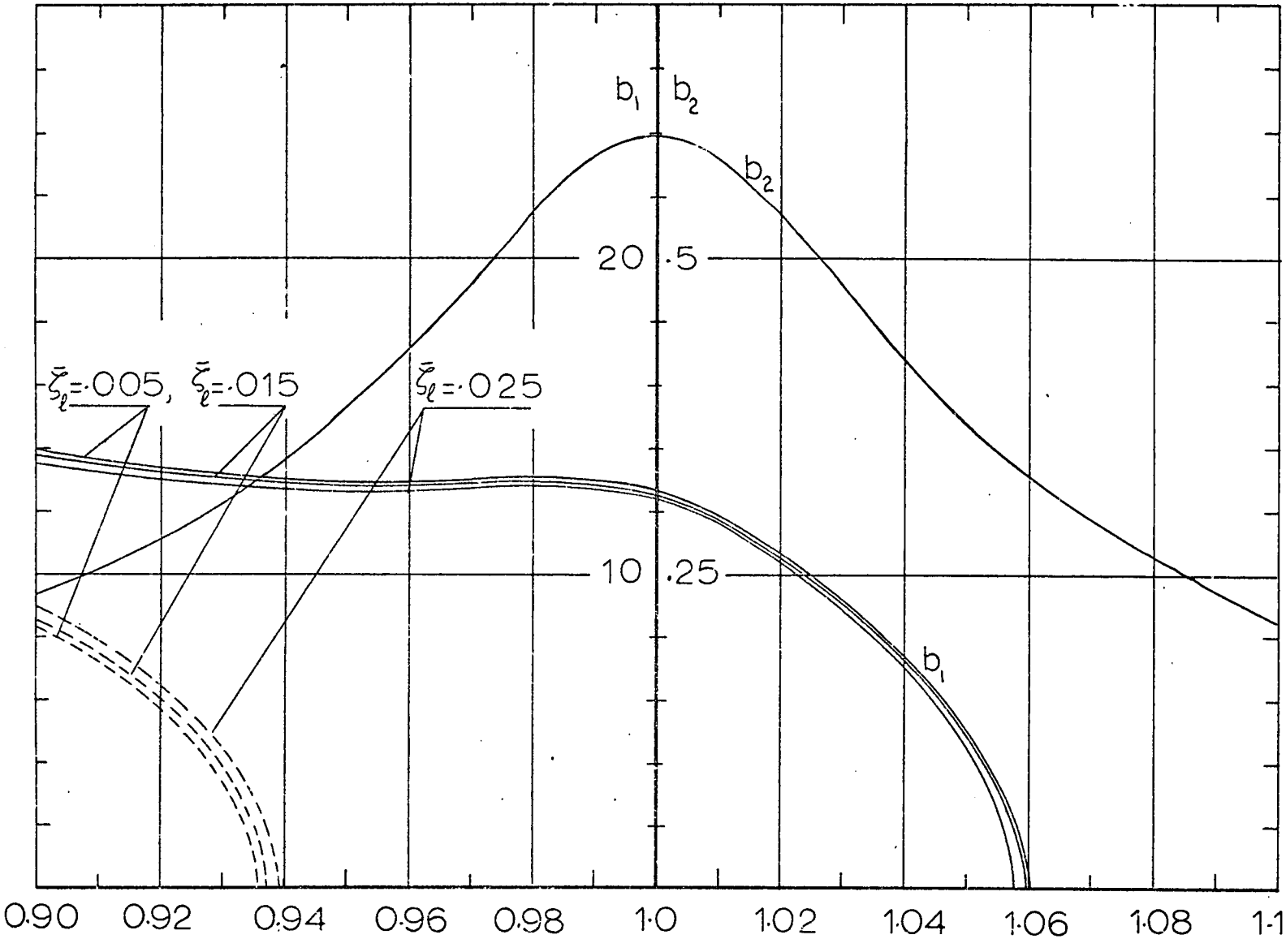


Fig(III·10) Response of Two Mode Interaction under Parametric Excitation, $r_{s1}$= 2·0, h/a = 2·0, $\epsilon$ = ·005, $\bar{\zeta}_s$ = ·040

of $\bar{\zeta}_\ell$ and $\bar{\zeta}_{s1}$, and two values of the excitation amplitude parameter $\epsilon = 0.0025$ and $0.005$. It can be noticed that there are two real solutions for $b_1$, one is given by the dotted curve kf and the other is indicated by the full curve kmn in Fig. (III.5). Only the latter solution kmn, is observed experimentally. Hence the dotted curve of $b_1$ must be unstable. It can be seen that this curve is bounded by two vertical tangents where $\frac{db1}{dn} = \infty$, one is at $b_1 = 0$ (point f) and the other at the collapse amplitude defined by point k. From Figs. (III.5-10) it can be concluded that the collapse amplitude is governed mainly by the fluid damping ratio $\bar{\zeta}_\ell$ and the excitation amplitude $\bar{\zeta}_0$ (or $\epsilon$).

It is seen also that when the forcing frequency is increased from "1" to "f" the fluid amplitude remains identically zero; it then jumps from "f" to "a" and follows the continuous curve amn. With decreasing forcing frequency the fluid response follows the curve nmak until the collapse amplitude is reached (point k). In this particular case the behaviour of the fluid response is typical of a nonlinear soft system.

In connection with the response of the main mass, it is seen that there is a remarkable difference between the two solutions (III.31, 38). While the solution (III.31) gives a suppression effect to the motion of the main mass, the cubic solution (III.38) brings it back up to the linear solution level (III.33) as shown in Fig. (III.5). To clarify that apparent contradiction,

consider conditions at resonance ($\gamma = 0.0$), assuming the liquid is inviscid, ($\bar{\zeta}_\ell = 0.0$) and ignoring the vertical sloshing effect ($L_1 = 0.0$). In this case the three solutions of the main mass are:

$b_2 = 0.0$ (i) from the quadratic solution (III.31)

$b_2 = \pm 1/\eta_{s1}$ (ii) from the linear resonance solution (III.33)

$b_2 = \pm \frac{1}{4} c_{12} b_1^2$ (iii) from the cubic solution (III.38)

$b_1$ can be obtained by solving (III.39) after inserting the relevant coefficients, it gives:

$$\frac{c_{12}^4 \eta_{s1}^2 b_1^8}{16} - c_{12}^2 b_1^4 = 0$$

This equation has the solutions;

$$b_1^4 = 0 \quad \text{or} \quad b_1^4 = \frac{16}{c_{12}^2 \eta_{s1}^2}$$

Substituting the second solution in (iii) gives:

$$b_2 = \pm \frac{1}{\eta_{s1}}$$

which coincides with the linear resonance solution (ii).

This implies that if the liquid free surface does not contribute any vertical force the structure response would be similar to that of a single degree of freedom system. The amplitude response curves $b_2$ shown in Figs. (III.5-10) indicate that the liquid sloshing effect on the main mass is very tiny and disappears when h/a increases. The liquid sloshing generates horizontal forces which are reacted by the vertical guides to the tank motion. These forces

are significant when the container is released to horizontal motion, and such a situation will be investigated in Chapters (IV,V).

In the present case, however, the effects of the cubic terms in $\epsilon^2$ in the governing equations of motion are very important in defining the characteristics of the system properly. Moreover, the coupling between the liquid motion and the structure is so weak that it can be imagined that the two equations (III.15, 16) are decoupled in the sense that the liquid is subjected to a direct parametric excitation Z which is the solution of the linear equation (III.16) if $L_1$ were equated to zero.

## III.3 Stability of the Steady-State Solutions

The stability of the steady-state solutions of equations (III.30) or (III.37) could be investigated by imposing a small perturbation from these solutions and examining the subsequent motion. If the motion following the perturbation decreases with time, the solution is called stable, if the motion increases with time, the solution is unstable. The steady-state solution of (III.30) or (III.37) will be denoted by the superscript (0). Let

$$\begin{aligned} b_1 &= b_1^{(0)} + \delta_1 e^{\lambda T} & \theta &= \theta^{(0)} + \delta_3 e^{\lambda T} \\ b_2 &= b_2^{(0)} + \delta_2 e^{\lambda T} & \varphi &= \varphi^{(0)} + \delta_4 e^{\lambda T} \end{aligned} \qquad \text{(III.40)}$$

where $\delta_i$ are assumed to be small. Stable solutions correspond to the values of $\lambda$ with a negative real part, while positive values indicate unstable motion. Introducing (III.40) in (III.30) or (III.37), neglecting products of $\delta_i$ leads to the following set of homogeneous algebraic equations.

$$\begin{bmatrix} D_{11}-\lambda & D_{12} & D_{13} & D_{14} \\ D_{21} & D_{22}-\lambda & D_{23} & D_{24} \\ D_{31} & D_{32} & D_{33}-\lambda & D_{34} \\ D_{41} & D_{42} & D_{43} & D_{44}-\lambda \end{bmatrix} \begin{Bmatrix} \delta_1 \\ \delta_2 \\ \delta_3 \\ \delta_4 \end{Bmatrix} = \begin{Bmatrix} 0 \\ 0 \\ 0 \\ 0 \end{Bmatrix} \qquad \text{(III.41)}$$

where $D_{ij}$ are the derivatives of $\dot{b}_1$, $\dot{b}_2$, $\dot{\theta}$, and $\dot{\varphi}$ of (III.30) or (III.37) with respect to $b_1$, $b_2$, $\theta$ and $\varphi$ respectively and are given in Appendix (III.A).

Equations (III.41) are homogeneous in $\delta_i$ and nontrivial solution will exist only if the determinant of the coefficients is zero. Expanding the determinant gives;

$$A_4\lambda^4 + A_3\lambda^3 + A_2\lambda^2 + A_1\lambda + A_0 = 0 \qquad \text{(III.42)}$$

the coefficient $A_i$ corresponding to equations (III.30) and (III.37) are given in Appendix (III.B).

The question of stability reduces to an examination of the roots of (III.42). The values of the roots of (III.42) are dependent upon the physical properties of the system and the detuning parameter $\gamma$. So for a particular system configuration the behaviour of the roots is dependent on $\gamma$ only. The location of these roots in the $\lambda$ plane as $\gamma$ is changing gives a direct measure of the degree of stability in the system. This method is powerful only when the characteristic equation is of low order, as a direct analytical solution for a higher order equation is laborious. In many cases it is sufficient to know whether or not the roots have a negative real part. A necessary and sufficient condition that the equation (III.42) has only

roots with negative real part is that $A_i > 0$ and all the Hurwitz determinants $H_i$ should also be positive [R6];

$$H_1 = A_1$$

$$H_2 = \begin{vmatrix} A_1 & A_0 \\ A_3 & A_2 \end{vmatrix} \quad , \quad H_3 = \begin{vmatrix} A_1 & A_0 & 0 \\ A_3 & A_2 & A_1 \\ 0 & A_4 & A_3 \end{vmatrix} \qquad \text{(III.43)}$$

Inserting solutions (III.31, 32) in the coefficients $A_i$ given in Appendix (III.B) and $H_i$, and evaluating their numerical values shows that $A_0$ and $A_3$ are always positive while $A_1$, $A_2$, $H_2$ and $H_3$ are negative. This implies that the steady-state solutions (III.31-32) are unstable in the frequency range spanned by the response of $b_1$.

In connection with the third order steady-state solutions, the stability test is performed by inserting numerical values of the two solutions indicated by the dotted and full curves in Fig. (III.5-10) One of these solutions (the dotted one) is always unstable and the other solution (full curve $b_1$) is stable except at the regions in the neighbourhood of its terminals where collapse occurs.

## III.4 Conclusions

The response of a structure system containing a liquid subjected to parametric excitation has been investigated theoretically. It has been found that the second order perturbation solution (in $\epsilon$) was not adequate enough to predict the response of the system. Third order terms (in $\epsilon^2$) were considered and the corresponding solution showed an essential difference from the second order solution. Unlike the response of the autoparametric vibration absorber [H5], the

fluid free surface sloshing forces do not act with a significant absorber effect in the vertical direction and consequently the response of the main mass is identically a linear resonance single degree of freedom system.

Because the linear theory gives zero sloshing force in the vertical direction and predicts higher forces in the lateral direction, it is anticipated that the fluid structure coupling will be more significant if the lateral constraints are released. This case will be studied in the next Chapter.

## APPENDIX (III.A)

Values of $D_{ij}$ in (III.41)

$$D_{11} = 0$$

$$D_{12} = 2\eta_\ell \, b_1/b_2$$

$$D_{13} = -\, 2b_1(2\gamma - C_{12}b_1^2)$$

$$D_{14} = b_1(2\gamma - C_{12}b_1^2)$$

$$D_{21} = 0.5 \, L_1 \, \eta_\ell b_1/b_2$$

$$D_{22} = -\, \eta_{s1}$$

$$D_{23} = -\, 0.25 \, L_1 b_1^2(2\gamma - C_{12}b_1^2)/b_2$$

$$D_{24} = -\, 4\gamma b_2$$

$$D_{31} = -\, 2C_{12}b_1$$

$$D_{32} = -(2\gamma - C_{12}b_1^2)/b_2$$

$$D_{33} = -\, 4\eta_\ell$$

$$D_{34} = 2\eta_\ell$$

$$D_{41} = 0.25 \, L_1 b_1 (2\gamma - C_{12}b_1^2)/b_2^2$$

$$D_{42} = 4\gamma/b_2$$

$$D_{43} = 0.5 \, L_1 \eta_\ell b_1^2/b_2^2$$

$$D_{44} = -\, \eta_{s1}$$

for the second order solution equate $C_{12}$ to zero.

## APPENDIX (III.B)

Coefficients of (III.42) for the second order solution (III.31, 32) are:

$$A_4 = 1.0$$

$$A_3 = 2(\eta_{s1} + 2\eta_\ell)$$

$$A_2 = -8L_1 b_1^2 + 16\gamma^2 + \eta_{s1}(8\eta_\ell + \eta_{s1})$$

$$A_1 = 4\eta_\ell(\eta_{s1}^2 + 16\gamma^2) - L_1(b_1/b_2)^2[2\eta_\ell^2\eta_{s1} + 4\eta_\ell^3 + \gamma^2\eta_{s1} + 8\gamma^2\eta_\ell] + 4\gamma L_1\eta_\ell^2(b_1/b_2)^2 b_1 - 8\gamma\eta_\ell(\eta_{s1} + 4\eta_\ell)/b_2$$

$$A_0 = L_1\gamma^2(b_1/b_2)^2\left\{L_1(b_1/b_2)^2(2\eta_\ell^2 + \gamma^2) + 4(4\eta_\ell^2 + 4\gamma^2 - \eta_\ell\eta_{s1})\right\}$$

Coefficients of (III.42) for the third order solution (III.38, 39) are:

$$A_4 = 1.0$$

$$A_3 = 2(\eta_{s1} + 2\eta_\ell)$$

$$A_2 = [\eta_{s1}^2 + 16\gamma^2 + 8\eta_{s1}\eta_\ell - 2L_1\eta_\ell^2(\frac{b_1}{b_2})^2 - 4C_{12}b_1^2(2\gamma - C_{12}b_1^2) - \frac{L_1}{4}\eta_{s1}(\frac{b_1}{b_2})^2(2\gamma - C_{12}b_1^2)^2]$$

$$A_1 = 4\eta_\ell(16\gamma^2 + \eta_{s1}^2) - 16L_1 b_1^2(\frac{\eta_{s1}}{2} + \eta_\ell) - 2b_1^2(2\gamma - C_{12}b_1^2)(\frac{L_1\gamma\eta_\ell}{b_2^2} + 4C_{12}\eta_{s1})$$

$$A_0 = L_1\eta_\ell^2(\frac{b_1}{b_2})^2[L_1(\frac{b_1}{b_2})^2 - 4\eta_{s1}\eta_\ell - 8C_{12}\gamma b_1^2] + b_1^2(2\gamma - C_{12}b_1^2)[4C_{12}(16\gamma^2 - \eta_{s1}^2) + 8L_1\eta_\ell^2\frac{\gamma}{b_2^2} + L_1C_{12}(\frac{b_1}{b_2})^2(2\gamma - \eta_{s1}\eta_\ell)] + L_1(\frac{b_1}{b_2})^2(2\gamma - C_{12}b_1^2)^2[\frac{L_1}{2}\eta_\ell^2\frac{b_1}{b_2} + 2(\gamma - \eta_\ell\eta_{s1})] + \frac{L_1^2}{16}(\frac{b_1}{b_2})^4(2\gamma - C_{12}b_1^2)^4$$

# CHAPTER (IV)

## FLUID-STRUCTURE INTERACTION WHEN THE FLUID CONTAINER IS FREE TO MOVE LATERALLY

IV.1

In this Chapter, the general situation of the system shown in Figure (II.1) will be considered. The fluid container will oscillate laterally when the conditions of autoparametric resonance are fulfilled. Under these circumstances autoparametric coupling will take place between the fluid free surface motion, the tank lateral and vertical motions and the vertical motion of the main mass. The first antisymmetric sloshing mode will be considered and equations (II.34,38,39 and 40) take the form;

The dynamic free surface equation (II.34) becomes:

$$\dot{\alpha}_{11} - [g + \ddot{\xi} - \frac{6}{5\ell}(\dot{X}_d^2 + X_d\ddot{X}_d)]a_{11} + 0.1045682\,\lambda_{11}^2\dot{\alpha}_{11}\,a_{11}^2$$

$$- 0.2810256\,\lambda_{11}^3\alpha_{11}^2\,a_{11}\,\tanh\lambda_{11}h$$

$$- [\ddot{X}_d - \frac{6}{5\ell}\ddot{\xi}X_d + \frac{36}{25\ell^2}X_d(X_d\ddot{X}_d + \dot{X}_d^2)]\frac{2a}{(\xi_{11}^2 - 1)J_1(\xi_{11})} = 0 \qquad \text{(IV.1)}$$

The kinematic free surface equation (II.38) becomes;

$$\dot{a}_{11} + (\lambda_{11}\tanh\lambda_{11}h)\alpha_{11} - 0.122515\,\lambda_{11}^3\alpha_{11}\,a_{11}^2\,\tanh\lambda_{11}h = 0 \qquad \text{(IV.2)}$$

The equation of motion along the vertical direction (II.39) becomes;

$$(M_o + m_{t1})\ddot{\xi} + C_{s1}\dot{\xi} + K_{s1}\xi - \frac{0.202\pi\rho\alpha_{11}^2}{\cosh^2\lambda_{11}h} - \frac{6}{5\ell} m_{t1}(\dot{X}_d^2 + X_d\ddot{X}_d)$$

$$= K_{s1}\xi \cos\Omega t \qquad \text{(IV.3)}$$

The equation of motion along the horizontal direction (II.40) becomes;

$$m_{t1}\ddot{X}_d + C_{s2}\dot{X}_d + (K_{s2} - \frac{6}{5\ell} m_{t1}\ddot{\xi})X_d + \frac{36}{25\ell^2} m_{t1}X_d(X_d\ddot{X}_d + \dot{X}_d^2)$$

$$- \frac{\pi\rho a}{\lambda_{11}}\dot{\alpha}_{11} J_1(\xi_{11}).\tanh\lambda_{11}h = 0 \qquad \text{(IV.4)}$$

Elimination of $\alpha_{11}$ and $\dot{\alpha}_{11}$ results in the three equations:-

$$\ddot{a}_{11} + \omega_{11}^2 a_{11} = -\omega_{11}^2 \frac{\ddot{\xi}}{g} a_{11} - \lambda_{11}^2 a_{11}(0.227083\, a_{11}\ddot{a}_{11} + 0.5260556\, \dot{a}_{11}^2)$$

$$- \frac{6}{5\ell}\lambda_{11}[\dot{X}_d^2 + X_d\ddot{X}_d]a_{11}.\tanh\lambda_{11}h$$

$$- [\ddot{X}_d - \frac{6}{5\ell}\ddot{\xi}X_d + \frac{36}{25\ell^2} X_d(X_d\ddot{X}_d + \dot{X}_d^2)] \frac{2\xi_{11}.\tanh\lambda_{11}h}{(\xi_{11}^2 - 1)J_1(\xi_{11})}$$

.....(IV.5)

$$\ddot{\xi} + 2\omega_{s1}\zeta_{s1}\dot{\xi} + \omega_{s1}^2\xi = \frac{6}{5\ell}J_2(\dot{X}_d^2 + X_d\ddot{X}_d) + \frac{0.202\, J_1}{h\xi_{11}^2 \sinh^2\lambda_{11}h}\dot{a}_{11}^2$$

$$+ \omega_{s1}^2 \xi_o \cos\Omega t \qquad \text{(IV.6)}$$

$$\ddot{X}_d + 2\omega_{s2}\zeta_{s2}\dot{X}_d + \omega_{s2}^2 X_d = \frac{6}{5\ell}\ddot{\xi}X_d - \frac{36}{25\ell^2} X_d(X_d\ddot{X}_d + \dot{X}_d^2)$$

$$+ \frac{J_3 J_1(\xi_{11})}{(\frac{h}{a})\xi_{11}^2}[-\ddot{a}_{11} - .122515\lambda_{11}^2 a_{11}(a_{11}\ddot{a}_{11} + 2\dot{a}_1^2)]$$

..... (IV.7)

where:

$$\omega_{11}^2 = g\lambda_{11}\tanh\lambda_{11}h \qquad \mu_1 = m_\ell/(M_o + m_{t\ell})$$

$$\omega_{s1}^2 = K_{s1}/(M_o + m_{t\ell}) \qquad \mu_2 = m_{t\ell}/(M_o + m_{t\ell})$$

$$\omega_{s2}^2 = K_{s2}/m_{t\ell} \qquad \mu_3 = m_\ell/m_{t\ell}$$

The nondimensional parameters used in Chapter (III) take the form;

$$\tau = \omega_{11}t \qquad \epsilon = \xi_o/a$$

$$\begin{Bmatrix} a_{11} \\ \xi \\ X_d \end{Bmatrix} = \frac{\epsilon}{\lambda_{11}\tanh\lambda_{11}h} \begin{Bmatrix} A_{11} \\ Z \\ X \end{Bmatrix}$$

$$\begin{Bmatrix} \sigma \\ r_{s1} \\ r_{s2} \end{Bmatrix} = \frac{1}{\omega_{11}} \begin{Bmatrix} \Omega \\ \omega_{s1} \\ \omega_{s2} \end{Bmatrix}, \quad \begin{Bmatrix} \bar{\zeta}_\ell \\ \bar{\zeta}_{s1} \\ \bar{\zeta}_{s2} \end{Bmatrix} = \epsilon \begin{Bmatrix} \zeta_\ell \\ \zeta_{s1} \\ \zeta_{s2} \end{Bmatrix} \qquad \text{(IV.8)}$$

Introducing (IV.8) in (IV.5-7) gives;

$$A_{11}'' + 2\epsilon\zeta_\ell A_{11}' + A_{11} + C_o X'' = -\epsilon Z''(A_{11} - C_2 X) - \epsilon^2 \left\{ A_{11}(C_1 A_{11} A_{11}'' + \bar{C}_1 A_{11}'^2) - C_3 A_{11}(X'^2 + XX'') + C_4 X(XX'' + X'^2) \right\} \qquad \text{(IV.9)}$$

$$X'' + 2\epsilon r_{s2}\zeta_{s2}X' + r_{s2}^2 X + k_o A_{11}'' = k_1 XZ'' - \epsilon^2 \left\{ k_1^2 X(XX'' + X'^2) + k_2 A_{11}(A_{11}A_{11}'' + 2A_{11}'^2) \right\} \qquad \text{(IV.10)}$$

$$Z'' + 2\epsilon r_{s1}\zeta_{s1}Z' + r_{s1}^2 Z = \epsilon \left\{ L_2(X'^2 + XX') + L_1 A_{11}'^2 + f\cos\sigma\tau \right\} \qquad \text{(IV.11)}$$

$$C_o = \frac{2\xi_{11}\tanh\lambda_{11}h}{(\xi_{11}^2-1)J_1(\xi_{11})} \qquad C_1 = \frac{0.227083}{\tanh^2\lambda_{11}h}$$

$$C_2 = \frac{2.4}{(\ell/a)(\xi_{11}^2-1)J_1(\xi_{11})} \qquad C_1 = \frac{0.5260556}{\tanh^2\lambda_{11}h}$$

$$C_4 = C_2C_3 \qquad C_3 = \frac{1.2}{(\ell/a)\xi_{11}\tanh\lambda_{11}h} \qquad \text{(IV.12)}$$

$$L_1 = \frac{0.202\ \mu_1}{\xi_{11}^3(h/a)\tanh\lambda_{11}h.\sinh^2\lambda_{11}h}, \qquad L_2 = \mu_2\ C_3$$

$$f = [r_{s1}^2\xi_{11}\tanh\lambda_{11}h]/\epsilon \qquad K_o = \mu_3 J_1(\xi_{11})/[\xi_{11}^2(h/a)]$$

$$K_1 = C_3 \qquad K_2 = .122515\ k_c/\tanh^2\lambda_{11}h$$

A fluid free surface damping term has been introduced in (IV.9).

## IV.2 Transformation into a Principal Co-ordinate System

Any possible solution for equations (IV.9-11) gives the total motion as a sum of responses in its characteristic modes of vibration. In order to derive the solution in terms of these modes (principal modes) transformation from generalised co-ordinates to principal ones should be carried out. In an undamped linear vibration system the principal co-ordinates of a system are the natural co-ordinates and each principal mode responds to an applied force as a single degree of freedom system, i.e. the modes are decoupled.

When the damping is considered, other principal co-ordinates known as "damped principal co-ordinates[B8]" exist. Bishop and Gladwell[B8] showed that the general representation of the damping has the effect of coupling the principal modes of the system, "so that

a force which would have excited just one principal mode in the undamped system now excites other modes as well". Due to the lack of experimental information of the nature and influence of damping and its imprecise value there is no simple mathematical theory to represent it properly. Furthermore there is no conclusive experimental evidence to show whether the damping does in fact couple the modes or not. Any evidence of coupling that may appear in the experimental results does not refer only to the presence of off-diagonal damping terms because other sources of coupling, such as non-linear coupling of modes, may have a great influence.

It is common practice to carry out the transformation, first, for the undamped linear homogeneous equations and then introduce damping terms after the equations have been transformed into principal co-ordinates. Simplifications can be achieved by assuming viscous damping and the modal damping matrix is taken to be diagonal thus implying that the modes are not coupled by damping forces in the structure.

Many standard references[B7, C6] consider some special cases in which the damping matrix is diagonalised by a transformation into principal co-ordinates. One of these cases is known as "proportional damping" where the damping matrix is a linear combination of the mass and stiffness matrix. Rayleigh[R4] showed that such systems possess classical principal modes. Caughey[C1] proved that the necessary and sufficient condition for a damped dynamic system to have classical principal modes is that the damping matrix be diagonalised by the same transformation which uncouples the undamped system.

Recently, Hasselman[H4] has shown that the off-diagonal terms in the undamped principal co-ordinates are, in some cases, of the same order as the diagonal ones. He assumed viscous damping to devise a

method of measuring the off-diagonal terms in the principal damping matrix. The method is based on the coincident and quadrature - Co-quad - technique currently employed to measure modal frequencies and damping[H4].

Due to the presence of nonlinear coupling terms, it is convenient to transform the linear undamped homogeneous equations (IV.9 and IV.10) and then introduce damping terms into the principal co-ordinate equation. In this case, viscous damping will be introduced and the normal damping matrix will be taken to be diagonal.

$$\begin{bmatrix} 1 & C_o \\ k_o & 1 \end{bmatrix} \begin{Bmatrix} A_{11} \\ X \end{Bmatrix} + \begin{bmatrix} 1 & 0 \\ 0 & r_{s2}^2 \end{bmatrix} \begin{Bmatrix} A_{11} \\ X \end{Bmatrix} = 0 \qquad \text{(IV.13)}$$

Apply the linear transformation;

$$\begin{Bmatrix} A_{11} \\ X \end{Bmatrix} = [R] \begin{Bmatrix} P_1 \\ P_2 \end{Bmatrix} \qquad \text{(IV.14)}$$

Such that in $P_i$, the linear equations of motion are all independent or uncoupled, and [R] is a nonsingular real square matrix.

To determine [R] let:-

$$\begin{aligned} A_{11} &= Ae^{i\lambda\tau} \\ X &= Be^{i\lambda\tau} \end{aligned} \qquad \text{(IV.15)}$$

Substituting (IV.15) into (IV.13) gives two equations whose non-trivial solution exists if the determinant

$$\begin{vmatrix} 1 & -\lambda^2 & -C_o\lambda^2 \\ k_o\lambda^2 & & r_{s2}^2 - \lambda^2 \end{vmatrix} = 0 \qquad \text{(IV.16)}$$

The characteristic equation (IV.16) has two roots for $\lambda^2$ given by;

$$\lambda_{1,2}^2 = \frac{1 + r_{s2}^2 \pm \sqrt{(1+r_{s2})^2 - 4(1-C_ok_o)r_{s2}^2}}{2(1 - C_ok_o)} \qquad \text{(IV.17)}$$

The eigenvectors corresponding to $\lambda_1^2$ and $\lambda_2^2$ are;

$$\begin{Bmatrix} A \\ B \end{Bmatrix}_1 = \begin{Bmatrix} 1 \\ \frac{1-\lambda_1^2}{C_o\lambda_1^2} \end{Bmatrix} \quad , \quad \begin{Bmatrix} A \\ B \end{Bmatrix}_2 = \begin{Bmatrix} 1 \\ \frac{1-\lambda_2^2}{C_o\lambda_2^2} \end{Bmatrix} \qquad \text{(IV.18)}$$

The transformation matrix [R] can now be constructed as

$$[R] = \begin{bmatrix} 1 & 1 \\ \frac{1-\lambda_1^2}{C_o\lambda_1^2} & \frac{1-\lambda_2^2}{C_o\lambda_2^2} \end{bmatrix} = \begin{bmatrix} 1 & 1 \\ n_1 & n_2 \end{bmatrix} \qquad \text{(IV.19)}$$

where

$$\left.\begin{aligned} n_1 &= \frac{1-\lambda_1^2}{C_o\lambda_1^2} \\ n_2 &= \frac{1-\lambda_2^2}{C_o\lambda_2^2} \end{aligned}\right\} \qquad \text{(IV.20)}$$

Introducing (IV.19) in (IV.14) and invoking (IV.20)

$$\left.\begin{aligned} A_{11} &= P_1 + P_2 \\ X &= n_1P_1 + n_2P_2 \end{aligned}\right\} \qquad \text{(IV.21)}$$

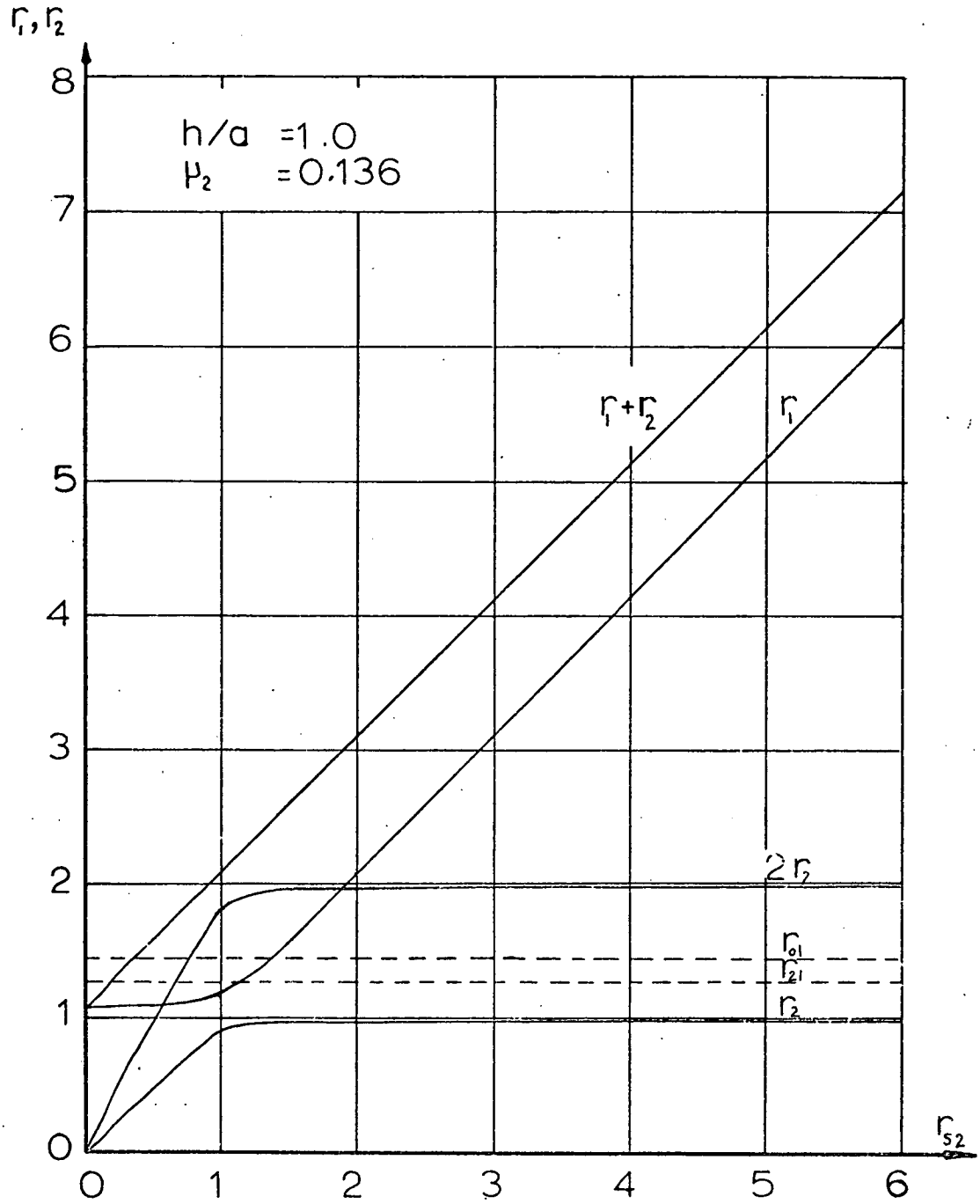


Fig.(IV.1) Relation Between Normal Modes Frequencies and Natural Frequency of Upper Structure.

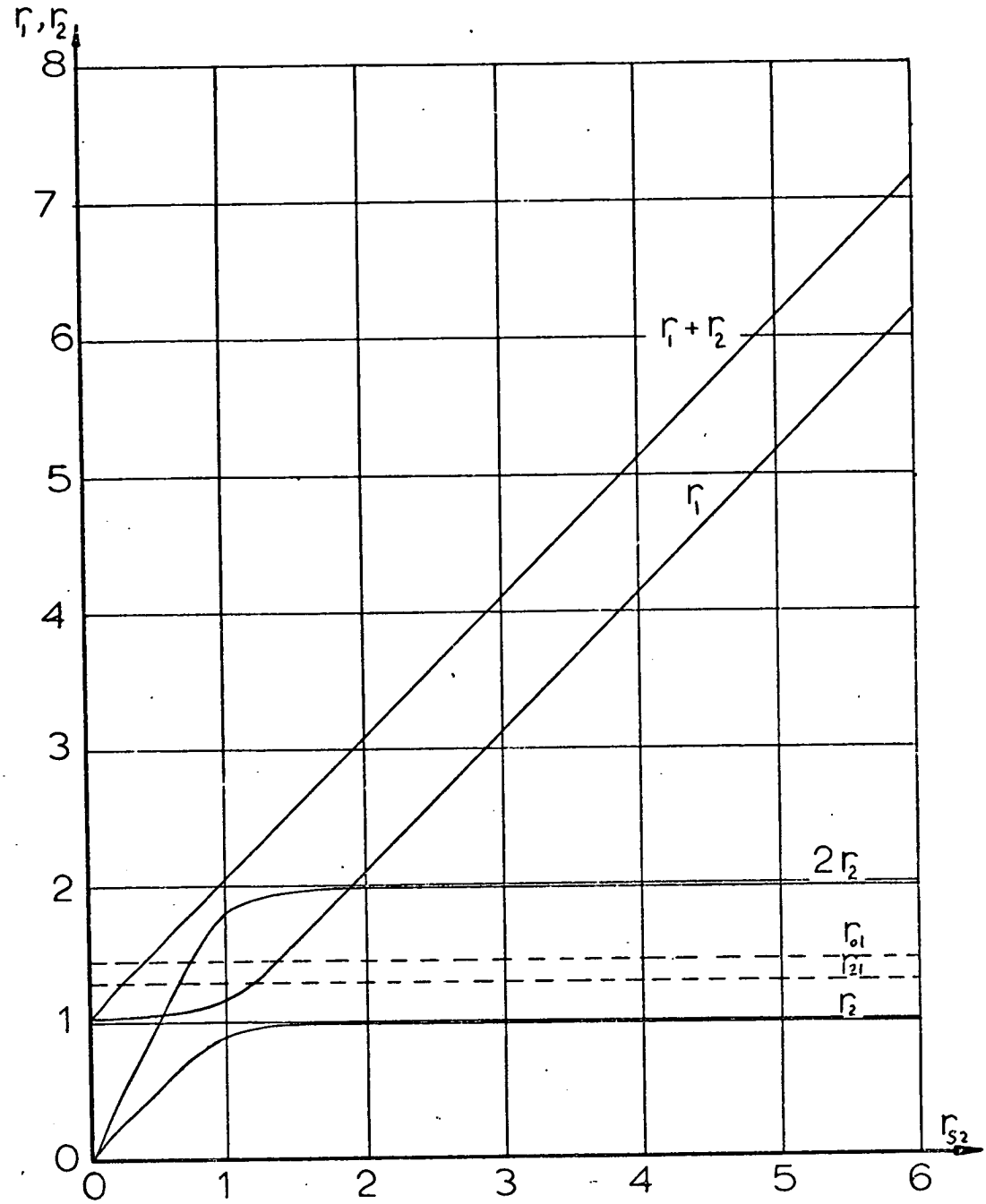


Fig.(IV.2)Relation Between Normal Modes Frequencies and Natural Frequency of Upper Structure.( h /a =1.5, $\mu_2$=0.19).

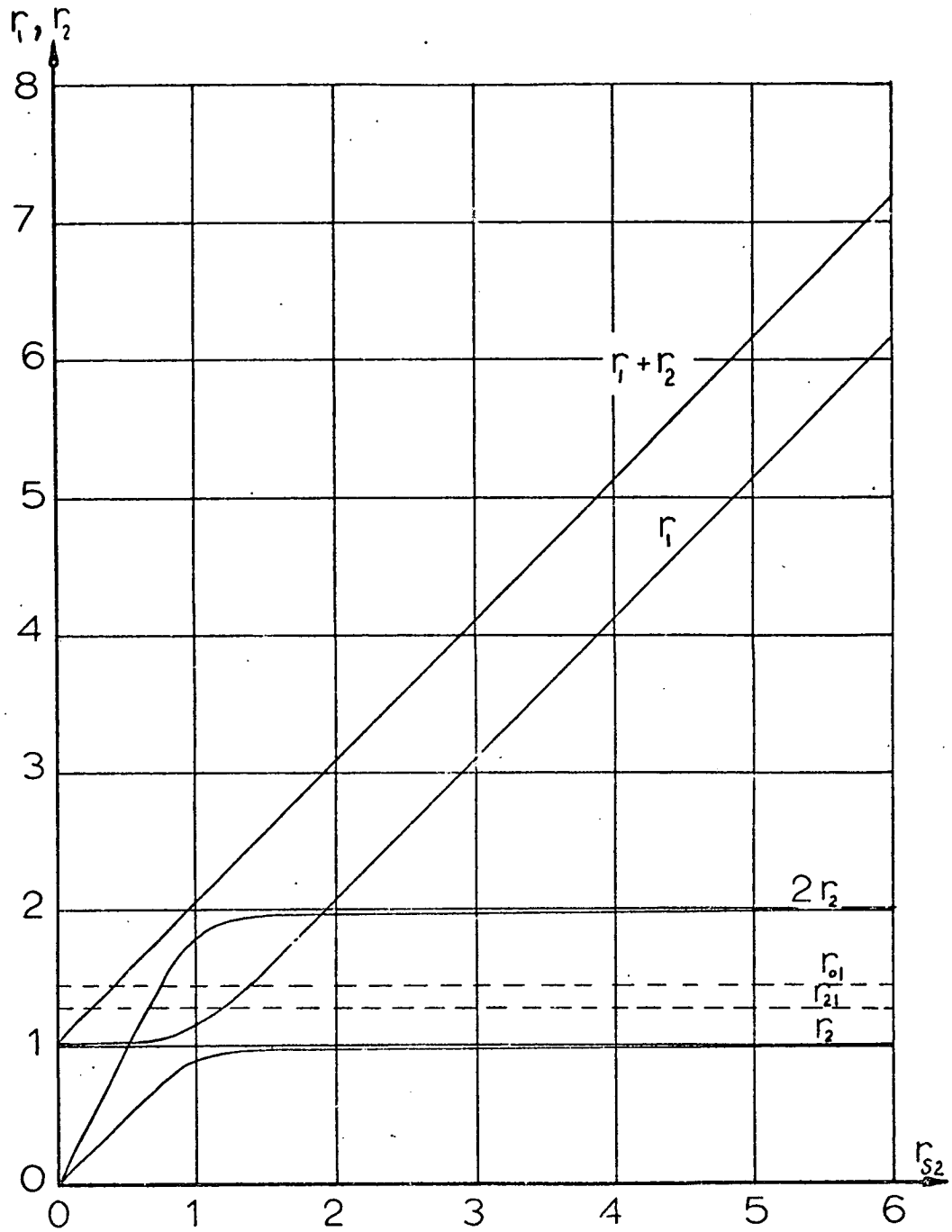


Fig.(IV·3) Relation Between Normal Modes Frequencies and Natural Frequency of Upper Structure. ( $h/a = 2.0$ , $\mu_2 = 0.24$ )

The transformation (IV.14) can now be introduced into (IV.13) and pre-multiplying by $\begin{bmatrix} 1 & C_o \\ k_o & 1 \end{bmatrix}^{-1}[R]^{-1}$ gives;

$$\begin{bmatrix} 1 & 0 \\ 0 & 1 \end{bmatrix} \begin{Bmatrix} P_1'' \\ P_2'' \end{Bmatrix} + \begin{bmatrix} r_1^2 & 0 \\ 0 & r_2^2 \end{bmatrix} \begin{Bmatrix} P_1 \\ P_2 \end{Bmatrix} = 0 \qquad \text{(IV.22)}$$

where

$$r_1^2 = \lambda_1^2 \quad \text{and} \quad r_2^2 = \lambda_2^2$$

Relationships of $r_1$ and $r_2$ versus structure frequency $r_{s2}$ are given in Figs (IV.1-3) for different fluid depth ratios. The generalised co-ordinate Z becomes $P_3$ in the principal co-ordinate frame.

Introducing into (IV.22) a diagonal damping matrix whose diagonal terms are the damping corresponding to each mode, equations (IV.9-11) can be written in the principal damped co-ordinate system as:

$$\begin{aligned} P_1'' + S_1^2\nu^2 P_1 = \epsilon \Big\{ & \epsilon^{-1}(S_1^2\nu^2 - r_1^2)P_1 - 2r_1\zeta_1 P_1' - C_5 P_1 P_3'' - C_6 P_2 P_3'' \Big\} \\ & + \epsilon^2 \Big\{ C_7 P_1^2 P_1'' + C_8 P_1^2 P_2'' + C_9 P_1 P_2 P_1'' + C_{10} P_1 P_2 P_2'' \\ & + C_{11} P_2^2 P_1'' + C_{12} P_2^2 P_2'' + C_{13} P_1 P_1'^2 + C_{14} P_1 P_1' P_2' \\ & + C_{15} P_2 P_1' P_2' + C_{16} P_2 P_2'^2 + C_{17} P_2 P_1'^2 + C_{18} P_1 P_1'^2 \Big\} \end{aligned} \qquad \text{(IV.23)}$$

$$P_2'' + S_2^2\nu^2 P_2 = \epsilon\left\{\epsilon^{-1}(S_2^2\nu^2 - r_2^2)P_2 - 2r_2\zeta_2 P_2' + K_3 P_1 P_3'' + K_4 P_2 P_3''\right\}$$
$$+ \epsilon^2\left\{K_5 P_1^2 P_1'' + K_6 P_1^2 P_2'' + 2K_6 P_1 P_2 P_1'' + 2K_7 P_1 P_2 P_2''\right.$$
$$+ K_7 P_2^2 P_2'' + K_8 P_2^2 P_2'' + K_9 P_1 P_1'^2 + 2K_{10} P_1 P_1' P_2'$$
$$\left. + 2K_{11} P_2 P_1' P_2' + K_{11} P_1 P_2'^2 + K_{10} P_2 P_1'^2 + K_{12} P_2 P_2'^2\right\} \qquad \text{(IV.24)}$$

$$P_3'' + S_3^2\nu^2 P_3 = \epsilon\left\{\epsilon^{-1}(S_3^2\nu^2 - r_3^2)P_3 - 2r_3\zeta_3 P_3' + L_3 P_1'^2 + L_4 P_1' P_2'\right.$$
$$+ L_5 P_2'^2 + L_6 P_1 P_1'' + L_7 P_1 P_2'' + L_7 P_2 P_1''$$
$$\left. + L_8 P_2 P_2'' + f\cos(n\nu\tau)\right\} \qquad \text{(IV.25)}$$

Where the constants $C_i$, $K_i$ and $L_i$ are given in Appendix (IV.A) The forcing frequency $\sigma$ has been replaced by $n\nu$ where n is a + ve real number and $\nu$ is in the neighbourhood of one of the principal mode frequencies. $S_1$, $S_2$ and $S_3$ are +ve real numbers such that $|S_i^2\nu^2 - r_i^2| < \epsilon$.

Applying the approximate asymptotic solution as explained in Chapter (III), the solutions take the form,

$$\left.\begin{aligned} P_1 &= P_1\cos(r_1\tau + \varphi) + \epsilon a_1 + \ldots \\ P_2 &= P_2\cos(r_2\tau + \theta) + \epsilon b_1 + \ldots \\ P_3 &= P_3\cos(r_3\tau + \gamma) + \epsilon d_1 + \ldots \end{aligned}\right\} \qquad \text{(IV.26)}$$

As defined in Chapter (III), the amplitudes $P_1$, $P_2$ and $P_3$, and phases $\varphi$, $\theta$, and $\gamma$ are slowly-time varying.

Substituting (IV.26) in (IV.23-25) yields the following approximate equations up to the second order terms in $\epsilon$

$$[P_1'' - P_1(r_1+\varphi')^2]\cos(r_1\tau+\varphi)-[P_1\varphi''+2P_1'(r_1+\varphi')]\sin(r_1\tau+\varphi)+\epsilon a_1''$$

$$+ S_1^2\nu^2[P_1\cos(r_1\tau+\varphi)+\epsilon a_1+\ldots]$$

$$= \epsilon\Big\{\epsilon^{-1}(S_1^2\nu^2-r_1^2)[P_1\cos(r_1\tau+\varphi)+\epsilon a_1+\epsilon^2 a_2]$$

$$- 2r_1\zeta_1[-r_1P_1\sin(r_1\tau+\varphi)+\epsilon a_1']$$

$$+C_5r_3^2P_1P_3\cos(r_1\tau+\varphi)\cos(r_3\tau+\gamma)-\epsilon C_5[P_1d_1''\cos(r_1\tau+\varphi)-r_3^2a_1P_3\cos(r_3\tau+\gamma)]$$

$$+C_6r_3^2P_2P_3\cos(r_2\tau+\theta)\cos(r_3\tau+\gamma)-\epsilon C_6[P_2d_1''\cos(r_2\tau+\theta)-r_3^2b_1P_3\cos(r_3\tau+\gamma)]\Big\}$$

$$+\epsilon^2\Big\{-C_7r_1^2P_1^3\cos^3(r_1\tau+\varphi)-P_1^2P_2(C_8r_2^2+C_9r_1^2)\cos^2(r_1\tau+\varphi)\cos(r_2\tau+\theta)$$

$$-P_1P_2^2(C_{10}r_2^2+C_{11}r_1^2)\cos(r_1\tau+\varphi)\cos^2(r_2\tau+\theta)-C_{12}r_2^2P_2^3\cos^3(r_2\tau+\theta)$$

$$+C_{13}r_1^2P_1^3\cos(r_1\tau+\varphi)\sin^2(r_1\tau+\varphi)+\tfrac{1}{2}C_{14}r_1r_2P_1^2P_2\sin(2r_1\tau+2\varphi)\sin(r_2\tau+\theta)$$

$$+\tfrac{1}{2}C_{15}r_1r_2P_1P_2^2\sin(r_1\tau+\varphi)\sin(2r_2\tau+2\theta)+C_{16}r_2^2P_2^3\cos(r_2\tau+\theta)\sin^2(r_2\tau+\theta)$$

$$+C_{17}r_1^2P_1^2P_2\sin^2(r_1\tau+\varphi)\cos(r_2\tau+\theta)+C_{18}r_2^2P_1P_2^2\cos(r_1\tau+\varphi)\sin^2(r_2\tau+\theta)\Big\}$$

.....(IV.27)

$$[P_2'' - P_2(r_2+\theta')^2]\cos(r_2\tau+\theta)-[P_2\theta''+2P_2'(r_2+\theta')]\sin(r_2\tau+\theta)+\epsilon b_1''$$

$$+ S_2^2\nu^2[P_2\cos(r_2\tau+\theta)+\epsilon b_1+\ldots]$$

$$= \epsilon\Big\{\epsilon^{-1}(S_2^2\,{}^2-r_2^2)[P_2\cos(r_2\tau+\theta)+\epsilon b_1+\epsilon^2 b_2]$$

(IV.28) continued.....

$$-2r_2\zeta_2[-r_2P_2\sin(r_2\tau+\theta)+\epsilon b_1']$$

$$-K_3r_3^2P_1P_3\cos(r_1\tau+\varphi)\cos(r_3\tau+\gamma)+\epsilon K_3[P_1d_1''\cos(r_1\tau+\varphi)-r_3^2a_1P_3\cos(r_3\tau+\gamma)]$$

$$-K_4r_3^2P_2P_3\cos(r_2\tau+\theta)\cos(r_3\tau+\gamma)+\epsilon K_4[P_2d_1''\cos(r_2\tau+\theta)-r_3^2b_1P_3\cos(r_3\tau+\gamma)]$$

$$+\epsilon^2\Big\{-K_5r_1^2P_1^3\cos^3(r_1\tau+\varphi)-K_6P_1^2P_2(r_2^2+2r_1^2)\cos^2(r_1\tau+\varphi)\cos(r_2\tau+\theta)$$

$$-K_7P_1P_2^2(2r_2^2+r_1^2)\cos(r_1\tau+\varphi)\cos^2(r_2\tau+\theta)-K_8r_2^2P_2^3\cos^3(r_2\tau+\theta)$$

$$+K_9r_1^2P_1^3\cos(r_1\tau+\varphi)\sin^2(r_1\tau+\varphi)+K_{10}r_1r_2P_1^2P_2\sin(2r_1\tau+2\varphi)\sin(r_2\tau+\theta)$$

$$+K_{11}r_1r_2P_1P_2^2\sin(r_1\tau+\varphi)\sin(2r_2\tau+2\theta)+K_{11}r_2^2P_1P_2^2\cos(r_1\tau+\varphi)\sin^2(r_2\tau+\theta)$$

$$+K_{10}r_1^2P_1^2P_2\sin^2(r_1\tau+\varphi)\cos(r_2\tau+\theta)+K_{12}r_2^2P_2^3\cos(r_2\tau+\theta)\sin^2(r_2\tau+\theta)\Big\}$$

.....(IV.28)

$$[P_3''-P_3(r_3+\gamma')^2]\cos(r_3\tau+\gamma)-[P_3\gamma''+2P_3'(r_3+\gamma')]\sin(r_3\tau+\gamma)+\epsilon d_1''$$

$$+S_3^2V^2[P_3\cos(r_3\tau+\gamma)+\epsilon d_1+\ldots]$$

$$=\epsilon\Big\{\epsilon^{-1}(S_3^2V^2-r_3^2)[P_3\cos(r_3\tau+\gamma)+\epsilon d_1+\epsilon^2d_2]$$

$$-2r_3\zeta_3[-r_3P_3\sin(r_3\tau+\gamma)+\epsilon d_1']$$

$$+L_3[r_1^2P_1^2\sin^2(r_1\tau+\varphi)-2\epsilon r_1a_1'P_1\sin(r_1\tau+\varphi)]$$

$$+L_4r_1r_2P_1P_2\sin(r_1\tau+\varphi)\sin(r_2\tau+\theta)-\epsilon L_4[r_1b_1'P_1\sin(r_1\tau+\varphi)$$

$$+r_2a_1'P_2\sin(r_2\tau+\theta)]$$

(IV.29) continued.....

$$+ L_5[r_2^2P_2^2\sin^2(r_2\tau+\theta)-2\epsilon r_2 b_1' P_2\sin(r_2\tau+\theta)]$$

$$+ L_6[-r_1^2P_1^2\cos^2(r_1\tau+\varphi)+\epsilon(a_1''-a_1 r_1^2)P_1\cos(r_1\tau+\varphi)]$$

$$- L_7 r_2^2 P_1 P_2\cos(r_1\tau+\varphi)\cos(r_2\tau+\theta)+\epsilon L_7[b_1'' P_1\cos(r_1\tau+\varphi)-r_2^2 a_1 P_2\cos(r_2\tau+\theta)]$$

$$- L_7 r_1^2 P_1 P_2\cos(r_1\tau+\varphi)\cos(r_2\tau+\theta)+\epsilon L_7[a_1'' P_2\cos(r_2\tau+\theta)-r_1^2 b_1 P_1\cos(r_1\tau+\varphi)]$$

$$+ L_8[-r_2^2P_2^2\cos^2(r_2\tau+\theta)+\epsilon(b_1''-b_1 r_2^2)P_2\cos(r_2\tau+\theta)] + f\cos(n\nu\tau) \Big\} \quad \text{(IV.29)}$$

The fundamental variational equations are obtained by equating terms of zero order in $\epsilon$ in equations (IV.27-29);

$$\left.\begin{aligned}
-2r_1P_1\varphi' &= \left\{\epsilon^{-1}(S_1^2\nu^2-r_1^2)P_1\right\} \\
-2r_1P_1' &= 0 \\
-2r_2P_2\theta' &= \epsilon\left\{\epsilon^{-1}(S_2^2\nu^2-r_2^2)P_2\right\} \\
-2r_2P_2' &= 0 \\
-2r_3P_3\gamma' &= \epsilon\left\{\epsilon^{-1}(S_3^2\nu^2-r_3^2)P_3\right\} \\
-2r_3P_3' &= 0
\end{aligned}\right\} \quad \text{(IV.30)}$$

On the other hand the first order terms of $\epsilon$ in (IV.27-29) give the first order perturbation equations as;

$$\ddot{a}_1+r_1^2 a_1 = 2r_1^2\zeta_1 P_1 \sin(r_1\tau+\varphi)$$
$$+ \tfrac{1}{2}C_5 r_3^2 P_1 P_3 \left\{\cos[(r_3-r_1)\tau+\gamma-\varphi]+\cos[(r_3+r_1)\tau+\gamma+\varphi]\right\}$$
$$+ \tfrac{1}{2}C_6 r_3^2 P_2 P_3 \left\{\cos[(r_3-r_2)\tau+\gamma-\theta]+\cos[(r_3+r_2)\tau+\gamma+\theta]\right\} \qquad \text{(IV.31)}$$

This equation contains secular terms which exhibit nonlinear resonance if:-

$$\left.\begin{aligned} r_3 &= 2r_1 \\ r_3 &= r_1+r_2 \\ r_3 &= r_1-r_2 \end{aligned}\right\} \qquad \text{(IV.32)}$$

$$\ddot{b}_1+r_2^2 b_1 = 2r_2^2\zeta_2 P_2 \sin(r_2\tau+\theta)$$
$$- \tfrac{1}{2}K_3 r_3^2 P_1 P_3 \left\{\cos[(r_3-r_1)\tau+\gamma-\varphi]+\cos[(r_3+r_1)\tau+\gamma+\varphi]\right\}$$
$$- \tfrac{1}{2}K_4 r_3^2 P_2 P_3 \left\{\cos[(r_3-r_2)\tau+\gamma-\theta]+\cos[(r_3+r_2)\tau+\gamma+\theta]\right\} \qquad \text{(IV.33)}$$

Resonance occurs if;

$$\left.\begin{aligned} r_3 &= r_1+r_2 \\ r_3 &= r_2-r_1 \\ r_3 &= 2r_2 \end{aligned}\right\} \qquad \text{(IV.34)}$$

Finally;

$$\ddot{d}_1+r_3^2 d_1 = 2r_3^2\zeta_3 P_3 \sin(r_3\tau+\gamma)+\tfrac{1}{2}L_3 r_1^2 P_1^2[1-\cos(2r_1\tau+2\varphi)]$$
$$+ \tfrac{1}{2}L_4 r_1 r_2 P_1 P_2 \left\{\cos[(r_1-r_2)\tau+\varphi-\theta]-\cos[(r_1+r_2)\tau+\varphi+\theta]\right\}$$
$$+ \tfrac{1}{2}L_5 r_2^2 P_2^2[1-\cos(2r_2\tau+2\theta)]-\tfrac{1}{2}L_6 r_1^2 P_1^2[1+\cos(2r_1\tau+2\varphi)]$$

(IV.35) continued.....

$$- \tfrac{1}{2}L_7 r_2^2 P_1 P_2 \left\{ \cos[(r_1-r_2)\tau+\varphi-\theta]+\cos[(r_1+r_2)\tau+\varphi+\theta] \right\}$$

$$- \tfrac{1}{2}L_7 r_1^2 P_1 P_2 \left\{ \cos[(r_1-r_2)\tau+\varphi-\theta]+\cos[(r_1+r_2)\tau+\varphi+\theta] \right\}$$

$$- \tfrac{1}{2}L_8 r_2^2 P_2^2 [1+\cos(2r_2\tau+2\theta)] + f\cos(n\nu\tau) \qquad \text{(IV.35)}$$

This equation contains two kinds of resonance, these are;

a) Nonlinear internal resonance which occurs at:

$$\left.\begin{aligned} r_3 &= r_1+r_2 \\ r_3 &= r_1-r_2 \\ r_3 &= 2r_1 \\ r_3 &= 2r_2 \end{aligned}\right\} \qquad \text{(IV.36a)}$$

b) External resonance, due to the forcing function term, which occurs at

$$r_3 = n\nu \qquad \text{(IV.36b)}$$

It is evident from (IV.32, 34, 36a) that there are four cases of internal resonance, two of these are sum and difference of two normal frequencies (some investigators call them conjugate frequencies[M7]), and the others take place at twice the normal frequencies of modes 1 or 2. The analysis of each case will be given in the subsequent sections.

## IV.3 Autoparametric Resonance of the Summed Type

In this section vibrations of the so-called "summed type" under parametric excitation are treated. The frequencies of the system are governed by the following relations;

$$\left.\begin{aligned} r_3 &= r_1+r_2 \\ r_3 &= n\nu \end{aligned}\right\} \qquad \text{(IV.37)}$$

The resonant terms in equations (IV.31, 33, 35) corresponding to resonance conditions (IV.37) must be removed to the variational equations (Iv.30). The resulting first order perturbation equations become;

$$a_1''+r_1^2a_1 = \tfrac{1}{2}C_5r_3^2P_1P_3\left\{\cos(r_2\tau+\gamma-\varphi)+\cos[(2r_1+r_2)\tau+\gamma+\varphi]\right\}$$

$$+\tfrac{1}{2}C_6r_3^2P_2P_3\cos[(2r_2+r_1)\tau+\gamma+\theta]$$

The particular solution of this equation is;

$$a_1 = \frac{C_5r_3P_1P_3}{2(r_1-r_2)}\cos(r_2\tau+\gamma-\varphi)-\frac{C_5r_3P_1P_3}{2(3r_1+r_2)}\cos[(2r_1+r_2)\tau+\gamma+\varphi]$$

$$-\frac{C_6r_3P_2P_3}{8r_2}\cos[(2r_2+r_1)\tau+\gamma+\theta] \qquad \text{(IV.38)}$$

$$b_1''+r_2^2b_1 = -\tfrac{1}{2}K_3r_3^2P_1P_3\cos[(2r_1+r_2)\tau+\gamma+\varphi]-\tfrac{1}{2}K_4r_3^2P_2P_3\left\{\cos(r_1\tau+\gamma-\theta)\right.$$

$$\left.+\cos[(2r_1+r_2)\tau+\gamma+\theta]\right\}$$

The steady state solution of this equation is;

$$b_1 = \frac{K_3r_3P_1P_3}{8r_1}\cos[(2r_1+r_2)\tau+\gamma+\varphi]+\frac{K_4r_3P_2P_3}{2(r_1-r_2)}\cos(r_1\tau+\gamma-\theta)$$

$$+\frac{K_4r_3P_2P_3}{2(3r_2+r_1)}\cos[(2r_2+r_1)\tau+\gamma+\theta] \qquad \text{(IV.39)}$$

Finally,

$$d_1'' + r_3^2 d_1 = \tfrac{1}{2}r_1^2(L_3-L_6)P_1^2 - \tfrac{1}{2}r_1^2(L_3+L_6)P_1^2\cos(2r_1\tau+2\varphi) + \tfrac{1}{2}r_2^2(L_5-L_8)P_2^2$$

$$-\tfrac{1}{2}r_2^2(L_5+L_8)P_2^2\cos(2r_2\tau+2\theta) + \tfrac{1}{2}[L_7(r_1^2+r_2^2)+L_4 r_1 r_2]P_1 P_2\cos[(r_1-r_2)\tau+\varphi-\theta]$$

The solution is found in the form;

$$d_1 = \tfrac{1}{2}(L_3-L_6)\left(\frac{r_1}{r_3}\right)^2 P_1^2 + \tfrac{1}{2}(L_5-L_8)\left(\frac{r_2}{r_3}\right)^2 P_2^2 - \tfrac{1}{2}(L_3+L_6)\left(\frac{r_1^2}{r_3^2-4r_1^2}\right)P_1^2\cos(2r_1\tau+2\varphi)$$

$$- \tfrac{1}{2}(L_5+L_8)\left(\frac{r_2^2}{r_3^2-4r_2^2}\right)P_2^2\cos(2r_2\tau+2\theta) + \frac{1}{8}\left[\frac{L_7(r_1^2+r_2^2)+L_4 r_1 r_2}{r_1 r_2}\right]P_1 P_2\cos[(r_1-r_2)\tau+\varphi-$$

.....(IV.40)

Terms of second order in $\epsilon^2$ in equations (IV.27-29) give the second order perturbation equations

$$a_2'' + r_1^2 a_2 = -2r_1\zeta_1 a_1' - C_5[P_1 d_1''\cos(r_1\tau+\varphi) - r_3^2 a_1 P_3\cos(r_3\tau+\gamma)]$$

$$- C_6[P_2 d_1''\cos(r_2\tau+\theta) - r_3^2 b_1 P_3\cos(r_3\tau+\gamma)] - C_7 r_1^2 P_1^3\cos^3(r_1\tau+\varphi)$$

$$-(C_8 r_2^2 + C_9 r_1^2)P_1^2 P_2\cos^2(r_1\tau+\varphi)\cos(r_2\tau+\theta) - C_{12} r_2^2 P_2^3\cos^3(r_2\tau+\theta)$$

$$-(C_{10} r_2^2 + C_{11} r_1^2)P_1 P_2^2\cos(r_1\tau+\varphi)\cos^2(r_2\tau+\theta) + C_{13} r_1^2 P_1^3\cos(r_1\tau+\varphi)\cdot$$

$$\cdot\sin^2(r_1\tau+\varphi)$$

$$+ \tfrac{1}{2}C_{14} r_1 r_2 P_1^2 P_2\sin(2r_1\tau+2\varphi)\sin(r_2\tau+\theta) + \tfrac{1}{2}C_{15} r_1 r_2 P_1 P_2^2\sin(r_1\tau+\varphi)$$

$$\sin(2r_2\tau+2\theta)$$

$$+ C_{16} r_2^2 P_2^3\cos(r_2\tau+\theta)\sin^2(r_2\tau+\theta) + C_{17} r_1^2 P_1^2 P_2\sin^2(r_1\tau+\varphi)\cos(r_2\tau+\theta)$$

$$+ C_{18} r_2^2 P_1 P_2^2\cos(r_1\tau+\varphi)\sin^2(r_2\tau+\theta) \qquad \text{(IV.41)}$$

$$b_2''+r_2^2b_2 = -2r_2\zeta_2b_1'+K_3[P_1d_1''\cos(r_1\tau+\varphi)-r_3^2a_1P_3\cos(r_3\tau+\gamma)]-K_5r_1^2P_1^3\cos^3(r_1\tau+\varphi)$$

$$+K_4[P_2d_1''\cos(r_2\tau+\theta)-r_3^2b_1P_3\cos(r_3\tau+\gamma)]-K_6P_1^2P_2(r_2^2+2r_1^2)\cos^2(r_1\tau+\varphi)\cdot\cos(r_2\tau+\theta)$$

$$-K_7P_1P_2^2(2r_2^2+r_1^2)\cos(r_1\tau+\varphi)\cos^2(r_2\tau+\theta)-K_8r_2^2P_2^3\cos^3(r_2\tau+\theta)$$

$$+K_9r_1^2P_1^3\cos(r_1\tau+\varphi)\sin^2(r_1\tau+\varphi)+K_{10}r_1r_2P_1^2P_2\sin(2r_1\tau+2\varphi)\sin(r_2\tau+\theta)$$

$$+K_{11}r_1r_2P_1P_2^2\sin(r_1\tau+\varphi)\sin(2r_2\tau+2\theta)+K_{11}r_2^2P_1P_2^2\cos(r_1\tau+\varphi)\sin^2(r_2\tau+\theta)$$

$$+K_{10}r_1^2P_1^2P_2\sin^2(r_1\tau+\varphi)\cos(r_2\tau+\theta)+K_{12}r_2^2P_2^3\cos(r_2\tau+\theta)\sin^2(r_2\tau+\theta)$$

.....(IV.42)

$$d_2''+r_3^2d_2 = -2r_3\zeta_3d_1'-2L_3r_1a_1'P_1\sin(r_1\tau+\varphi)-L_4r_1b_1'P_1\sin(r_1\tau+\varphi)$$

$$-L_4r_2a_1'P_2\sin(r_2\tau+\theta)-2L_5r_2b_1'P_2\sin(r_2\tau+\theta)$$

$$+L_6(a_1''P_1-a_1r_1^2P_1)\cos(r_1\tau+\varphi)+L_7[b_1''P_1\cos(r_1\tau+\varphi)$$

$$-r_1^2a_1P_2\cos(r_2\tau+\theta)+a_1''P_2\cos(r_2\tau+\theta)-r_1^2b_1P_1\cos(r_1\tau+\varphi)]$$

$$+L_8(b_1''P_2-b_1r_2^2P_2)\cos(r_2\tau+\theta) \qquad \text{(IV.43)}$$

Extracting the terms that give the resonance condition $r_3=r_1+r_2$ from equations (IV.41-43) gives

$$[C_{574}r_1^2P_1^3+C_{556}r_3^2P_1P_3^2+C_{618}r_2^2P_1P_2^2]\cos(r_1\tau+\varphi)$$

from equation (IV.42)

$$[K_{482}r_2^2P_2^3+K_{361}r_1^2P_1^2P_2+K_{344}r_3^2P_2P_3^2]\cos(r_2\tau+\theta)$$

(IV.44) continued.....

and from equation (IV.43)

$$[L_{43}r_1^2P_1^2P_3+L_{45}r_2^2P_2^2P_3]\cos(r_3\tau+\gamma) \qquad \text{(IV.44)}$$

Constants in (IV.44) are given in Appendix (IV.B).

The addition of resonant terms of the first and second order to the variational equations gives the following variational equations;

$$\left.\begin{aligned}
-2r_1P_1\varphi' &= \epsilon\left\{\epsilon^{-1}(S_1^2\nu^2-r_1^2)P_1+\tfrac{1}{2}C_6r_3^2P_2P_3\cos(\gamma-\varphi-\theta)\right\} \\
&\quad +\epsilon^2P_1\left\{C_{574}r_1^2P_1^2+C_{556}r_3^2P_3^2+C_{618}r_2^2P_2^2\right\} \\
-2r_1P_1' &= \epsilon\left\{2r_1^2\zeta_1P_1-\tfrac{1}{2}C_6r_3^2P_2P_3\sin(\gamma-\varphi-\theta)\right\} \\
-2r_2P_2\theta' &= \epsilon\left\{\epsilon^{-1}(S_2^2\nu^2-r_2^2)P_2-\tfrac{1}{2}K_3r_3^2P_1P_3\cos(\gamma-\varphi-\theta)\right\} \\
&\quad +\epsilon^2P_2\left\{K_{482}r_2^2P_2^2+K_{361}r_1^2P_1^2+K_{314}r_3^2P_3^2\right\} \\
-2r_2P_2' &= \epsilon\left\{2r_2^2\zeta_2P_2+\tfrac{1}{2}K_3r_3^2P_1P_3\sin(\gamma-\varphi-\theta)\right\} \\
-2r_3P_3\gamma' &= \epsilon\left\{\epsilon^{-1}(S_3^2\nu^2-r_3^2)P_3-\tfrac{1}{2}r_3^2L_{47}P_1P_2\cos(\gamma-\varphi-\theta)+f\cos\gamma\right\} \\
&\quad +\epsilon^2P_3\left\{L_{43}r_1^2P_1^2+L_{45}r_2^2P_2^2\right\} \\
-2r_3P_3' &= \epsilon\left\{2r_3^2\zeta_3P_3-\tfrac{1}{2}r_3^2L_{47}P_1P_2\sin(\gamma-\varphi-\theta)+f\sin\gamma\right\}
\end{aligned}\right\} \qquad \text{(IV.45)}$$

Introducing the following transformation variables;

$$
\left.
\begin{aligned}
P_i &= b_i\left[\frac{\sqrt{f}}{r_3\ \sqrt{|L_{47}|}}\right] & \tau &= 2T/\epsilon\sqrt{f\,|L_{47}|}\\
\gamma &= \frac{r_3^2 - \nu^2}{r_3\,\epsilon\sqrt{f\,|L_{47}|}} & \eta_i &= \zeta_i\, r_i\left[\frac{2}{\sqrt{f\,|L_{47}|}}\right]\\
S_1 &= r_1/r_3 & S_2 &= r_2/r_3\\
\psi &= \gamma - \varphi - \theta & S_3 &= 1\\
& & \delta &= \frac{\epsilon}{r_3\,|L_{47}|}\sqrt{\frac{f}{|L_{47}|}}
\end{aligned}
\right\} \qquad \text{(IV.46)}
$$

equations (IV.45) take the form

$$
\left.
\begin{aligned}
-b_1\dot{\varphi} &= -S_1\gamma b_1 + \tfrac{1}{2}\left(\frac{C_6}{S_1\,|L_{47}|}\right) b_2 b_3 \cos\psi\\
&\quad + \delta\, b_1\left\{C_{574} S_1 b_1^2 + \frac{C_{556}}{S_1}\, b_3^2 + C_{618}\left(\frac{S_2^2}{S_1}\right) b_2^2\right\} && \text{(a)}\\
-\dot{b_1} &= \eta_1 b_1 - \tfrac{1}{2}\left(\frac{C_6}{S_1\,|L_{47}|}\right) b_2 b_3 \sin\psi && \text{(b)}\\
-b_2\dot{\theta} &= -S_2\gamma b_2 - \tfrac{1}{2}\left(\frac{K_3}{S_2\,|L_{47}|}\right) b_1 b_3 \cos\psi\\
&\quad + \delta b_2\left\{K_{482} S_2 b_2^2 + K_{361}\left(\frac{S_1^2}{S_2}\right) b_1^2 + \frac{K_{344}}{S_2}\, b_3^2\right\} && \text{(c)}\\
-\dot{b_2} &= \eta_2 b_2 + \tfrac{1}{2}\left(\frac{K_3}{S_2\,|L_{47}|}\right) b_1 b_3 \sin\psi && \text{(d)}\\
-b_3\dot{\gamma} &= -\gamma b_3 - \tfrac{1}{2}\,\frac{L_{47}}{|L_{47}|}\, b_1 b_2 \cos\psi + \cos\gamma\\
&\quad + \delta b_3\left[L_{43} S_1^2 b_1^2 + L_{45} S_2^2 b_2^2\right] && \text{(e)}\\
-\dot{b_3} &= \eta_3 b_3 - \tfrac{1}{2}\,\frac{L_{47}}{|L_{47}|}\, b_1 b_2 \sin\psi + \sin\gamma && \text{(f)}
\end{aligned}
\right\} \qquad \text{(IV.47)}
$$

where prime denotes differentiation with respect to the new time parameter T.

The steady-state solution of this set of equations can be obtained by setting the left hand side to zero, however the resulting six nonlinear algebraic equations are incompatible because they contain only five unknowns. This means either that one or more of the variables do not achieve steady state or that one of the equations is related to another through their coefficients (which implies that the virtual number of these equations is five). These equations are consistent only if the damping of the first two normal modes is neglected. This situation leads to four algebraic equations with four unknowns.

The behaviour of each possible case will be investigated separately.

Case A $\eta_1 = \eta_2 = 0$

In order to simplify the analysis the third order terms are dropped as the numerical values of their coefficients are very small compared to those of the second order. The resulting equations are;

$$\left.\begin{aligned} -S_1\gamma b_1 \pm \tfrac{1}{2}\left(\frac{C_6}{S_1|L_{47}|}\right)b_2 b_3 &= 0 \\ S_2\gamma b_2 \pm \tfrac{1}{2}\left(\frac{K_3}{S_2|L_{47}|}\right)b_1 b_3 &= 0 \\ \gamma b_3 \pm \tfrac{1}{2}\frac{L_{47}}{|L_{47}|}b_1 b_2 &= \cos\gamma \\ -\eta_3 b_3 &= -\sin\gamma \end{aligned}\right\} \qquad \text{(IV.48)}$$

The solution of these equations is

$$b_3 = -\frac{4S_1^2 S_2^2 \gamma^2}{C_6 K_3} L_{47}^2 \qquad \text{(IV.49)}$$

$$b_1^2 = -\frac{C_6}{K_3}\frac{S_2^2}{S_1^2} b_2^2 \qquad \text{(IV.50)}$$

$$b_2^2 = 4\frac{S_1^2}{C_6}\left\{ \left|L_{47}\right|\gamma^2 \pm \sqrt{-\frac{K_3 C_6}{4 S_1^2 S_2^2} - \gamma^2 {}^2{}_3 L_{47}^2} \right\} \qquad \text{(IV.51)}$$

There is another solution can be obtained with $b_1 = b_2 = 0$, and $b_3$ given by

$$b_3 = \frac{1}{\sqrt{\gamma^2 + \eta_3^2}} \qquad \text{(IV.52)}$$

which is a normal resonance solution.

The amplitude response curves are determined for two different cases of fluid depth ratios $\frac{h}{a} =$ 1, and 2, and for two excitation parameters $\in = 0.021$, and 0.0105. From the relationship of $r_1$ and $r_2$ vis. $r_{s2}$ given in Figs. (IV.1-3) the value of $r_{s2}$ can be defined for the condition $r_3 = r_1 + r_2 \approx 2.0$. Having obtained $r_{s2}$ the length of the leaf springs L/a can be determined from Fig. (VI.6) for the relevant top masses. With these data the constants in (IV.49-51) are determined. Figs. (IV.4-9) depict the theoretical curves for $b_1$, $b_2$ and $b_3$. It has been indicated in similar studies [H5, B4] that the points of vertical tangency on the response curves $b_1$ and $b_2$ are important as they define the boundaries of the region of parametric instability of these modes. Two kinds of vertical tangents exist on each side of the resonance frequency n=1, the first occurs at the forcing frequency where $b_1 = b_2 = 0.0$. At this frequency $b_3$ in (IV.49) is equal to $b_3$ in (IV.52) and the values of $b_1$ and $b_2$ jump from point A to point B on $b_1$ and C on $b_2$ Fig. (IV.4). The responses of $b_1$ and

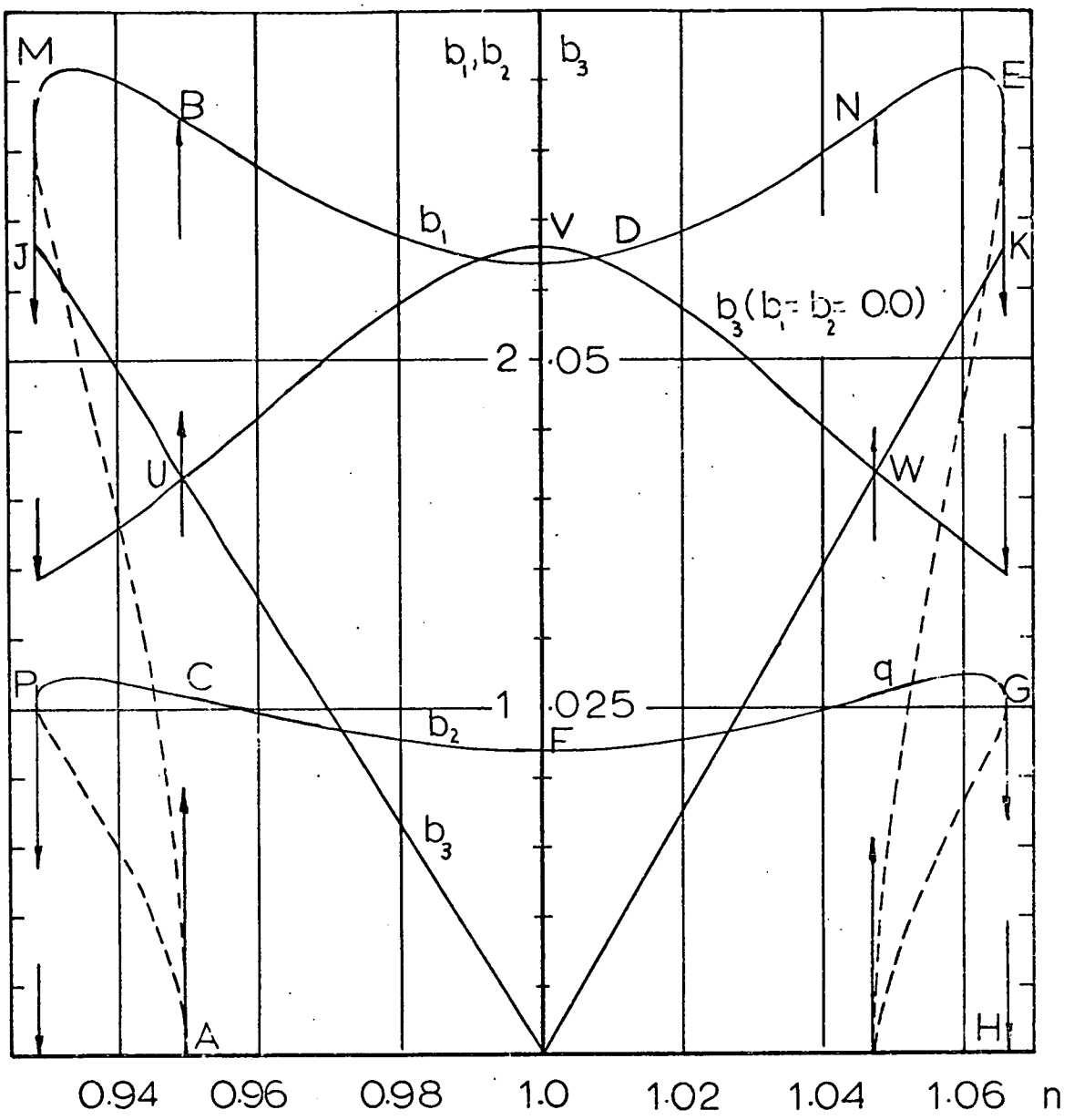


Fig.(IV.4) Three Mode Interaction, $\Gamma_3 = \Gamma_1 + \Gamma_2$

($\epsilon = 0.021$, $h/a = 1.0$, $l/a = 2.55$, $\bar{\zeta}_3 = 0.05$

$\bar{\zeta}_1 = \bar{\zeta}_2 = 0.0$)

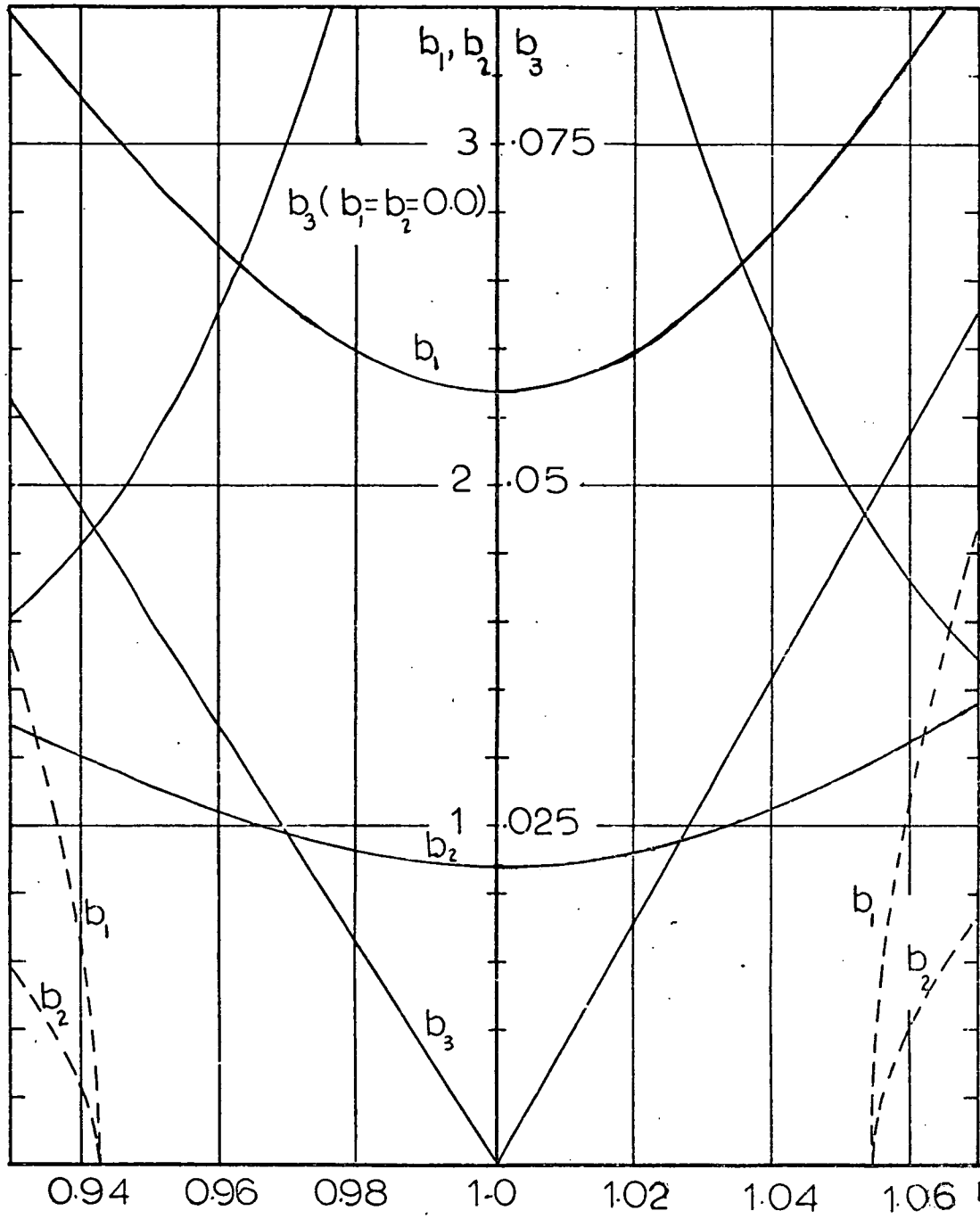


Fig(IV.5) Three Mode Interaction, $\Omega_3 = \Omega_1 + \Omega_2$

( $\epsilon = 0.021$, $h/a = 1.0$, $l/a = 2.55$, $\bar{\zeta}_3 = 0.025$

$\bar{\zeta}_1 = \bar{\zeta}_2 = 0.0$ )

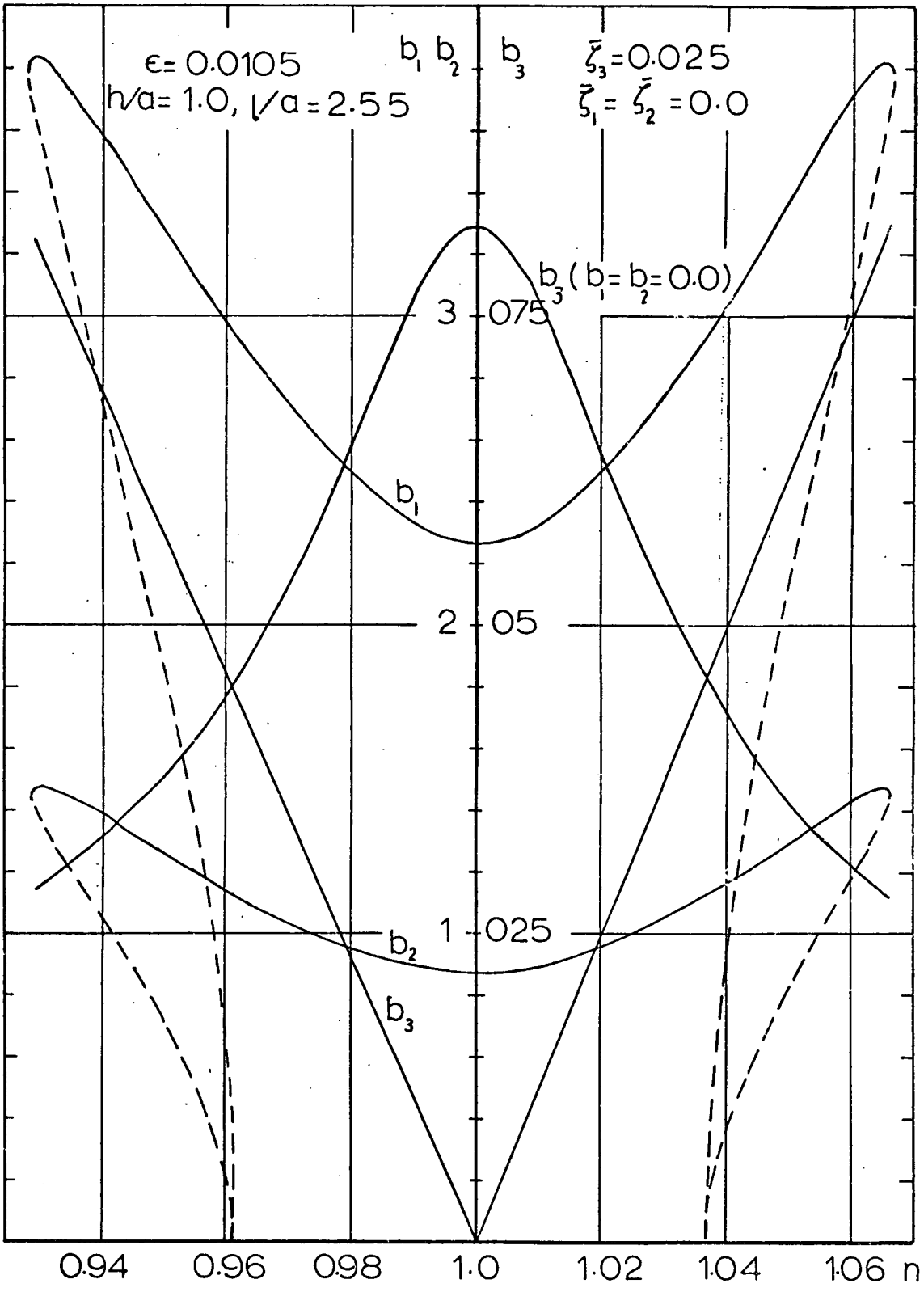


Fig.(IV.6) Three Mode Interaction, $r_3 = r_1 + r_2$

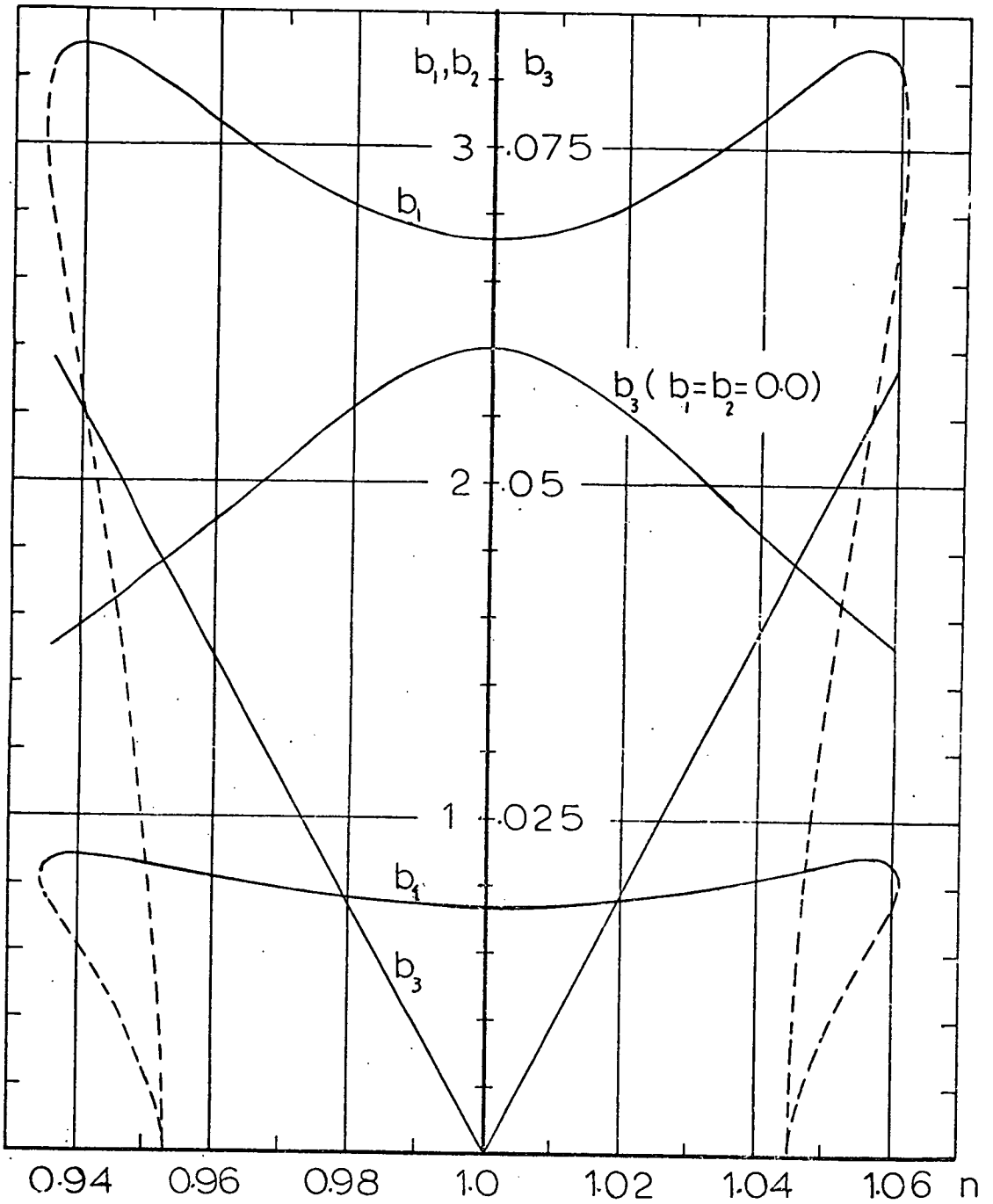


Fig(IV·7) Three Mode Interaction, $r_3 = r_1 + r_2$
($\epsilon$=.021, h/a=2.0, l/a=2.5, $\bar{\zeta}_3$=0.05, $\bar{\zeta}_1=\bar{\zeta}_2$=0.0)

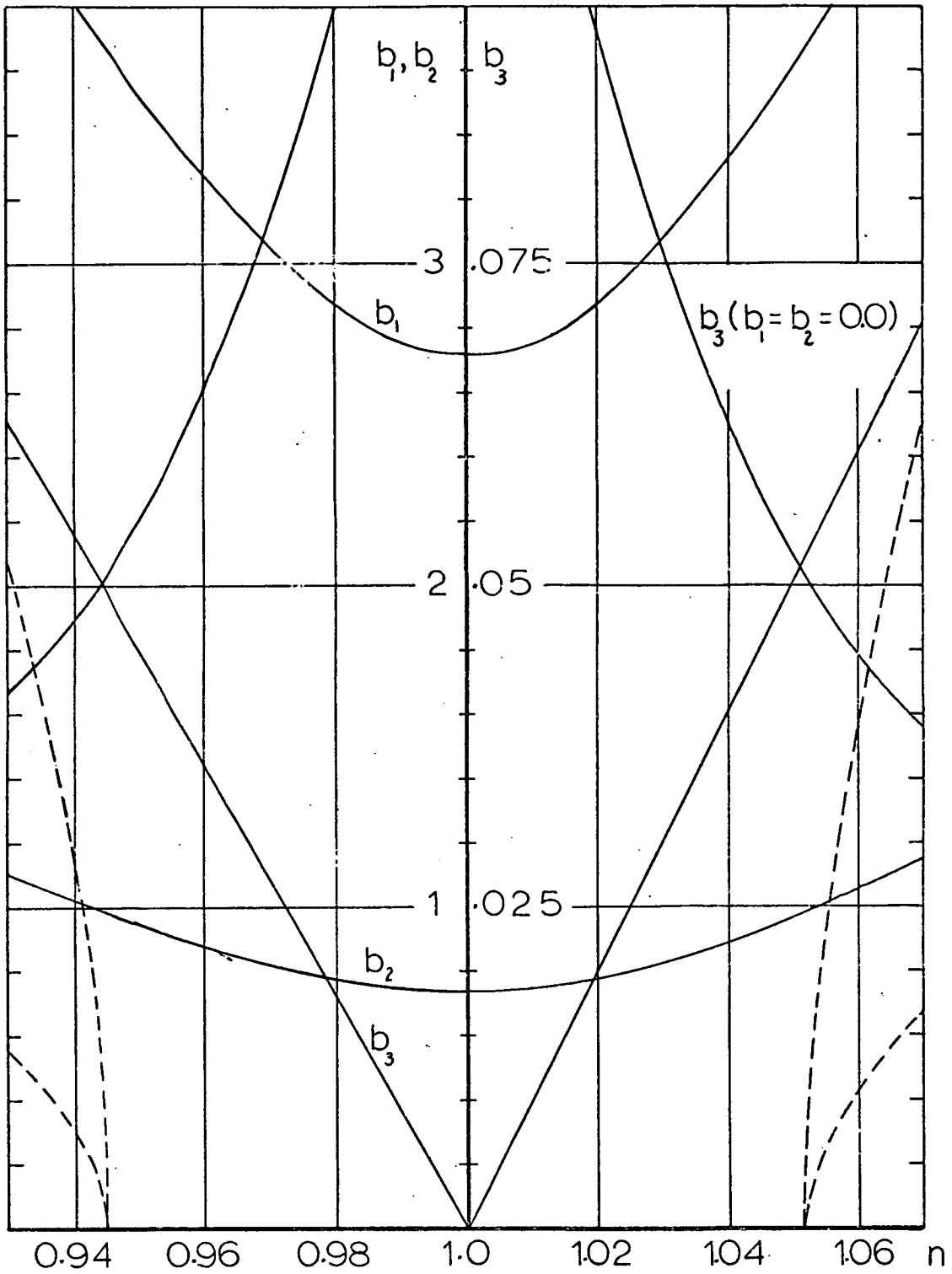


Fig(IV. 8) Three Mode Interaction, $r_3 = r_1 + r_2$
($\epsilon$=.021, h/a = 2, l/a = 2.5, $\bar{\zeta}_3$ =0.025, $\bar{\zeta}_1 = \bar{\zeta}_2$ =0.0)

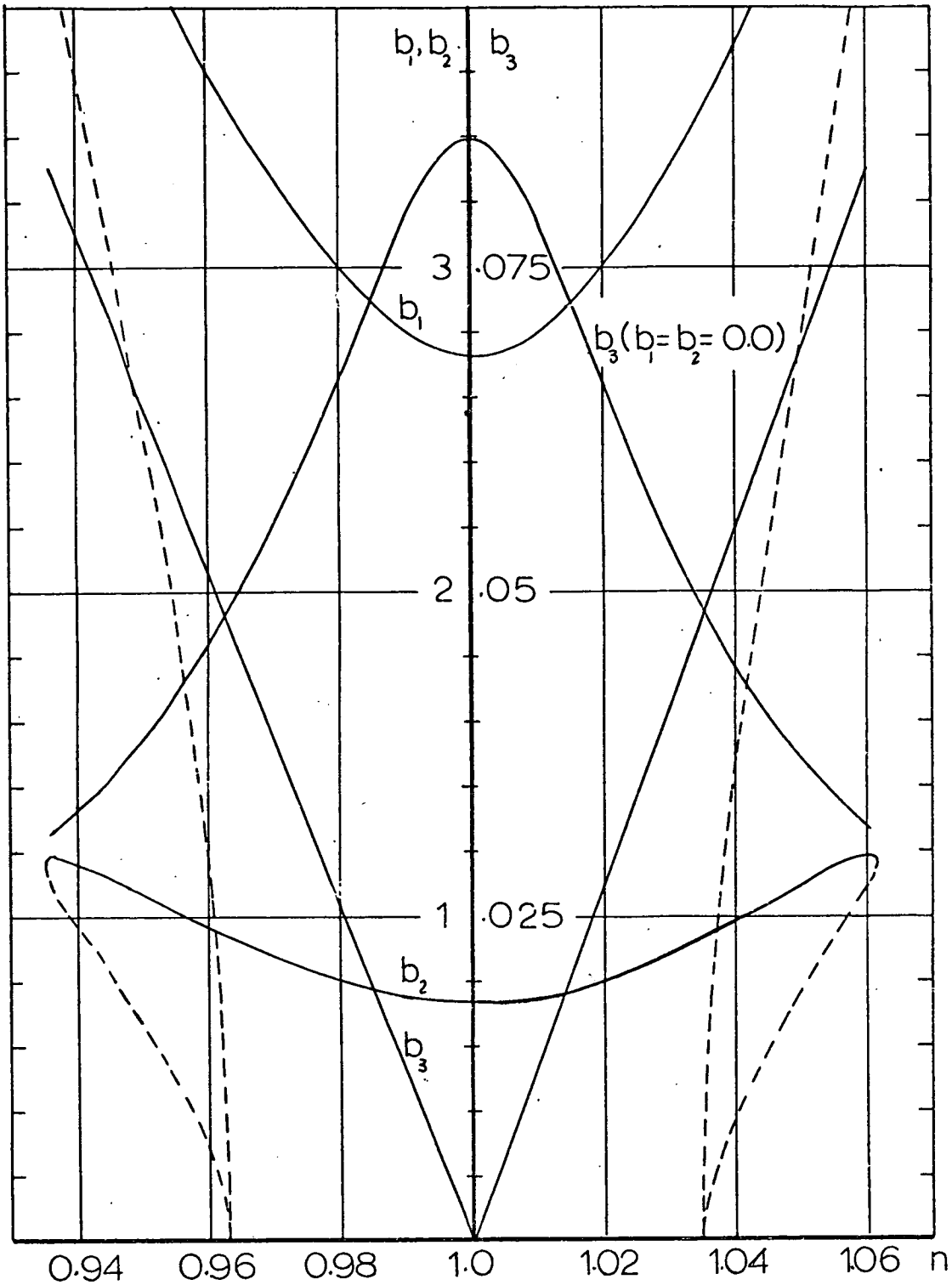


Fig(IV.9) Three Mode Interaction, $r_3 = r_1 + r_2$
($\epsilon$=.0105, h/a=2, l/a = 2.5, $\bar{\zeta}_3$ =.025, $\bar{\zeta}_1 = \bar{\zeta}_2$ =0.0 )

$b_2$ follow the curves BDE and CFG respectively with peaks at E and G at which $\frac{db_1}{dn} = \frac{db_2}{dn} = \infty$, (the second kind of vertical tangency), and the values $b_1$ and $b_2$ drop to point H. The mode $b_3$ is suppressed through the autoparametric action and meets the n axis at n=1.0 because $\zeta_1 = \zeta_2 = 0.0$, and instead of the linear resonance response of $b_3$ represented by equation (IV.52) and the curve UVW, the large response occurs in the first and second modes which exhibit large peaks on either side of resonance n=1. Haxton and Barr[H5] showed that if the internal resonance, in the present case $r_3 = r_1 + r_2$, is not met precisely the effect of imperfect tuning in this respect is to shift the diagram of Fig. (IV.4) to left or to right of n=1.

Case B $\eta_1/\eta_2 = S_1/S_2$

This relation is generated as a condition for consistency of the six equations, which are reduced to five if this condition holds. The damping ratios relation can be easily realised if the possible steady-state solutions of (IV.47), after neglecting third order terms, are considered.

Setting the left hand side of equations (IV.47) to zero and considering (IV.47a,c) gives

$$\frac{b_1^2}{b_2^2} = \left(\frac{S_2}{S_1}\right)^2 \left(\frac{C_6}{\bar{K}_3}\right) \qquad \text{(IV.53)}$$

where $\bar{K}_3 = -K_3$.

Considering (IV.47 b,d) gives

$$\frac{b_1^2}{b_2^2} = \frac{S_2}{S_1}\frac{\eta_2}{\eta_1}\frac{C_6}{\bar{K}_3} \qquad \text{(IV.54)}$$

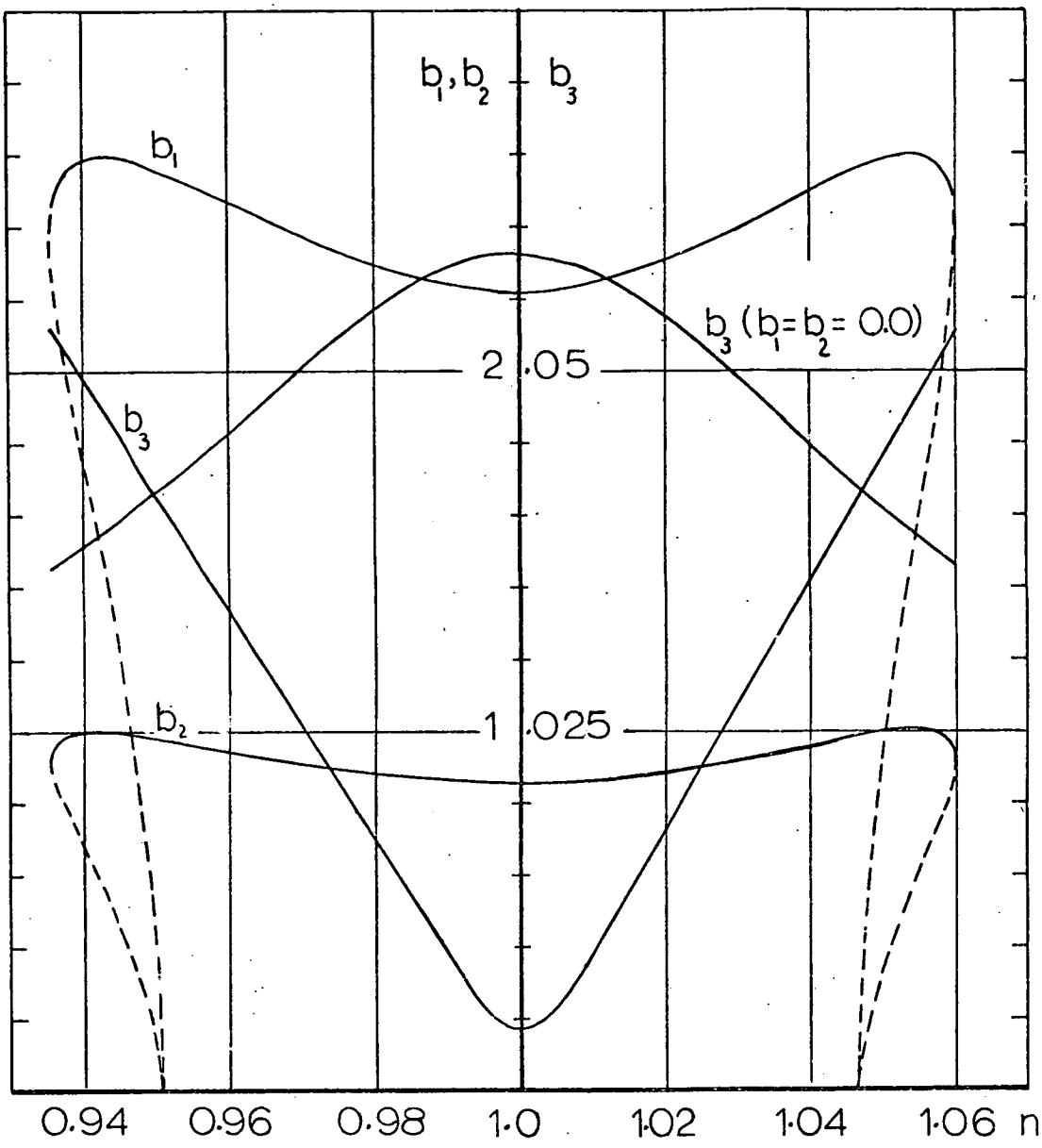


Fig.(IV.10) Three Mode Interaction, $r_3 = r_1 + r_2$
($\epsilon$=.021, h/a=1.0, l/a=2.55, $\bar{\zeta}_3$=.05, $\bar{\zeta}_1 = \bar{\zeta}_2$=.005)

$$\eta_1 / \eta_2 = r_1 / r_2$$

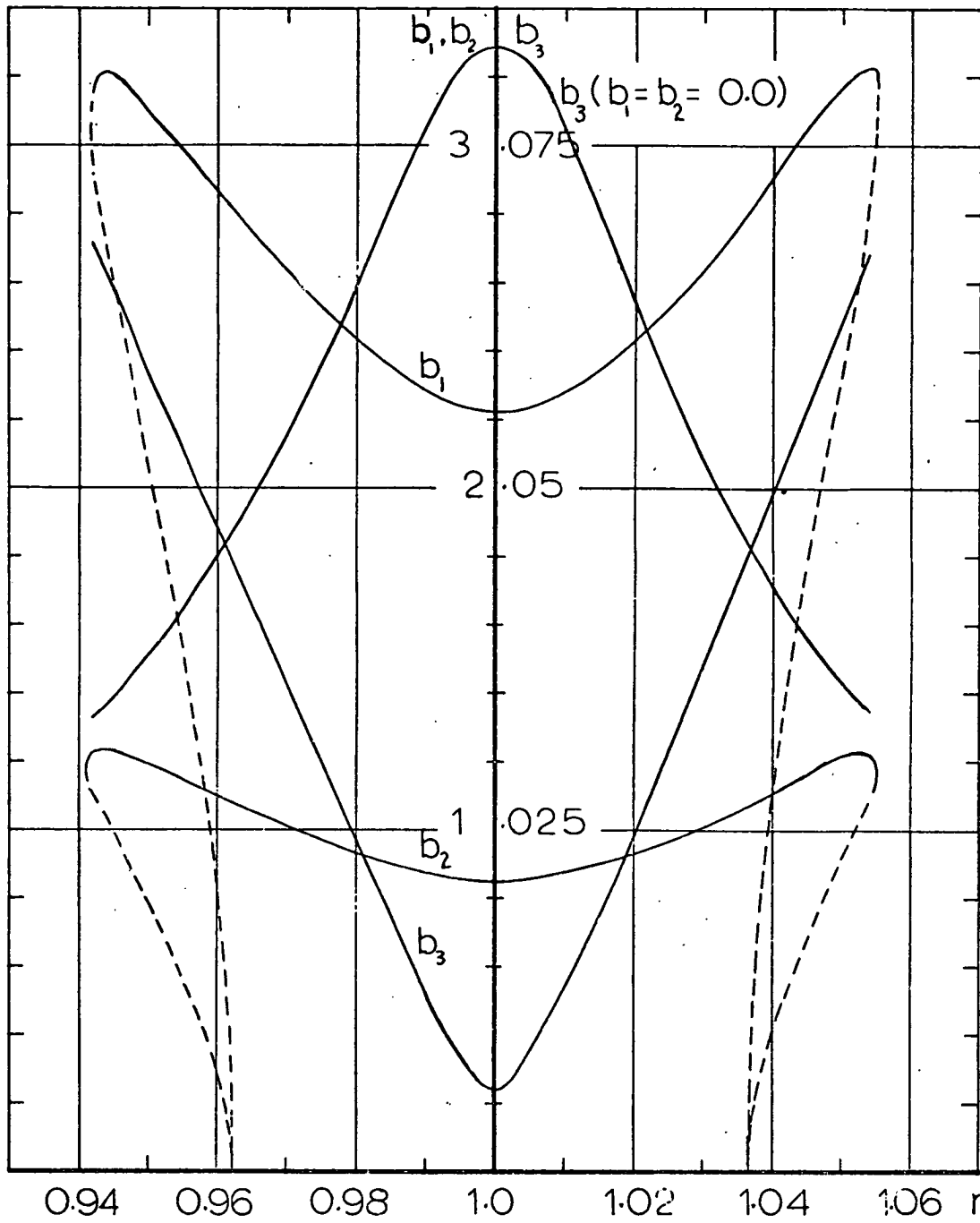


Fig(IV.11) Three Mode Interaction, $r_3 = r_1 + r_2$
($\epsilon$=·0105, h/a=1.0, l/a=2.55, $\bar{\zeta}_3$=·025, $\bar{\zeta}_1 = \bar{\zeta}_2$=.005)

$$\eta_1 / \eta_2 = r_1 / r_2$$

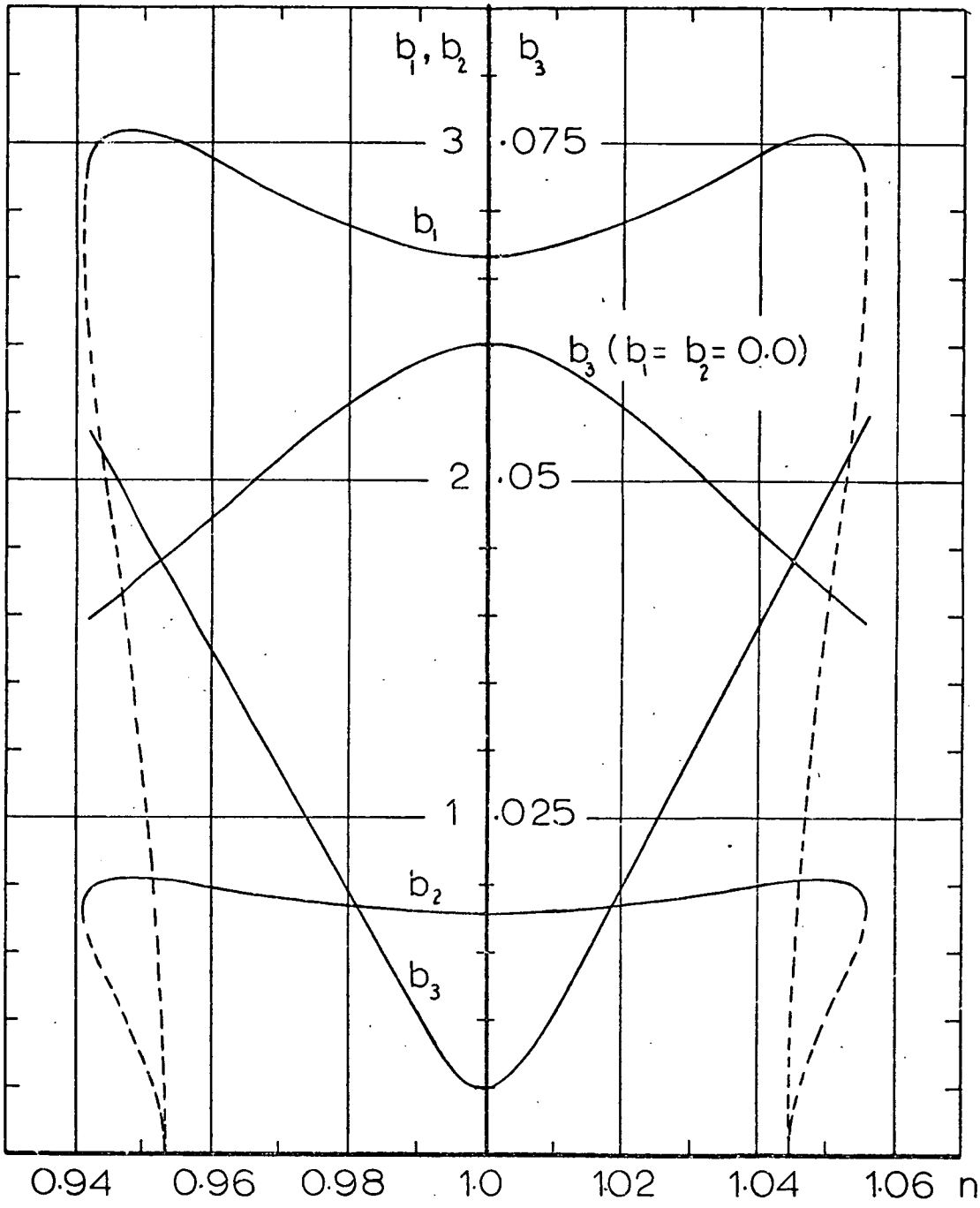


Fig.(IV.12) Three Mode Interaction, $r_3 = r_1 + r_2$
($\epsilon = .021$, $h/a = 2$, $l/a = 2.5$, $\bar{\zeta}_3 = .05$, $\bar{\zeta}_1 = \bar{\zeta}_2 = .005$)

$$\eta_1/\eta_2 = r_1/r_2$$

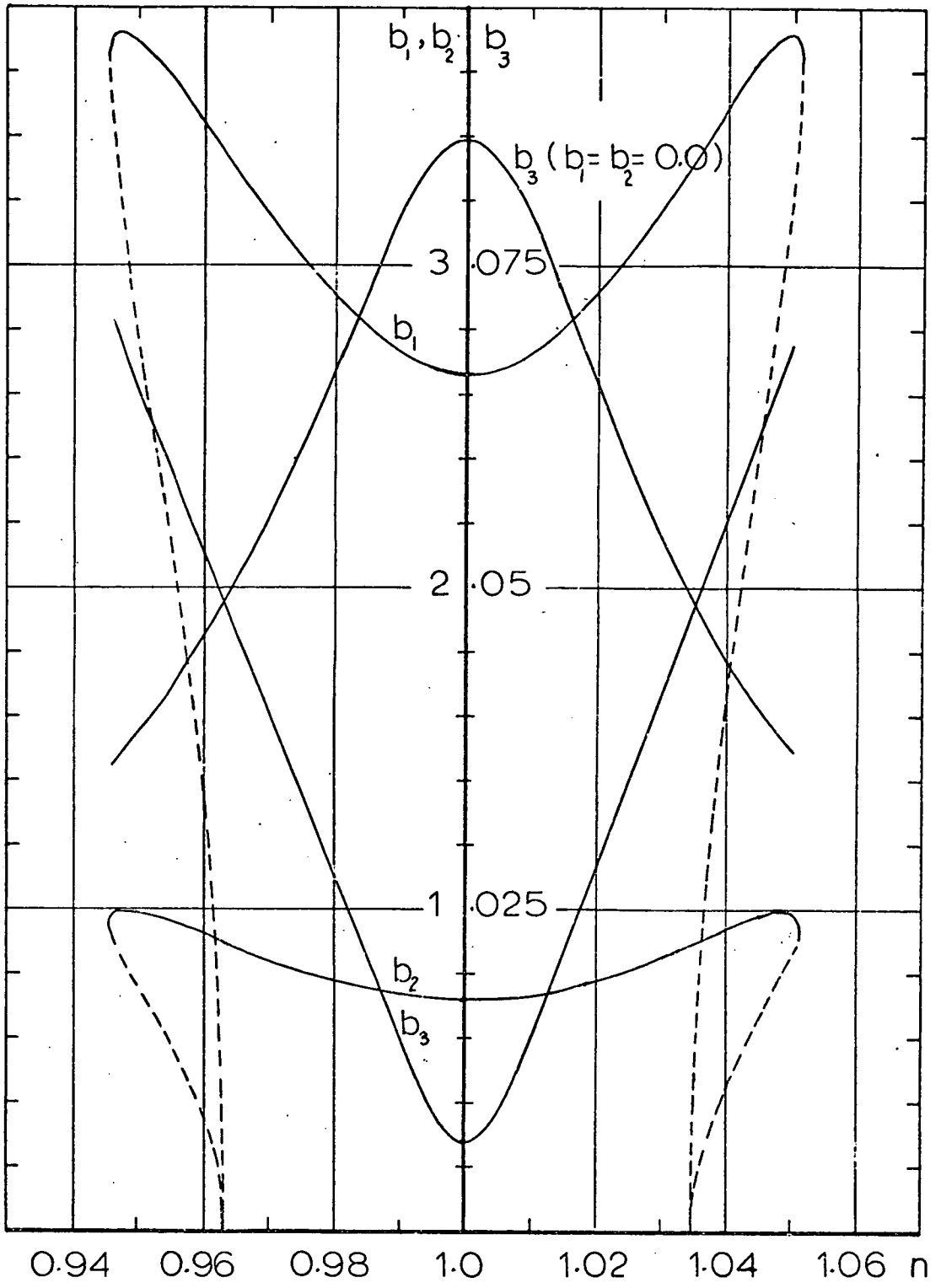


Fig(IV·13) Three Mode Interaction, $r_3 = r_1 + r_2$
($\epsilon$=.0105, h/a=2, l/a=2.5, $\bar{\zeta}_3$=.025, $\bar{\zeta}_1 = \bar{\zeta}_2$=.005)

$\eta_1/\eta_2 = r_1/r_2$

Another solution is obtained by squaring (IV.47a), (IV.47b) and adding and squaring (IV.47c), (IV.47d) and adding, the resulting relations are divided to give;

$$\frac{b_1^2}{b_2^2} = \left(\frac{S_2}{S_1}\right)^2\left(\frac{C_6}{\bar{K}_3}\right)\sqrt{\frac{[\gamma^2 + (\eta_2/S_2)^2]}{[\gamma^2 + (\eta_1/S_1)^2]}} \qquad \text{(IV.55)}$$

It can be seen that (IV.52-55) are consistent if $\eta_2/\eta_1 = S_2/S_1$. If this condition holds the other amplitudes are given by;

$$b_3^2 = 4S_1^2S_2^2\left(\frac{L_{47}^2}{C_6\,\bar{K}_3}\right)(\gamma^2 + \eta_1^2/S_1^2) \qquad \text{(IV.56)}$$

and

$$b_2^2 = -4S_1^2\left(\frac{L_{47}}{C_6}\right)(\gamma^2 - \eta_1\eta_3) \pm 2\frac{S_1}{C_6}\sqrt{\frac{\bar{K}_3C_6}{S_2^2} - 4\gamma^2L_{47}^2(\eta_1 + S_1\eta_3)^2} \qquad \text{(IV.57)}$$

The amplitude response curves given by (IV.54, 56, 57) are shown in Figs. (IV.10-13). The influence of $\eta_1$ (or $\eta_2$) on the behaviour of the system appears by the offset amplitude of $b_3$ at n=1.

Case C $\eta_1/\eta_2 \neq S_1/S_2$

If the relation $\eta_1/\eta_2 = S_1/S_2$ is not satisfied, then the solution of equation (IV.47) with the presence of their left hand terms should be investigated. However, the available tools of analysis appear to be inadequate to find an explicit analytical solution. A numerical solution of the simultaneous equations will give an idea as to whether the system possesses a steady state or not. Inserting the six equations in a CSMP (Continuous System Modeling Program) simulation and using the Milne integration routine gives the results shown in Figs. (IV.14,15). With zero initial

conditions for $b_1$ and $b_2$ the CSMP simulation is indetermined since there will be terms involving division (zero by zero) such as $b_2 b_3 / b_1$ and the result is $(\frac{0}{0})$ which is invalid. Initial values for $b_1$ and $b_2$ should be assumed. The importance of this fact may be visualised in the experimental work in which the steady state responses cannot be created unless initial values have been applied. The numerical results show that a steady state solution could be achieved only for the amplitudes $b_1, b_2, b_3$ and the phase $\gamma$ but $\varphi$ and $\theta$ exhibit only unsteady solution whose degree of unsteadiness decreases as $n \rightarrow 1$. At n=1 the system possesses a complete steady state. The normal resonance curve does not exist within the frequency range $n \approx 1 \pm 0(\epsilon)$ where the autoparametric action takes place, and the upper branches of $b_1$ and $b_2$ are obtained. The peaks or collapse amplitudes that are found in cases (A) and (B) do not appear as the solution is virtually unstable. The positions where $b_3$ changes its behaviour from normal linear resonance response to that similar to autoparametric absorber define the region of stable modes for $b_1$ and $b_2$.

The CSMP simulation does not delineate the complete picture of the stable solution of $b_1$, $b_2$ and $b_3$, where the parts MB,NE on $b_1$; PC, qG on $b_2$ and UJ,WK on $b_3$ of Fig. (IV.4) do not exist in Figs. (IV.14,15). These parts could appear in the CSMP solution if the proper initial conditions were inserted. The transient solution for selected detuning parameters (n=1.04 and 1.0) is delineated in Figs. (IV.16,17). For n=1 it is evident that the interaction takes place in a form of energy exchange between the first two modes and the third mode.

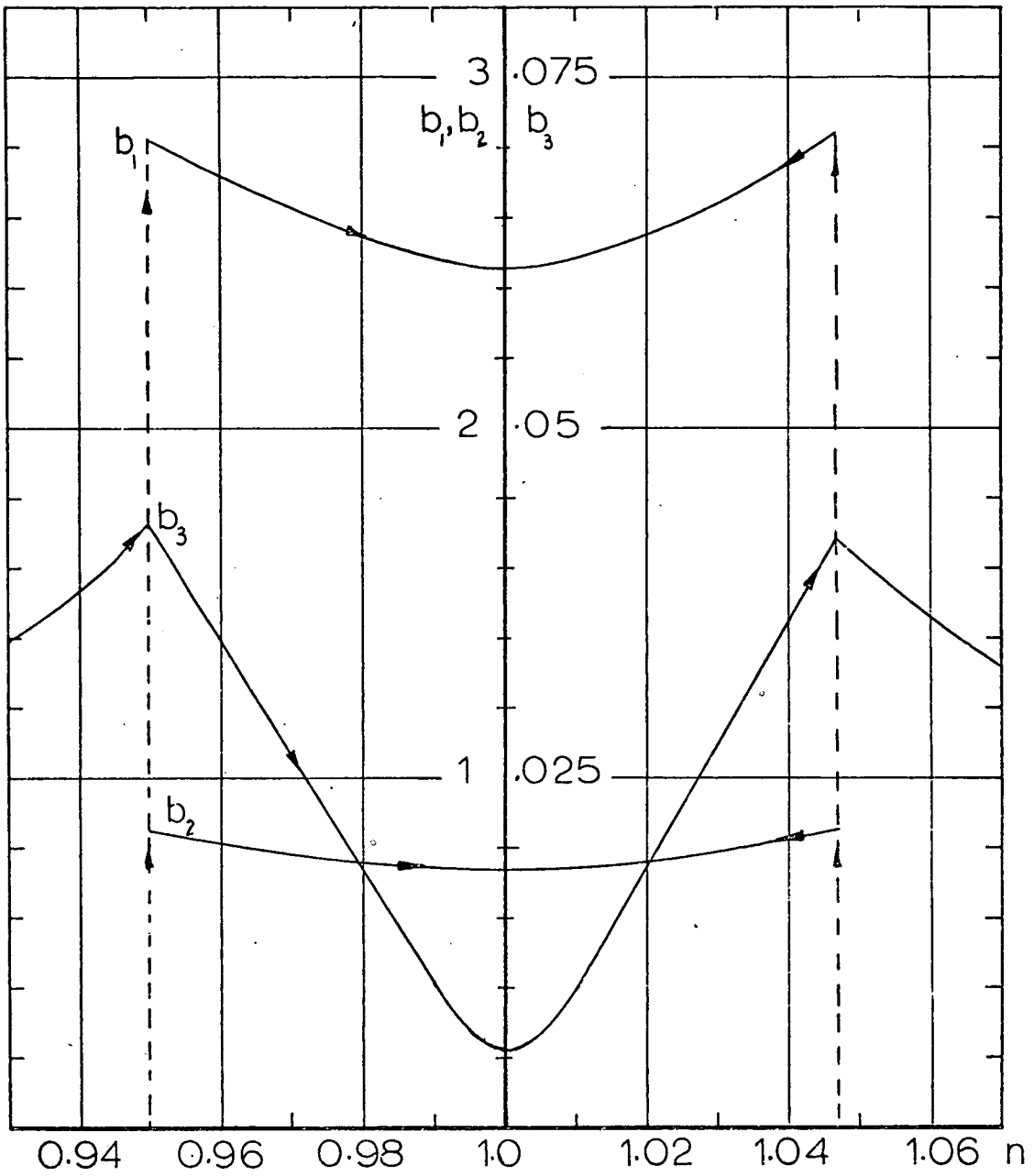


Fig(IV·14) CSMP Solution of Three Mode Interaction when $\eta_1/\eta_2 \neq r_1/r_2$, $r_3 = r_1 + r_2$ ($\epsilon$ =·021 ,h/a=1, l/a = 2·55, $\bar{\zeta}_3$ =·05, $\bar{\zeta}_1$ =·005 $\bar{\zeta}_2$ =·0085)

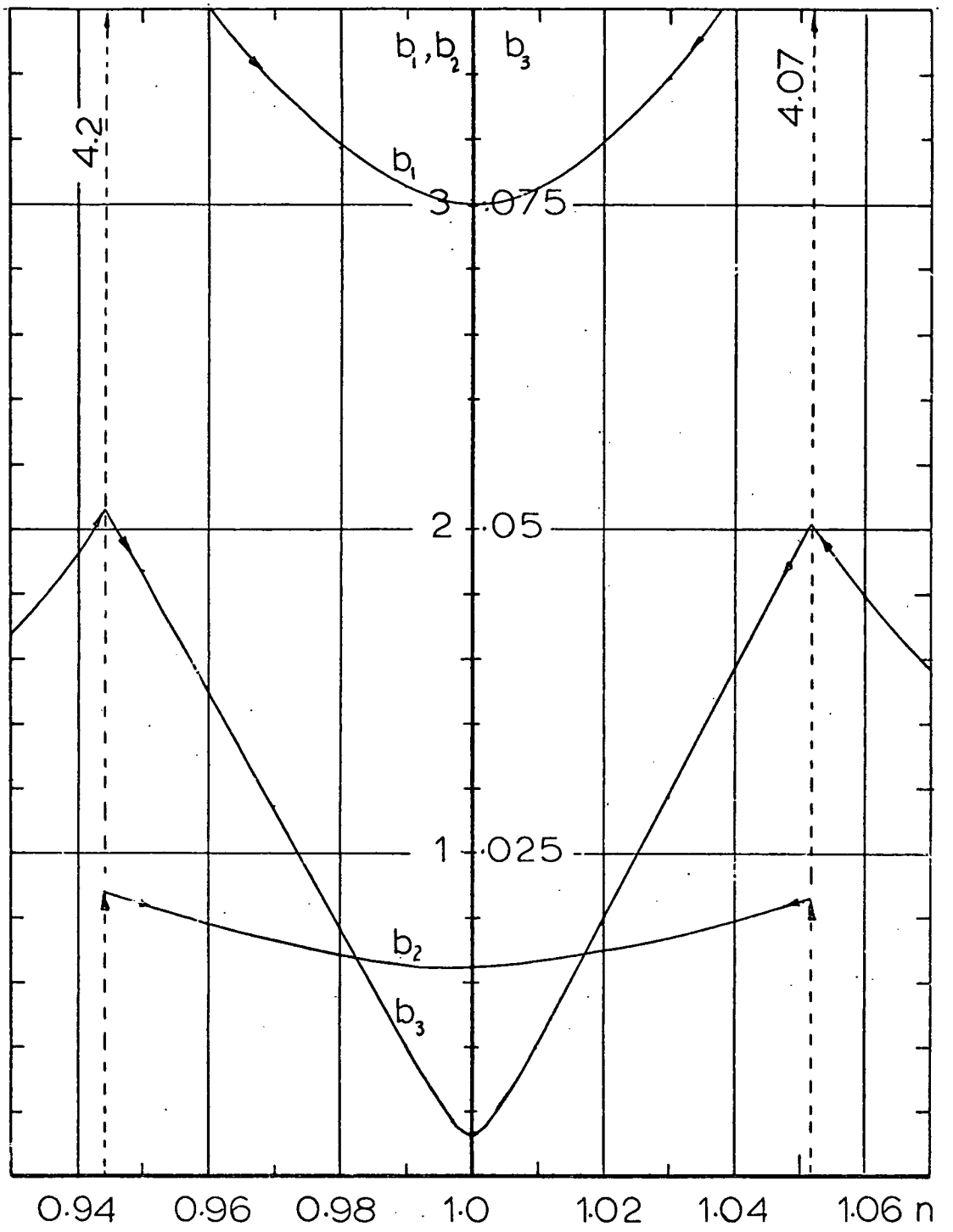


Fig (IV.15) CSMP Solution of Three Mode Interaction when $\eta_1/\eta_2 \neq r_1/r_2$, $r_3 = r_1 + r_2$ ($\epsilon$=·021, h/a = 2, l/a = 2·5, $\bar{\zeta}_3$ =·05, $\bar{\zeta}_1$ =·0025 $\bar{\zeta}_3$ =·004)

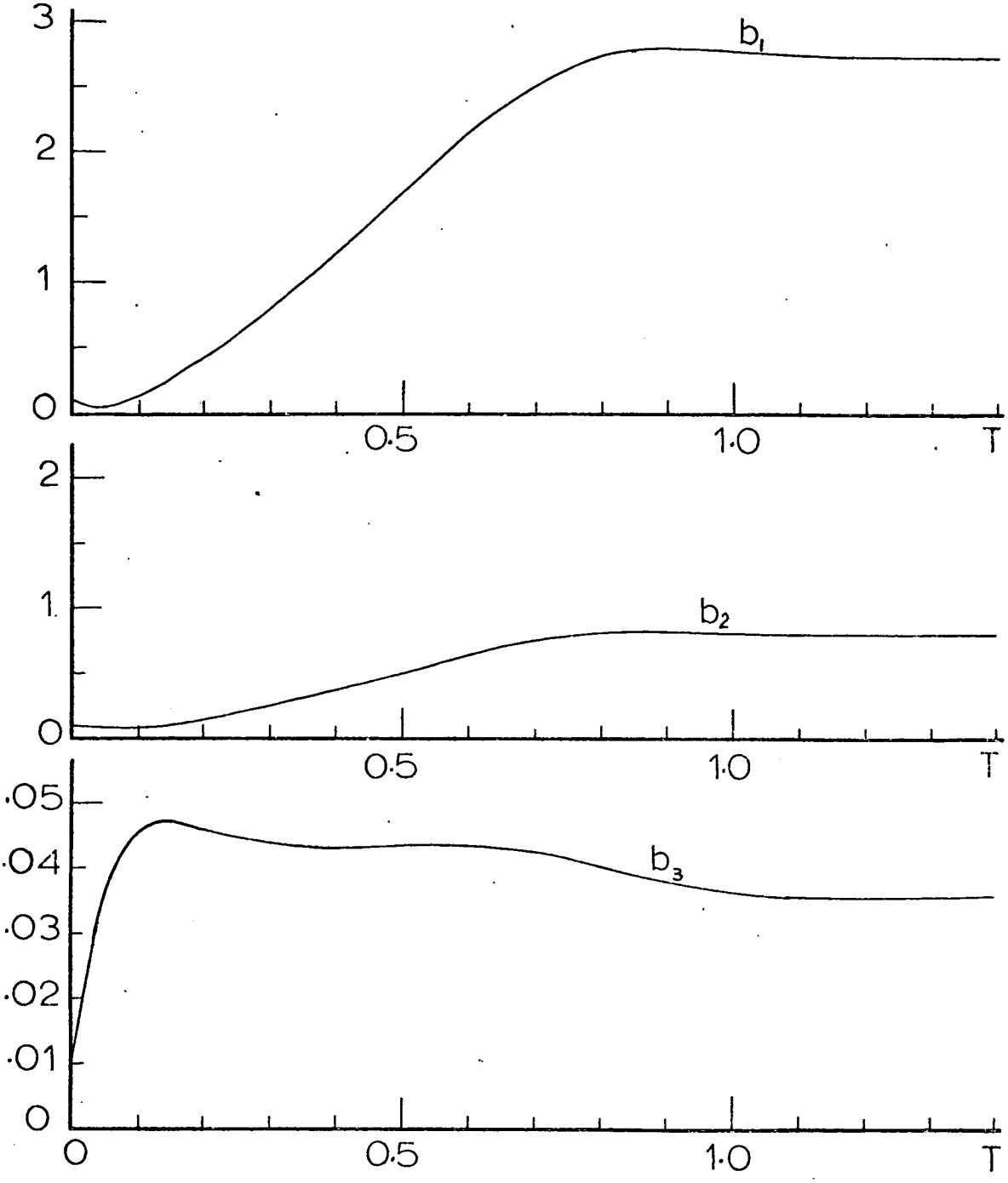


Fig(IV.16) CSMP Transient Response of Three Mode Interaction, $r_3 = r_1 + r_2$, $\eta_1/\eta_2 \neq r_1/r_2$ $n = 1.04$, $\epsilon = .021$, $h/a = 1.0$, $l/a = 2.55$, $\bar{\zeta}_1 = .005$ $\bar{\zeta}_2 = .0085$, $\bar{\zeta}_3 = .05$

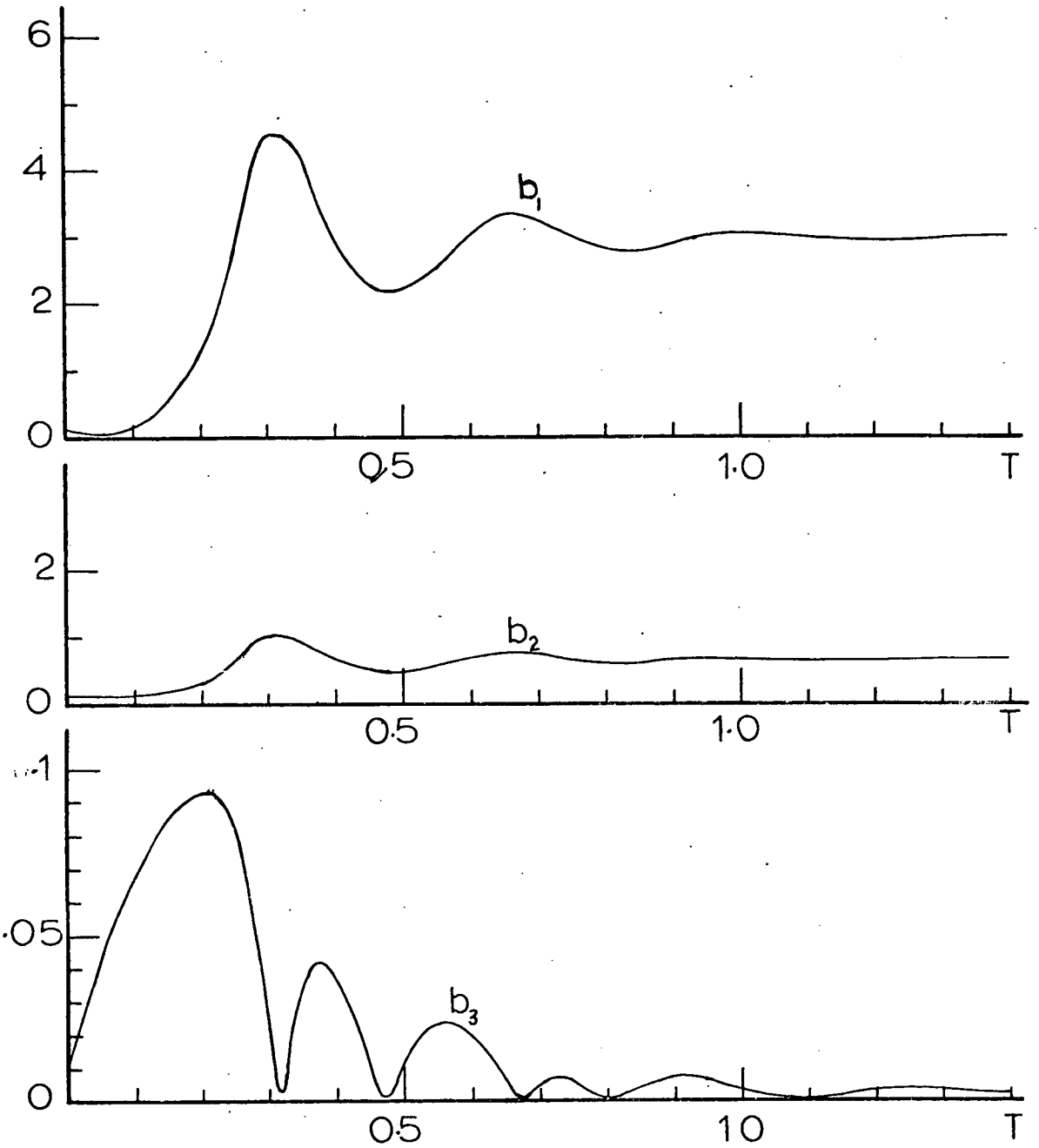


Fig(IV·17) CSMP Transient Solution of Three Mode Interaction, $r_3 = r_1 + r_2$, $\eta_1/\eta_2 \neq r_1/r_2$, $\epsilon = \cdot 021$ $h/a = 2$, $l/a = 2.5$, $n = 1.0$, $\bar{\zeta}_1 = \cdot 0025$, $\bar{\zeta}_2 = \cdot 004$ $\bar{\zeta}_3 = \cdot 05$

## IV.4 Autoparametric Resonance of Differential Type

$$\left.\begin{aligned} r_3 &= r_1 - r_2 \\ r_3 &= n\nu \end{aligned}\right\} \qquad \text{(IV.58)}$$

Considering quadratic terms in the first order perturbation equations (IV.31, 33 and 35) and transferring terms which resonate under conditions (IV.58), the variational equations become;

$$\left.\begin{aligned}
-2r_1P_1\dot{\varphi} &= \epsilon\left\{\epsilon^{-1}(S_1^2\nu^2 - r_1^2)P_1 + \tfrac{1}{2}C_6 r_3^2 P_2 P_3 \cos(\gamma+\theta-\varphi)\right\} \\
-2r_1\dot{P}_1 &= \epsilon\left\{2r_1^2\zeta_1 P_1 - \tfrac{1}{2}C_6 r_3^2 P_2 P_3 \sin(\gamma+\theta-\varphi)\right\} \\
-2r_2P_2\dot{\theta} &= \epsilon\left\{\epsilon^{-1}(S_2^2\nu^2 - r_2^2)P_2 + \tfrac{1}{2}\bar{K}_3 r_3^2 P_1 P_3 \cos(\gamma+\theta-\varphi)\right\} \\
-2r_3\dot{P}_2 &= \epsilon\left\{2r_2^2\zeta_2 P_2 + \tfrac{1}{2}\bar{K}_3 r_3^2 P_1 P_3 \sin(\gamma+\theta-\varphi)\right\} \\
-2r_3P_3\dot{\gamma} &= \epsilon\left\{\epsilon^{-1}(S_3^2\nu^2 - r_3^2)P_3 - \tfrac{1}{2}r_3^2 L_{74} P_1 P_2 \cos(\gamma+\theta-\varphi) + f\cos\gamma\right\} \\
-2r_3\dot{P}_3 &= \epsilon\left\{2r_3^2\zeta_3 P_3 - \tfrac{1}{2}r_3^2 L_{74} P_1 P_2 \sin(\gamma+\theta-\varphi) + f\sin\gamma\right\}
\end{aligned}\right\} \qquad \text{(IV.59)}$$

where

$$\bar{K}_3 = -K_3$$

$$L_{74} = L_7(r_1^2+r_2^2) - L_4 r_1 r_2$$

These equations are transformed to a simple form by using the following parameters:-

$$P_i = \frac{b_i}{r_3}\sqrt{\frac{f}{|L_{74}|}} \quad , \quad \tau = \frac{2T}{\epsilon\sqrt{f|L_{74}|}} \quad , \quad \gamma = \frac{r_3^2 - \nu^2}{\epsilon r_3\sqrt{f|L_{74}|}}$$

$$\eta_i = \frac{2r_i\zeta_i}{\sqrt{f|L_{74}|}} \quad , \quad S_1 = r_1/r_3 \ , \ S_2 = \frac{r_2}{r_3} \ , \ S_3 = 1$$

$$\psi_1 = \gamma + \theta - \varphi$$

.....(IV.60)

Introducing (IV.60) into (IV.59) gives;

$$\left.\begin{aligned}
-b_1\dot{\varphi} &= -S_1\gamma b_1 + \tfrac{1}{2}\left(\frac{C_6}{S_1|L_{74}|}\right)b_2b_3\cos\psi_1 \\
-\dot{b_1} &= \eta_1 b_1 - \tfrac{1}{2}\left(\frac{C_6}{S_1|L_{74}|}\right)b_2b_3\sin\psi_1 \\
-b_2\dot{\theta} &= -S_2\gamma b_2 + \tfrac{1}{2}\left(\frac{\bar{K}_3}{S_2|L_{74}|}\right)b_1b_3\cos\psi_1 \\
-\dot{b_2} &= \eta_2 b_2 + \tfrac{1}{2}\left(\frac{\bar{K}_3}{S_2|L_{74}|}\right)b_1b_3\sin\psi_1 \\
-b_3\dot{\gamma} &= -\gamma b_3 - \tfrac{1}{2}\left(\frac{L_{74}}{|L_{74}|}\right)b_1b_2\cos\psi_1 + \cos\gamma \\
-\dot{b_3} &= \eta_3 b_3 - \tfrac{1}{2}\left(\frac{L_{74}}{|L_{74}|}\right)b_1b_2\sin\psi_1 + \sin\gamma
\end{aligned}\right\} \qquad (IV.61)$$

Setting the left hand side of (IV.61) to zero, one redundant equation is obtained as in the previous section. Proceeding on the same lines of analysis for the various cases:

Case A) $\eta_1 = \eta_2 = 0$

The solution is found to be,

$$\left.\begin{aligned} b_3 &= \frac{2\gamma S_1 S_2 L_{74}}{\sqrt{C_6 \bar{K}_3}} \\ b_1 &= \pm b_2 \frac{S_2}{S_1} \sqrt{\frac{C_6}{\bar{K}_3}} \\ b_2^2 &= \frac{4}{C_6} S_1^2 \left\{ - L_{74}\gamma^2 \pm \sqrt{\frac{\bar{K}_3 C_6}{4S_1^2 S_2^2} - L_{74}^2 \gamma^2 \eta_3^2} \right\} \end{aligned}\right\} \quad \text{(IV.62)}$$

There is another solution with $b_1 = b_2 = 0$ and $b_3$ is given by (IV.52). Theoretical amplitude responses are given in Figs. (IV.18,19) and follow the same argument as section ( IV.3).

Case B) $\eta_1/\eta_2 = s_1/s_2$

The solution is,

$$b_3 = \pm 2S_1 S_2 \left| L_{74} \right| \sqrt{\frac{[\gamma^2 + (\eta_1/S_1)^2}{C_6 \bar{K}_3}}$$

$$b_1^2 = \left(\frac{C_6}{\bar{K}_3}\right)\left(\frac{S_2}{S_1}\right)^2 b_2^2$$

$$b_2^2 = -4\left(\frac{L_{74} S_1^2}{C_6}\right)(\gamma^2 - \eta_1\eta_3) \pm 2\frac{S_1}{C_6}\sqrt{\frac{\bar{K}_3 C_6}{S_2^2} - 4\gamma^2 L_{74}^2 (\eta_1 + S_1\eta_3)^2}$$

.....(IV.63)

The main features of this solution are similar to those of section IV.3B, and the response curves are delineated in Figs. (IV.20, 21).

Case C) $\eta_1/\eta_2 \neq s_1/s_2$

The same treatment and comments as given in IV.3C are applied for this case. Numerical solutions using the CSMP simulation

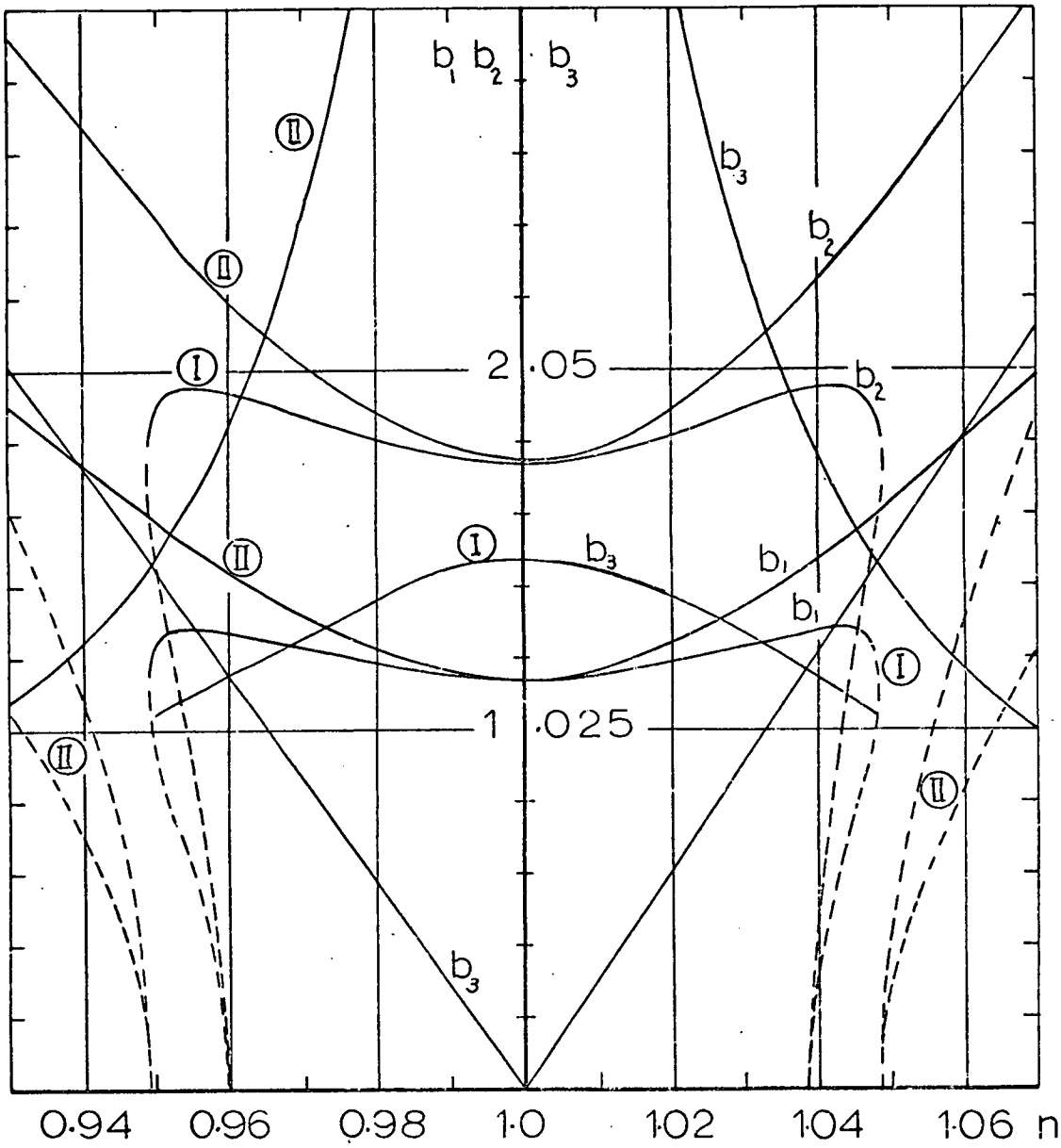


Fig(IV.18) Three Mode Interaction, $\gamma_3 = \gamma_1 - \gamma_2$
($\epsilon = 021$, $h/a = 1$, $l/a = 1.22$, $\bar{\zeta}_1 = \bar{\zeta}_2 = 0.0$
(I) $\bar{\zeta}_3 = 0.05$, (II) $\bar{\zeta}_3 = 0.01$)

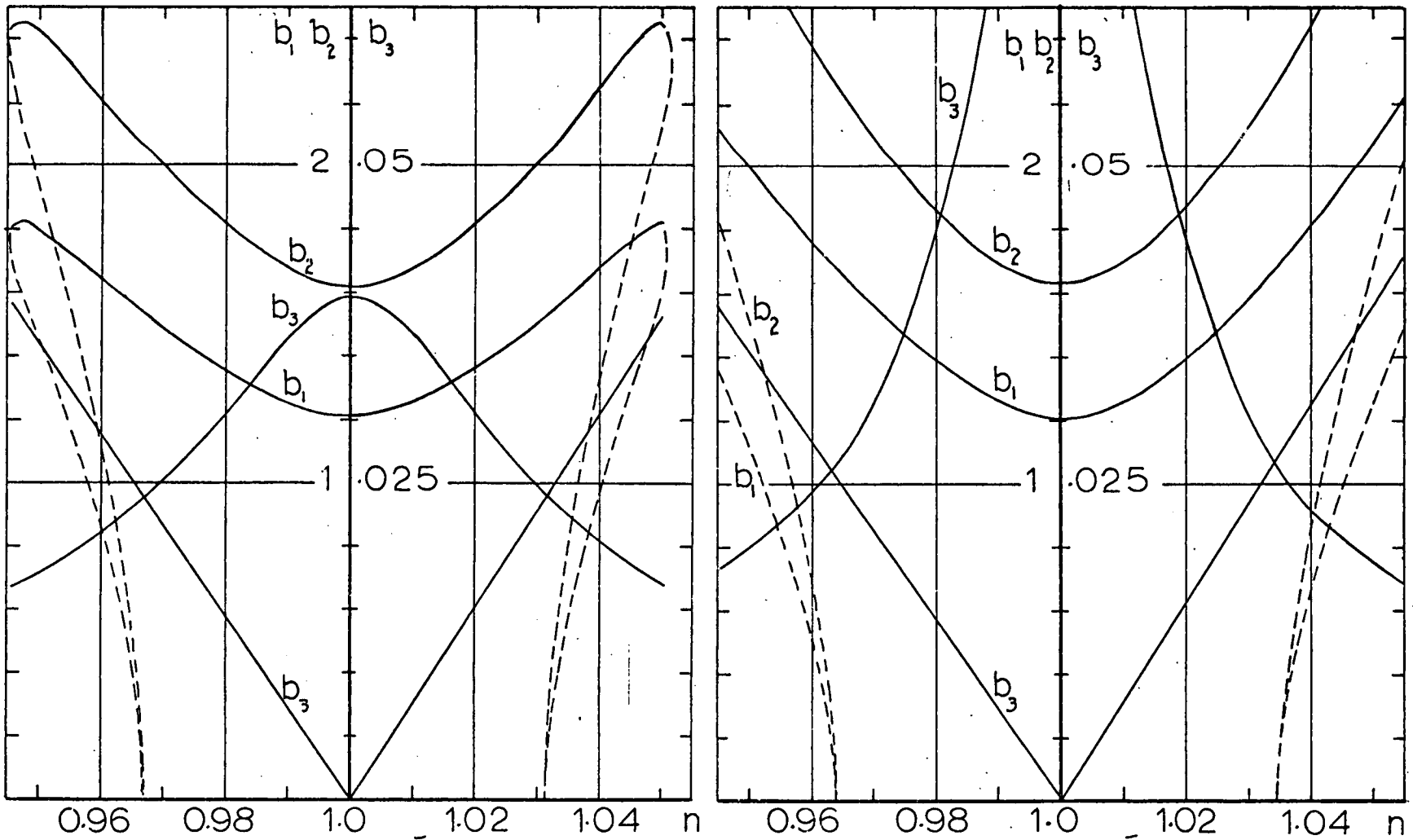


(a) $\bar{\zeta}_3 = 0.025$ (b) $\bar{\zeta}_3 = 0.01$

Fig(IV.19) Three Mode Interaction, $r_3 = r_1 - r_2$

($\epsilon$=.0105, $h/a = 2$, $l/a = 1.22$, $\bar{\zeta}_1 = \bar{\zeta}_2 = 0.0$)

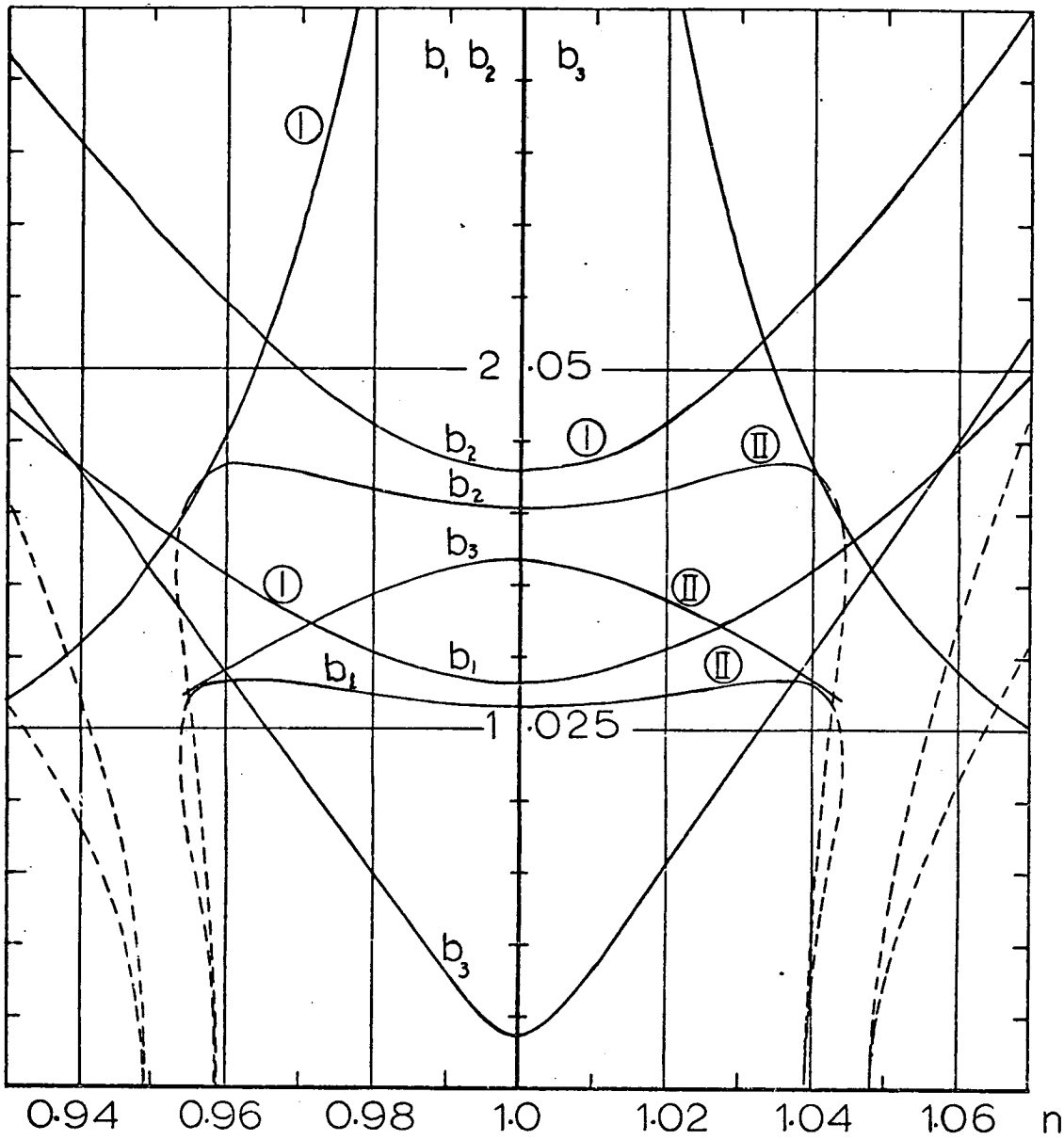


Fig (IV·20) Three Mode Interaction, $r_3 = r_1 - r_2$
($\epsilon$=.021, $h/a = 1.0$, $l/a = 1.22$, $\eta_1/\eta_2 = r_1/r_2$
$\bar{\zeta}_1 = \bar{\zeta}_2 = 0.005$, (I) $\bar{\zeta}_3 = .01$ (II) $\bar{\zeta}_3 = .05$

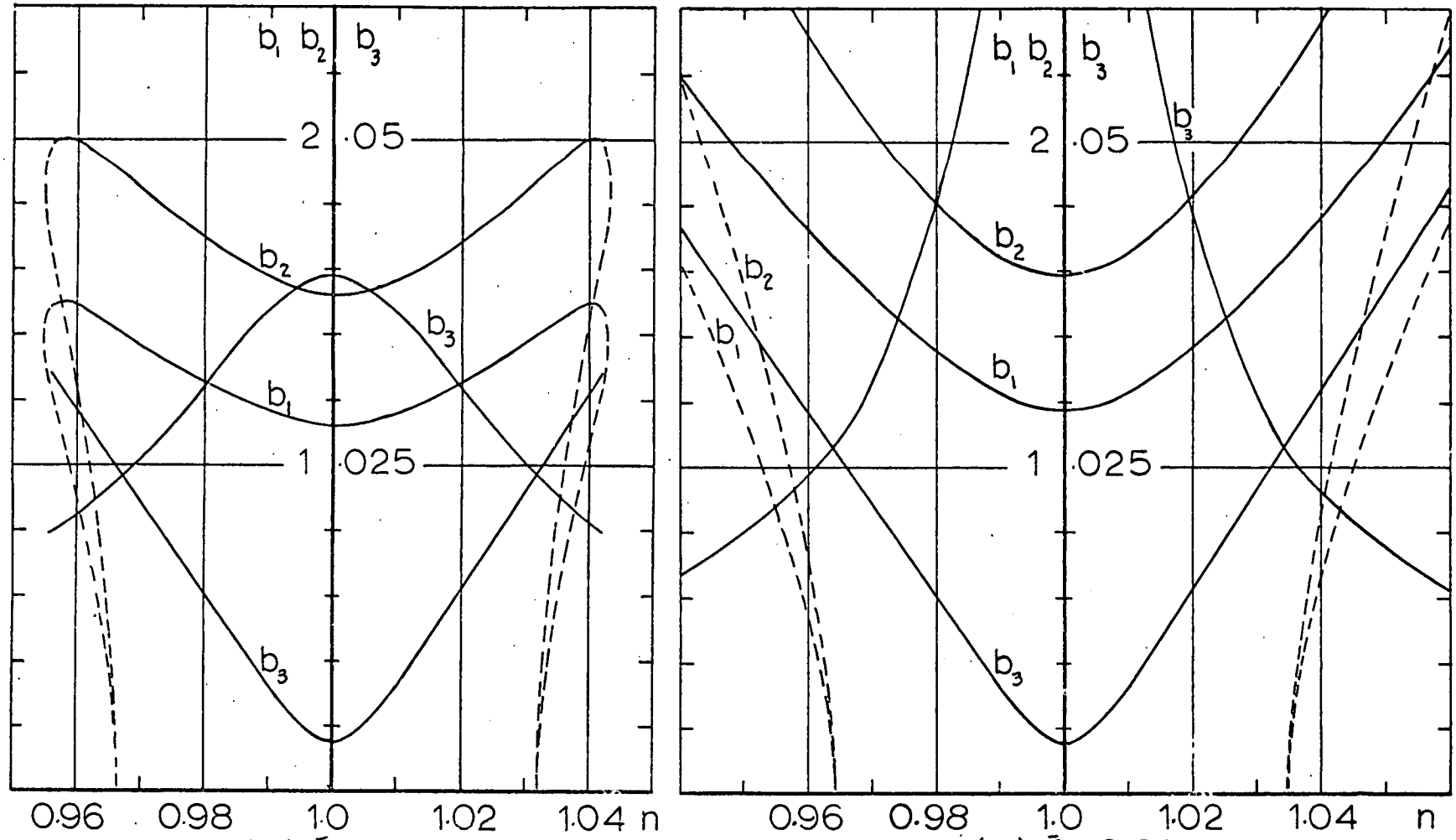


Fig(IV·21) Three Mode Interaction, $r_3 = r_1 - r_2$, $\eta_1/\eta_2 = r_1/r_2$

($\epsilon$=·0105, $h/a = 2$, $l/a = 1.22$, $\bar{\zeta}_1 = \bar{\zeta}_2 = .005$)

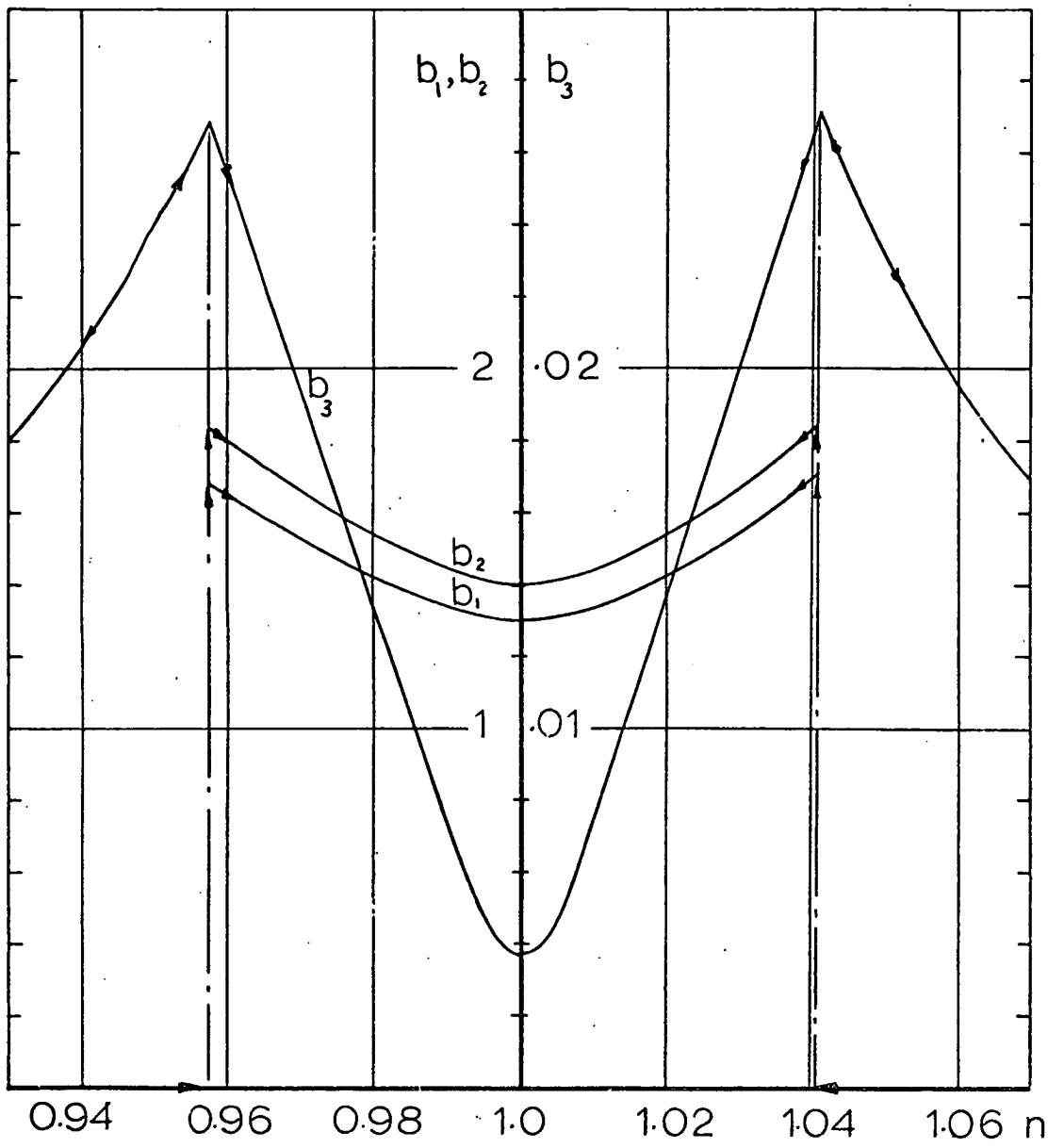


Fig(IV.22) CSMP Solution of Three Mode Interaction, when $\eta_1/\eta_2 \neq r_1/r_2$ , $r_3 = r_1 - r_2$ ( $\epsilon = .0105$, $h/a = 1$, $l/a = 1.22$, $\bar{\zeta}_3 = .025$, $\bar{\zeta}_1 = .0025$, $\bar{\zeta}_2 = .005$ )

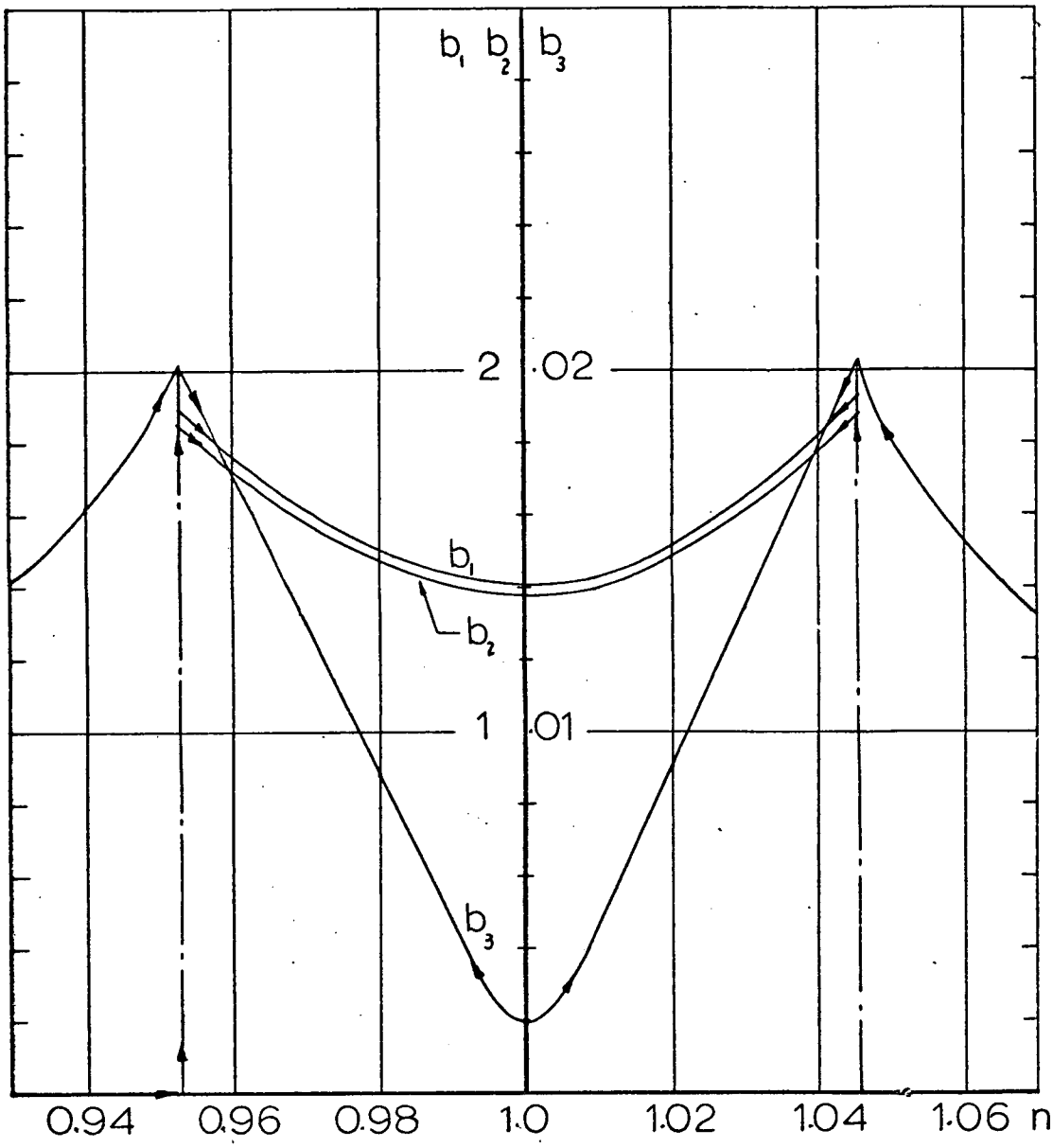


Fig (IV.23) CSMP Solution of Three Mode Interaction $r_3 = r_1 - r_2$, $\eta_1/\eta_2 \neq r_1/r_2$, $\bar{\zeta}_3 = .025$ $\bar{\zeta}_1 = .0025$, $\bar{\zeta}_2 = .005$, $\epsilon = .0105$, $h/a = 2$, $l/a = 1.2$

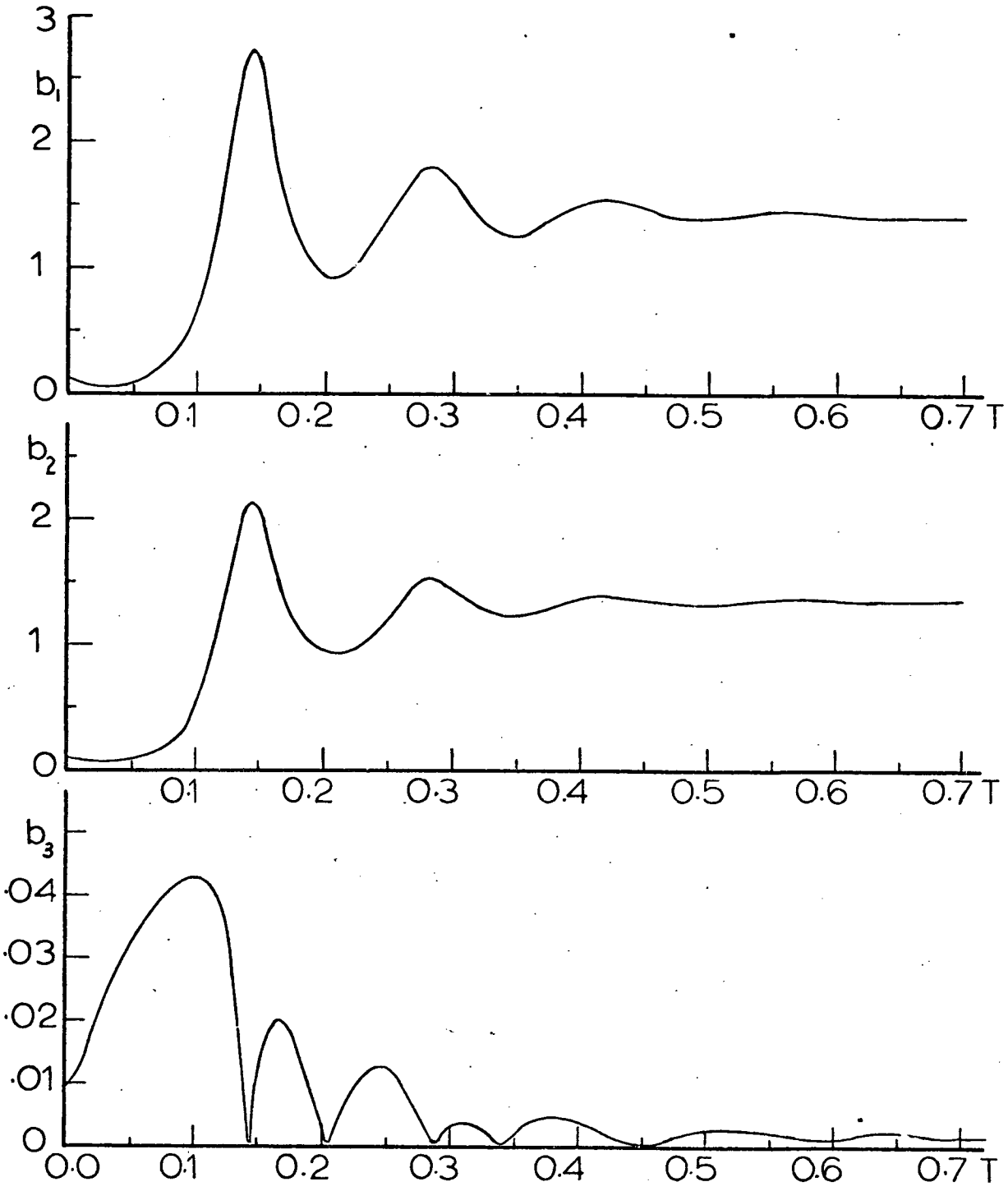


Fig(IV.24) Simulate (CSMP) Model Response of Three Mode Interaction, $r_3 = r_1 - r_2$
$\eta_1/\eta_2 \neq r_1/r_2$, $\epsilon = .0105$, $h/a = 2$, $l/a = 1.22$
$\bar{\zeta}_1 = .0025$, $\bar{\zeta}_2 = .005$, $\bar{\zeta}_3 = .025$, $n = 1.0$

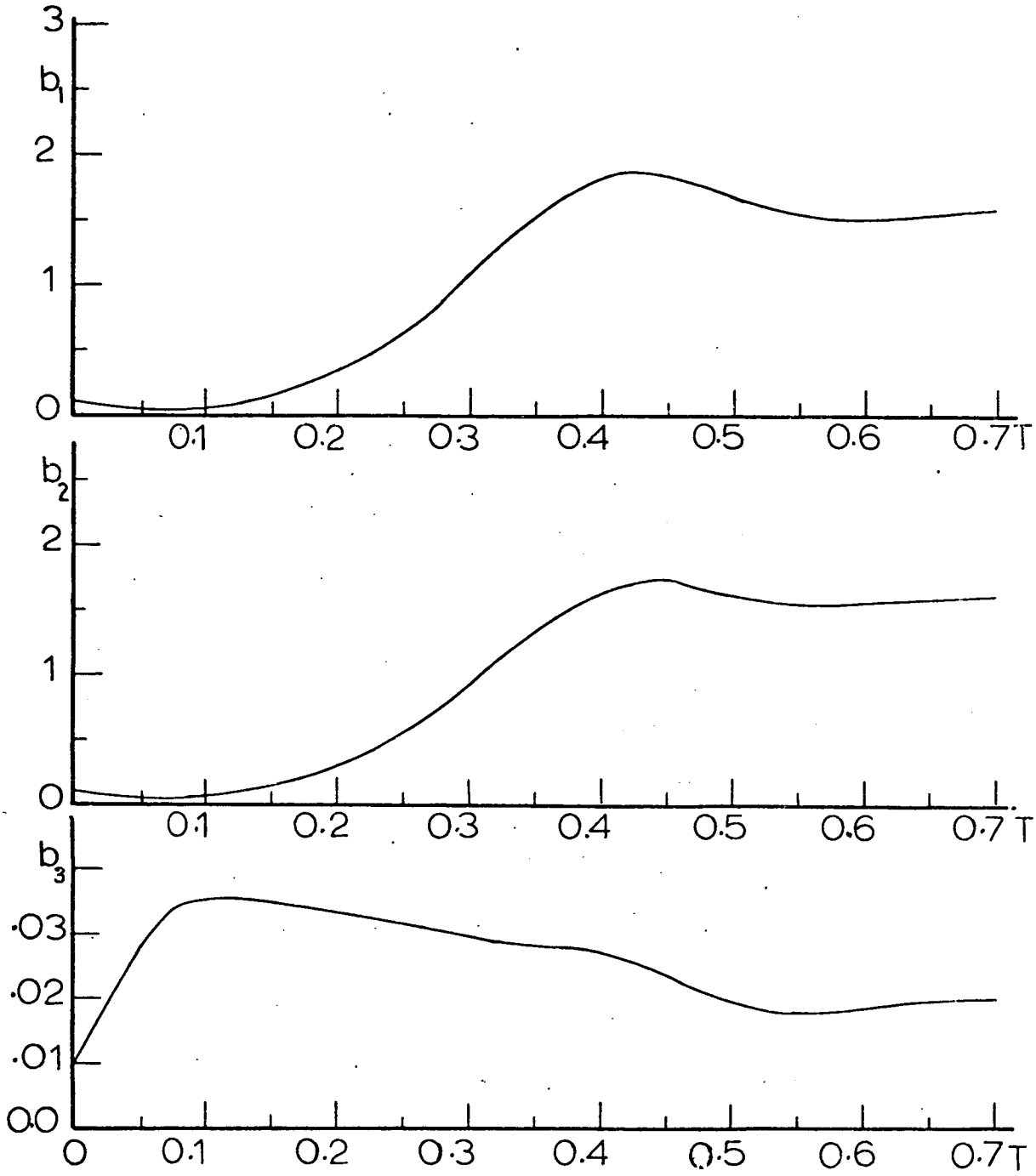


Fig(IV·25) CSMP Transient solution of Three Mode Interaction, $r_3 = r_1 - r_2$, $n = 0.97$, $h/a = 1.0$, $l/a = 1.22$, $\epsilon = 0.0105$ $\bar{\zeta}_1 = 0.0025$, $\bar{\zeta}_2 = 0.005$, $\bar{\zeta}_3 = 0.025$

are shown in Figs. (IV.22, 23). The transient solution for n=1, and 0.97 are depicted in Figs. (IV.24, 25).

## IV.5 Autoparametric Resonance of the Principal Type (Modes 1,3)

This kind of resonance takes place between the first and third modes;

$$\left.\begin{aligned} r_3 &= 2r_1 \\ r_3 &= n\nu \end{aligned}\right\} \qquad \text{(IV.64)}$$

The second mode has no influence on the frequency response of the system. The variational equations of this case are;

$$\left.\begin{aligned} -2r_1P_1\varphi' &= \epsilon\left\{\epsilon^{-1}(S_1^2\,{}^2-r_1^2)P_1 + \tfrac{1}{2}C_5r_3^2P_1P_3\cos(\gamma-2\varphi)\right\} \\ -2r_1P_1' &= \epsilon\left\{2r_1^2\zeta_1P_1 - \tfrac{1}{2}C_5r_3^2P_1P_3\sin(\gamma-2\varphi)\right\} \\ -2r_3P_3\gamma' &= \epsilon\left\{\epsilon^{-1}(S_3^2\,{}^2-r_3^2)P_3 - \tfrac{1}{2}L_{36}r_1^2P_1^2\cos(\gamma-2\varphi)+f\cos\gamma\right\} \\ -2r_3P_3' &= \epsilon\left\{2r_3^2\zeta_3P_3 - \tfrac{1}{2}L_{36}r_1^2P_1^2\sin(\gamma-2\varphi)+f\sin\gamma\right\} \end{aligned}\right\} \qquad \text{(IV.65)}$$

where:

$$L_{36} = L_3 + L_6$$

With the following transformation parameters:

$$\left.\begin{aligned} P_i &= \frac{1}{r_3}\sqrt{\frac{f}{|L_{36}|}}\,b_i \quad , \quad \tau = \frac{2T}{\epsilon\sqrt{f|L_{36}|}} \\ \gamma &= \frac{r_3^2-\nu^2}{\epsilon r_3\sqrt{f|L_{36}|}} \quad , \quad \eta_i = \frac{2r_i}{\epsilon\sqrt{f|L_{36}|}} \\ S_1 &= \frac{r_1}{r_3} = 0.5 \end{aligned}\right\} \qquad \text{(IV.66)}$$

equations (IV.65) become:

$$\left.\begin{aligned} -b_1\varphi' &= -.5\gamma b_1 + \frac{C_5}{|L_{36}|}\, b_1 b_3 \cos(\gamma-2\varphi) \\ -b_1' &= \eta_1 b_1 - \frac{C_5}{|L_{36}|}\, b_1 b_3 \sin(\gamma-2\varphi) \\ -b_3\gamma' &= -\gamma b_3 - \frac{1}{8}\frac{L_{36}}{|L_{36}|}\, b_1^2 \cos(\gamma-2\varphi) + \cos\gamma \\ -b_3' &= \eta_3 b_3 - \frac{1}{8}\frac{L_{36}}{|L_{36}|}\, b_1^2 \sin(\gamma-2\varphi) + \sin\gamma \end{aligned}\right\} \qquad \text{(IV.67)}$$

Seeking again steady-state solutions of (IV.67), it is found, contrary to the previous two sections that these equations are compatible and have the solution;

$$b_3 = \tfrac{1}{2}\frac{|L_{36}|}{C_5}\sqrt{\gamma^2 + 4\eta_1^2} \qquad \text{(a)}$$

and

$$b_1^2 = -\frac{4}{C_5}\left\{L_{36}(\gamma^2 - 2\eta_1\eta_2) \pm |L_{36}|\sqrt{4\left(\frac{C_5}{L_{36}}\right)^2 - \gamma^2(\eta_3+2\eta_1)^2}\right\} \qquad \text{(b)}$$

.....(IV.68)

There is also another possible solution with $b_1 = 0$ and $b_3$ given by (IV.52). Examination of the theoretical solutions (IV.68) shows that there is only one real solution for $b_1$ defined by the vertical tangency at $b_1 \doteq 0$ at which $b_3$ is changed from linear resonance (IV.52) to an autoparametric absorber response (IV.68a). Figs. (IV.26.-29) show the amplitude response curves for different fluid depth ratios.

IV.6 Autoparametric Resonance of Principal Type (Modes 2, and 3)

$$\left.\begin{aligned} r_3 &= 2r_2 \\ r_3 &= n\gamma \end{aligned}\right\} \qquad \text{(IV.69)}$$

This case is similar to the previous section but the interaction will take place between the second and third modes. The variational equations are found to take the form;

$$\left.\begin{aligned}
-2r_2P_2\dot{\theta} &= \epsilon\left\{\epsilon^{-1}(S_2^2\nu^2 - r_2^2)P_2 - \tfrac{1}{2}K_4r_3^2P_2P_3\cos(\gamma-2\theta)\right\}\\
-2r_2\dot{P}_2 &= \epsilon\left\{2r_2^2\zeta_2P_2 + \tfrac{1}{2}K_4r_3^2P_2P_3\sin(\gamma-2\theta)\right\}\\
-2r_3P_3\dot{\gamma} &= \epsilon\left\{\epsilon^{-1}(S_3^2\,{}^2 - r_3^2)P_3 - \tfrac{1}{2}L_{58}r_2^2P_2^2\cos(\gamma-2\theta)+f\cos\gamma\right\}\\
-2r_3\dot{P}_3 &= \epsilon\left\{2r_3^2\zeta_3P_3 - \tfrac{1}{2}L_{58}r_2^2P_2^2\sin(\gamma-2\theta)+f\sin\gamma\right\}
\end{aligned}\right\} \quad (IV.70)$$

where

$$L_{58} = L_5 + L_8$$

Using the transformation parameters;

$$\left.\begin{aligned}
P_i &= \frac{1}{r_3}\sqrt{\frac{f}{|L_{58}|}}\,b_i & \tau &= \frac{2T}{\sqrt{f|L_{58}|}}\\
\gamma &= \frac{r_3^2 - \nu^2}{\epsilon r_3^2\sqrt{f|L_{58}|}} & \eta_i &= \frac{2r_i\zeta_i}{\sqrt{f|L_{58}|}}\\
S_2 &= \frac{r_2}{r_3} = \tfrac{1}{2} & S_3 &= 1
\end{aligned}\right\} \quad (IV.71)$$

equations (IV.70) take the form;

$$\left.\begin{aligned}
-b_2\theta &= -0.5\gamma b_2 - \frac{K_4}{|L_{58}|}b_2b_3\cos(\gamma-2\theta)\\
-b_2 &= \eta_2b_2 + \frac{K_4}{|L_{58}|}b_2b_3\sin(\gamma-2\theta)\\
-b_3\gamma &= -\gamma b_3 - \frac{1}{8}\frac{L_{58}}{|L_{58}|}b_2^2\cos(\gamma-2\theta)+\cos\gamma\\
-b_3 &= +\eta_3b_3 - \frac{1}{8}\frac{L_{58}}{|L_{58}|}b_2^2\sin(\gamma-2\theta)+\sin\gamma
\end{aligned}\right\} \quad (IV.72)$$

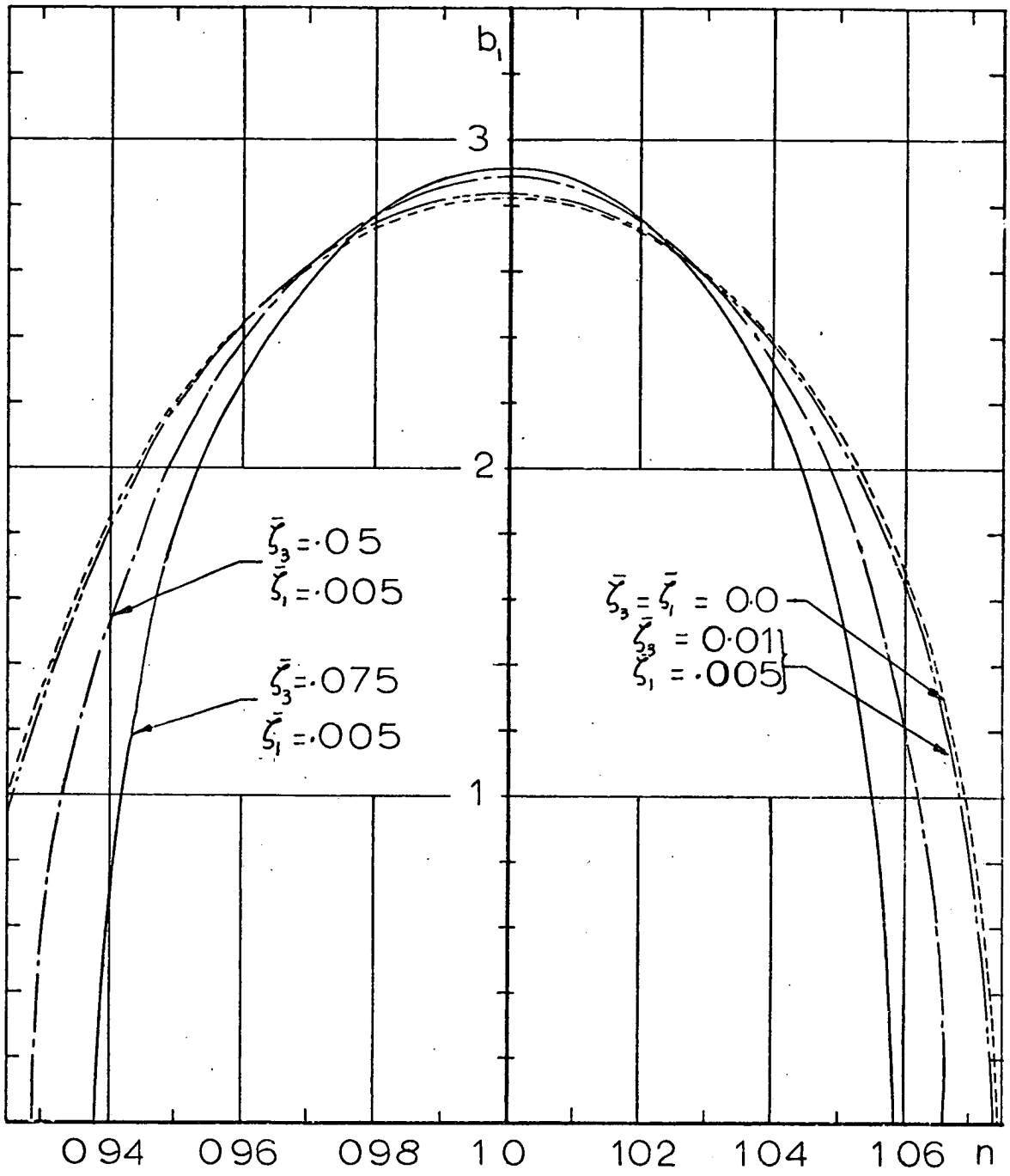


Fig(IV.26) First Mode Response in Two Mode Interaction, $r_3 = 2r_1$, $\epsilon = .0105$, $h/a = 1.0$ $l/a = 2.55$

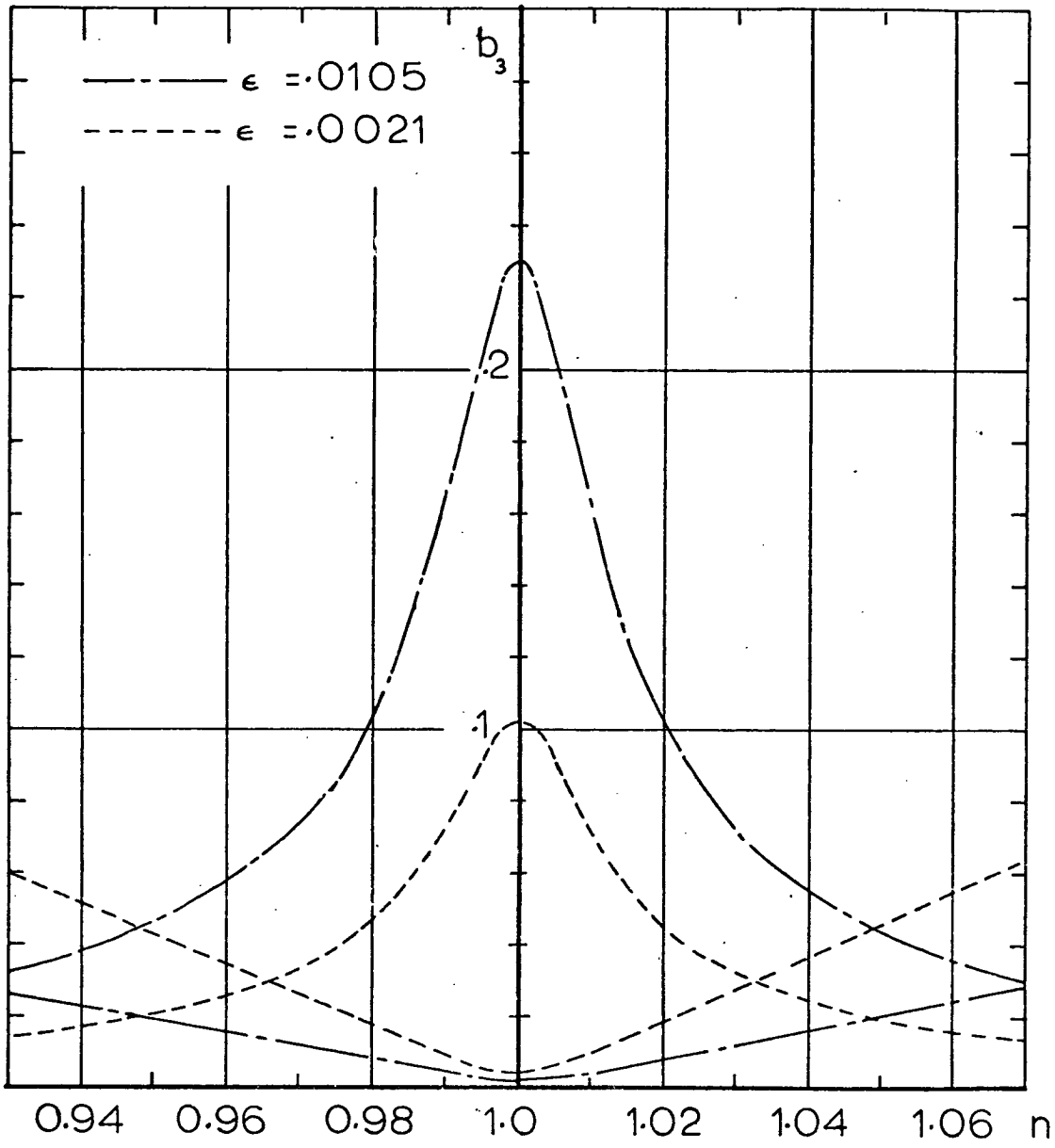


Fig.(IV.27) Main Mass Response in Two Mode Interaction, $r_3 = 2\,r_1$, $h/a = 1.0$, $l/a = 2.55$, $\bar{\zeta}_3 = 0.01$ , $\bar{\zeta}_1 = 0.005$

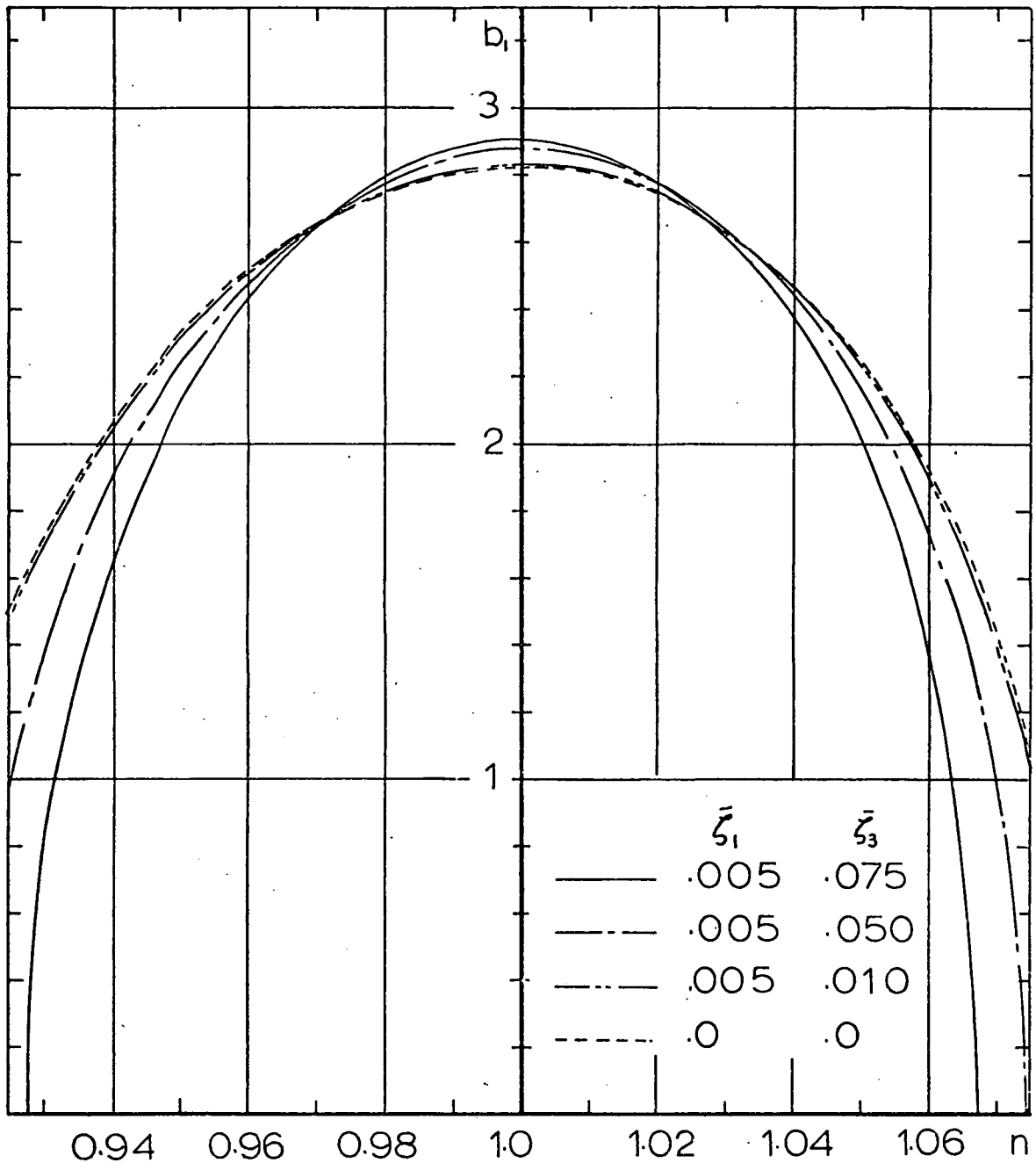


Fig(IV.28) First Mode Response in Two Mode Interaction, $r_3 = 2r_1$, $\epsilon = .0105$, $h/a = 2.0$ $l/a = 2.5$

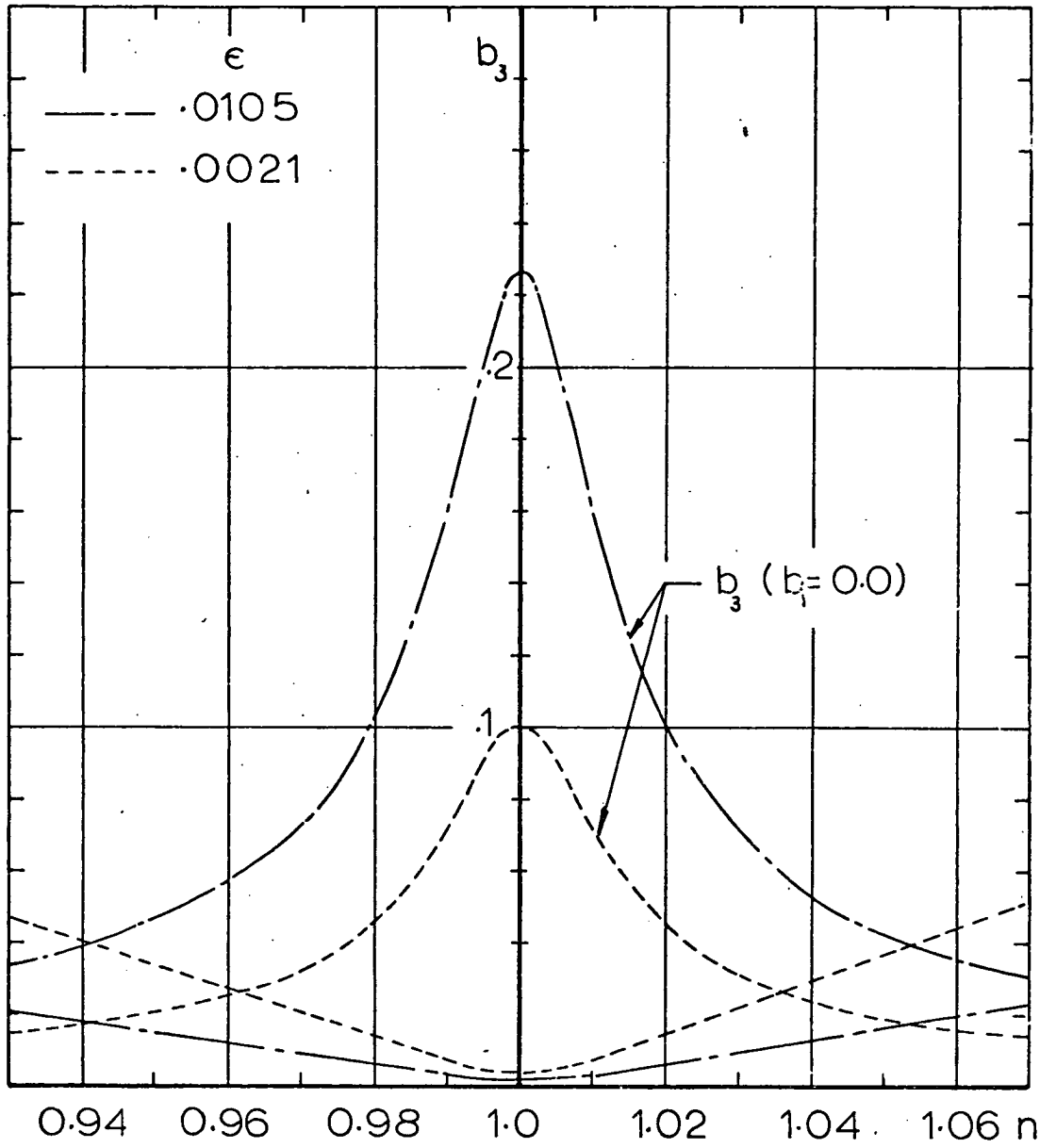


Fig (IV.29) Main Mass Response in Two Mode Interaction, $r_3 = 2r_1$, $h/a = 2$, $l/a = 2.5$ $\bar{\zeta}_3 = 0.01$, $\bar{\zeta}_1 = 0.005$

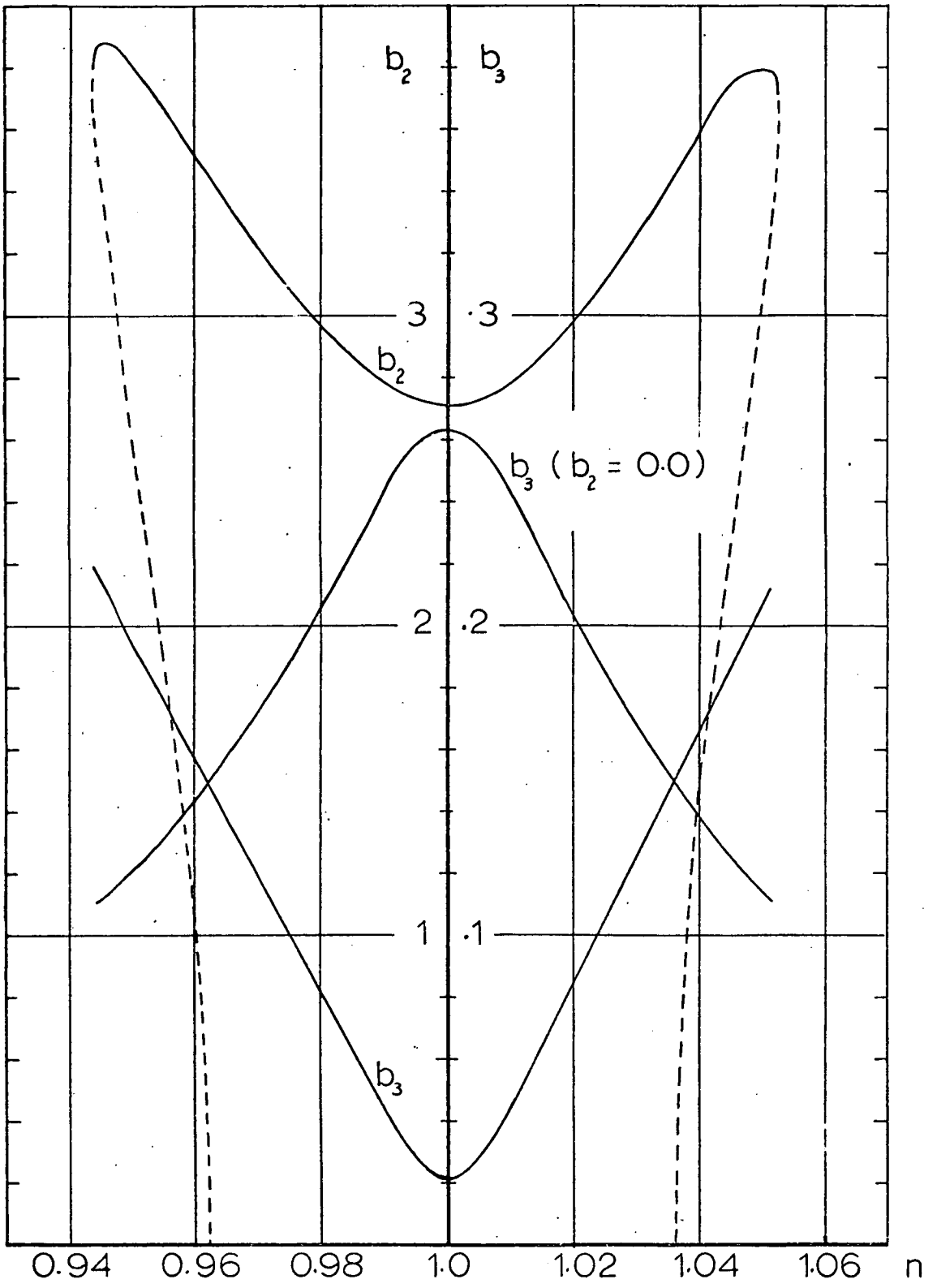


Fig(IV·30) Two Mode Interaction, $r_3 = 2\, r_2$
( $\epsilon$=.021, h/a= 1·0, l/a= 2·55, $\bar{\zeta}_2$ =·005, $\bar{\zeta}_3$ =·025)

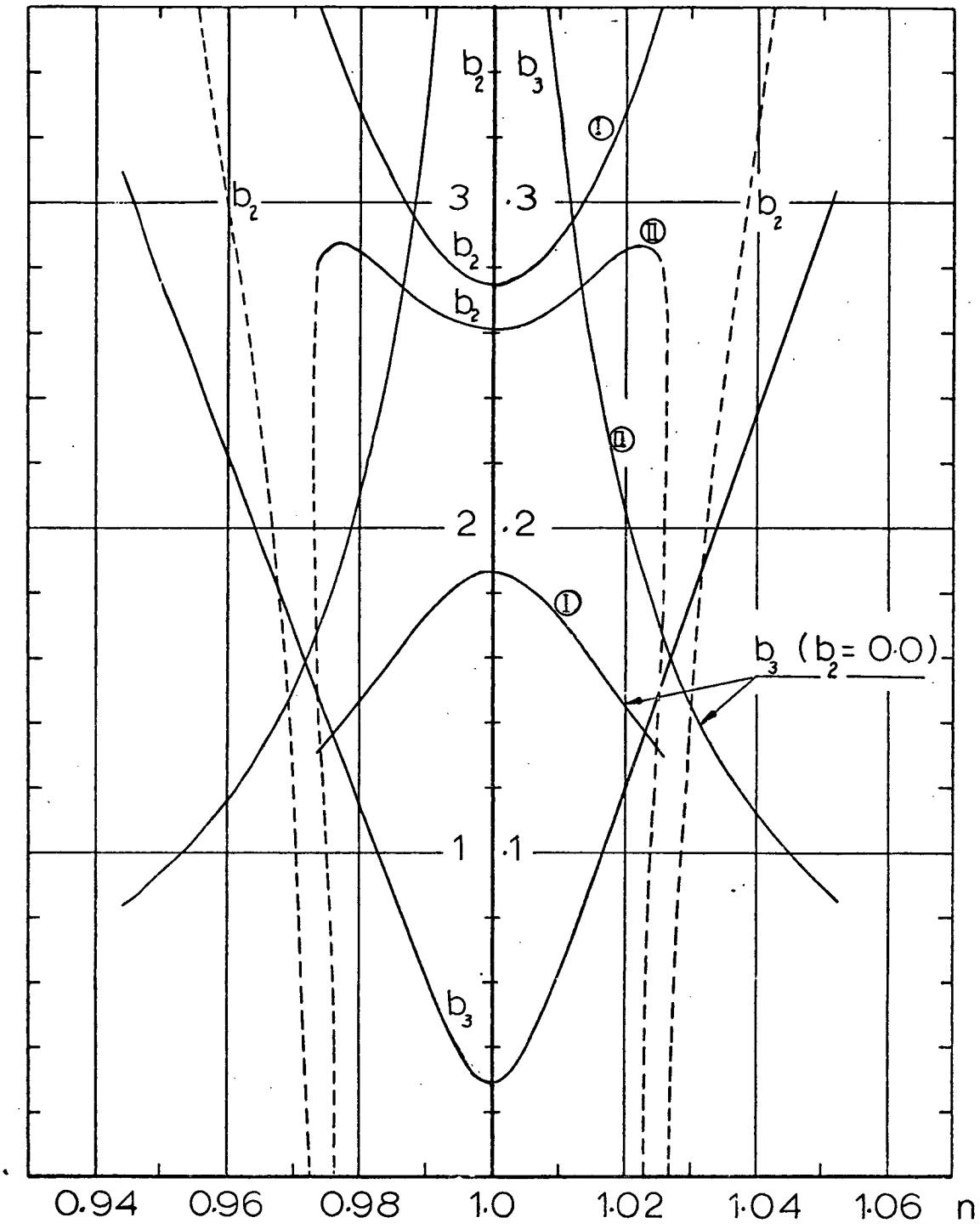


Fig(IV.31) Two Mode Interaction, $r_3 = 2r_2$
($\epsilon = 0{\cdot}0105$, $h/a = 1$, $l/a = 2.55$, $\bar{\zeta}_2 = {\cdot}005$
① $\bar{\zeta}_3 = {\cdot}025$; ② $\bar{\zeta}_3 = {\cdot}01$)

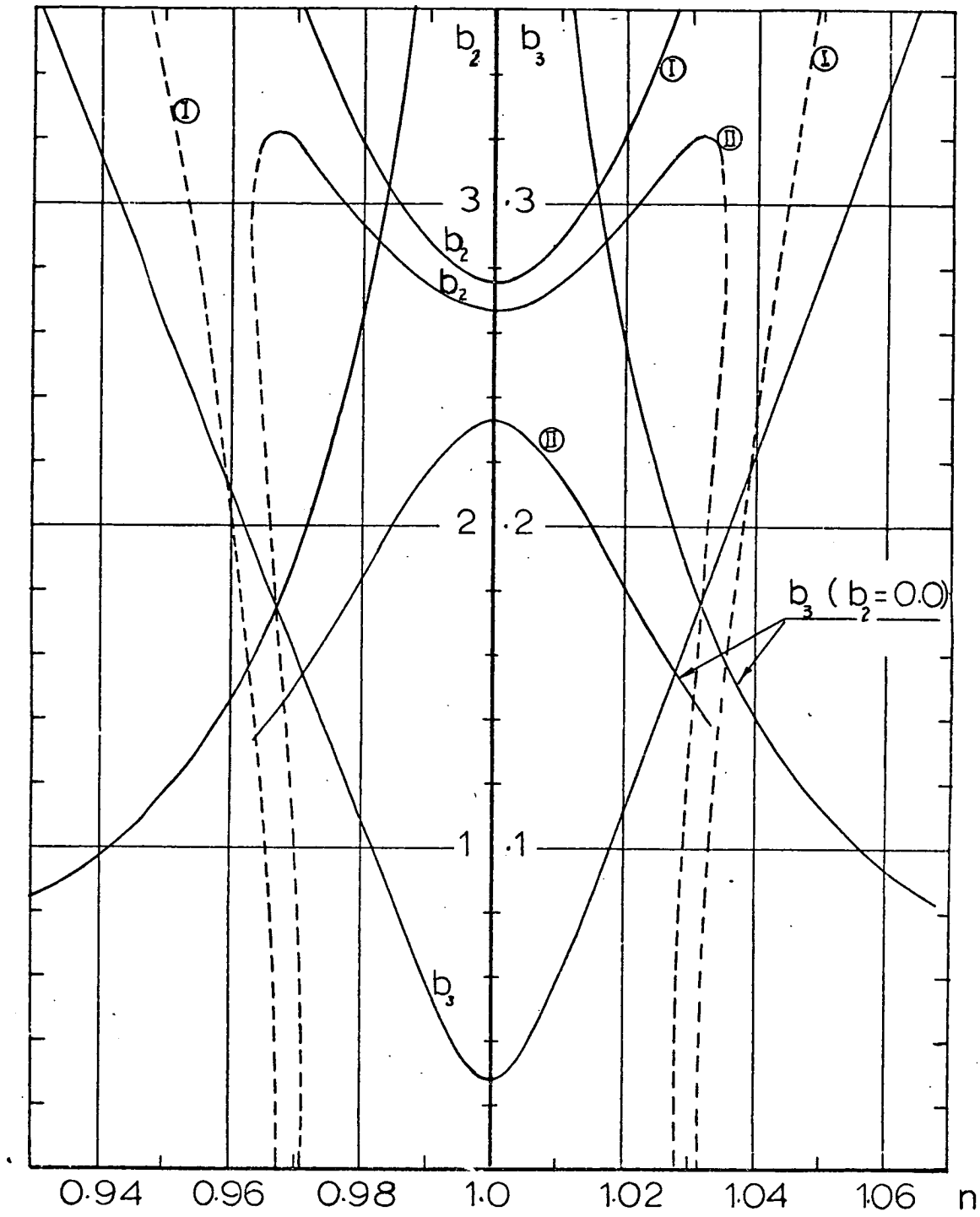


Fig.(IV.32) Two Mode Interaction, $r_3 = 2r_2$
($\epsilon$=·021, h/a = 2, l/a = 2.5, $\bar{\zeta}_2$ = ·005,
① $\bar{\zeta}_3$ = ·01 , ② $\bar{\zeta}_3$ = ·025 )

Again the steady-state solution is given by

$$|b_3| = \tfrac{1}{2}\frac{|L_{58}|}{K_4}\sqrt{\frac{\gamma^2}{4}+\eta_2^2}$$

$$b_2^2 = \frac{4}{K_4}\left\{L_{58}(\gamma^2 - 2\eta_2\eta_3) \pm |L_{58}|\sqrt{4(\frac{K_4}{L_{58}})^2 - \gamma^2(\eta_3+2\eta_2)^2}\right\} \qquad \text{(IV.73)}$$

The theoretical curves of $b_3$ and $b_2$ vis. the forcing frequency are given in Figs. (IV.30-32). The action of this case is similar to that of an autoparametric vibration absorber [H5] in every respect. $b_2$ has two branches, the upper branch is stable while the lower branch is unstable and bounded by two vertical tangents, $\frac{db_2}{d\gamma} = \infty$.

## IV.7 General Stability Considerations

It has been indicated in the previous four sections that there are two possible kinds of steady-state solution, one gives non-zero amplitude response in the vicinity of $n \approx 1 \pm 0(\epsilon)$, and the other gives a linear resonance response for the main mass with zero-response for the other amplitudes. In the first two sections, stability analysis appears rather difficult because of the incompatibility of the steady-state equations of the system. However, previous stability studies of a compatible autoparametric system together with the stability of the fluid free surface will be useful in anticipating some remarkable features of the stability of the present problem. As the fluid container is mounted in such a way that longitudinal and lateral motions are possible, the fluid free surface can undergo the following types of motions;

a) Suppose that, in the first instance, the tank receives purely vertical harmonic excitation at a frequency below double the fluid natural frequency ($\Omega < 2\omega_{11}$). The behaviour of the free surface of

the fluid is mainly governed by the Mathieu stability chart and, as long as the excitation amplitude and frequency are not in one of the instability regions, the free surface remains identically zero and the system follows the solution (IV.52).

b) As the amplitude and frequency of the main mass approach the instability boundary, the free surface starts to move back-and-forth, this sloshing motion exerts a lateral force which causes lateral oscillation of the container with its structure system. This in turn acts as a lateral excitation to the liquid and energy exchange between the two systems will proceed until either a steady-state condition is achieved or the resulting motion becomes a beating type. In the steady state case the fluid motion has a constant peak wave height and a single nodal diameter perpendicular to the direction of excitation. Eulitz and Glasser[E1] showed that as the excitation frequency (structure lateral frequency) increases the fluid wave height increases. Then, at a frequency a little less than the natural frequency, the nodal diameter begins to rotate and the peak wave height varies. This unstable behaviour takes place up to a frequency a little above the fluid natural frequency, where once again the steady state fluid motion has a constant peak wave height and a single nodal diameter perpendicular to the direction of excitation. An additional increase in the excitation frequency from this stable point reduces the wave height until the cycle begins again as the next resonance is approached. They concluded also that unstable sloshing will occur only when the peak acceleration of a fluid particle on the free surface becomes equal to the acceleration due to gravity (i.e. at $\eta\omega_{11}^2 = g$).

Although many investigators have reported the rotational motion of the fluid free surface about the vertical axis of symmetry, they gave different descriptions of its manner. Abramson, Chu, and Dodge[A2] described the essential features of that motion as an apparent "rotation" of the liquid superimposed on the normal sloshing motion which results in a type of "beating" motion.

Hutton[H12] classified the fluid motion into three types, stable planar, stable nonplanar, and unstable. Stable planar motion is a steady-state fluid motion with a constant peak wave height and a stationary single nodal diameter perpendicular to the direction of excitation. Stable nonplanar motion is a steady-state fluid motion with a constant peak wave height and a single nodal diameter that rotates at a constant speed around the tank. This motion has the appearance of a surface wave travelling around the tank at a constant speed and in a single direction. Unstable motion is a fluid motion that never attains a steady-state harmonic response, the peak wave height and nodal diameter rotation rate and direction continually change with time. The surface wave may build up and then decay, it may rotate first in one direction, then stop and rotate the other way. At times, the wave may slosh for several cycles in a plane perpendicular to the plane in which the tank is being driven, then rotate around and slosh in the driven plane for several cycles.

This complex motion has been attributed to a strong coupling between the two orthogonal directions, Lateral and transverse, where the slosh frequencies are the same in both directions, causing unstable motion to occur rapidly, unlike the case of a rectangular tank where the two natural frequencies in these directions are different.

In connection with the other type of system response, where the steady state may not be achieved and beating results due to the continuous exchange of energy between the two modes, it has been shown in a paper by Asmis and Tso[A5] that the amplitude of the beating decreases as the internal detuning increases. For large internal detuning the amplitude of beating becomes so small that for most purposes, the system can be considered as having reached steady-state. However, the CSMP simulation solution described in Sections IV.3,4 shows that with the autoparametric resonance condition satisfied exactly ($\gamma = 0$) the system can achieve a complete steady-state. This latter result has been also obtained by Asmis and Tso.

These concepts lead to the following conclusions;

1) At zero detuning ($\gamma = 0$) the system may or may not achieve a steady-state depending on the internal resonance detuning, which determines the state of the fluid free surface.

2) The vertical tangents $\frac{db_1}{dn} = \infty$ and/or $\frac{db_1}{dn} = \infty$ at $b_1 = b_2 = 0$ determines the boundaries of identically zero planar motion.

## IV.8 Conclusions

Autoparametric coupling of the structure vibration modes with the fluid antisymmetric sloshing mode has been investigated theoretically. Nonlinear analysis up to the second order terms in $\epsilon$ has generated four possible cases of internal resonance. The contribution of higher terms, say in $\epsilon^2$, was found to be negligible, although further internal resonance conditions, such as $r_3 = 3r_1$, $r_3 = 3r_2$, $r_3 = 2r_1+r_2$, $r_3 = r_1+2r_2$ and many others arise. In general it has been shown that the first two normal modes act as an autoparametric absorber for the third mode.

When the third mode frequency equals the sum or difference of the first two mode frequencies, $r_3 = r_1 \pm r_2$, the system may not achieve a steady-state depending on the damping relation between the first modes; $\eta_1 : \eta_2$, as well as the detuning frequency parameter $\gamma$. There are two cases under which the system achieves a steady-state, namely $\eta_1 = \eta_2 = 0$, or $\eta_1 : \eta_2 = r_1 : r_2$. If $\eta_1 \neq \eta_2 \neq 0$ and $\eta_1/\eta_2 \neq r_1/r_2$ the unsteadiness takes place in the phases of the modes 1 and 2 and tends to a steady state as $\gamma \rightarrow 0$ $(n \rightarrow 1)$. At $\gamma = 0$ the system is completely stable within the scope of the present analysis. However, previous studies on the behaviour of fluid near its natural frequency predicts unsteady, unstable nonplanar fluid free surface motion which affects the stability of the system near $\gamma \approx 0$.

The other two internal resonance conditions occur between the third mode and one of the other two modes, i.e. either $r_3 = 2r_1$, or $r_3 = 2r_2$. In both cases there are two forcing frequencies which determine the region of autoparametric action. The responses of the absorber modes are different in both cases but the behaviour of the third mode is similar to that of the case of three mode interaction. The condition $r_3 = 2r_1$ gives one real solution for the mode 1, while the condition $r_3 = 2r_2$ gives two solutions for the mode 2 one is stable and the other is unstable.

These theoretical predictions will be checked experimentally in Chapter (VI).

## APPENDIX (IV.A)

Constants of equation (IV.23)

$$C_5 = 1 - C_2 n_1 \qquad C_6 = 1 - C_2 n_2$$

$$C_7 = C_3 n_1^2 + C_4 n_1^3 - C_1 \qquad C_8 = C_4 n_1^2 n_2 + C_3 n_1 n_2 - C_1$$

$$C_9 = 2C_4 n_1^2 n_2 + C_3(n_1^2 + n_1 n_2) - 2C_1$$

$$C_{10} = 2C_4 n_1 n_2^2 + n_2 C_3(n_2 + n_1) - 2C_1$$

$$C_{11} = C_4 n_1 n_2^2 + C_3 n_1 n_2 - C_1 \qquad C_{12} = C_4 n_2^3 + C_3 n_2^2 - C_1$$

$$C_{13} = C_4 n_1^3 + C_3 n_1^2 - \bar{C}_1 \qquad C_{14} = 2C_4 n_1^2 n_2 + 2C_3 n_1 n_2 - 2\bar{C}_1$$

$$C_{15} = 2C_4 n_1 n_2^2 + 2C_3 n_1 n_2 - 2\bar{C}_1 \qquad C_{16} = C_4 n_2^3 + C_3 n_2^2 - \bar{C}_1$$

$$C_{17} = C_4 n_1^2 n_2 + C_3 n_1^2 - \bar{C}_1 \qquad C_{18} = C_4 n_1 n_2^2 + C_3 n_2^2 - \bar{C}_1$$

Constantsof equation (IV.24)

$$K_3 = n_1 K_1 \qquad K_4 = n_2 K_1$$

$$K_5 = -K_2 - K_1^2 n_1^3 \qquad K_6 = -K_2 - K_1^2 n_1^2 n_2$$

$$K_7 = -K_2 - K_1^2 n_1 n_2^2 \qquad K_8 = -K_2 - K_1^2 n_2^3$$

$$K_9 = -2K_2 - K_1^2 n_1^3 \qquad K_{10} = -2K_2 - K_1^2 n_1^2 n_2$$

$$K_{11} = -2K_2 - K_1^2 n_1 n_2^2 \qquad K_{12} = -2K_2 - K_1^2 n_2^3$$

Constants of equations (IV.25)

$$L_3 = L_2 n_1^2 + L_1 \qquad L_4 = 2L_2 n_1 n_2 + 2L_1$$

$$L_5 = L_2 n_2^2 + L_1 \qquad L_6 = L_2 n_1^2$$

$$L_7 = L_2 n_1 n_2 \qquad L_8 = L_2 n_2^2$$

## APPENDIX (IV.B)

Constants of terms in (IV.44) are,

$$C_{574} = -\frac{C_5 r_1^2(L_3+L_6)}{(r_3^2 - 4r_1^2)} - \frac{3}{4} C_7 + \frac{1}{4} C_{13}$$

$$C_{556} = \frac{C_5^2 r_3(r_1+r_2)}{2(r_1-r_2)(3r_1+r_2)} + \frac{C_6 K_3 r_3}{16 r_1}$$

$$C_{618} = \frac{C_6[L_7(r_1^2+r_2^2) + L_4 r_1 r_2]}{16 r_1 r_2^3}(r_1-r_2)^2 - \tfrac{1}{2}(C_{10}-C_8) - \tfrac{1}{2} C_{11}(\frac{r_1}{r_2})^2$$

$$K_{482} = \frac{K_4 r_2^2(L_5+L_8)}{(r_3^2-4r_2^2)} - \frac{3}{4} K_8 + \frac{1}{4} K_{12}$$

$$K_{361} = \frac{-K_3[L_7(r_1^2+r_2^2) + L_4 r_1 r_2](r_1-r_2)^2}{16 r_1^3 r_2} - \tfrac{1}{2} K_6(\frac{r_2}{r_1})^2 - K_6 + \tfrac{1}{2} K_{10}$$

$$K_{344} = \frac{1}{16}(\frac{r_3}{r_2})K_3 C_6 - \tfrac{1}{2}\frac{K_4^2 r_3^2}{(r_1-r_2)(3r_2+r_1)}$$

$$L_{43} = -\frac{L_3 C_5 r_2 r_3}{2r_1(r_1-r_2)} - \frac{L_3 C_5 r_3(2r_1+r_2)}{2r_1(3r_1+r_2)} + \frac{L_4 K_4 r_2(2r_1+r_2)}{16 r_1^2}$$
$$- \frac{L_6 C_5 r_2^2 r_3}{4r_1^2(r_1-r_2)} + \frac{L_6 C_5 r_3(2r_1+r_2)^2}{4r_1^2(3r_1+r_2)} - \frac{L_6 C_5 r_3}{4(r_1-r_2)} + \frac{L_6 C_5 r_3}{4(3r_1+r_2)}$$
$$- \frac{L_7 K_3 r_3(5r_1^2 + 4r_1 r_2 + r_2^2)}{16 r_1^3}$$

$$L_{45} = -\frac{L_4 C_6 r_3(2r_2+r_1)}{16 r_2^2} - \frac{L_5 K_4 r_1 r_3}{2r_2(r_1-r_2)} + \frac{L_5 K_4 r_3(2r_2+r_1)}{2r_2(3r_2+r_1)}$$
$$+ \frac{L_6 C_6 r_3(r_1^2 + 2r_1 r_2 + 2r_2^2)}{8 r_2^3} - \frac{L_8 K_4 r_1^2 r_3}{4r_2^2(r_1-r_2)}$$
$$- \frac{L_8 K_4 r_3(2r_2+r_1)^2}{4r_2^2(3r_2+r_1)} - \frac{1}{4} L_8 K_4 r_3[\frac{1}{(r_1-r_2)} + \frac{1}{(3r_2+r_1)}]$$

# CHAPTER (V)

## AUTOPARAMETRIC COUPLING UNDER TWO SIMULTANEOUS INTERNAL RESONANCE CONDITIONS

V.1

It is evident from the previous chapter that the dangerous autoparametric coupling of the liquid and structure first modes is governed mainly by the internal resonance conditions. It is useful to extend the analysis by considering more sloshing modes and discovering the corresponding critical autoparametric resonance conditions.

Previous theoretical studies [D2], of the coupling of liquid free surface modes in rigid containers subjected to parametric excitation has shown that the modes (0,1), and (0,2) are secondary when the primary is (1,1). Accordingly the analysis in the present chapter will be confined to these three sloshing modes, sketched in Fig. (V.1), together with the modes of the structure.

The dynamic free surface condition equation (II.31) leads to the following equations

$$-[\ddot{X}_d - \frac{6}{5\ell}\ddot{\xi}X_d + \frac{36}{25\ell^2}X_d(X_d\ddot{X}_d + \dot{X}_d^2)]\frac{2a}{(\xi_{11}^2-1)J_1(\xi_{11})} - \dot{\alpha}_{11}$$

$$- [g + \ddot{\xi} - \frac{6}{5\ell}(\dot{X}_d^2 + X_d\ddot{X}_d)]a_{11} + s_{11} = 0 \qquad (V.1)$$

$$\dot{\alpha}_{01} - [g + \ddot{\xi} - \frac{6}{5\ell}(\dot{X}_d^2 + X_d\ddot{X}_d)]a_{01} + s_{01} = 0 \qquad (V.2)$$

$$\dot{\alpha}_{21} - [g + \ddot{\xi} - \frac{6}{5\ell}(\dot{X}_d^2 + X_d\ddot{X}_d)]a_{21} + s_{21} = 0 \qquad (V.3)$$

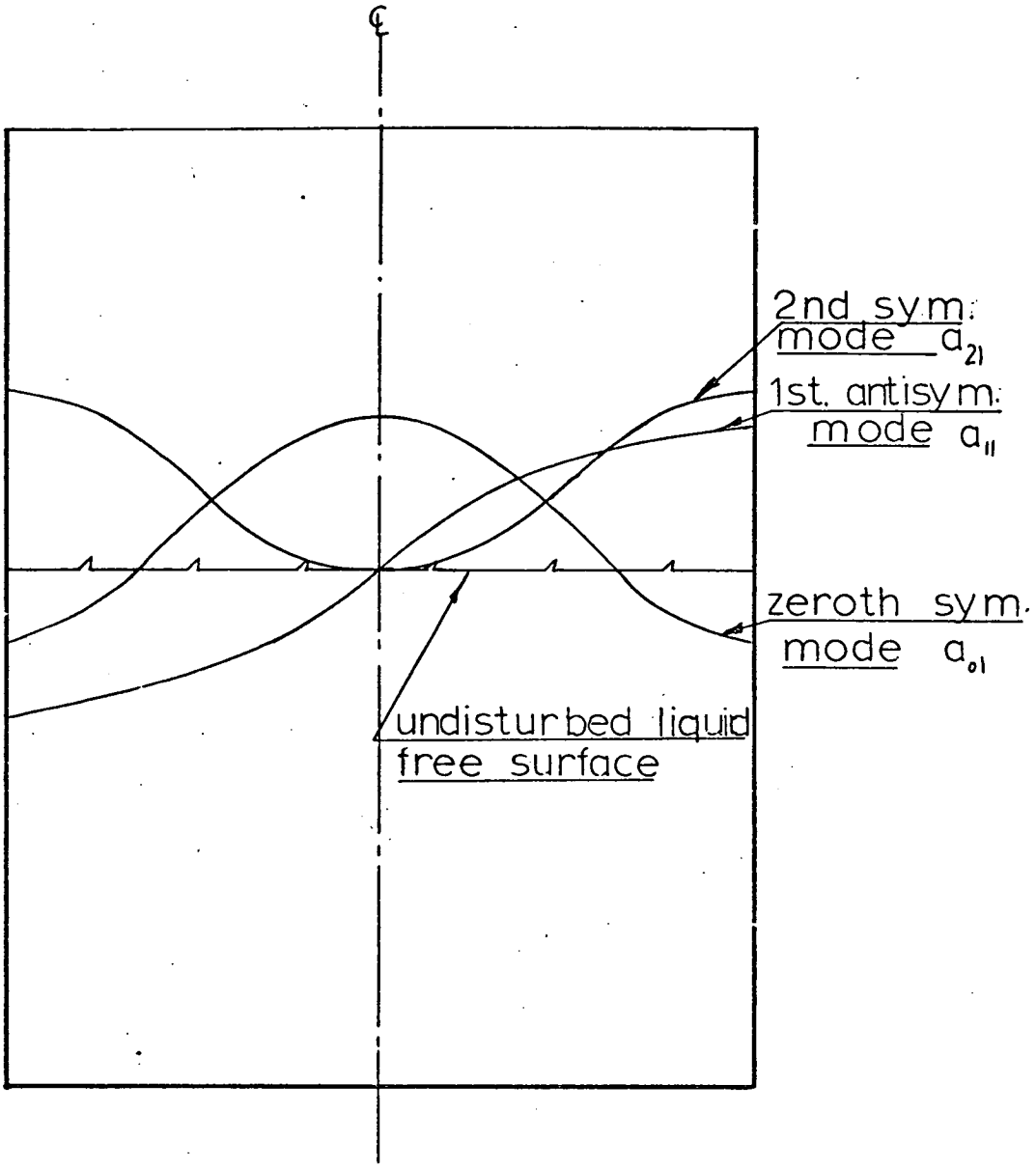


Fig(V.1 ) Liquid Sloshing Modes Considered in chapter V.

The kinematic free surface condition; equation (II.35) gives:

$$a_{11} + (\lambda_{11}\tanh\lambda_{11}h)\alpha_{11} + h_{11} = 0 \qquad (V.4)$$

$$a_{o1} + (\lambda_{01}\tanh\lambda_{01}h)\alpha_{01} + h_{01} = 0 \qquad (V.5)$$

$$a_{21} + (\lambda_{21}\tanh\lambda_{21}h)\alpha_{21} + h_{21} = 0 \qquad (V.6)$$

where the nonlinear functions $S_{mn}$ and $h_{mn}$ are determined by using (II.33) and (II.37) which give:

$$S_{11} = 0.1045682\lambda_{11}^2\dot{\alpha}_{11}a_{11}^2 - 0.2810256\lambda_{11}^3\alpha_{11}^2 a_{11}\tanh\lambda_{11}h$$

$$- 0.3446801\,\lambda_{11}\dot{\alpha}_{01}a_{11}\tanh\lambda_{01}h - 0.1655938\,\lambda_{11}\dot{\alpha}_{11}a_{01}\tanh\lambda_{11}h$$

$$+ 0.1987524\,\lambda_{11}\dot{\alpha}_{11}a_{21}\tanh\lambda_{11}h + 0.3297066\,\lambda_{11}\dot{\alpha}_{21}a_{11}\tanh\lambda_{11}h$$

$$+ \alpha_{01}\alpha_{11}\lambda_{11}^2[0.3570485 + 0.3446801\tanh\lambda_{01}h.\tanh\lambda_{11}h]$$

$$- \alpha_{11}\alpha_{21}\lambda_{11}^2[0.2725628 + 0.3297066\tanh\lambda_{21}h.\tanh\lambda_{11}h]$$

$$S_{01} = -\alpha_{11}^2\lambda_{11}^2[0.0696505 - 0.0614991\tanh^2\lambda_{11}h] - 0.1229981\,\lambda_{11}\dot{\alpha}_{11}a_{11}\tanh\lambda_{11}h$$

$$S_{21} = -\alpha_{11}^2\lambda_{11}^2[-0.0655181 + 0.1751103\tanh^2\lambda_{11}h] + 0.3502201\,\lambda_{11}\dot{\alpha}_{11}a_{11}\tanh\lambda_{11}h$$

$$h_{11} = -0.122515\lambda_{11}^3\alpha_{11}a_{11}^2\tanh\lambda_{11}h - 0.3603956\lambda_{11}^2\alpha_{01}a_{11} + 0.1914547\lambda_{11}^2\alpha_{11}a_{01}$$

$$+ 0.2744914\lambda_{11}^2\alpha_{21}a_{11} - 0.0738103\lambda_{11}^2\alpha_{11}a_{21}$$

$$h_{01} = -0.2612992\lambda_{11}^2\alpha_{11}a_{11}$$

$$h_{21} = 0.4812568\lambda_{11}^2\alpha_{11}a_{11}$$

Introducing these fluid modes, the overall system equations of motion become;

Equation of motion in the vertical direction:

$$M_o\ddot{\xi} + C_{s1}\dot{\xi} + K_{s1}\xi + m_t(\ddot{\xi} - \frac{6}{5\ell}\dot{X}_d^2 - \frac{6}{5\ell}X_d\ddot{X}_d)$$
$$+ \rho\int_o^a\int_o^{2\pi}\Big\{\tilde{\Phi}_t - \tfrac{1}{2}(\tilde{\Phi}_r^2 + \frac{1}{r^2}\tilde{\Phi}_\theta^2 + \tilde{\Phi}_z^2) + (\ddot{\xi} - \frac{6}{5\ell}\dot{X}_d^2 - \frac{6}{5\ell}X_d\ddot{X}_d)h$$
$$- r[\ddot{X}_d - \frac{6}{5\ell}X_d\ddot{\xi} - \frac{36}{25\ell^2}X_d(X_d\ddot{X}_d + \dot{X}_d^2)]\cos\theta\Big\}\, r\,d\theta\,dr$$
$$= \omega_{s1}^2\xi_o\cos\Omega t \qquad (V.7)$$

Equation of motion in the horizontal direction

$$m_t\ddot{X}_d + C_{s2}\dot{X}_d + K_{s2}X_d - \frac{6}{5\ell}m_{t\ell}\ddot{\xi}X_d + \frac{36}{25\ell^2}m_tX_d(X_d\ddot{X}_d + \dot{X}_d^2)$$
$$- \rho\int_{-h}^{o}\int_o^{2\pi}\Big\{\tilde{\Phi} - \tfrac{1}{2}(\tilde{\Phi}_r^2 + \frac{1}{r^2}\tilde{\Phi}_\theta^2 + \tilde{\Phi}_z^2) - [\ddot{\xi} - \frac{6}{5\ell}(\dot{X}_d^2 - \frac{6}{5\ell}X_d\ddot{X}_d)]Z$$
$$- a[\ddot{X}_d - \frac{6}{5\ell}\ddot{\xi}X_d - \frac{36}{25\ell^2}X_d(X_d\ddot{X}_d + \dot{X}_d^2)]\cos\theta\Big\}\, a\cos\theta.d\theta.dz = 0 \qquad (V.8)$$

The evaluation of the integrals will be considerably simplified by using the orthogonal and recurrence relations in Appendix A of Chapter (II). Performing the integrals in (V.7, 8) gives

$$[M_o + m_{t\ell}]\ddot{\xi} + C_{s1}\dot{\xi} + K_{s1}\xi - \frac{6}{5\ell}m_{t\ell}(\dot{X}_d^2 + X_d\ddot{X}_d) - \frac{0.202\pi\alpha_{11}^2\rho}{\cosh^2\lambda_{11}h} = \omega_{s1}^2\xi_o\cos\Omega t$$

.....(V.7)

$$m_{t\ell}\ddot{X}_d + C_{s2}\dot{X}_d + K_{s2}X_d - \frac{6}{5\ell}m_{t\ell}\ddot{\xi}X_d + \frac{36}{25\ell^2}m_{t\ell}X_d(X_d\ddot{X}_d + \dot{X}_d^2)$$
$$- \pi\frac{\rho a}{\lambda}\alpha_{11}J_1(\xi_{11})\tanh(\lambda_{11}h)$$
$$+ \tfrac{\pi}{2}\rho a\,\lambda_{21}\alpha_{11}\alpha_{21}\Big\{\frac{J_1(\xi_{11})J_2(\xi_{21})}{\cosh\lambda_{11}h.\cosh\lambda_{21}h}\Big[\frac{1 + 0.5\xi_{11}\xi_{21}}{\xi_{21}(\xi_{11}+\xi_{21})}\sinh((\lambda_{11}+\lambda_{21})h)$$
$$+ \frac{1 - 0.5\xi_{11}\xi_{21}}{\xi_{21}(\xi_{21}-\xi_{11})}\sinh((\lambda_{21}-\lambda_{11})h)\Big]\Big\}$$
$$+ \tfrac{\pi}{2}\rho a\,\lambda_{11}\alpha_{01}\alpha_{11}\Big\{\frac{J_o(\xi_{01})J_1(\xi_{11})}{\cosh\lambda_{01}h.\cosh\lambda_{11}h}\Big[\frac{\xi_{01}\sinh[(\lambda_{01}+\lambda_{11})h]}{(\xi_{01}+\xi_{11})}$$
$$- \frac{\xi_{01}\sinh[(\lambda_{01}-\lambda_{11})h]}{(\xi_{01}-\xi_{11})}\Big\} = 0 \qquad (V.8)$$

Eliminating $\alpha_{mn}$ and $\dot{\alpha}_{mn}$ from (V.1-8) and using the following non-dimensional parameters;

$$\tau = \omega_{11} t$$

$$\epsilon = \xi_o / a$$

$$\begin{Bmatrix} \sigma \\ r_{s1} \\ r_{s2} \\ r_{o1} \\ r_{21} \end{Bmatrix} = \frac{1}{\omega_{11}} \begin{Bmatrix} \Omega \\ \omega_{s1} \\ \omega_{s2} \\ \omega_{o1} \\ \omega_{21} \end{Bmatrix} , \quad \begin{Bmatrix} A_{11} \\ A_{o1} \\ A_{21} \\ Z \\ X \end{Bmatrix} = \frac{\lambda_{11} \tanh \lambda_{11} h}{\epsilon} \begin{Bmatrix} a_{11} \\ a_{o1} \\ a_{21} \\ \xi \\ X_d \end{Bmatrix} \tag{V.9}$$

$$\begin{Bmatrix} \bar{\zeta}_{s1} \\ \bar{\zeta}_{s2} \end{Bmatrix} = \epsilon \begin{Bmatrix} \zeta_{s1} \\ \zeta_{s2} \end{Bmatrix} , \quad \begin{Bmatrix} \mu_1 \\ \mu_2 \end{Bmatrix} = \frac{1}{M_o + m_{t1}} \begin{Bmatrix} m_1 \\ m_{t1} \end{Bmatrix} , \quad \mu_3 = \frac{m_1}{m_{t1}}$$

the following five equations are obtained:

$$\begin{aligned} \ddot{A}_{11} + A_{11} + C_o \ddot{X} = \epsilon \Big\{ & C_2 X\ddot{Z} - A_{11}\ddot{Z} + C_1 A_{o1}\ddot{A}_{11} - C_5 \ddot{A}_{11} A_{21} - C_6 \dot{A}_{o1}\dot{A}_{11} \\ & - C_7 \dot{A}_{11}\dot{A}_{21} - C_8 \ddot{A}_{o1} A_{11} + C_9 A_{11}\ddot{A}_{21} \Big\} \\ & + \epsilon^2 \Big\{ C_{10} A_{11}^2 \ddot{A}_{11} - C_4 X(X\ddot{X} + \dot{X}^2) + C_{11} A_{11}\dot{A}_{11}^2 \\ & + C_3 A_{11}(\dot{X}^2 + X\ddot{X}) \Big\} \end{aligned} \tag{V.10}$$

$$\begin{aligned} \ddot{A}_{o1} + r_{o1}^2 A_{o1} = \epsilon & \Big\{ N_1 A_{11}\ddot{A}_{11} - N_2 \dot{A}_{11}^2 - r_{o1}^2 A_{o1}\ddot{Z} \Big\} \\ & + \epsilon^2 N_3 A_{o1}(\dot{X}^2 + X\ddot{X}) \end{aligned} \tag{V.11}$$

$$\begin{aligned} \ddot{A}_{21} + r_{21}^2 A_{21} = \epsilon & \Big\{ M_1 A_{11}\ddot{A}_{11} + M_2 \dot{A}_{11}^2 - r_{21}^2 A_{21}\ddot{Z} \Big\} \\ & + \epsilon^2 M_3 A_{21}(\dot{X}^2 + X\ddot{X}) \end{aligned} \tag{V.12}$$

$$\ddot{Z} + r_{s1}^2 Z = \epsilon \left\{ L_1 \dot{A}_{11}^2 + L_2(\dot{X}^2 + X\ddot{X}) - 2r_{s1}\zeta_{s1}\dot{Z} \right\}$$
$$+ \xi_{11} r_{s1}^2 \tanh(\lambda_{11} h).\cos\sigma\tau \qquad (V.13)$$

$$\ddot{X} + r_{s2}^2 X + K_o \ddot{A}_{11} = \epsilon \left\{ K_1 \ddot{Z}X - 2r_{s2}\zeta_{s2}\dot{X} + K_2 A_{o1}\ddot{A}_{11} - K_3 \ddot{A}_{11} A_{21} \right.$$
$$\left. - K_4 \dot{A}_{11}\dot{A}_{o1} - K_5 \dot{A}_{11}\dot{A}_{21} - K_6 \ddot{A}_{o1} A_{11} + K_7 \ddot{A}_{21} A_{11} \right\}$$
$$+ \epsilon^2 \left\{ - K_1^2 X(X\ddot{X} + \dot{X}^2) + K_8 A_{11}^2 \ddot{A}_{11} + K_9 A_{11}\dot{A}_{11}^2 \right\} \qquad (V.14)$$

$A_{11}$, $A_{o1}$ and $A_{21}$ are the nondimensional amplitudes of the first antisymmetric, zero symmetric and second symmetric sloshing modes respectively, Z is the vertical amplitude of the main mass, and X is the amplitude of the tank lateral oscillations. The constants of equations (V.10-14) are defined in Appendix (V.I).

Transforming (V.10-14) into principal coordinates by using the transformation (IV.14), introducing a linear diagonal damping matrix after transformation, and taking $Z=P_3$, $A_{o1}=P_4$, and $A_{21}=P_5$ allows equations (V.10-14) to be written in the form:

$$\ddot{P}_1 + S_1^2 \nu^2 P_1 = \epsilon \left\{ \epsilon^{-1}(S_1^2\nu^2 - r_1^2)P_1 - 2r_1\zeta_1\dot{P}_1 - C_{12}P_1\ddot{P}_3 - C_{13}P_2\ddot{P}_3 + C_1\ddot{P}_1 P_4 + C_1\ddot{P}_2 P_4 \right.$$
$$- C_5\ddot{P}_1 P_5 - C_5\ddot{P}_2 P_5 - C_6\dot{P}_1\dot{P}_4 - C_6\dot{P}_2\dot{P}_4 - C_7\dot{P}_1\dot{P}_5$$
$$\left. - C_7\dot{P}_2\dot{P}_5 - C_8 P_1\ddot{P}_4 - C_8 P_2\ddot{P}_4 + C_9 P_1\ddot{P}_5 + C_9 P_2\ddot{P}_5 \right\}$$
$$+ \epsilon^2 \left\{ C_{14}\ddot{P}_1 P_1^2 + C_{15}\ddot{P}_1 P_1 P_2 + C_{16}\ddot{P}_2 P_2^2 + C_{17} P_1^2\ddot{P}_2 + C_{18} P_1 P_2 \ddot{P}_2 \right.$$
$$+ C_{19} P_2^2\ddot{P}_2 + C_{20} P_1\dot{P}_1^2 + C_{21} P_1\dot{P}_1\dot{P}_2 + C_{22} P_1\dot{P}_2^2 + C_{23}\dot{P}_1^2 P_2$$
$$\left. + C_{24}\dot{P}_1\dot{P}_2 P_2 + C_{25} P_2\dot{P}_2^2 \right\} \qquad (V.15)$$

$$\ddot{P}_2+S_2^2\nu^2P_2=\epsilon\Big\{\epsilon^{-1}(S_2^2\nu^2-r_2^2)P_2-2r_2\zeta_2P_2+K_{10}P_1\ddot{P}_3+K_{11}P_2\ddot{P}_3+K_2\ddot{P}_1P_4+K_2\ddot{P}_2P_4$$
$$-K_3\ddot{P}_1P_5-K_3\ddot{P}_2P_5-K_4\dot{P}_1\dot{P}_4-K_4\dot{P}_2\dot{P}_4-K_5\dot{P}_1\dot{P}_5-K_5\dot{P}_2\dot{P}_5$$
$$-K_6P_1\ddot{P}_4-K_6P_2\ddot{P}_4+K_7P_1\ddot{P}_5+K_7P_2\ddot{P}_5\Big\}$$
$$+\epsilon^2\Big\{K_{12}P_1^2\ddot{P}_1+2K_{13}P_1\ddot{P}_1P_2+K_{14}\ddot{P}_1P_2^2+K_{13}P_1^2\ddot{P}_3+2K_{14}P_1P_2\ddot{P}_2$$
$$+K_{15}P_2^2\ddot{P}_2+K_{16}P_1\dot{P}_1^2+2K_{17}P_1\dot{P}_1\dot{P}_2+K_{18}P_1\dot{P}_2^2+K_{17}\dot{P}_1^2P_2$$
$$+2K_{18}\dot{P}_1\dot{P}_2P_2+K_{19}\dot{P}_1^2P_2\Big\} \qquad (V.16)$$

$$\ddot{P}_3+S_3^2\nu^2P_3=\epsilon\Big\{\epsilon^{-1}(S_3^2\nu^2-r_3^2)P_3-2r_3\zeta_3\dot{P}_3+L_3\dot{P}_1^2+L_4\dot{P}_1\dot{P}_2+L_5\dot{P}_2^2$$
$$+L_6P_1\ddot{P}_1+L_7P_1\ddot{P}_2+L_7\ddot{P}_1P_2+L_8P_2\ddot{P}_2+f\cos\sigma\tau\Big\} \qquad (V.17)$$

$$\ddot{P}_4+S_4^2\nu^2P_4=\epsilon\Big\{\epsilon^{-1}(S_4^2\nu^2-r_4^2)P_4-2r_4\zeta_4\dot{P}_4+N_1P_1\ddot{P}_1+N_1P_1\ddot{P}_2+N_1\ddot{P}_1P_2$$
$$+N_1P_2\ddot{P}_2-2N_2\dot{P}_1\dot{P}_2-N_2\dot{P}_2^2-r_4^2\ddot{P}_3P_4-N_2\dot{P}_1\Big\}$$
$$+\epsilon^2\Big\{N_4\dot{P}_1^2P_4+2N_5\dot{P}_1\dot{P}_2P_4+N_6\dot{P}_2^2P_4+N_4P_1\ddot{P}_1P_4$$
$$+N_5P_1\ddot{P}_2P_4+N_5\ddot{P}_1P_2P_4+N_6P_2\ddot{P}_2P_4\Big\} \qquad (V.18)$$

$$\ddot{P}_5+S_5^2\nu^2P_5=\epsilon\Big\{\epsilon^{-1}(S_5^2\nu^2-r_5^2)P_5-2r_5\zeta_5\dot{P}_5+M_1P_1\ddot{P}_1+M_1P_1\ddot{P}_2+M_1\ddot{P}_1P_2$$
$$+M_1P_2\ddot{P}_2+M_2\dot{P}_1^2+2M_2\dot{P}_1\dot{P}_2+M_2\dot{P}_2^2-r_5^2\ddot{P}_3P_5\Big\}$$
$$+\epsilon^2\Big\{M_4\dot{P}_1^2P_5+2M_5\dot{P}_1\dot{P}_2P_5+M_6\dot{P}_2^2P_5+M_4P_1\ddot{P}_1P_5$$
$$+M_5P_1\ddot{P}_2P_5+M_5\ddot{P}_1P_2P_5+M_6P_2\ddot{P}_2P_5\Big\} \qquad (V.19)$$

The new constants of these equations are given in Appendix (V.II).

The cubic nonlinearities in equations (V.15,16,18,19) are not very important in the present chapter because quadratic nonlinearities such as $P_1\ddot{P}_3$ and $P_2\ddot{P}_3$ are quite adequate to define the characteristics of the system.

Following the same argument as in chapter (III) for the method of solution, the following asymptotic solutions for equations (V.15-19) are assumed.

$$\begin{aligned}
P_1 &= P_1(\tau)\cos[r_1\tau + \varphi(\tau)] + \epsilon a_1 + \dots \\
P_2 &= P_2(\tau)\cos[r_2\tau + \theta(\tau)] + \epsilon b_1 + \dots \\
P_3 &= P_3(\tau)\cos[r_3\tau + \gamma(\tau)] + \epsilon d_1 + \dots \\
P_4 &= P_4(\tau)\cos[r_4\tau + \alpha(\tau)] + \epsilon u_1 + \dots \\
P_5 &= P_5(\tau)\cos[r_5\tau + \delta(\tau)] + \epsilon v_1 + \dots
\end{aligned} \tag{V.20}$$

Introducing (V.20) into (V.15-19) gives;

$$\begin{aligned}
&[\ddot{P}_1 - P_1(r_1+\dot{\varphi})^2]\cos(r_1\tau+\varphi) - [P_1\ddot{\varphi} + 2(r_1+\dot{\varphi})\dot{P}_1]\sin(r_1\tau+\varphi) + \epsilon\ddot{a}_1 \\
&\quad + S_1^2\nu^2[P_1\cos(r_1\tau+\varphi) + \epsilon a_1 + \dots] \\
&= \epsilon\Big\{\epsilon^{-1}(S_1^2\nu^2 - r_1^2)\,[P_1\cos(r_1\tau+\varphi) + \epsilon a_1] + 2r_1^2\zeta_1 P_1\sin(r_1\tau+\varphi) \\
&\quad + C_{12}r_3^2 P_1P_3\cos(r_1\tau+\varphi)\cos(r_3\tau+\gamma) + C_{13}r_3^2P_2P_3\cos(r_2\tau+\theta)\cos(r_3\tau+\gamma) \\
&\quad + (C_8r_4^2 - C_1r_1^2)P_1P_4\cos(r_1\tau+\varphi)\cos(r_4\tau+\alpha) + (C_8r_4^2 - C_1r_2^2)P_2P_4\cos(r_2\tau+\vartheta)\cos(r_4\tau+\gamma) \\
&\quad + (C_5r_1^2 - C_9r_5^2)P_1P_5\cos(r_1\tau+\varphi)\cos(r_5\tau+\delta) + (C_5r_2^2 - C_9r_5^2)P_2P_5\cos(r_2\tau+\theta)\cos(r_5\tau+\delta) \\
&\quad - C_6r_1r_4P_1P_4\sin(r_1\tau+\varphi)\sin(r_4\tau+\alpha) - C_6r_2r_4P_2P_4\sin(r_2\tau+\theta)\sin(r_4\tau+\alpha) \\
&\quad - C_7r_1r_5P_1P_5\sin(r_1\tau+\varphi)\sin(r_5\tau+\delta) - C_7r_2r_5P_2P_5\sin(r_2\tau+\theta)\sin(r_5\tau+\delta)\Big\}
\end{aligned} \tag{V.21}$$

$$[\ddot{P}_2-P_2(r_2+\dot{\theta})^2]\cos(r_2\tau+\theta)-[P_2\ddot{\theta}+2\dot{P}_2(r_2+\dot{\theta})]\sin(r_2\tau+\theta)+\epsilon\ddot{b}_1$$

$$+S_1^2\nu^2[P_2\cos(r_2\tau+\theta)+\epsilon b_1+\ldots.]$$

$$=\epsilon\Big\{\bar{\epsilon}^1(S_1^2\nu^2-r_2^2)[P_2\cos(r_2\tau+\theta)+\epsilon b_1]+2r_2^2\zeta_2P_2\sin(r_2\tau+\theta)$$

$$-K_{10}r_3^2P_1P_3\cos(r_1\tau+\varphi)\cos(r_3\tau+\gamma)-K_{11}r_3^2P_2P_3\cos(r_2\tau+\theta)\cos(r_3\tau+\gamma)$$

$$+(K_6r_4^2-K_2r_1^2)P_1P_4\cos(r_1\tau+\varphi)\cos(r_4\tau+\alpha)+(K_6r_4^2-K_2r_2^2)P_2P_4\cos(r_2\tau+\theta)\cos(r_4\tau+\alpha)$$

$$+(K_3r_1^2-K_7r_5^2)P_1P_5\cos(r_1\tau+\varphi)\cos(r_5\tau+\delta)+(K_3r_2^2-K_7r_5^2)P_2P_5\cos(r_2\tau+\theta)\cos(r_5\tau+\delta)$$

$$-K_4r_1r_4P_1P_4\sin(r_1\tau+\varphi)\sin(r_4\tau+\alpha)-K_4r_2r_4P_2P_4\sin(r_2\tau+\theta)\sin(r_4\tau+\alpha)$$

$$-K_5r_1r_5P_1P_5\sin(r_1\tau+\varphi)\sin(r_5\tau+\delta)-K_5r_2r_5P_2P_5\sin(r_2\tau+\theta)\sin(r_5\tau+\delta)\Big\}$$

.....(V.22)

$$[\ddot{P}_3-P_3(r_3+\dot{\gamma})^2]\cos(r_3\tau+\gamma)-[P_3\ddot{\gamma}+2\dot{P}_3(r_3+\dot{\gamma})]\sin(r_3\tau+\gamma)+\epsilon\ddot{d}_1$$

$$+S_3^2\nu^2[P_3\cos(r_3\tau+\gamma)+\epsilon d_1+\ldots]$$

$$=\epsilon\Big\{\bar{\epsilon}^1(S_3^2\nu^2-r_3^2)[P_3\cos(r_3\tau+\gamma)+\epsilon d_1]-2r_3^2\zeta_3P_3\sin(r_3\tau+\gamma)$$

$$+L_3r_1^2P_1^2\sin^2(r_1\tau+\varphi)+L_4r_1r_2P_1P_2\sin(r_1\tau+\varphi)\sin(r_2\tau+\theta)$$

$$L_5r_2^2P_2^2\sin^2(r_2\tau+\theta)-L_6r_1^2P_1^2\cos^2(r_1\tau+\varphi)$$

$$-L_7(r_1^2+r_2^2)P_1P_2\cos(r_1\tau+\varphi)\cos(r_2\tau+\varphi)-L_8r_2^2P_2^2\cos^2(r_2\tau+\theta)$$

$$+f\cos(n\nu\tau)\Big\} \qquad (V.23)$$

$$[\ddot{P}_4-P_4(r_4+\dot{\alpha})^2]\cos(r_4\tau+\alpha)-[P_4\ddot{\alpha}+2\dot{P}_4(r_4+\dot{\alpha})]\sin(r_4\tau+\alpha)+\epsilon\ddot{u}_1$$

$$+S_4^2\nu^2[P_4\cos(r_4\tau+\alpha)+\epsilon u_1+\ldots]$$

$$=\epsilon\Big\{\bar{\epsilon}^1(S_4^2\nu^2-r_4^2)[P_4\cos(r_4\tau+\alpha)+\epsilon u_1]+2r_4^2\zeta_4P_4\sin(r_4\tau+\alpha)$$

$$-N_1 r_1^2 P_1^2 \cos^2(r_1\tau+\varphi) - N_1 r_2^2 P_1 P_2 \cos(r_1\tau+\varphi)\cos(r_2\tau+\theta)$$

$$-N_1 r_1^2 P_1 P_2 \cos(r_1\tau+\varphi)\cos(r_2\tau+\theta) - N_1 r_2^2 P_2^2 \cos^2(r_2\tau+\theta)$$

$$-N_2 r_1^2 P_1^2 \sin^2(r_1\tau+\varphi) - 2N_2 r_1 r_2 P_1 P_2 \sin(r_1\tau+\varphi)\sin(r_2\tau+\theta)$$

$$-N_2 r_2^2 P_2^2 \sin^2(r_2\tau+\theta) + r_3^2 r_4^2 P_3 P_4 \cos(r_3\tau+\gamma)\cos(r_4\tau+\alpha)\Big\} \qquad (V.24)$$

$$[\ddot{P}_5 - P_5(r_5+\dot{\delta})^2]\cos(r_5\tau+\delta) - [P_5\ddot{\delta} + 2\dot{P}_5(r_5+\dot{\delta})]\sin(r_5\tau+\delta) + \epsilon\ddot{V}_1$$

$$+S_5^2\nu^2[P_5\cos(r_5\tau+\delta)+\epsilon V_1+\ldots]$$

$$= \epsilon\Big\{\epsilon^{-1}(S_5^2\nu^2 - r_5^2)[P_5\cos(r_5\tau+\delta)+\epsilon V_1] + 2r_5^2\zeta_5 P_5 \sin(r_5\tau+\delta)$$

$$-M_1 r_1^2 P_1^2 \cos^2(r_1\tau+\varphi) - M_1 r_2^2 P_1 P_2 \cos(r_1\tau+\varphi)\cos(r_2\tau+\theta)$$

$$-M_1 r_1^2 P_1 P_2 \cos(r_1\tau+\varphi)\cos(r_2\tau+\theta) - M_1 r_2^2 P_2^2 \cos^2(r_2\tau+\theta)$$

$$+M_2 r_1^2 P_1^2 \sin^2(r_1\tau+\varphi) + 2M_2 r_1 r_2 P_1 P_2 \sin(r_1\tau+\varphi)\sin(r_2\tau+\theta)$$

$$+M_2 r_2^2 P_2^2 \sin^2(r_2\tau+\theta) + r_3^2 r_5^2 P_3 P_5 \cos(r_3\tau+\gamma)\cos(r_5\tau+\delta)\Big\} \qquad (V.25)$$

The fundamental variational equations corresponding to this set of equations are:

$$\left.\begin{aligned}
-2r_1 P_1 \dot{\varphi} &= \epsilon\Big\{\epsilon^{-1}(S_1^2\nu^2 - r_1^2)P_1\Big\} \\
-2r_1 \dot{P}_1 &= 0 \\
-2r_2 P_2 \dot{\theta} &= \epsilon\Big\{\epsilon^{-1}(S_2^2\nu^2 - r_2^2)P_2\Big\} \\
-2r_2 \dot{P}_2 &= 0 \\
-2r_3 P_3 \dot{\gamma} &= \epsilon\Big\{\epsilon^{-1}(S_3^2\nu^2 - r_3^2)P_3\Big\} \\
-2r_3 \dot{P}_3 &= 0
\end{aligned}\right\} \qquad (V.26)$$

$$
\left.
\begin{aligned}
-2r_4P_4\dot{\alpha} &= \epsilon\left\{\epsilon^{-1}(S_4^2\nu^2-r_4^2)P_4\right\}\\
-2r_4\dot{P}_4 &= 0\\
-2r_5P_5\dot{\delta} &= \epsilon\left\{\epsilon^{-1}(S_5^2\nu^2-r_5^2)P_5\right\}\\
-2r_5\dot{P}_5 &= 0
\end{aligned}
\right\}
$$

The first order perturbation equations are obtained by collecting terms of order $\epsilon$ in equations (V.21-25). The resulting equations are given as follows:

$$
\begin{aligned}
\ddot{a}_1+r_1^2a_1 = {} & 2r_1^2\zeta_1P_1\sin(r_1\tau+\varphi)+\tfrac{1}{2}C_{12}r_3^2P_1P_3\left\{\cos[(r_1+r_3)\tau+\varphi+\gamma]+\cos[(r_3-r_1)\tau+\gamma-\varphi]\right\}\\
&+\tfrac{1}{2}C_{13}r_3^2P_2P_3\left\{\cos[(r_3+r_2)\tau+\gamma+\varphi]+\cos[(r_3-r_2)\tau+\gamma-\theta]\right\}\\
&+\tfrac{1}{2}(C_8r_4^2-C_1r_1^2)P_1P_4\left\{\cos[(r_4+r_1)\tau+\alpha+\varphi]+\cos[(r_4-r_1)\tau+\alpha-\varphi]\right\}\\
&+\tfrac{1}{2}(C_8r_4^2-C_1r_2^2)P_2P_4\left\{\cos[(r_4+r_2)\tau+\alpha+\theta]+\cos[(r_4-r_2)\tau+\alpha-\theta]\right\}\\
&+\tfrac{1}{2}(C_5r_1^2-\tfrac{1}{2}C_9r_5^2)P_1P_5\left\{\cos[(r_5+r_1)\tau+\delta+\varphi]+\cos[(r_5-r_1)\tau+\delta-\varphi]\right\}\\
&+\tfrac{1}{2}(C_5r_2^2-\tfrac{1}{2}C_9r_5^2)P_2P_5\left\{\cos[(r_5+r_2)\tau+\delta+\theta]+\cos[(r_5-r_2)\tau+\delta-\theta]\right\}\\
&-\tfrac{1}{2}C_6r_1r_4P_1P_4\left\{\cos[(r_4-r_1)\tau+\alpha-\varphi]-\cos[(r_4+r_1)\tau+\alpha+\varphi]\right\}\\
&-\tfrac{1}{2}C_6r_2r_4P_2P_4\left\{\cos[(r_4-r_2)\tau+\alpha-\theta]-\cos[(r_4+r_2)\tau+\alpha+\theta]\right\}\\
&-\tfrac{1}{2}C_7r_1r_5P_1P_5\left\{\cos[(r_5-r_1)\tau+\delta-\varphi]-\cos[(r_5+r_1)\tau+\delta+\varphi]\right\}\\
&-\tfrac{1}{2}C_7r_2r_5P_2P_5\left\{\cos[(r_5-r_2)\tau+\delta-\theta]-\cos[(r_5+r_2)\tau+\delta+\theta]\right\}
\end{aligned}
\qquad (V.27)
$$

As indicated in Chapter (III), there are some secular terms in equation (V.27) giving rise to instability in the steady state solution of the first order perturbation terms, when one or more of the following internal resonance relations are met:

$$\left.\begin{array}{ll} r_3 = 2r_1 & r_3 = r_1 \pm r_2 \\ r_4 = 2r_1 & r_4 = r_1 \pm r_2 \\ r_5 = 2r_1 & r_5 = r_1 + r_2 \end{array}\right\} \qquad (V.28)$$

The first order perturbation terms of equation (V.22) are:

$$\begin{aligned} \ddot{b}_1 + r_2^2 b_2 = {} & 2r_2^2 \zeta_2 P_2 \sin(r_2\tau+\theta) - \tfrac{1}{2}K_{10} r_3^2 P_1 P_3 \left\{\cos[(r_3+r_1)\tau+\gamma+\varphi]+\cos[(r_3-r_1)\tau+\gamma-\varphi]\right\} \\ & -\tfrac{1}{2}K_{11} r_3^2 P_2 P_3 \left\{\cos[(r_3+r_2)\tau+\gamma+\theta]+\cos[(r_3-r_2)\tau+\gamma-\theta]\right\} \\ & +\tfrac{1}{2}(K_6 r_4^2 - K_2 r_1^2) P_1 P_4 \left\{\cos[(r_4+r_1)\tau+\alpha+\varphi]+\cos[(r_4-r_1)\tau+\alpha-\varphi]\right\} \\ & +\tfrac{1}{2}(K_6 r_4^2 - K_2 r_2^2) P_2 P_4 \left\{\cos[(r_4+r_2)\tau+\alpha+\theta]+\cos[(r_4-r_2)\tau+\alpha-\theta]\right\} \\ & +\tfrac{1}{2}(K_3 r_1^2 - K_7 r_5^2) P_1 P_5 \left\{\cos[(r_5+r_1)\tau+\delta+\varphi]+\cos[(r_5-r_1)\tau+\delta-\varphi]\right\} \\ & +\tfrac{1}{2}(K_3 r_2^2 - K_7 r_5^2) P_2 P_5 \left\{\cos[(r_5+r_2)\tau+\delta+\theta]+\cos[(r_5-r_2)\tau+\delta-\theta]\right\} \\ & -\tfrac{1}{2}K_4 r_1 r_4 P_1 P_4 \left\{\cos[(r_4-r_1)\tau+\alpha-\varphi]-\cos[(r_4+r_1)\tau+\alpha+\varphi]\right\} \\ & -\tfrac{1}{2}K_4 r_2 r_4 P_2 P_4 \left\{\cos[(r_4-r_2)\tau+\alpha-\theta]-\cos[(r_4+r_2)\tau+\alpha+\theta]\right\} \\ & -\tfrac{1}{2}K_5 r_1 r_5 P_1 P_5 \left\{\cos[(r_5-r_1)\tau+\delta-\varphi]-\cos[(r_5+r_1)\tau+\delta+\varphi]\right\} \\ & -\tfrac{1}{2}K_5 r_2 r_5 P_2 P_5 \left\{\cos[(r_5-r_2)\tau+\delta-\theta]-\cos[(r_5+r_2)\tau+\delta+\theta]\right\} \end{aligned} \qquad (V.29)$$

This equation contains resonant terms at the following frequency relations:

$$\left.\begin{array}{ll} r_3 = 2r_2 & r_3 = r_1 \pm r_2 \\ r_4 = 2r_2 & r_4 = r_1 \pm r_2 \\ r_5 = 2r_2 & r_5 = r_1 \pm r_2 \end{array}\right\} \qquad (V.30)$$

The first order perturbation terms of equation (V.23) are:

$$\ddot{d}_1+r_3^2 d_1=2r_3^2\zeta_3 P_3\sin(r_3\tau+\gamma)+\tfrac{1}{2}(L_3-L_6)r_1^2P_1^2[1-\cos(2r_1\tau+2\varphi)]$$
$$+\tfrac{1}{2}L_4 r_1 r_2 P_1 P_2\left\{\cos[(r_1-r_3)\tau+\varphi-\theta]+\cos[(r_1+r_2)\tau+\varphi+\theta]\right\}$$
$$+\tfrac{1}{2}(L_5-L_8)r_2^2P_2^2[1-\cos(2r_2\tau+2\theta]$$
$$-\tfrac{1}{2}L_7(r_1^2+r_2^2)P_1P_2\left\{\cos[(r_1-r_2)\tau+\varphi-\theta]+\cos[(r_1+r_2)\tau+\varphi+\theta]\right\}$$
$$+f\cos(n\nu\tau) \qquad (V.31)$$

Two types of resonance are found in this equation:

$$\left.\begin{array}{ll} \text{i) the external resonance} & r_3 = n\nu \\ \text{ii) the internal resonance} & r_3 = 2r_1 \\ & r_3 = 2r_2 \\ & r_3 = r_1 \pm r_2 \end{array}\right\} \qquad (V.32)$$

The first order perturbation terms of equations (V.24) are:-

$$\ddot{u}_1+r_4^2 u_1 = 2r_4^2\zeta_4 P_4\sin(r_4\tau+\alpha)-\tfrac{1}{2}(N_1+N_2)(r_1^2P_1^2+r_2^2P_2^2)$$
$$+\tfrac{1}{2}(N_2-N_1)r_1^2P_1^2\cos(2r_1\tau+2\varphi)+\tfrac{1}{2}(N_2-N_1)r_2^2P_2^2\cos(2r_2\tau+2\theta)$$
$$-\tfrac{1}{2}N_1(r_1^2+r_2^2)P_1P_2\left\{\cos[(r_1+r_2)\tau+\varphi+\theta]+\cos[(r_1-r_2)\tau+\varphi-\theta]\right\}$$
$$-N_2 r_1 r_2 P_1 P_2\left\{\cos[(r_1-r_2)\tau+\varphi-\theta]-\cos[(r_1+r_2)\tau+\varphi+\theta]\right\}$$
$$+\tfrac{1}{2}r_3^2r_4^2P_3P_4\left\{\cos[(r_3+r_4)\tau+\gamma+\alpha]+\cos[(r_3-r_4)\tau+\gamma-\alpha]\right\} \qquad (V.33)$$

Resonance occurs at:

$$\begin{array}{ll} r_3 = 2r_4 & r_4=2r_2 \\ r_4 = 2r_1 & r_4=2r_1\pm r_2 \end{array} \qquad (V.34)$$

Finally the first order perturbation terms of equation (V.25) are:

$$\ddot{V}_1+r_5^2V_1 = 2r_5^2\zeta_5P_5\sin(r_5\tau+\delta)-\tfrac{1}{2}(M_1-M_2)(r_1^2P_1^2+r_2^2P_2^2)$$

$$-\tfrac{1}{2}(M_1+M_2)r_1^2P_1^2\cos(2r_1\tau+2\varphi)-\tfrac{1}{2}(M_1+M_2)r_2^2P_2^2\cos(2r_2\tau+2\theta)$$

$$-\tfrac{1}{2}M_1(r_1^2+r_2^2)P_1P_2\left\{\cos[(r_1+r_2)\tau+\varphi+\theta]+\cos[(r_1-r_2)\tau+\varphi-\theta]\right\}$$

$$+M_2r_1r_2P_1P_2\left\{\cos[(r_1-r_2)\tau+\varphi-\theta]-\cos[(r_1+r_2)\tau+\varphi+\theta]\right\}$$

$$-\tfrac{1}{2}r_3^2r_5^2P_3P_5\left\{\cos[(r_3+r_5)\tau+\gamma+\delta]+\cos[(r_3-r_5)\tau+\gamma-\delta]\right\} \qquad (V.35)$$

Internal resonance relations of this equation are:

$$r_3 = 2r_5 \qquad r_5 = 2r_2$$

$$r_5 = 2r_1 \qquad r_5 = r_1 \pm r_2 \qquad (V.36)$$

V.2 Classification of Resonance Conditions: Relations(V.28,30, 32,34,and36) can be combined to give the following autoparametric resonance conditions:

$$\left.\begin{array}{ll}
1)\ r_3 = r_1+r_2 & 2)\ r_3 = r_1+r_2 \\
\quad = r_4 & \quad = r_5 \\
\quad = n\nu & \quad = n\nu \\
\\
3)\ r_3 = 2r_2 & 4)\ r_3 = 2r_2 \\
\quad = r_4 & \quad = 2r_5 \\
\quad = n\nu & \quad = n\nu \\
\\
5)\ r_3 = r_1-r_2 & 6)\ r_3 = r_1-r_2 \\
\quad = r_4 & \quad = r_5 \\
\quad = n\nu & \quad = n\nu \\
\\
7)\ r_3 = 2r_1 & 8)\ r_3 = 2r_2 \\
\quad = n\nu & \quad = n\nu \\
\\
9)\ r_3 = 2r_4 & 10)\ r_3 = 2r_5 \\
\quad = n\nu & \quad = n\nu
\end{array}\right\} \qquad (V.37)$$

The last four conditions represent principal parametric resonance conditions for four modes of the system. Conditions 7 and 8 have been investigated in Chapter (IV) and the last two conditions lead to an analysis similar to Chapter (III). In the following sections study will be confined to the first six conditions.

V.3 Condition(1)

$$r_3 = r_1 + r_2 \\ = r_4 \qquad = n\nu$$

The autoparametric interaction takes place between four modes, the first two normal modes $P_1, P_2$, the vertical main mass motion $P_3$ and the zeroth symmetric liquid sloshing mode $P_4$. The resonance terms corresponding to the present condition will be removed from equations (V.27, 29, 31, 33) and inserted in the fundamental variational equations (V.26). The resulting variational equations become;

$$-2r_1P_1\dot{\varphi} = \epsilon\left\{\epsilon^{-1}(S_1^2\nu^2 - r_1^2)P_1 + \tfrac{1}{2}C_{13}r_3^2P_2P_3\cos(\gamma-\theta-\varphi) - \tfrac{1}{2}C_{816}r_3^2P_2P_4\cos(\alpha-\theta-\varphi)\right\}$$

$$-2r_1\dot{P}_1 = \epsilon\left\{2r_1^2\zeta_1P_1 - \tfrac{1}{2}C_{13}r_3^2P_2P_3\sin(\gamma-\theta-\varphi) + \tfrac{1}{2}C_{816}r_3^2P_2P_4\sin(\alpha-\theta-\varphi)\right\}$$

$$-2r_2P_2\dot{\theta} = \epsilon\left\{\epsilon^{-1}(S_2^2\nu^2 - r_2^2)P_2 - \tfrac{1}{2}K_{10}r_3^2P_1P_3\cos(\gamma-\theta-\varphi) - \tfrac{1}{2}K_{426}r_3^2P_1P_4\cos(\alpha-\theta-\varphi)\right\}$$

$$-2r_2\dot{P}_2 = \epsilon\left\{2r_2^2\zeta_2P_2 + \tfrac{1}{2}K_{10}r_3^2P_1P_3\sin(\gamma-\theta-\varphi) + \tfrac{1}{2}K_{426}r_3^2P_1P_4\sin(\alpha-\theta-\varphi)\right\}$$

$$-2r_3P_3\dot{\gamma} = \epsilon\left\{\epsilon^{-1}(S_3^2\nu^2 - r_3^2)P_3 - \tfrac{1}{2}L_{477}r_3^2P_1P_2\cos(\gamma-\varphi-\theta) + f\cos\gamma\right\}$$

$$-2r_3\dot{P}_3 = \epsilon\left\{2r_3^2\zeta_3P_3 - \tfrac{1}{2}L_{477}r_3^2P_1P_2\sin(\gamma-\varphi-\theta) + f\sin\gamma\right\}$$

$$-2r_4P_4\dot{\alpha} = \epsilon\left\{\epsilon^{-1}(S_4^2\nu^2 - r_4^2)P_4 - \tfrac{1}{2}N_{112}r_3^2P_1P_2\cos(\alpha-\theta-\varphi)\right\}$$

$$-2r_4\dot{P}_4 = \epsilon\left\{2r_4^2\zeta_4P_4 - \tfrac{1}{2}N_{112}r_3^2P_1P_2\sin(\alpha-\theta-\varphi)\right\} \qquad (V.38)$$

where

$$C_{816} = C_1 S_2^2 + C_6 S_2 S_4 - C_8 S_4^2$$

$$K_{426} = K_4 S_1 S_4 + K_2 S_1^2 - K_6 S_4^2$$

$$L_{477} = L_4 S_1 S_2 + L_7 (S_1^2 + S_2^2)$$

$$N_{112} = N_1 (S_1^2 + S_2^2) - N_2 S_1 S_2$$

$$S_1 = r_1/r_3 \ , \ S_2 = r_2/r_3 \ , \ S_4 = r_4/r_3$$

Introducing the following parameters;

$$\left.\begin{aligned} P_i &= \frac{b_i \sqrt{f}}{r_3 \sqrt{|L_{pqr}|}} & \tau &= \frac{2T}{\epsilon \sqrt{f\,|L_{pqr}|}} & \psi_1 &= \theta + \varphi \\ \eta_i &= \frac{2 r_i \zeta_i}{\sqrt{f\,|L_{pqr}|}} & \gamma &= \frac{r_3^2 - \nu^2}{r_3 \epsilon \sqrt{f\,|L_{pqr}|}} & \psi_2 &= \theta - \varphi \\ & & & & \psi_3 &= 2\theta \end{aligned}\right\} \qquad (V.39)$$

equations (V.38) take the form;

$$-S_1 b_1 \dot{\varphi} = -S_1^2 \gamma b_1 + \tfrac{1}{2} \frac{C_{13}}{|L_{477}|} b_2 b_3 \cos(\gamma - \psi_1) - \tfrac{1}{2} \frac{C_{816}}{|L_{477}|} b_2 b_4 \cos(\alpha - \psi_1)$$

$$-S_1 \dot{b_1} = S_1 \eta_1 b_1 - \tfrac{1}{2} \frac{C_{13}}{|L_{477}|} b_2 b_3 \sin(\gamma - \psi_1) + \tfrac{1}{2} \frac{C_{816}}{|L_{477}|} b_2 b_4 \sin(\alpha - \psi_1)$$

$$-S_2 b_2 \dot{\theta} = -S_2^2 \gamma b_2 - \tfrac{1}{2} \frac{K_{10}}{|L_{477}|} b_1 b_3 \cos(\gamma - \psi_1) - \tfrac{1}{2} \frac{K_{426}}{|L_{477}|} b_1 b_4 \cos(\alpha - \psi_1)$$

$$-S_2 \dot{b_2} = S_2 \eta_2 b_2 + \tfrac{1}{2} \frac{K_{10}}{|L_{477}|} b_1 b_3 \sin(\gamma - \psi_1) + \tfrac{1}{2} \frac{K_{426}}{|L_{477}|} b_1 b_4 \sin(\alpha - \psi_1)$$

$$-b_3 \dot{\gamma} = -\gamma b_3 - \tfrac{1}{2} \frac{L_{477}}{|L_{477}|} b_1 b_2 \cos(\gamma - \psi_1) + \cos\gamma$$

$$-\dot{b_3} = \eta_3 b_3 - \tfrac{1}{2} \frac{L_{477}}{|L_{477}|} b_1 b_2 \sin(\gamma - \psi_1) + \sin\gamma$$

$$-S_4 b_4 \dot{\alpha} = -S_4^2 \gamma b_4 - \tfrac{1}{2} \frac{N_{112}}{|L_{477}|} b_1 b_2 \cos(\alpha - \psi_1)$$

$$-S_4 \dot{b_4} = S_4 \eta_4 b_4 - \tfrac{1}{2} \frac{N_{112}}{|L_{477}|} b_1 b_2 \sin(\alpha - \psi_1) \qquad (V.40)$$

To obtain the steady state solution, the left hand sides of equations (V.40) are equated to zero, however the resulting algebraic equations are not compatible since their number is greater than the number of unknowns. Such a situation has been treated in Chapter (IV) by considering some special cases. Again some special cases of (V.40) will be investigated.

a) $\eta_1 = \eta_2 = \eta_4 = 0$

This condition results in the five compatible equations

$$\left.\begin{aligned}
&-S_1^2\gamma b_1 \pm \tfrac{1}{2}\frac{C_{13}}{|L_{477}|}\, b_2 b_3 \mp \tfrac{1}{2}\frac{C_{816}}{|L_{477}|}\, b_2 b_4 = 0\\
&S_2^2\gamma b_2 \pm \tfrac{1}{2}\frac{K_{10}}{|L_{477}|}\, b_1 b_3 \pm \frac{K_{426}}{|L_{477}|}\, b_1 b_4 = 0\\
&\gamma b_3 \pm \tfrac{1}{2}\frac{L_{477}}{|L_{477}|}\, b_1 b_2 = \cos\gamma\\
&\eta_3 b_3 = -\sin\gamma\\
&S_4^2\gamma b_4 \pm \tfrac{1}{2}\frac{N_{112}}{|L_{477}|}\, b_1 b_2 = 0
\end{aligned}\right\} \quad (V.41)$$

The analytical solution of equations (V.41) is found to be:

the zero symmetric sloshing amplitude $b_4$:

$$b_4 = \frac{-0.5\, N_{112}}{\gamma S_4^2 |L_{477}|}\, b_1 b_2 \qquad (V.42a)$$

the first normal mode amplitude $b_1$:

$$b_1^2 = \frac{\gamma C_{13} S_2^2 b_2^2}{\left[\dfrac{(K_{10}C_{816} + C_{13}K_{426})}{4\gamma L_{477}^2 S_4^2} N_{112}\right] b_2^2 - \gamma K_{10} S_1^2} \qquad (V.42b)$$

the vertical mass motion amplitude $b_3$

$$b_3 = \frac{2\gamma}{C_{13}}\left[\frac{|L_{477}|S_1^2}{b_2^2} - \frac{C_{816}N_{112}}{4S_4^2\gamma^2}\right]b_1 b_2 \qquad (V.42c)$$

where the second normal mode amplitude $b_2$ is given by the solution of the quadratic equation in $b_2^2$:

$$\left\{\frac{S_2^2 C_{816}N_{112}}{2S_4^2}\left[\gamma^2+\eta_3^2 - \gamma\frac{L_{477}}{|L_{477}|}\right] + \tfrac{1}{4}C_{13}S_2^2\gamma\right\}b_2^4$$

$$+\left\{2S_1^2S_2^2\gamma L_{477}\left[\gamma^2 - \frac{|L_{477}|C_{816}N_{112}}{L_{477}\cdot C_{13}\cdot S_4^2}(\gamma^2+\tfrac{2}{3})\right] - \frac{N_{112}(K_{10}C_{816}+C_{13}K_{426})}{4L_{477}^2S_4^2\gamma}\right\}b_2^2$$

$$+\gamma S_1^2\left[\frac{4\gamma^2S_1^2S_2^2L_{477}^2(\gamma^2+\frac{2}{3})}{C_{13}} + K_{10}\right] = 0 \qquad (V.42d)$$

The amplitude-response curves $b_1, b_2, b_3$ and $b_4$ are shown in Figs. (V.2-5) for two values of liquid depth ratio h/a = 1, and 2, and for a perturbation parameter $\epsilon = 0.0105$. The characteristic of the theoretical solution of the four mode interaction is rather complex and differs from the case of the three mode interaction of chapter (IV). Because the damping parameters $\eta_1, \eta_2$ and $\eta_4$ were assumed zero, the amplitude response curves are not bounded on both sides of n=1. It is anticipated, from the previous chapter, that the damping causes the cross over at which the amplitudes collapse. However, there are some remarkable features that can be deduced from vertical tangents of the graphs in Fig. (V.2,3). When the forcing frequency increases from G to A, a jump AB occurs in the first two normal amplitudes $b_1$ and $b_2$ (Figs. (V.2a,b)) and the zero symmetric sloshing amplitude $b_4$ (Fig. (V.3d)) while the main mass amplitude $b_3$ follows the linear resonance curve HIB. The first normal mode

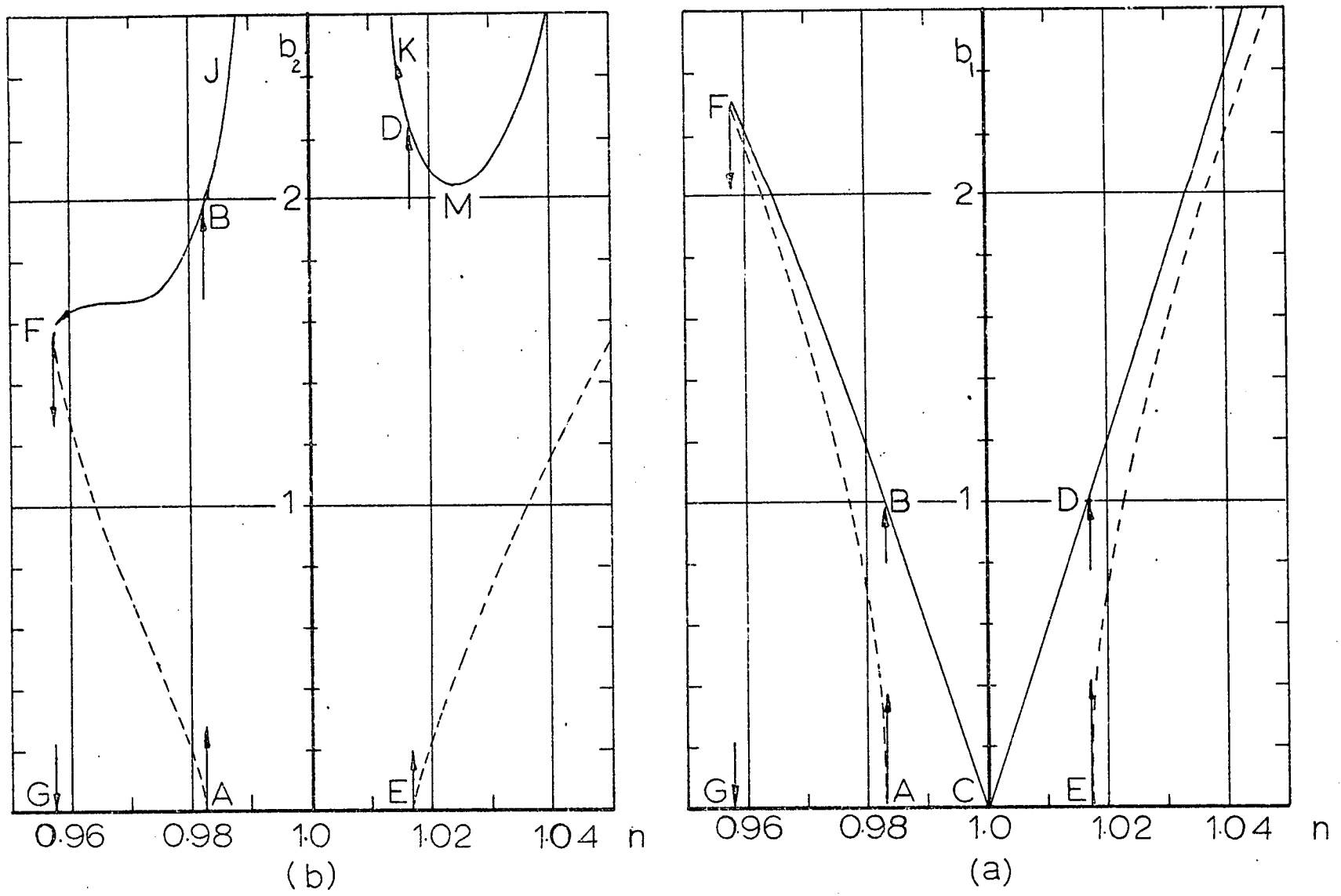


Fig(V. 2) Theoretical Response of the First Two Normal Modes, $r_3 = r_1 + r_2 = r_4$, $h/a = 1.0$, $\epsilon = 0.0105$, $l/a = 4.5$, $\zeta = 0.0275$

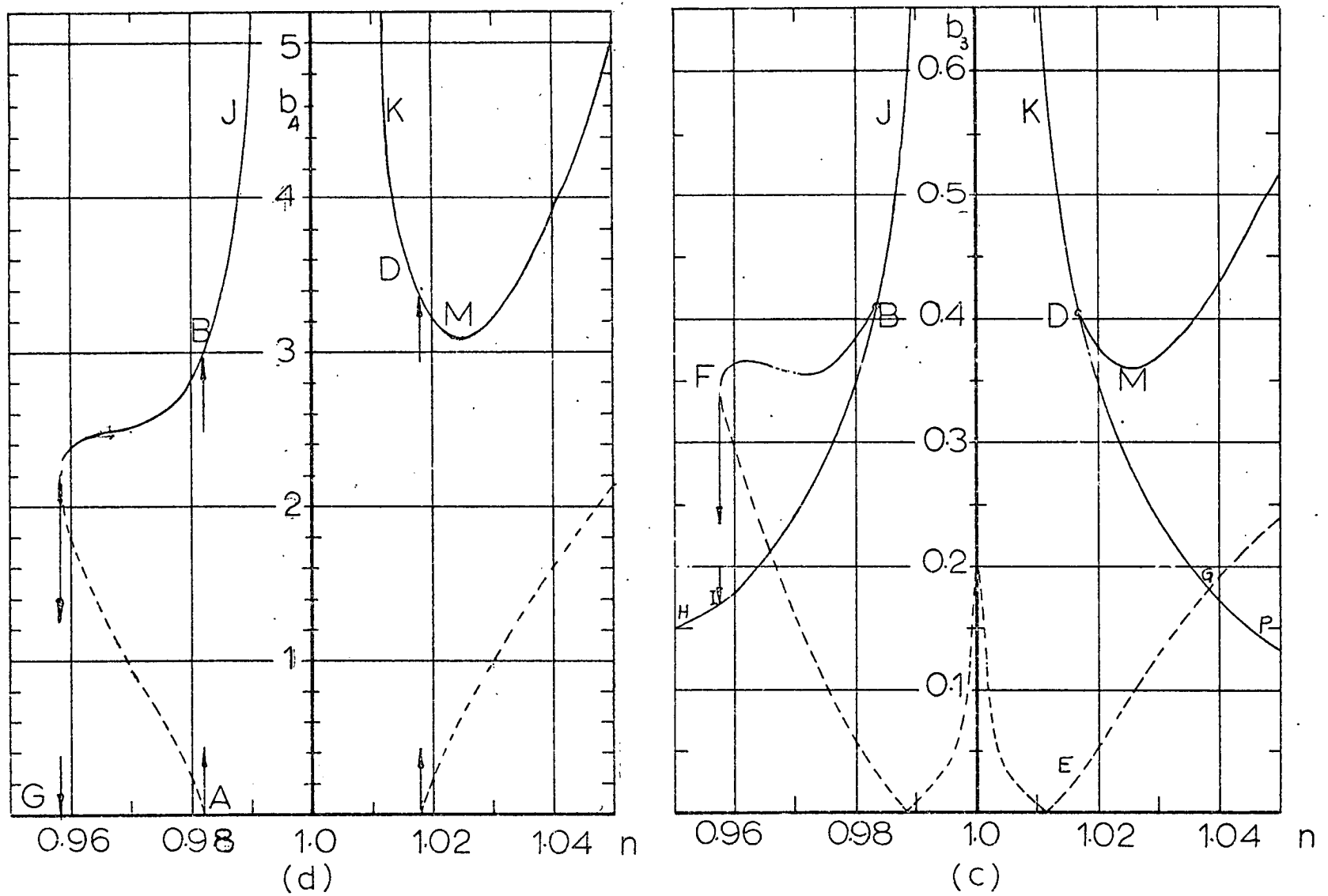


Fig(V. 3) Main Mass Amplitude $b_3$ and the Zeroth Symmetric Liquid Amplitude $b_4$ Responses. conditions as in fig.(v.2)

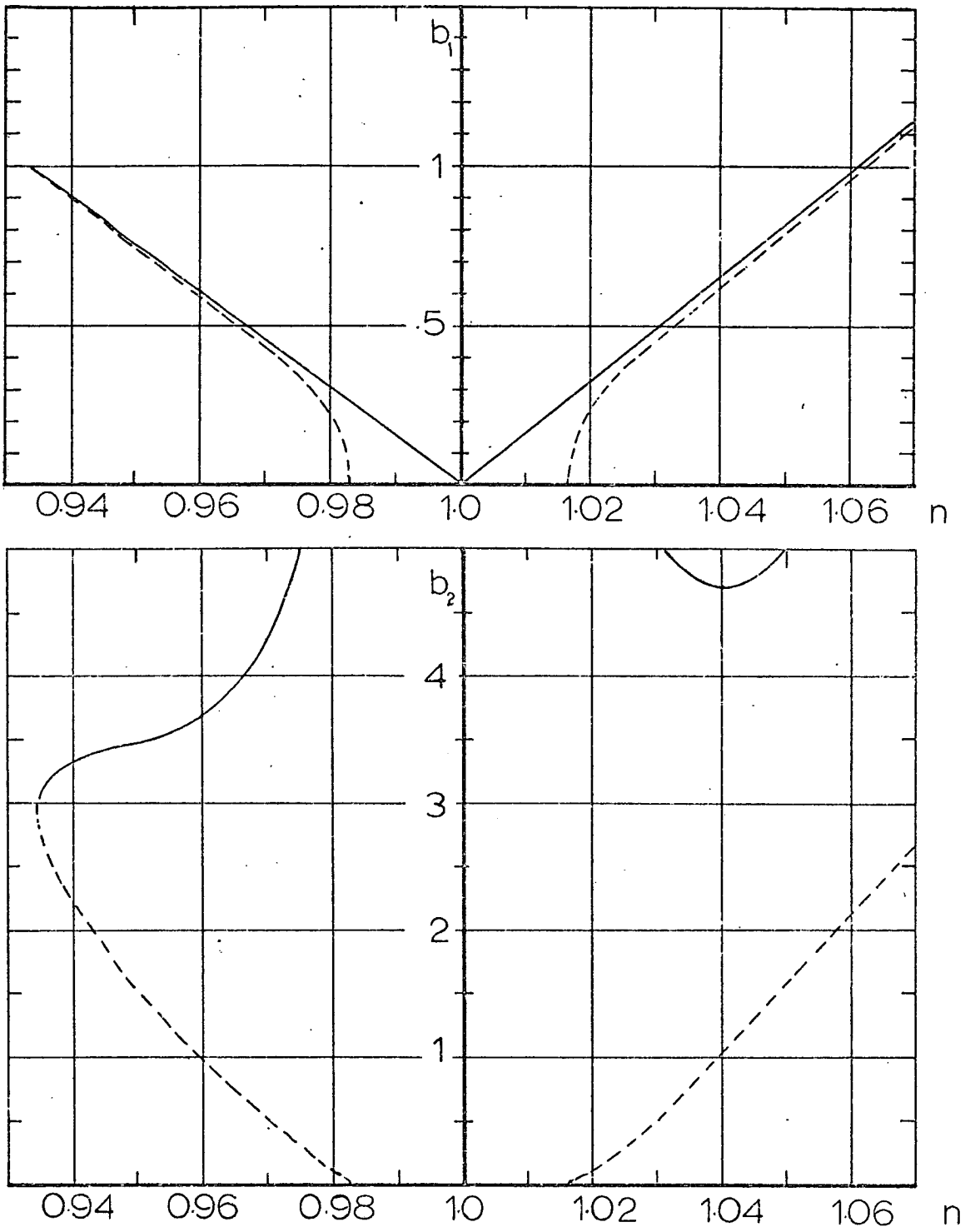


Fig(V. 4 ) Response of the First Two Modes Under Two Internal Resonance Conditions

$$r_3 = r_1 + r_2, \qquad r_3 = r_4$$

$h/a = 2.0$, $l/a = 4.1$, $\epsilon = .0105$, $\bar{\zeta}_{s1} = .0275$

$\bar{\zeta}_1 = \bar{\zeta}_2 = \bar{\zeta}_4 = 0.0$

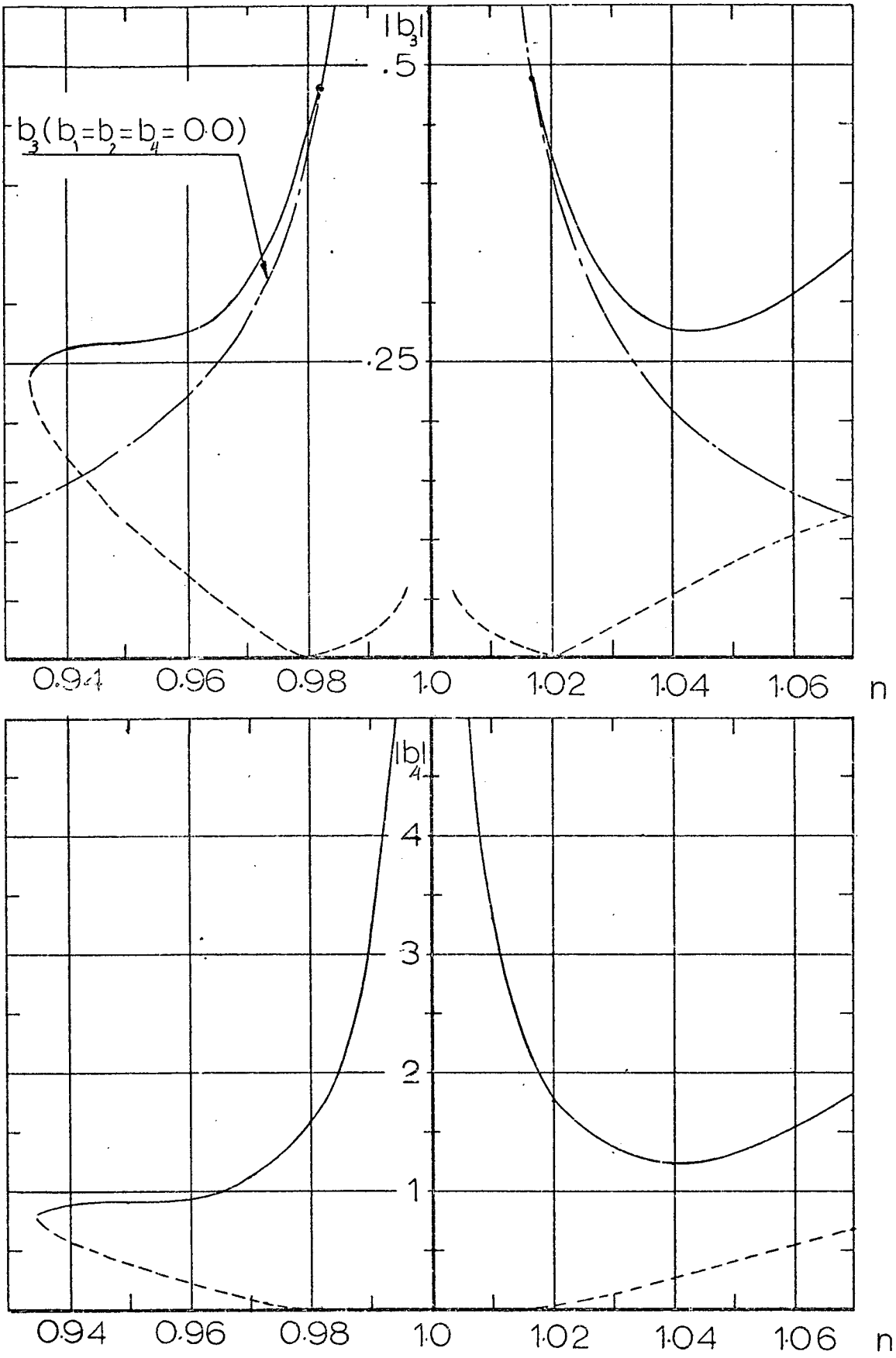


Fig(V.5) Response of the Main Mass $b_3$ and the Zeroth Symmetric Sloshing Mode $b_4$ under the conditions of fig(v.4)

amplitude $b_1$ exhibits a suppression effect BCD while the other modes follow the resonant curves BJKD with instability at n=1. A further increase in the forcing frequency causes a continuous decrease in $b_2$,$b_3$ and $b_4$ indicated by the path DM, while $b_2$ increases until its collapse which would have appeared if the damping parameters were included. When $b_4$ reaches its minimum value at M ($\frac{db_4}{dn} = 0$), the first antisymmetric sloshing mode dominates the liquid free surface motion until its collapse which brings the main mass response down to a point on the curve DGP. As the forcing frequency is decreased the system follows the paths indicated by the reversed arrows where the collapse location is defined on the left hand side of n = 1.0.

b) $\eta_1 \neq \eta_2 \neq \eta_4 \neq 0$

An attempt has been made to investigate equations (V.40) in a CSMP simulation, however it was difficult to observe any regular response in the numerical solution. The simulation showed that the system does not achieve any steady state solution during the long period of time inserted in the program, (T=150). The amplitudes $b_1$,$b_2$ and $b_4$ are increasing with time which indicates that the system is unstable.

V.4 Condition (2)

$$r_3 = r_1 + r_2$$
$$= r_5$$
$$= n\nu$$

Here the interaction takes place between the first two normal modes $P_1$, $P_2$ the vertical mass motion $P_3$, and the second symmetric sloshing mode $P_5$. Resonance terms corresponding to this condition are removed from the perturbation equations and inserted in the

fundamental variational equations which become:-

$$-2r_1P_1\dot{\varphi}=\epsilon\left\{\epsilon^{-1}(S_1^2\nu^2-r_1^2)P_1+\tfrac{1}{2}C_{13}r_3^2P_2P_3\cos(\gamma-\theta-\varphi)-\tfrac{1}{2}C_{759}r_3^2P_2P_5\cos(\delta-\theta-\varphi)\right\}$$

$$-2r_1\dot{P}_1=\epsilon\left\{2r_1^2\zeta_1P_1-\tfrac{1}{2}C_{13}r_3^2P_2P_3\sin(\gamma-\theta-\varphi)-\tfrac{1}{2}C_{759}r_3^2P_2P_5\sin(\delta-\theta-\varphi)\right\}$$

$$-2r_2P_2\dot{\theta}=\epsilon\left\{\epsilon^{-1}(S_2^2\nu^2-r_2^2)P_2-\tfrac{1}{2}K_{10}r_3^2P_1P_3\cos(\gamma-\theta-\varphi)-\tfrac{1}{2}K_{537}r_3^2P_1P_5\cos(\delta-\theta-\varphi)\right\}$$

$$-2r_2\dot{P}_2=\epsilon\left\{2r_2^2\zeta_2P_2+\tfrac{1}{2}K_{10}r_3^2P_1P_3\sin(\gamma-\theta-\varphi)+\tfrac{1}{2}K_{537}r_3^2P_1P_5\sin(\delta-\theta-\varphi)\right\}$$

$$-2r_3P_3\dot{\gamma}=\epsilon\left\{\epsilon^{-1}(S_3^2\nu^2-r_3^2)P_3-\tfrac{1}{2}L_{477}r_3^2P_1P_2\cos(\gamma-\theta-\varphi)+f\cos\gamma\right\}$$

$$-2r_3\dot{P}_3=\epsilon\left\{2r_3^2\zeta_3P_3-\tfrac{1}{2}L_{477}r_3^2P_1P_2\sin(\gamma-\theta-\varphi)+f\sin\gamma\right\}$$

$$-2r_5P_5\dot{\delta}=\epsilon\left\{\epsilon^{-1}(S_5^2\nu^2-r_5^2)P_5-\tfrac{1}{2}M_{112}r_3^2P_1P_2\cos(\delta-\theta-\varphi)\right\}$$

$$-2r_5\dot{P}_5=\epsilon\left\{2r_5^2\zeta_5P_5-\tfrac{1}{2}M_{112}r_3^2P_1P_2\sin(\delta-\theta-\varphi)\right\} \qquad (V.43)$$

where

$$C_{759}=C_7S_2S_5-C_5S_2^2+C_9S_5^2$$

$$K_{537}=K_5S_1S_5-K_3S_1^2+K_7S_5^2$$

$$L_{477}=L_4S_1S_2+L_7(S_2^2+S_1^2)$$

$$M_{112}=M_1(S_1^2+S_2^2)+M_2S_1S_2$$

$$S_i=r_i/r_3$$

Using (V.39), equations (V.43) can be written in the form:

$$-S_1b_1\dot{\varphi}=-S_1^2\gamma b_1+\frac{1}{2}\frac{C_{13}}{|L_{477}|}b_2b_3\cos(\gamma-\psi_1)-\frac{1}{2}\frac{C_{759}}{|L_{477}|}b_2b_5\cos(\delta-\psi_1)$$

$$-S_1\dot{b_1}=S_1\eta_1b_1-\frac{1}{2}\frac{C_{13}}{|L_{477}|}b_2b_3\sin(\gamma-\psi_1)+\frac{1}{2}\frac{C_{759}}{|L_{477}|}b_2b_5\sin(\delta-\psi_1)$$

$$-S_2b_2\dot{\theta}=-S_2\gamma b_2-\frac{1}{2}\frac{K_{10}}{|L_{477}|}b_1b_3\cos(\gamma-\psi_1)-\frac{1}{2}\frac{K_{537}}{|L_{477}|}b_1b_5\cos(\delta-\psi_1)$$

$$-S_2\dot{b_2} = S_2\eta_2 b_2 + \tfrac{1}{2}\frac{K_{10}}{|L_{477}|} b_1 b_3 \sin(\gamma-\psi_1) + \tfrac{1}{2}\frac{K_{537}}{|L_{477}|} b_1 b_5 \sin(\delta-\psi_1)$$

$$-b_3\dot{\gamma} = -\gamma b_3 - \tfrac{1}{2}\frac{L_{477}}{|L_{477}|} b_1 b_2 \cos(\gamma-\psi_1) + \cos\gamma$$

$$-\dot{b_3} = \eta_3 b_3 - \tfrac{1}{2}\frac{L_{477}}{|L_{477}|} b_1 b_2 \cos(\gamma-\psi_1) + \sin\gamma$$

$$-S_5 b_5 \dot{\delta} = -S_5^2 \gamma b_5 - \tfrac{1}{2}\frac{M_{112}}{|L_{477}|} b_1 b_2 \cos(\delta-\psi_1)$$

$$-S_5\dot{b_5} = S_5\gamma b_5 - \tfrac{1}{2}\frac{M_{112}}{|L_{477}|} b_1 b_2 \sin(\delta-\psi_1) \qquad \text{(V.44)}$$

Again, a set of incompatible equations is obtained when the left hand side are equated to zero. As in the previous condition a special case will be considered.

a) $\eta_1 = \eta_2 = \eta_5 = 0$

The response of the system is determined by the equations,

$$\left.\begin{aligned}
-S_1^2\gamma b_1 \pm \tfrac{1}{2}\frac{C_{13}}{|L_{477}|} b_2 b_3 \mp \tfrac{1}{2}\frac{C_{759}}{|L_{477}|} b_2 b_5 &= 0 \\
S_2^2\gamma b_2 \pm \frac{K_{10}}{|L_{477}|} b_1 b_3 \pm \tfrac{1}{2}\frac{K_{537}}{|L_{477}|} b_1 b_5 &= 0 \\
\gamma b_3 \pm \tfrac{1}{2}\frac{L_{477}}{|L_{477}|} b_1 b_2 &= \cos\gamma \\
\eta_3 b_3 &= -\sin\gamma \\
-S_5^2\gamma b_5 \mp \tfrac{1}{2}\frac{M_{112}}{|L_{477}|} b_1 b_2 &= 0
\end{aligned}\right\} \qquad \text{(V.45)}$$

The analytical solution of equations (V.45) can be obtained in a similar form to (V.42) as:

The second symmetric sloshing mode (amplitude $b_5$)

$$b_5 = \frac{-0.5M_{112}}{|L_{477}|\gamma S_5^2} b_1 b_2 \qquad \text{(V.46a)}$$

where the normal modes $b_1$ and $b_2$ have the relation

$$b_1^2 = \frac{\gamma C_{13} S_2^2 b_2^2}{\left[\frac{(K_{10}C_{759} + C_{13}K_{537})}{4\gamma L_{477}^2 S_5^2}\right] b_2^2 - \gamma K_{10} S_1^2} \tag{V.46b}$$

the amplitude of the vertical mass motion $b_3$:

$$b_3 = \frac{2\gamma}{C_{13}} \left[\frac{|L_{477}| S_1^2}{b_2^2} - \frac{C_{759}M_{112}}{4S_5^2 \gamma^2}\right] b_1 b_2 \tag{V.46c}$$

where $b_2$ is given by solving the quadratic equation in $b_2^2$:

$$\left\{\frac{S_2^2 C_{759} M_{112}}{2S_5^2}\left[\gamma^2 + \frac{2}{3} - \frac{\gamma L_{477}}{|L_{477}|}\right] + \tfrac{1}{4} C_{13} S_2^2 \gamma\right\} b_2^4$$

$$+\left\{2S_1^2 S_2^2 \gamma L_{477}\left[\gamma^2 - \frac{|L_{477}| C_{759} M_{112}}{L_{477} C_{13} S_5^2}\left(\gamma^2 + \frac{2}{3}\right)\right] - \frac{M_{112}(K_{10}C_{759} + C_{13}K_{537})}{4L_{477}^2 S_5^2 \gamma}\right\} b_2^2$$

$$+ \gamma S_1^2 \left[\frac{4\gamma^2 S_1^2 S_2^2 L_{477}^2 (\gamma^2 + \eta_3^2)}{C_{13}} + K_{10}\right] = 0 \tag{V.46d}$$

Figs. (V.6,7) depict the amplitude response curves for the case h/a = 1.0 and $\in$ = 0.0105. Again the system possesses an unstable solution in the neighbourhood of n=1 indicated by the unbounded response curves at that frequency region. At h/a = 2.0, equation (V.46d) has no real solution.

b) $\eta_1 \neq \eta_2 \neq \eta_5 \neq 0.0$

A CSMP simulation for the complete set of equation (V.44) gives an unsteady, unstable solution.

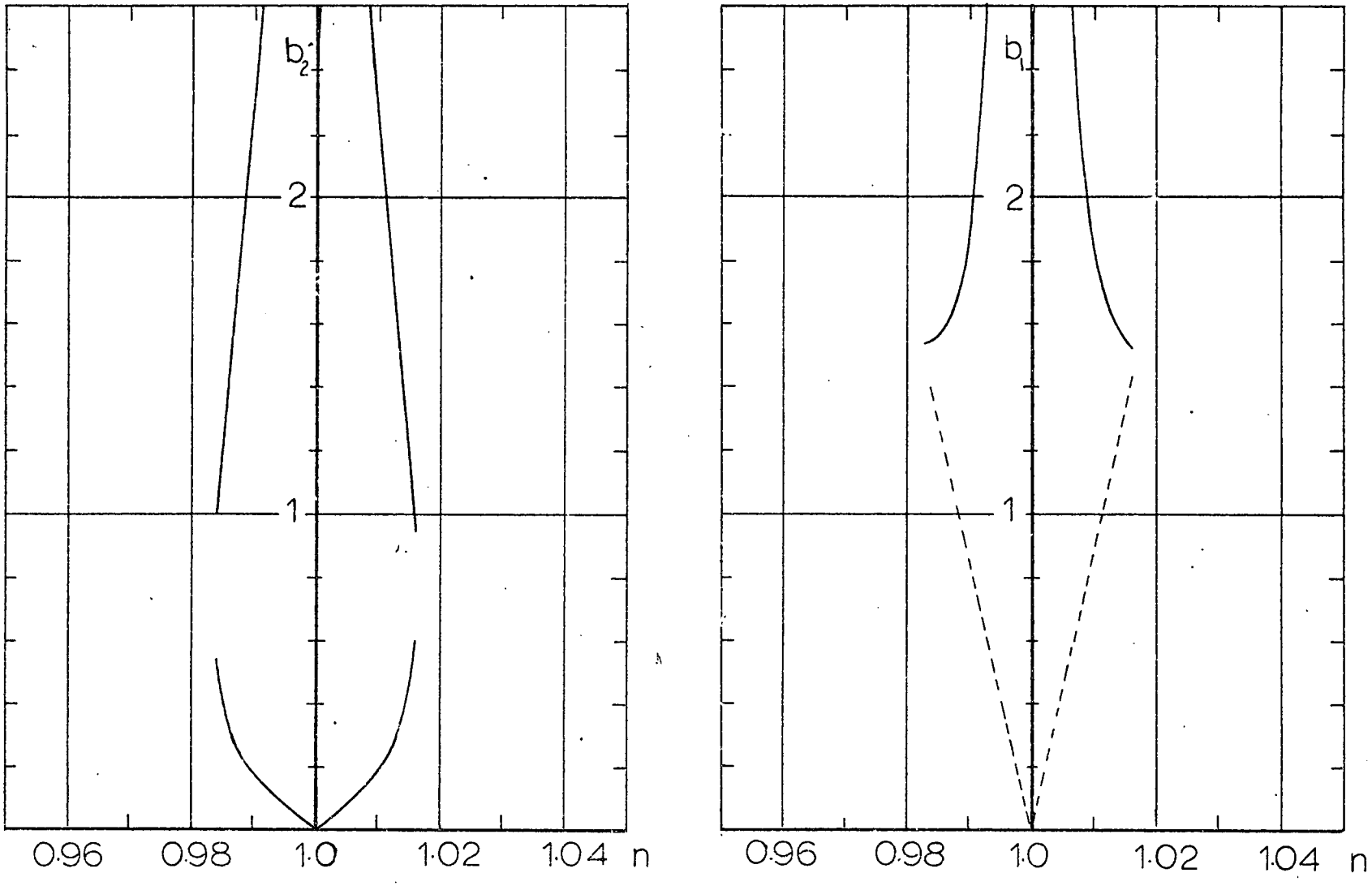


Fig(V. 6) Response of the First Two Normal Modes, $\Gamma_3 = \Gamma_1 + \Gamma_2 = \Gamma_5$, $h/a = 1.0$, $l/a = 5.25$, $\epsilon = 0.0105$, $\bar{\zeta}_{s_1} = .0275$, $\bar{\zeta}_1 = \bar{\zeta}_2 = \bar{\zeta}_5 = 0.0$

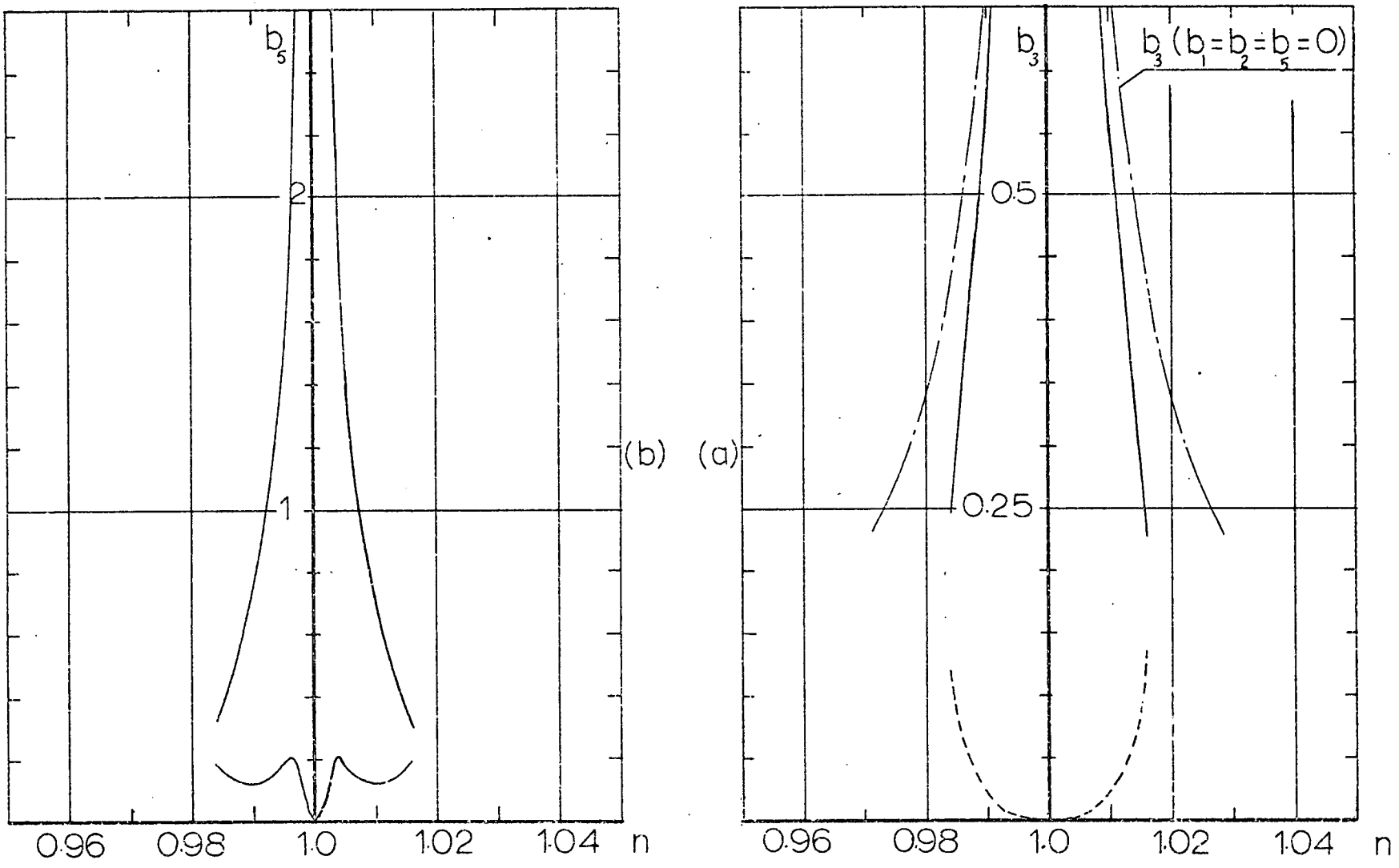


Fig(V. 7 ) Main Mass and Second Symmetric Sloshing Mode Responses
[data as of fig(V. 6 )]

V.5 Condition (3)

$$r_3 = 2r_2$$

$$= r_4$$

$$= n\nu$$

The interaction under this condition will take place between three modes, the second normal mode $P_2$, the main mass motion $P_3$, and the zeroth symmetric sloshing mode $P_4$. The variational equations of this case are found to be:

$$-2r_2P_2\dot{\theta} = \epsilon\left\{\epsilon^{-1}(S_2^2\nu^2-r_2^2)P_2-\tfrac{1}{2}K_{11}r_3^2P_2P_3\cos(\gamma-2\theta)-\tfrac{1}{2}K_{246}r_3^2P_2P_4\cos(\alpha-2\theta)\right\}$$

$$-2r_2\dot{P}_2 = \epsilon\left\{2r_2^2\zeta_2P_2+\tfrac{1}{2}K_{11}r_3^2P_2P_3\sin(\gamma-2\theta)+\tfrac{1}{2}K_{246}r_3^2P_2P_4\sin(\alpha-2\theta)\right\}$$

$$-2r_3P_3\dot{\gamma} = \epsilon\left\{\epsilon^{-1}(S_3^2\nu^2-r_3^2)P_3-\tfrac{1}{2}L_{58}r_2^2P_2^2\cos(\gamma-2\theta)+f\cos\gamma\right\}$$

$$-2r_3\dot{P}_3 = \epsilon\left\{2r_3^2\zeta_3P_3-\tfrac{1}{2}L_{58}r_2^2P_2^2\sin(\gamma-2\theta)+f\sin\gamma\right\}$$

$$-2r_4\dot{P}_4 = \epsilon\left\{\epsilon^{-1}(S_4^2\nu^2-r_4^2)P_4-\tfrac{1}{2}N_{12}r_2^2P_2^2\cos(\alpha-2\theta)\right\}$$

$$-2r_4\dot{P}_4 = \epsilon\left\{2r_4^2\zeta_4P_4-\tfrac{1}{2}N_{12}r_2^2P_2^2\sin(\alpha-2\theta)\right\} \qquad \text{(V.47)}$$

where:

$$K_{246} = K_2S_2^2+K_4S_1S_4-K_6S_4^2$$

$$L_{58} = L_5+L_8$$

$$N_{12} = N_1-N_2$$

Writing (V.47) in terms of the new variables (V.39):

$$-S_2 b_2 \dot{\theta} = -S_2^2 \gamma b_2 - \tfrac{1}{2} \frac{K_{11}}{|L_{58}|} b_2 b_3 \cos(\gamma - \psi_3) - \tfrac{1}{2} \frac{K_{246}}{|L_{58}|} b_2 b_4 \cos(\alpha - \psi_3)$$

$$-S_2 \dot{b_2} = S_2 \eta_2 b_2 + \tfrac{1}{2} \frac{K_{11}}{|L_{58}|} b_2 b_3 \sin(\gamma - \psi_3) + \tfrac{1}{2} \frac{K_{246}}{|L_{58}|} b_2 b_4 \sin(\alpha - \psi_3)$$

$$-b_3 \dot{\gamma} = -\gamma b_3 - \tfrac{1}{2} \frac{L_{58}}{|L_{58}|} S_2^2 b_2^2 \cos(\gamma - \psi_3) + \cos\gamma$$

$$-\dot{b_3} = \eta_3 b_3 - \tfrac{1}{2} \frac{L_{58}}{|L_{58}|} S_2^2 b_2^2 \sin(\gamma - \psi_3) + \sin\gamma$$

$$-S_4 b_4 \dot{\alpha} = -S_4^2 \gamma b_4 - \tfrac{1}{2} \frac{N_{12}}{|L_{58}|} S_2^2 b_2^2 \cos(\alpha - \psi_3)$$

$$-S_4 \dot{b_4} = S_4 \eta_4 b_4 - \tfrac{1}{2} \frac{N_{12}}{|L_{58}|} S_2^2 b_2^2 \sin(\alpha - \psi_3) \qquad \text{(V.48)}$$

On setting the left hand sides of (V.48) equal to zero, the resulting algebraic equations are consistent. The analytical solution of this set of equations was found to be rather difficult, however an algorithm DAVDEN, (IMP External Routine) due to Davidenko was used to solve the nonlinear algebraic equations of (V.48). The amplitude-response curves are displayed in Figs. (V.8,9) and show a discontinuity in the second normal mode response $b_2$ at n=1 while the main mass response $b_3$ and the zeroth symmetric sloshing response $b_4$ follow resonance curves near n=1. The response curves shown in these figures represent one of the solutions of (V.48), and other solutions could be obtained if another attempt were made by inserting suitable trial values of the $b_i$'s.

Special Case $\eta_2 = \eta_4 = 0$

This assumption reduces the algebraic equations of (V.48) to four equations whose solution is found to be:

the zeroth symmetric sloshing mode $b_4$:

$$b_4 = -\tfrac{1}{2\gamma} \frac{N_{12}}{|L_{58}|} \left(\frac{S_2^2}{S_4}\right) b_2^2 \qquad \text{(V.49a)}$$

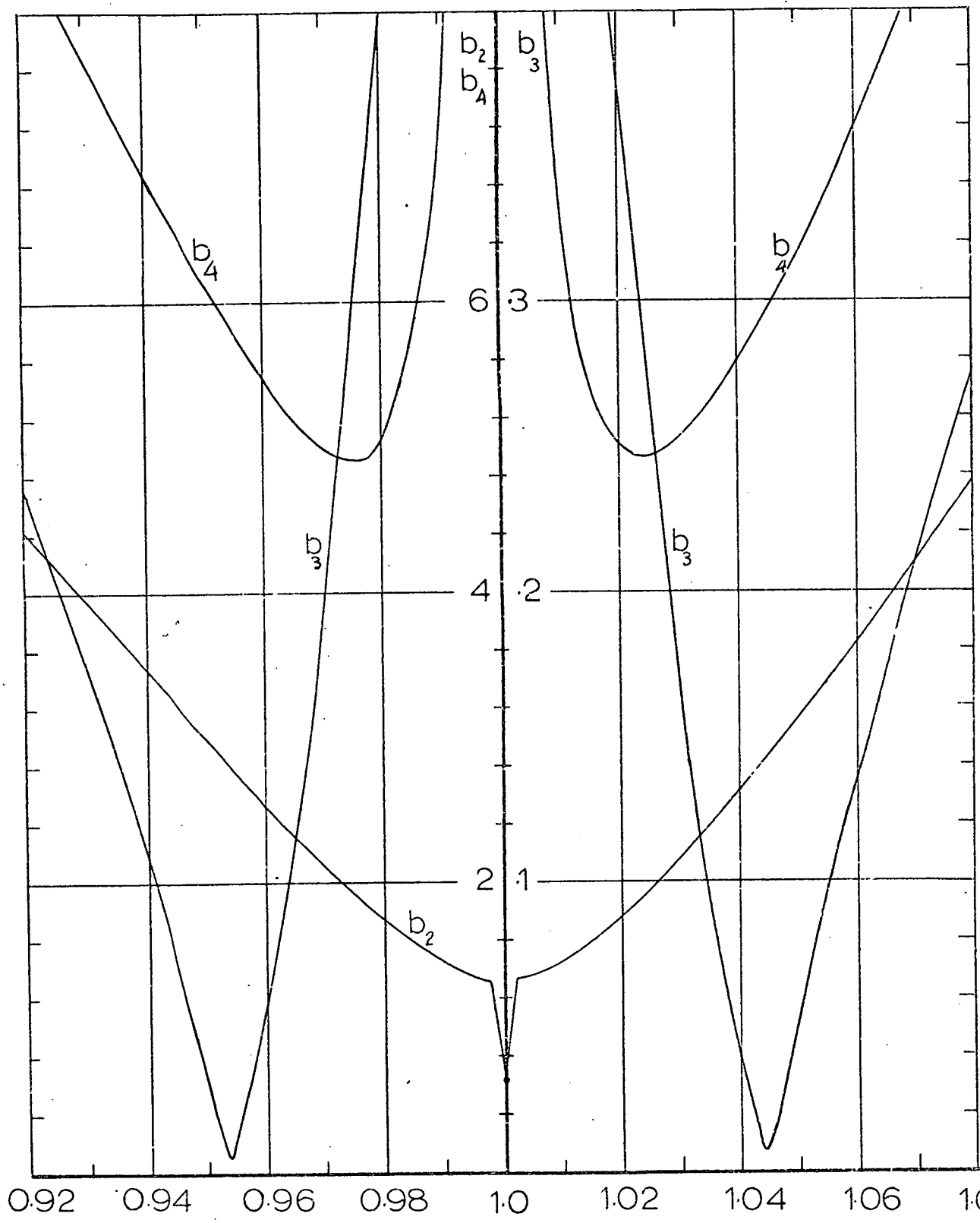


Fig(V.8) Three Mode Interaction under two internal resonance conditions, (Davidenko algorithm numerical solution), $h/a = 1.0$, $l/a = 2.88$, $\epsilon = .021$ $\bar{\zeta}_2 = \bar{\zeta}_4 = .005$, $\bar{\zeta}_{s1} = .0275$, $r_3 = 2r_2$, $r_3 = r_4$

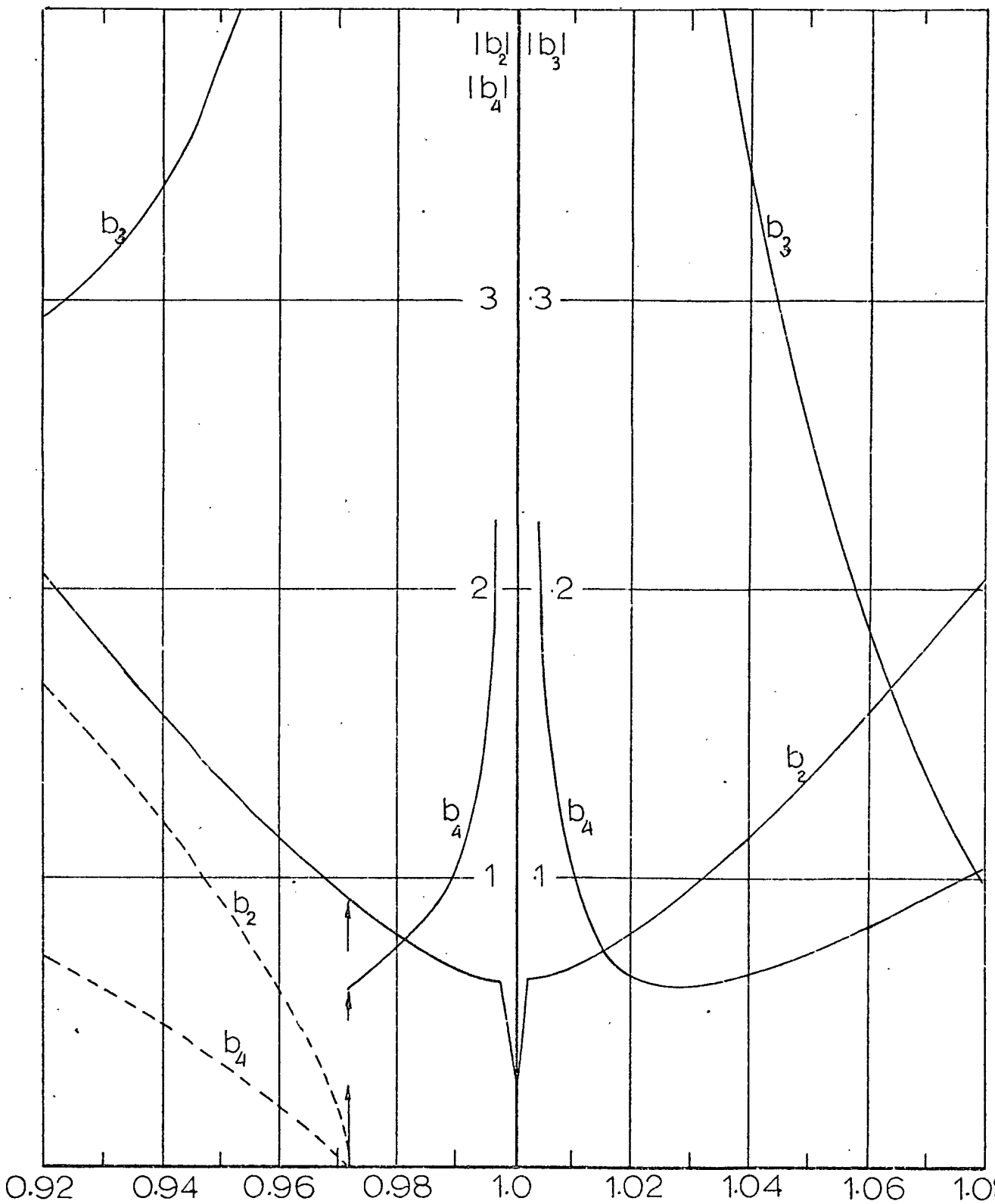


Fig(V·9) Three Mode Interaction, ( $r_3 = 2\, r_2$ , $r_3 = r_4$ )
(Davidenko algorithm solution) $h/a = 2.0$, $l/a = 2.88$
$\epsilon = .021$, $\bar{\zeta}_{s1} = .0275$, $\bar{\zeta}_2 = \bar{\zeta}_4 = .005$

the vertical main mass amplitude $b_3$:

$$b_3 = -\frac{2S_2^2\gamma|L_{58}|}{K_{11}} + \frac{K_{246}\cdot N_{12}}{2\gamma K_{11}|L_{58}|}\left(\frac{S_2}{S_4}\right)^2 b_2^2 \qquad \text{(V.49b)}$$

where the second normal mode amplitude $b_2$ is given by the solution of the quadratic equation in $b_2^2$:

$$\left\{\tfrac{1}{4}\left(\frac{S_2}{S_4}\right)^4\left[\frac{K_{246}\,N_{12}}{K_{11}|L_{58}|\gamma}\right]^2(\gamma^2+\eta_3^2) + \tfrac{1}{2}S_4^2\left[\left(\frac{S_2}{S_4}\right)^4\frac{K_{246}\cdot N_{12}}{L_{58}\cdot K_{11}} + \tfrac{1}{2}\right]\right\} b_2^4$$

$$-\frac{2S_2^4}{K_{11}}\left\{\frac{K_{246}\cdot N_{12}}{K_{11}\cdot S_4^2}(\gamma^2+\eta_3^2)+2\gamma^2 L_{58}\right\} b_2^2 + \left\{\frac{4S_2^4\gamma^2L_{58}^2}{K_{11}^2}(\gamma^2+\eta_3^2)-1\right\} = 0 \qquad \text{(V.49c)}$$

Equation (V.49c) has two real solutions shown in Fig. (V.10,12). The positions of vertical tangency determine the regions of instability in the system under the two internal resonance conditions $r_3 = 2r_2$ . $r_3=r_4$. The figures show that when the system is excited at a frequency below the resonance ($n<1$), the main mass response follows the response of a single degree of freedom system AB while $b_2$ and $b_4$ remain identically zero AB. A continuous increase in the forcing frequency brings the system in the region of autoparametric instability in which $b_2$ and $b_4$ jump to C, in the same time an autoparametric absorber effect appears in the response of the main mass CD. A further increase in n causes the zeroth symmetric sloshing mode $b_4$ to dominate the motion of the liquid free surface. This mode follows a typical resonant curve near n=1 while $b_2$ exhibits a discontinuity at n=1. At a frequency greater than resonance ($n>1$) there is another type of vertical tangency EF which brings $b_2$ and $b_4$ down to zero and $b_3$ follows again the linear resonance curve. Fig. (V.10b) shows another solution for the main mass indicated by the response JKLMN which may occur if the first antisymmetric sloshing mode is overcome by the motion of the zeroth symmetric sloshing mode,

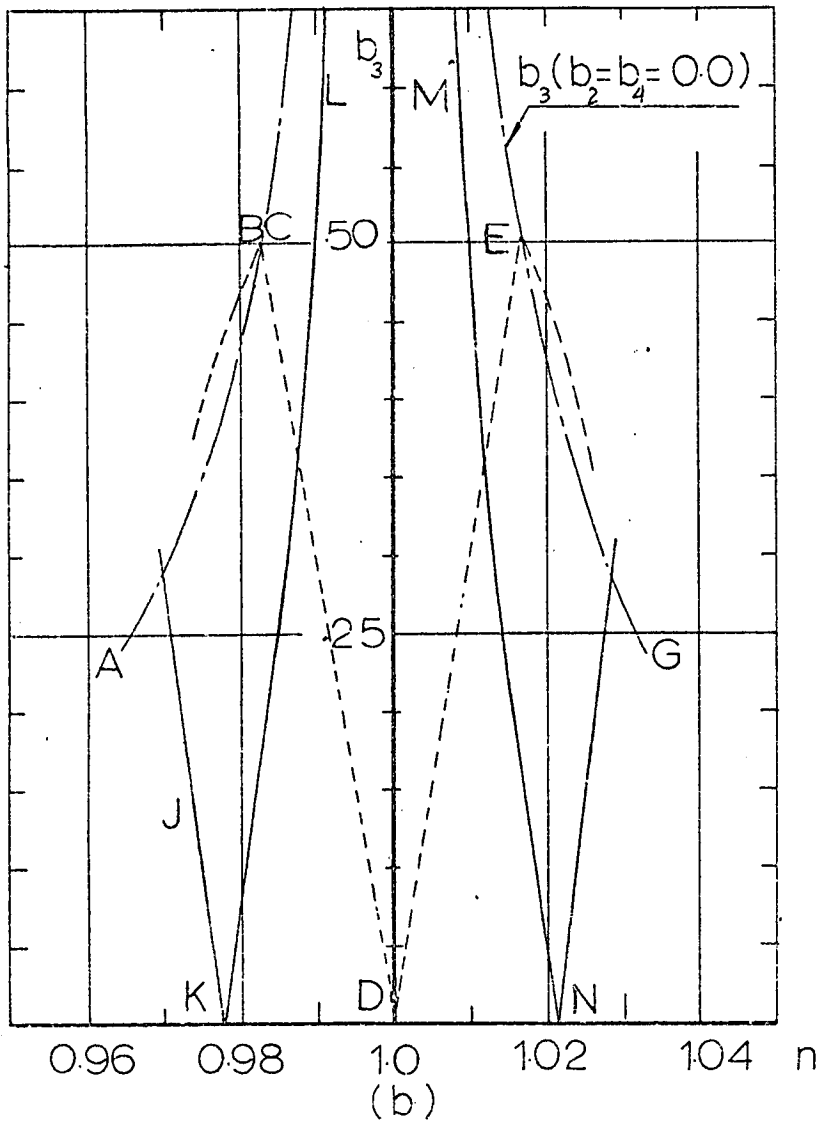


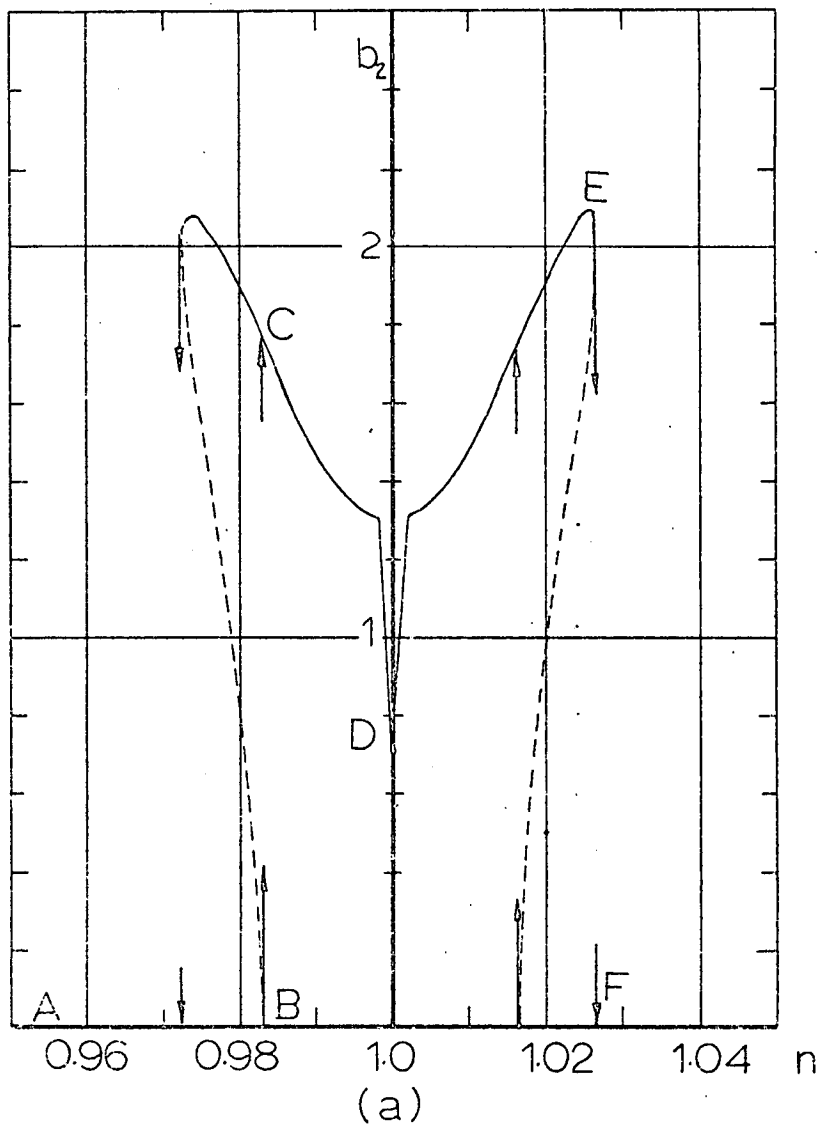


Fig(V.10) Second Normal Mode $b_2$ and Main Mass Amplitude $b_3$ Responses under the Resonance Condition, $r_3 = 2\,r_2 = r_4$, $h/a = 1.0$, $l/a = 2.8$, $\epsilon = 0.0105$ $\bar{\zeta}_2 = .0275$, $\bar{\zeta}_3 = \bar{\zeta}_4 = 0.0$

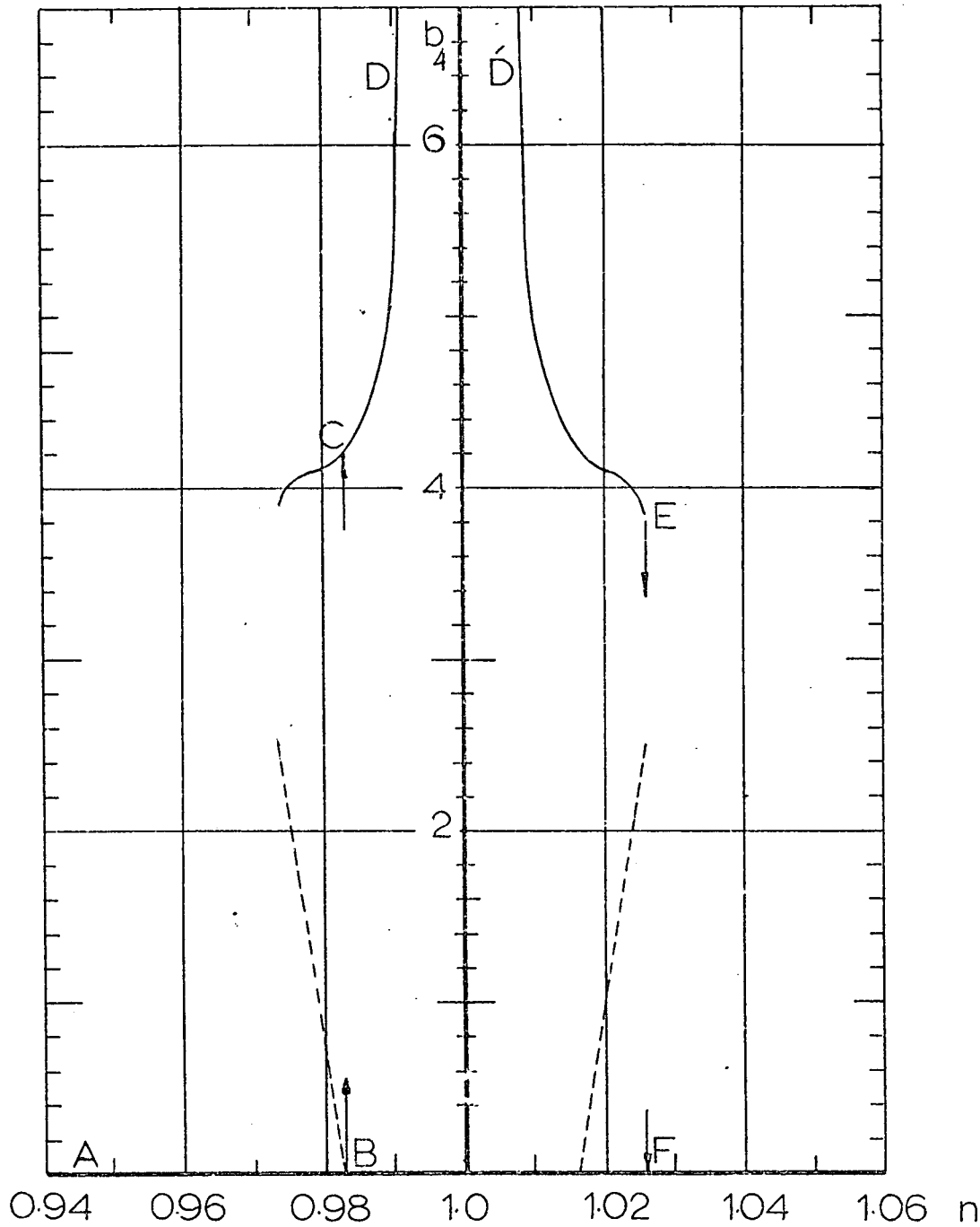


Fig(V.11 ) Response of the Zeroth Sloshing Mode, same constants of fig(v.10 )

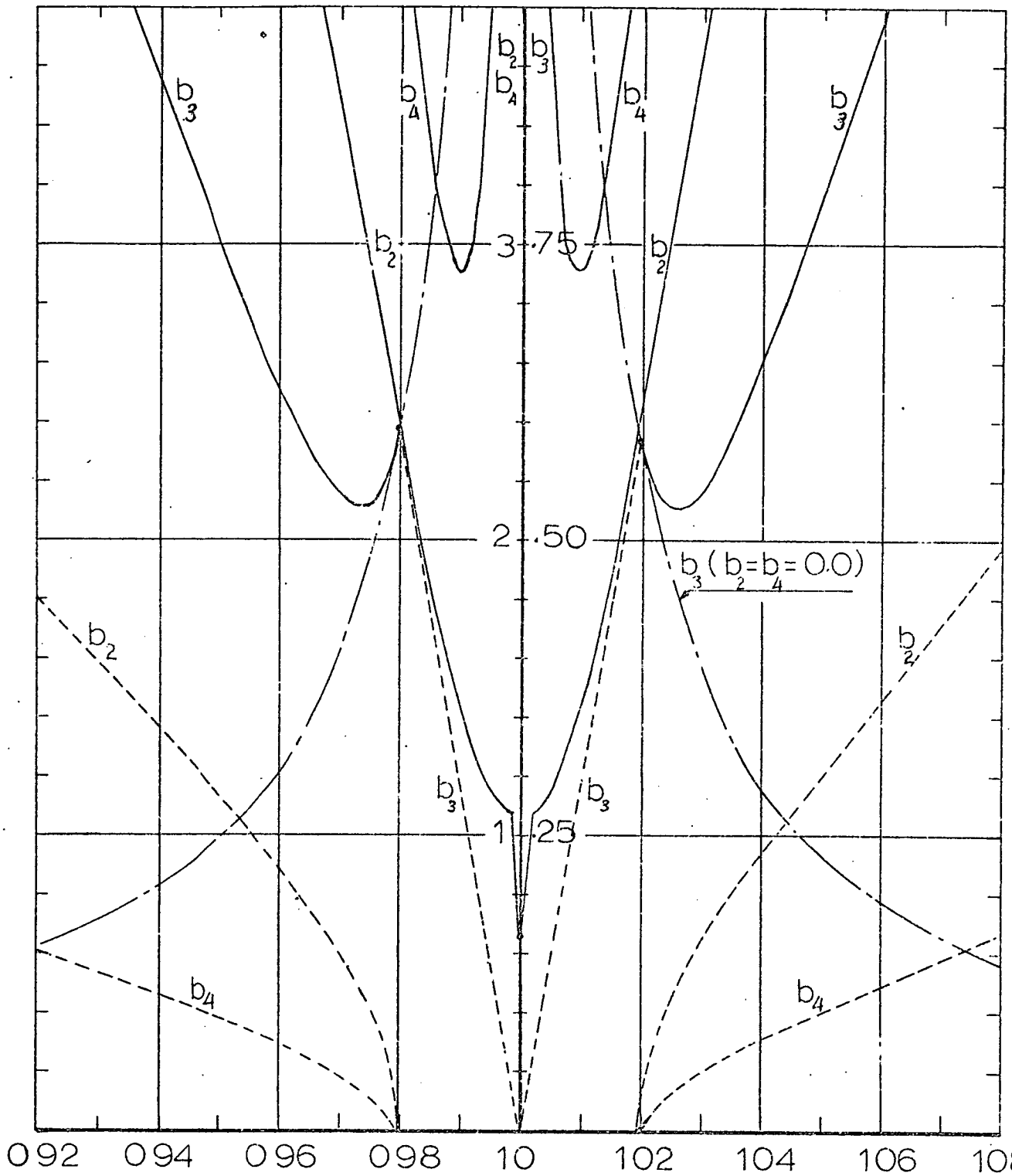


Fig(V.12) Three Mode Interaction under Two Internal Resonance Conditions, ($r_3 = 2r_2$, $r_3 = r_4$)
$h/a = 2.0$, $l/a = 2.88$, $\bar{\zeta}_{s1} = \cdot0275$, $\bar{\zeta}_2 = \bar{\zeta}_4 = 0.0$ $\epsilon = \cdot0105$

in that case there are two frequencies at K and N at which an absorbing effect in $b_3$ takes place.

V.6 Condition (4)

$$\begin{aligned} r_3 &= 2r_2 \\ &= r_5 \\ &= n\nu \end{aligned}$$

Following the same analysis of the previous condition and considering the second symmetric sloshing mode $P_5$ instead of the zeroth one, the following variational equations are found:

$$\begin{aligned}
-2r_2P_2\dot{\theta} &= \epsilon\left\{\epsilon^{-1}(S_2^2\nu^2-r_2^2)P_2-\tfrac{1}{2}K_{11}r_3^2P_2P_3\cos(\gamma-2\theta)-\tfrac{1}{2}K_{537}r_3^2P_2P_5\cos(\delta-2\theta)\right\} \\
-2r_2\dot{P}_2 &= \epsilon\left\{2r_2^2\zeta_2P_2+\tfrac{1}{2}K_{11}r_3^2P_2P_3\sin(\gamma-2\theta)+\tfrac{1}{2}K_{537}r_3^2P_2P_5\sin(\delta-2\theta)\right\} \\
-2r_3P_3\dot{\gamma} &= \epsilon\left\{\epsilon^{-1}(S_3^2\nu^2-r_3^2)P_3-\tfrac{1}{2}L_{58}r_2^2P_2^2\cos(\gamma-2\theta)+f\cos\gamma\right\} \\
-2r_3\dot{P}_3 &= \epsilon\left\{2r_3^2\zeta_3P_3-\tfrac{1}{2}L_{58}r_3^2P_2^2\sin(\gamma-2\theta)+f\sin\gamma\right\} \\
-2r_5P_5\dot{\delta} &= \epsilon\left\{\epsilon^{-1}(S_5^2\nu^2-r_5^2)P_5-\tfrac{1}{2}M_{12}r_2^2P_2^2\cos(\delta-2\theta)\right\} \\
-2r_5\dot{P}_5 &= \epsilon\left\{2r_5^2\zeta_5P_5-\tfrac{1}{2}M_{12}r_2^2P_2^2\sin(\delta-2\theta)\right\}
\end{aligned} \qquad (V.50)$$

where

$$K_{537} = K_5S_2S_5 - K_3S_2^2 - K_7S_5^2$$

$$L_{58} = L_5+L_8 \quad , \quad M_{12} = M_1+M_2$$

Writing (V.50) in terms of the new parameters(V.39):

$$\begin{aligned}
-S_2b_2\dot{\theta} &= -S_2^2\gamma b_2-\tfrac{1}{2}\frac{K_{11}}{|L_{58}|}b_2b_3\cos(\gamma-\psi_3)-\tfrac{1}{2}\frac{K_{537}}{|L_{58}|}b_2b_5\cos(\delta-\psi_3) \\
-S_2\dot{b}_2 &= S_2\eta_2b_2+\tfrac{1}{2}\frac{K_{11}}{|L_{58}|}b_2b_3\sin(\gamma-\psi_3)+\tfrac{1}{2}\frac{K_{537}}{|L_{58}|}b_2b_5\sin(\delta-\psi_3) \\
-b_3\dot{\gamma} &= -\gamma b_3-\tfrac{1}{2}\frac{L_{58}}{|L_{58}|}S_2^2b_2^2\cos(\gamma-\psi_3)+\cos\gamma
\end{aligned}$$

$$
\begin{aligned}
-b_3' &= \eta_3 b_3 - \tfrac{1}{2}\frac{L_{58}}{|L_{58}|} S_2^2 b_2^2 \sin(\gamma-\psi_3)+\sin\gamma \\
-S_5 b_5 \delta' &= -S_5^2 \gamma b_5 - \tfrac{1}{2}\frac{M_{12}}{|L_{58}|} S_2^2 b_2^2 \cos(\alpha-\psi_3) \\
-S_5 b_5' &= S_5 \eta_5 b_5 - \tfrac{1}{2}\frac{M_{12}}{|L_{58}|} S_2^2 b_2^2 \sin(\alpha-\psi_3)
\end{aligned}
\qquad (V.51)
$$

The steady state solution of equations (V.51) is obtained by using the Davidenko algorithm as described in condition 3. Figs. (V.13, 14) show the amplitude frequency response of the system for two values of liquid depth ratios h/a = 1, and 2, when $\epsilon = 0.0105$.

It is seen that when the forcing frequency is below resonance ($n<1$) both $b_2$ and $b_5$ are identically zero AB, and the main mass amplitude $b_3$ follows the linear resonance curve $\acute{A}\acute{B}$. At B instability occurs in $b_2$ and $b_4$ indicated by the jumps BC and $B\acute{C}$ respectively, the main mass shows a change in its response to the curve $\acute{B}DE$. Both the second symmetric sloshing mode $b_5$ and the main mass amplitude $b_3$ follow resonant curves at $n\approx 1$ with a discontinuity in $b_2$ at $n=1$. It is anticipated that there is a collapse in $b_2$ and $b_5$ somewhere at $n>1$ which is not indicated in the graph since the algorithm gives only one real solution.

Unlike the case of one internal resonance condition studied in Chapter (VI) in which the absorbing effect occurs once at n=1, the present case shows that there are two forcing frequencies $n=1 \pm O(\epsilon)$ at which the suppression takes place in $b_3$. This can be interpreted as the liquid free surface motion being dominated at n=1 mainly by the second sloshing mode $b_5$ which does not exert any lateral sloshing force and therefore does not participate in the autoparametric coupling; it is the first antisymmetric sloshing mode which, because it has a significant value at $n\gtrsim 1$, exerts the lateral sloshing force that interacted with the vertical mass motion $b_3$.

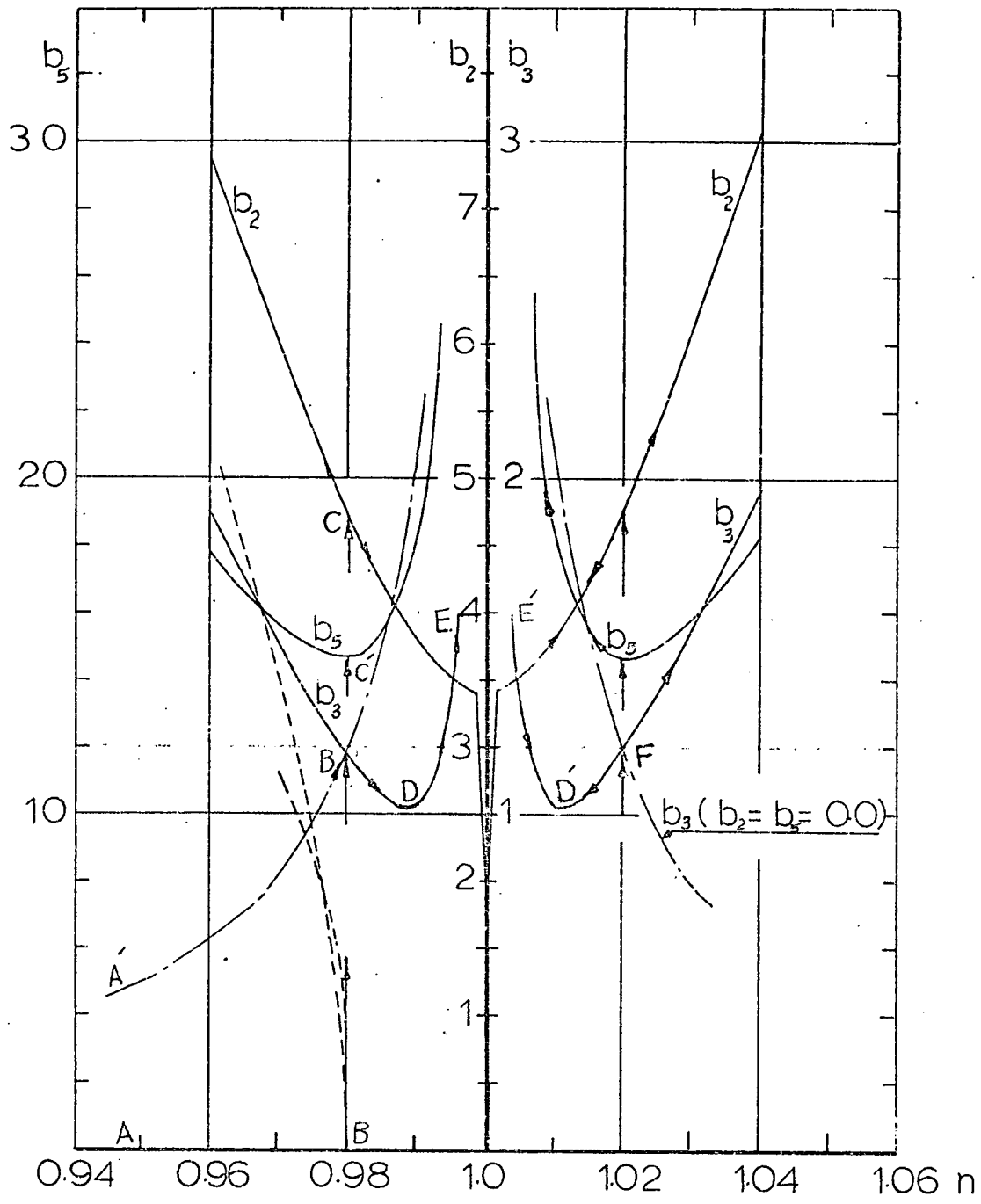


Fig(V.13) Three Mode Interaction ($r_3 = 2r_2$, $r_3 = r_5$)
(Davidenko algorithm solution)
$h/a = 1.0$ , $l/a = 3.13$ , $\epsilon = .0105$, $\bar{\zeta}_{s1} = .0275$
$\bar{\zeta}_2 = \bar{\zeta}_5 = 0.0$

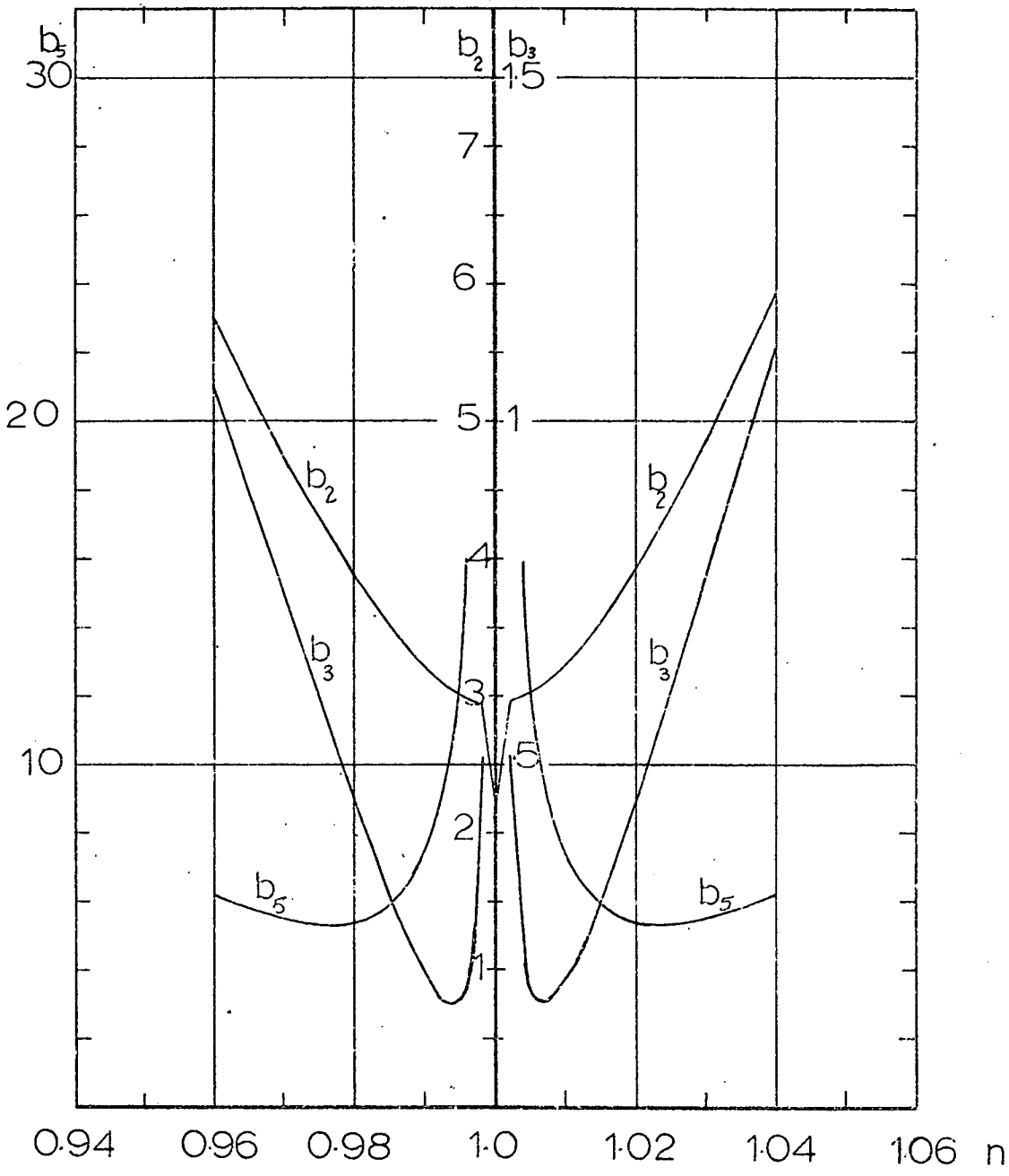


Fig(V.14) Three Mode Interaction, ( $r_3 = 2r_2$, $r_3 = r_5$) ( Davidenko algorithm solution), $h/a = 2.0$ $l/a = 3.13$, $\epsilon = .0105$, $\bar{\zeta}_{51} = .0275$, $\bar{\zeta}_2 = \bar{\zeta}_5 = .005$

A special case can be studied by assuming $\eta_2 = \eta_5 = 0$. This assumption simplifies the algebraic manipulation and yields an explicit analytic solution of the form:

The second symmetric sloshing amplitude $b_5$:

$$b_5 = -\frac{1}{2}\frac{M_{12}}{|L_{58}|}\left(\frac{S_2}{S_5}\right)^2\frac{b_2}{\gamma} \qquad (V.52a)$$

The vertical mass amplitude $b_3$:

$$b_3 = -\frac{2}{K_{11}}\gamma S_2^2\cdot|L_{58}| + \frac{K_{537}M_{12}}{2\gamma K_{11}|L_{58}|}\left(\frac{S_2}{S_5}\right)^2 b_2^2 \qquad (V.53b)$$

where $b_2$ is given by solving the equation

$$\left\{\frac{1}{4}\left(\frac{S_2}{S_5}\right)^4\left[\frac{M_{12}K_{537}}{\gamma|L_{58}|K_{11}}\right]^2\left(\gamma^2+\frac{2}{3}\right) + \frac{1}{2}S_5^2\left[\frac{K_{537}M_{12}}{L_{58}K_{11}}\left(\frac{S_2}{S_5}\right)^4 + 1\right]\right\} b_2^4$$

$$-\left\{\frac{2S_2^4}{K_{11}}\left[\frac{K_{537}M_{12}}{K_{11}S_5^2}\left(\gamma^2+\eta_3^2\right) + \gamma^2 L_{58}\right]\right\} b_2^2 + \left[\frac{2S_2^2\gamma|L_{58}|}{K_{11}}\right]^2\left(\gamma^2+\frac{2}{3}\right) - 1 = 0$$

.....(V.53c)

Figs. (V.15,16) show the amplitude frequency response curves $b_2, b_3$ and $b_5$. When the system is excited parametrically at frequency below resonance, the main mass amplitude $b_3$ follows the resonance curve AB, while both the second normal mode amplitude $b_2$ and the second symmetric sloshing mode $b_5$ are identically zero. With a continuous increase in the forcing frequency, the main mass follows the suppression curve BC at first with a sudden stimulation to the modes $b_2$ and $b_5$. The continuous increase in the second symmetric sloshing amplitude dominates the motion of the liquid free surface and the main mass then changes its response to another resonance curve CD. Because the curves are symmetric about n=1 the second half follows the direction of the indicated arrows.

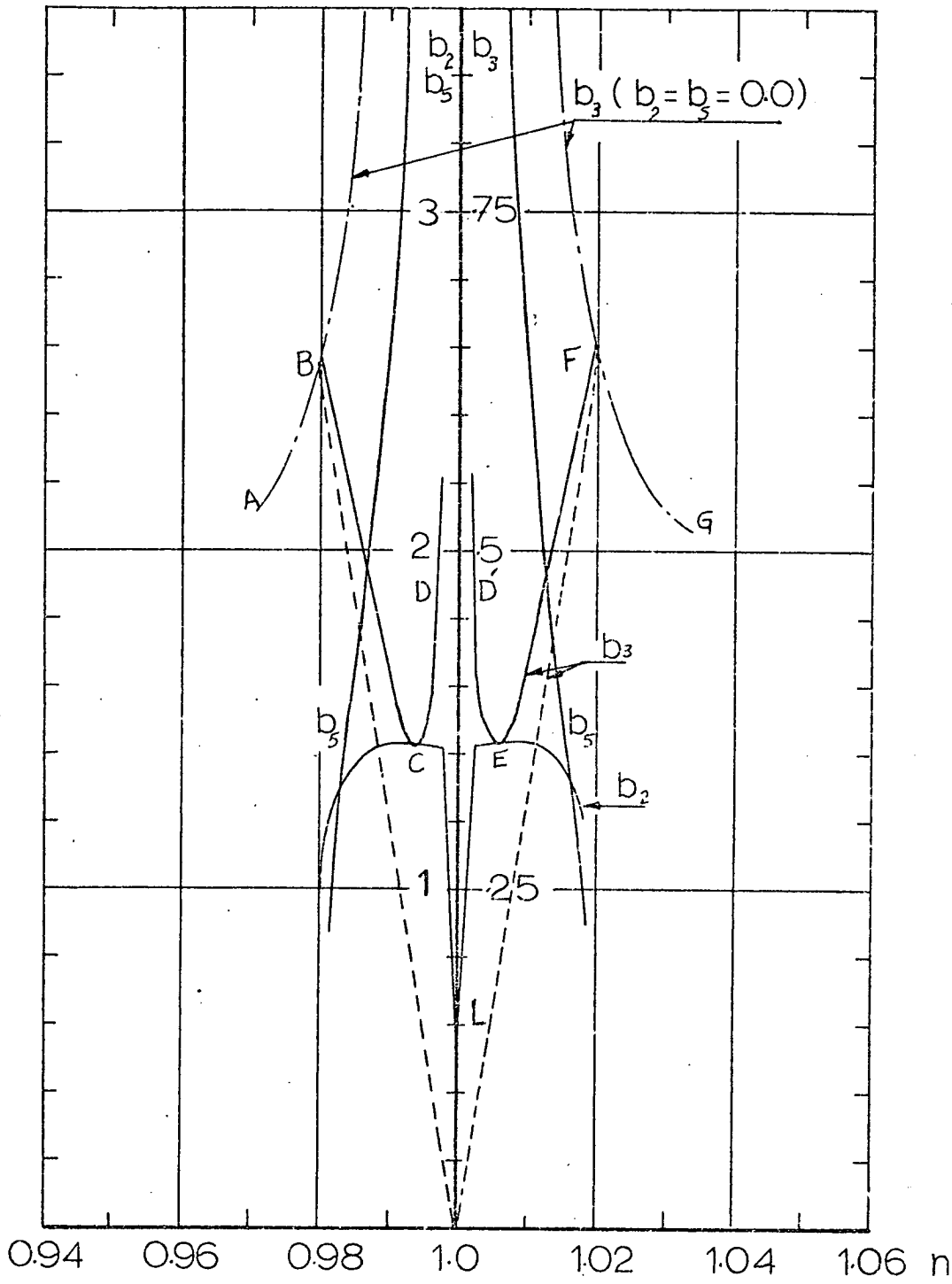


Fig(V.15) Three Mode Interaction under Two Internal Resonance Conditions, $r_3 = 2\,r_2$, $r_3 = r_5$ . . $h/a = 1.0$, $l/a = 3.06$, $\epsilon = 0.0105$, $\bar{\zeta}_{s1} = .0275$, $\bar{\zeta}_2 = \bar{\zeta}_5 = 0.0$

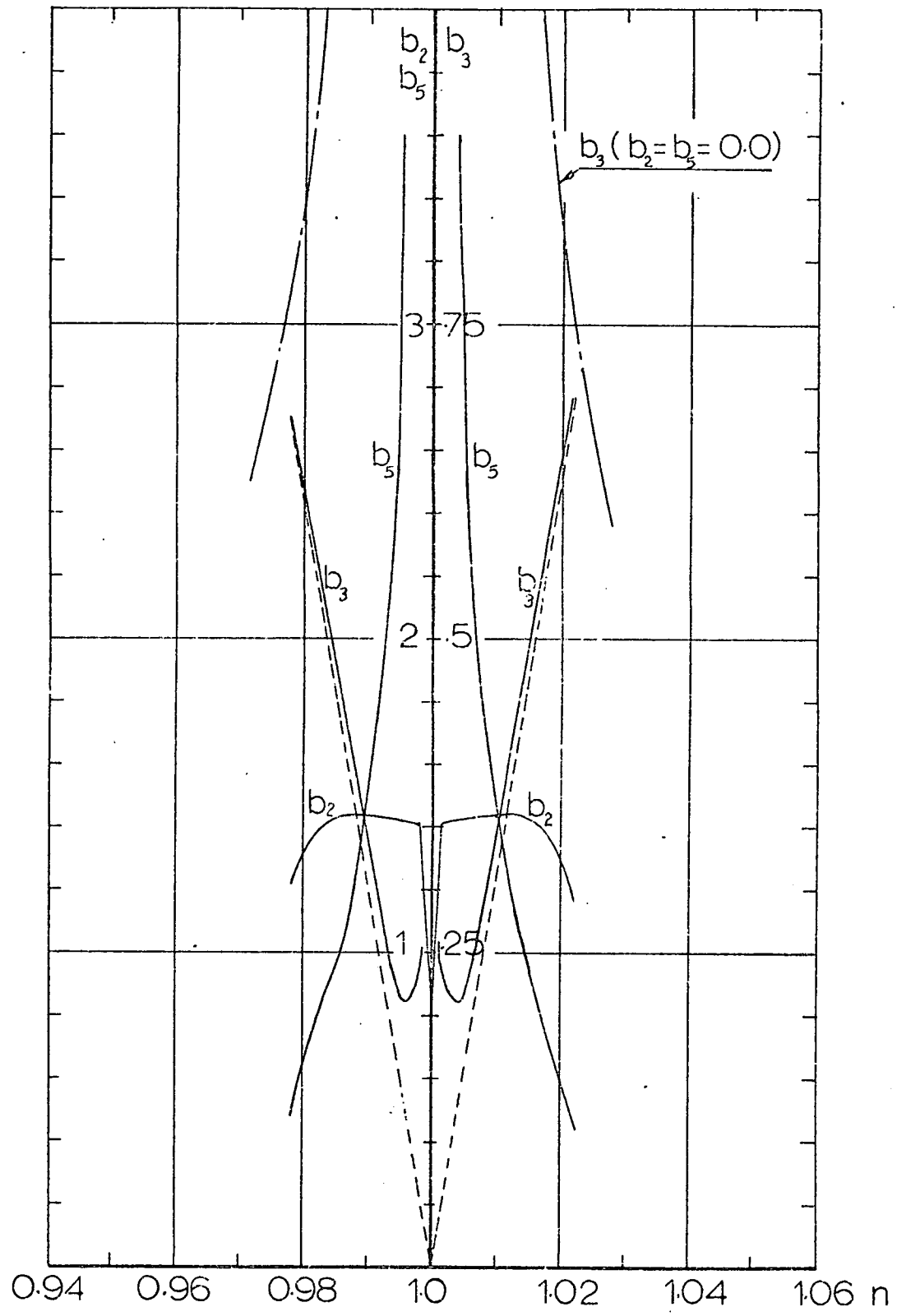


Fig(V.16)Three Mode Interaction, ($r_3 = 2r_2$, $r_3 = r_5$)
$h/a = 2.0$, $l/a = 3.13$, $\epsilon = .0105$, $\bar{\zeta}_{s1} = .0275$
$\bar{\zeta}_2 = \bar{\zeta}_5 = 0.0$

V.7 Condition 5:

$$r_3 = r_1 - r_2$$
$$= r_4$$
$$= n\nu$$

The modes considered in the present section are the same modes of section (V.3) however, here the internal resonance condition is of the difference type. The variational equations after using (V.39) are:

$$-S_1 b_1 \dot{\varphi} = -S_1^2 \gamma b_1 + \tfrac{1}{2} \frac{C_{13}}{|L_{747}|} b_2 b_3 \cos(\gamma + \psi_2) - \tfrac{1}{2} \frac{C_{681}}{|L_{747}|} b_2 b_4 \cos(\alpha + \psi_2)$$

$$-S_1 \dot{b}_1 = S_1 \eta_1 b_1 - \tfrac{1}{2} \frac{C_{13}}{|L_{747}|} b_2 b_3 \sin(\gamma + \psi_2) + \tfrac{1}{2} \frac{C_{681}}{|L_{747}|} b_2 b_4 \sin(\alpha + \psi_2)$$

$$-S_2 b_2 \dot{\theta} = -S_2^2 \gamma b_2 - \tfrac{1}{2} \frac{K_{10}}{|L_{747}|} b_1 b_3 \cos(\gamma + \psi_2) - \tfrac{1}{2} \frac{K_{246}}{|L_{747}|} b_1 b_4 \cos(\alpha + \psi_2)$$

$$-S_2 \dot{b}_2 = S_2 \eta_2 b_2 - \tfrac{1}{2} \frac{K_{10}}{|L_{747}|} b_1 b_3 \sin(\gamma + \psi_2) - \tfrac{1}{2} \frac{K_{246}}{|L_{747}|} b_1 b_4 \sin(\alpha + \psi_2)$$

$$-b_3 \dot{\gamma} = -\gamma b_3 - \tfrac{1}{2} \frac{L_{747}}{|L_{747}|} b_1 b_2 \cos(\gamma + \psi_2) + \cos\gamma$$

$$-\dot{b}_3 = \eta_3 b_3 - \tfrac{1}{2} \frac{L_{747}}{|L_{747}|} b_1 b_2 \sin(\gamma + \psi_2) + \sin\gamma$$

$$-S_4 b_4 \dot{\alpha} = -S_4^2 \gamma b_4 - \tfrac{1}{2} \frac{N_{21}}{|L_{747}|} b_1 b_2 \cos(\alpha + \psi_2)$$

$$-S_4 \dot{b}_4 = S_4 \eta_4 b_4 - \tfrac{1}{2} \frac{N_{21}}{|L_{747}|} b_1 b_2 \sin(\alpha + \psi_2) \qquad (V.54)$$

where

$$C_{681} = -C_6 S_2 S_4 - C_8 S_4^2 + C_1 S_2^2$$

$$K_{246} = K_2 S_1^2 + K_4 S_1 S_4 - K_6 S_4^2$$

$$L_{747} = -L_4 S_1 S_2 + L_7 (S_1^2 + S_2^2)$$

$$N_{21} = N_2 S_1 S_2 + N_1 (S_1^2 + S_2^2)$$

Setting the left hand sides of (V.54) to zero, gives eight equations and seven unknowns which implies that the system does not possess any steady solution. CSMP simulation did not give any regular response.

Special case $\eta_1 = \eta_2 = \eta_5 = 0$

Using this assumption gives the analytical solution:

the zeroth symmetric sloshing amplitude $b_4$;

$$b_4 = \frac{N_{21}}{2\gamma} \frac{b_1 b_2}{|L_{747}| S_4^2} \qquad (V.55a)$$

the first two normal modes $b_1$ and $b_2$ have the relation:

$$b_1^2 = \frac{\gamma C_{13} S_2^2 b_2^2}{\left[\frac{(K_{10}C_{681}+C_{13}K_{246})N_{21}}{4\gamma L_{747}^2 S_4^2}\right] b_2^2 - \gamma K_{10} S_1^2} \qquad (V.55b)$$

the vertical motion of the main mass $b_3$;

$$b_3 = \frac{2\gamma}{C_{13}} \left[\frac{|L_{747}|}{b_2^2} S_1^2 - \frac{C_{681} \cdot N_{21}}{4 S_4^2 \gamma^2}\right] b_1 b_2 \qquad (V.55c)$$

where $b_2$ is given by the solution of the equation:

$$\left\{ \tfrac{1}{2} S_2^2 \left[\frac{C_{681} N_{21}}{S_4^2} (\gamma^2 + \eta_3^2 - \frac{\gamma L_{747}}{|L_{747}|}) + \tfrac{1}{2} C_{13} \gamma\right] \right\} b_2^4$$

$$\left\{ 2 S_1^2 S_2^2 \gamma L_{747} \left[\gamma^2 - \frac{|L_{747}| C_{681} N_{21}}{L_{747} C_{13} S_4^2} (\gamma^2 + \eta_3^2)\right] - \frac{N_{21}(K_{10}C_{681}+C_{13}K_{246})}{4 L_{747}^2 S_4^2 \gamma} \right\} b_2^2$$

$$+ \gamma S_1^2 \left[\frac{4\gamma^2 S_1^2 S_2^2 L_{747}^2 (\gamma^2+\eta_3^2)}{C_{13}} + K_{10}\right] = 0 \qquad (V.55d)$$

Solving (V.55d) for the particular constants of the system, gives no real solution, so no results could be displayed. This leads to the conclusion that the system may not respond under the resonance condition of the present section.

V.8 Condition (6)

$$r_3 = r_1 - r_2$$
$$= r_5$$
$$= n\psi$$

Considering the second symmetric sloshing mode instead of the zeroth one, the previous section can be modified to involve the present four modes. The variational equations, after using the parameters (V.39) are:

$$-S_1 b_1 \varphi' = -S_1^2 \gamma b_1 + \tfrac{1}{2} \frac{C_{13}}{|L_{747}|} b_2 b_3 \cos(\gamma+\psi_2) - \tfrac{1}{2} \frac{C_{579}}{|L_{747}|} b_2 b_5 \cos(\delta+\psi_2)$$

$$-S_1 b_1' = S_1 \eta_1^2 b_1 - \tfrac{1}{2} \frac{C_{13}}{|L_{747}|} b_2 b_3 \sin(\gamma+\psi_2) + \tfrac{1}{2} \frac{C_{579}}{|L_{747}|} b_2 b_5 \sin(\delta+\psi_2)$$

$$-S_2 b_2 \theta' = -S_2^2 \gamma b_2 - \tfrac{1}{2} \frac{K_{10}}{|L_{747}|} b_1 b_3 \cos(\gamma+\psi_2) - \tfrac{1}{2} \frac{K_{753}}{|L_{747}|} b_1 b_5 \cos(\delta+\psi_2)$$

$$-S_2 b_2' = S_2 \eta_2 b_2 - \tfrac{1}{2} \frac{K_{10}}{|L_{747}|} b_1 b_3 \sin(\gamma+\psi_2) - \tfrac{1}{2} \frac{K_{753}}{|L_{747}|} b_1 b_5 \sin(\delta+\psi_2)$$

$$-b_3 \gamma' = -\gamma b_3 - \tfrac{1}{2} \frac{L_{747}}{|L_{747}|} b_1 b_2 \cos(\gamma+\psi_2) + \cos\gamma$$

$$-b_3' = \eta_3 b_3 - \tfrac{1}{2} \frac{L_{747}}{|L_{747}|} b_1 b_2 \sin(\gamma+\psi_2) + \sin\gamma$$

$$-S_5 b_5 \delta' = -S_5^2 \gamma b_5 - \tfrac{1}{2} \frac{M_{21}}{|L_{747}|} b_1 b_2 \cos(\delta+\psi_2)$$

$$-S_5 b_5' = S_5 \eta_5 b_5 - \tfrac{1}{2} \frac{M_{21}}{|L_{747}|} b_1 b_2 \sin(\delta+\psi_2) \qquad (V.56)$$

where

$$C_{579} = -C_5 S_2^2 - C_7 S_2 S_5 + C_9 S_5^2$$

$$K_{753} = K_7 S_5^2 + K_5 S_1 S_5 - K_3 S_1^2$$

$$L_{747} = -L_4 S_1 S_2 + L_7 (S_1^2 + S_2^2)$$

$$M_{21} = M_1 (S_1^2 + S_2^2) - M_2 S_1 S_2$$

Equations (V.56) are similar to (V.54) and have no steady state solution. Considering the special case by setting $\eta_1$ $\eta_2$, and $\eta_5$ equal zero a solution similar to (V.55) with the relevant constants of the present case. Again the resulting solution has no real response.

## V.9 Conclusions

Allowing more degrees-of-freedom for the motion of an auto-parametric system generates further internal resonance conditions. The response of the system near these critical conditions seems to be rather complex and exhibits unsteadiness or instability. It has been found that with a combination resonance of the summed type the system response is in general unsteady, while in the principal resonance it is steady. However, CSMP simulation showed unsteadiness of the system under the first four resonance conditions examined in this chapter. With a combination resonance of a difference type no response has been obtained by analytical and simulation methods.

The behaviour of the system, under two internal resonance conditions when one of the modes is externally excited is still obscure however, the present analysis needs further interpretation which can be obtained from the experimental observations and results given in Chapter (VI).

## APPENDIX (VI)

Constants of Equation (V.10)

$$c_0 = \frac{2\xi_{11}\tanh\lambda_{11}h}{(\xi_{11}^2-1)\,J_1(\xi_{11})}$$

$$c_1 = \frac{1}{\tanh\lambda_{11}h}\left[0.1655938 + \frac{.1914547}{\tanh\lambda_{11}h}\right]$$

$$c_2 = \frac{1.2}{(\ell/a)\xi_{11}\tanh\lambda_{11}h}$$

$$c_4 = c_2\,c_3$$

$$c_5 = \frac{1}{\tanh\lambda_{11}h}\left[0.1987524 + \frac{.0738103}{\tanh\lambda_{11}h}\right]$$

$$c_6 = \frac{1}{\tanh\lambda_{11}h}\left\{\frac{0.17244}{\tanh\lambda_{01}h} - \frac{.1914547}{\tanh\lambda_{11}h} - 0.479\tanh\lambda_{11}h\left[.3570485 + .34468\tanh\lambda_{01}h\tanh\lambda_{11}h\right]\right\}$$

$$c_7 = \frac{1}{\tanh\lambda_{11}h}\left\{\frac{.164694}{\tanh\lambda_{21}h} - \frac{.0738103}{\tanh\lambda_{11}h} + .602812\tanh\lambda_{11}h\left[.2725628 - 0.3297066\tanh\lambda_{21}h.\tanh\lambda_{11}h\right]\right\}$$

$$c_8 = \frac{0.17244}{\tanh\lambda_{11}h.\tanh\lambda_{01}h} - 0.1651$$

$$c_9 = \frac{0.164694}{\tanh\lambda_{11}h.\tanh\lambda_{21}h} - 0.197826$$

$$c_{10} = \frac{1}{\tanh^2\lambda_{11}h}\left\{0.0661179 - \frac{.0450739}{\tanh\lambda_{01}h.\tanh\lambda_{11}h} - \frac{0.1317559}{\tanh\lambda_{21}h.\tanh\lambda_{11}h}\right\}$$

$$c_{11} = \frac{1}{\tanh^2\lambda_{11}h}\left\{-.0780698 - \frac{0.0901478}{\tanh\lambda_{01}\tanh\lambda_{11}h} - \frac{.158107}{\tanh\lambda_{21}h.\tanh\lambda_{11}h} + 0.125498(0.3570485+0.3446801\tanh\lambda_{01}h\tanh\lambda_{11}h) + 0.288754(0.2725628+.3297066\tanh\lambda_{21}h\tanh\lambda_{11}h)\right\}$$

Constants of equation (V.11)

$$N_1 = \frac{1}{\tanh\lambda_{11}h}\left[0.25678\tanh\lambda_{01}h - \frac{0.2612992}{\tanh\lambda_{11}h}\right]$$

$$N_2 = \frac{1}{\tanh\lambda_{11}h}\left[\frac{0.2612992}{\tanh\lambda_{11}h} + \left(\frac{.1454}{\tanh^2\lambda_{11}h} - .12839\right)\tanh\lambda_{01}h\right]$$

$$N_3 = \frac{1.2\ r_{01}^2}{\xi_{11}(\ell/a)\tanh\lambda_{11}h}$$

Constants of equation (V.12)

$$M_1 = \frac{1}{\tanh\lambda_{11}h}\left[\frac{0.4812568}{\tanh\lambda_{11}h} - 0.5837\tanh\lambda_{21}h\right]$$

$$M_2 = \frac{1}{\tanh\lambda_{11}h}\left[\frac{0.4812568}{\tanh\lambda_{11}h} + \left(\frac{0.10919}{\tanh^2\lambda_{11}h} - 0.2918\right)\tanh\lambda_{21}h\right]$$

$$M_3 = \frac{1.2r_{21}^2}{\xi_{11}(\ell/a)\tanh\lambda_{11}h}$$

Constants of equation (V.13)

$$L_1 = \frac{0.202\ \mu_1}{\xi_{11}^3(h/a)\tanh\lambda_{11}h.\sinh^2\lambda_{11}h}$$

$$L_2 = \frac{1.2\ \mu_1}{(\ell/a)\xi_{11}\ \tanh\lambda_{11}h}$$

Constants of equation (V.14)

$$K_0 = \frac{\mu_3 J_1(\xi_{11})}{\xi_{11}^2(h/a)}$$

$$K_1 = \frac{1.2}{\xi_{11}(\ell/a)\tanh\lambda_{11}h}$$

$$K_2 = \frac{0.1914547\ \mu_3\ J_1(\xi_{11})}{\xi_{11}^2(h/a)\tanh^2\lambda_{11}h}$$

$$K_3 = \frac{0.0738103\ \mu_3\ J_1(\xi_{11})}{\xi_{11}^2(h/a)\tanh^2\lambda_{11}h}$$

$$K_4 = \frac{\mu_3}{\xi_{11}^2 (h/a)\tanh\lambda_{11}h}\left\{J_1(\xi_{11})\left[\frac{0.17244}{\tanh\lambda_{01}h} - \frac{0.1914547}{\tanh\lambda_{11}h}\right]\right.$$

$$\left. + \frac{.2395\ J_o(\xi_{01})J_1(\xi_{11})}{\sinh\lambda_{01}h.\sinh\lambda_{11}h}\left[\frac{\sinh[(\lambda_{01}+\lambda_{11})h]}{1.479} - \frac{\sinh[(\lambda_{01}-\lambda_{11}h]}{0.521}\right]\right\}$$

$$K_5 = \frac{\mu_3}{\xi_{11}^2 (h/a)\tanh\lambda_{11}h}\left\{J_1(\xi_{11})\left[\frac{0.1646948}{\tanh\lambda_{11}h} - \frac{0.0738103}{\tanh\lambda_{11}h}\right]\right.$$

$$+ \frac{J_1(\xi_{11})J_2(\xi_{21})}{2\sinh\lambda_{11}h.\sin\lambda_{21}h}\left[\frac{1+.5\xi_{11}\xi_{21}}{\xi_{21}(\xi_{21}+\xi_{11})}\cdot\sinh[(\lambda_{11}+\lambda_{21})h] + \frac{1-.5\xi_{11}\xi_{21}}{\xi_{21}(\xi_{21}-\xi_{11})}\cdot\right.$$

$$\left.\left.\sinh[(\lambda_{21}-\lambda_{11})h]\right]\right\}$$

$$K_6 = \frac{0.360395\ \mu_3 J_1(\xi_{11})}{\xi_{01}\xi_{11}(h/a)\ \tanh\lambda_{01}h.\tanh\lambda_{11}h}$$

$$K_7 = \frac{0.2744914\ \mu_3 J_1(\xi_{11})}{\xi_{11}\xi_{21}(h/a)\tanh\lambda_{21}h.\tanh\lambda_{11}h}$$

$$K_8 = \frac{\mu_3\ J_1(\xi_{11})}{\xi_{11}^2 (h/a)\tanh^2\lambda_{11}h}\left\{0.0322679 - \frac{.0450739}{\tanh\lambda_{01}h.\tanh\lambda_{11}h}\right.$$

$$\left. - \frac{.0790535}{\tanh\lambda_{11}h.\tanh\lambda_{21}h}\right\}$$

$$K_9 = \frac{\mu_3}{\xi_{11}^2 (h/a)\tanh^2\lambda_{11}h}\left\{J_1(\xi_{11})\left[0.0645358 - \frac{.0901478}{\tanh\lambda_{01}h.\tanh\lambda_{11}h}\right.\right.$$

$$\left. - \frac{.158107}{\tanh\lambda_{11}h.\tanh\lambda_{21}h}\right]$$

$$+ \frac{.2406284\ J_1(\xi_{11})J_2(\xi_{21})}{\tanh\lambda_{11}h.\sinh\lambda_{11}h.\sinh\lambda_{21}h}\left[\frac{1+.5\xi_{11}\xi_{21}}{\xi_{21}(\xi_{21}+\xi_{11})}\sinh[(\lambda_{11}+\lambda_{21})h]\right.$$

$$\left. + \frac{1-.5\xi_{11}\xi_{21}}{\xi_{21}(\xi_{21}-\xi_{11})}\sinh[(\lambda_{21}-\lambda_{11})h]\right]$$

$$- \frac{0.065749\ J_o(\xi_{01})\ J_1(\xi_{11})}{\tanh\lambda_{11}h.\sinh\lambda_{11}h.\sinh\lambda_{01}h}\left[\frac{\sinh[(\lambda_{01}+\lambda_{11})h]}{1.479} - \frac{\sinh[(\lambda_{01}-\lambda_{11})h]}{0.521}\right]\Bigg\}$$

## APPENDIX (V.II)

$$C_{12} = 1-n_1C_2$$

$$C_{13} = 1-n_2C_2$$

$$C_{14} = C_{10}-n_1^2(C_4n_1-C_3)$$

$$C_{15} = 2C_{10}-2C_4n_1^2n_2+C_3n_1(n_1+n_2)$$

$$C_{16} = C_{10}-n_1n_2(C_4n_2-C_3)$$

$$C_{17} = C_{10}-n_1n_2(C_4n_1-C_3)$$

$$C_{18} = 2C_{10}-2C_4n_1n_2^2+n_2(n_1+n_2)C_3$$

$$C_{19} = C_{10}-n_2^2(C_4n_2-C_3)$$

$$C_{20} = C_{11}+n_1^2(C_3-C_4n_1^2)$$

$$C_{21} = 2C_{11}+2n_1n_2(C_3-C_4n_1)$$

$$C_{22} = C_{11}+n_2^2(C_3-C_4n_1)$$

$$C_{23} = C_{11}+n_1^2(C_3-C_4n_2)$$

$$C_{24} = 2C_{11}+2n_1n_2(C_3-C_4n_2)$$

$$C_{25} = C_{11}+n_2^2(C_3-n_2C_4)$$

$$K_{10} = K_1n_1 \qquad K_{11} = K_1n_2$$

$$K_{12} = K_8-K_1^2n_1^3 \qquad K_{13} = K_8-K_1^2n_1^2n_2$$

$$K_{14} = K_8-K_1^2n_1n_2^2 \qquad K_{15} = K_8-K_1^2n_2^3$$

$$K_{16} = K_9-K_1^2n_1^3 \qquad K_{17} = K_9-K_1^2n_1^2n_2$$

$$K_{18} = K_9-K_1^2n_1n_2^2 \qquad K_{19} = K_9-K_1^2n_2^3$$

$$L_3 = L_1+n_1^2L_2 \qquad L_4 = 2(L_1+n_1n_2L_2)$$

$$L_5 = L_1+L_2n_2^2 \qquad L_6 = L_2n_1^2$$

$$L_7 = L_2n_1n_2 \qquad L_8 = L_2n_2^2$$

$$f = \frac{\xi_{11}r_{s1}^2}{\epsilon}\tanh\lambda_{11}h$$

$$N_4 = N_3 n_1^2 \qquad N_5 = N_3 n_1 n_2$$

$$N_6 = N_3 n_2^2$$

$$M_4 = M_3 n_1^2 \qquad M_5 = M_3 n_1 n_2$$

$$M_6 = M_3 n_2^2$$

# CHAPTER (VI)

## EXPERIMENTAL PROGRAMME AND RESULTS

The purpose of this Chapter is to explore the characteristics of the autoparametric systems studied in the previous three chapters and to check the validity of the theoretical results.

### VI.1.0 Apparatus

Figures (VI.1-3) show the basic layout of the rig. It consists of an upright circular perspex container of length 31.0 cm, inner diamater 9.5 cm and thickness 0.3 cm. The container is rigidly supported on a rectangular base made of dural (16.2 x 13.4 x 2.25 cm). Depending on the number of degrees of freedom required, the container and its base are supported vertically by either two rigid panels, (to give purely vertical tank motion, see Fig. VI.1), or four leaf springs (to permit lateral motion of the tank, see Fig. VI.2). The panels or leaf springs are attached at their lower ends to the main mass (a 16.2 x 13.4 x 3.6 cm piece of dural). An externally pressurised air lubricated bearing is placed in the centre of the main mass in order to guarantee its motion in purely vertical direction with negligible damping. The whole system is carried on a platform by two compression springs. The platform itself is connected directly to the head of a Pye-Ling vibrator type V1006 (maximum thrust 500 lbf). The excitation provided by the vibrator is controlled by an accurate function generator (Hewlett Packard type 203A) via a Pye-Ling power amplifier type PP1/2P. To prevent the full load being applied to the vibrator head the platform is suspended by four elastic ropes from a surrounding stationary frame. An adjustable dashpot - fitted between the main mass and a stationary point - provides

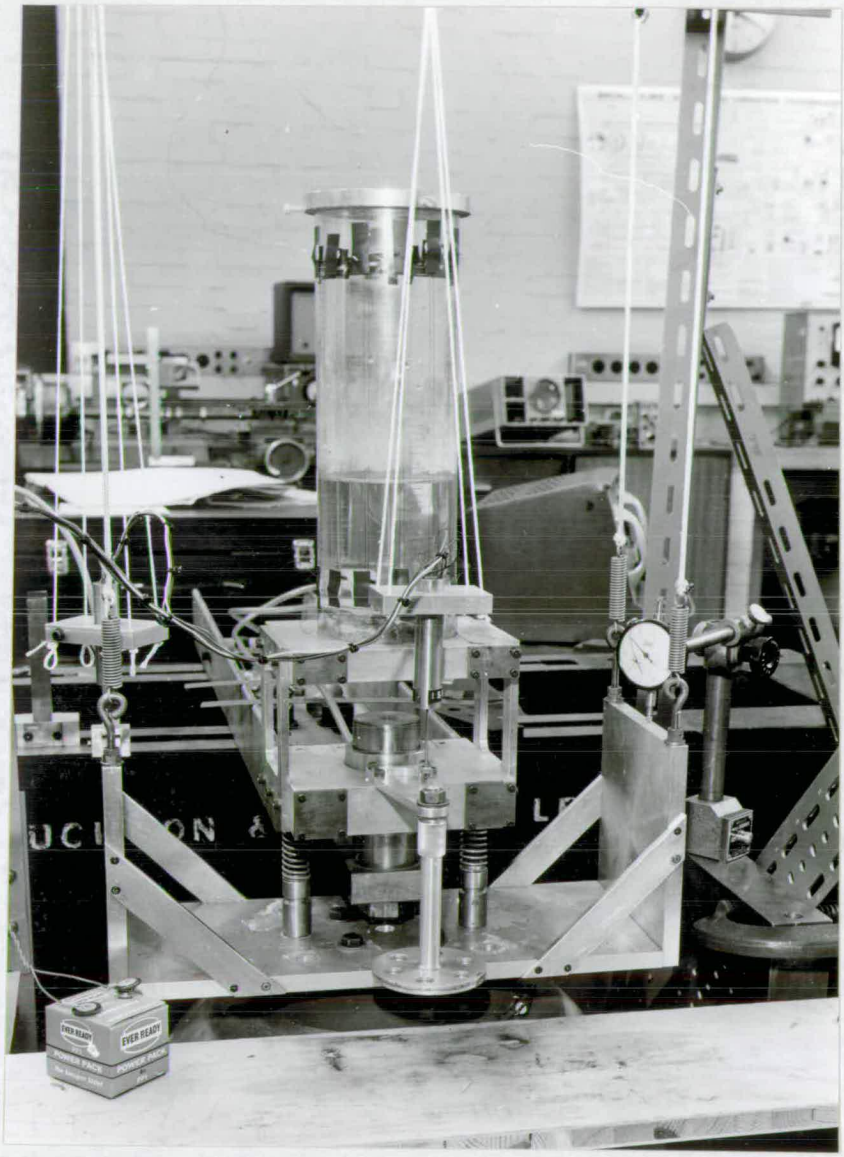


Fig(VI.1) Two Degrees of Freedom Experimental Apparatus.

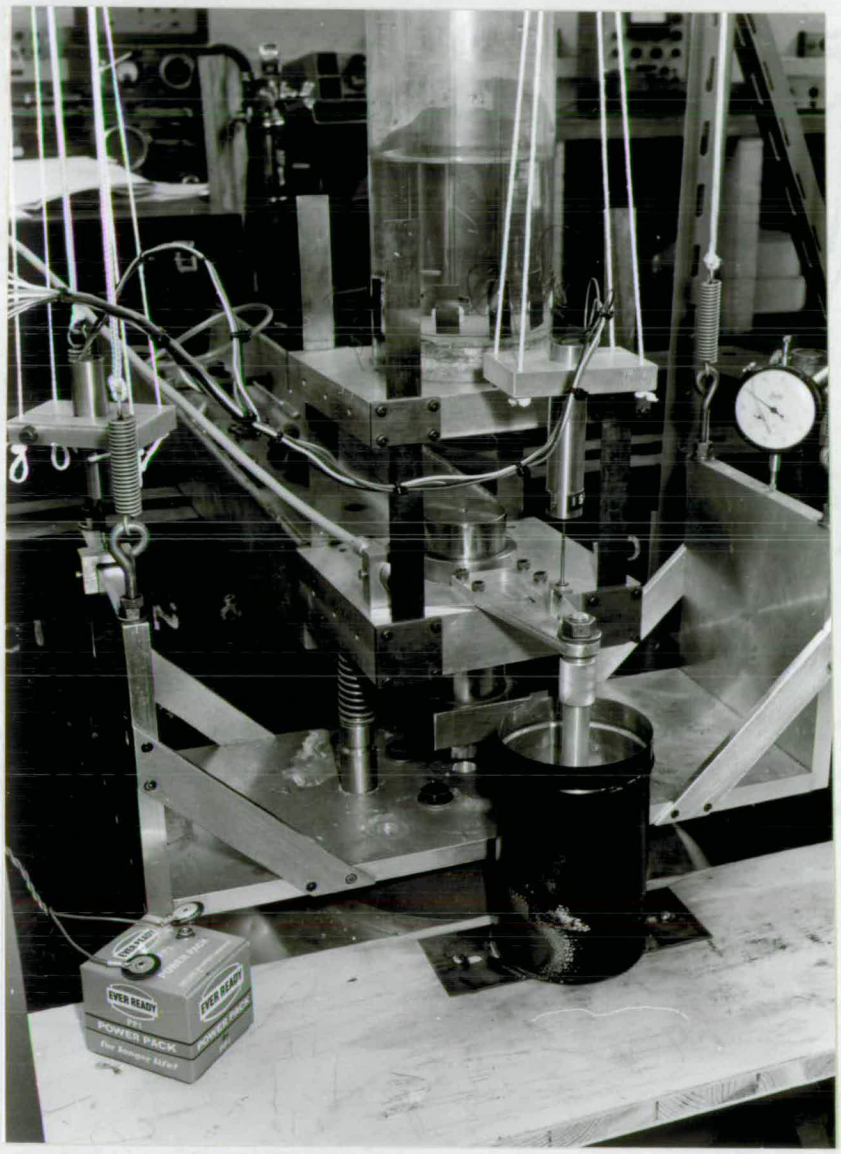


Fig(VI.2) Three Degrees of Freedom Experimental Apparatus.

1. Tank 2. Water
3. Liquid Wave Height Transducer ($\eta$)
4. Leaf Spring 5. Mains Mass
6. Compression Spring
7. Vibrator 8. Air Bearing
9. Linear Transducer $\xi_0$
10. Linear Transducer $\xi$
11. Adjustable Dashpot
12. Proximity Probe X
13. Two Parallel Wires to Prevent Main Mass Roll
14. Plat form

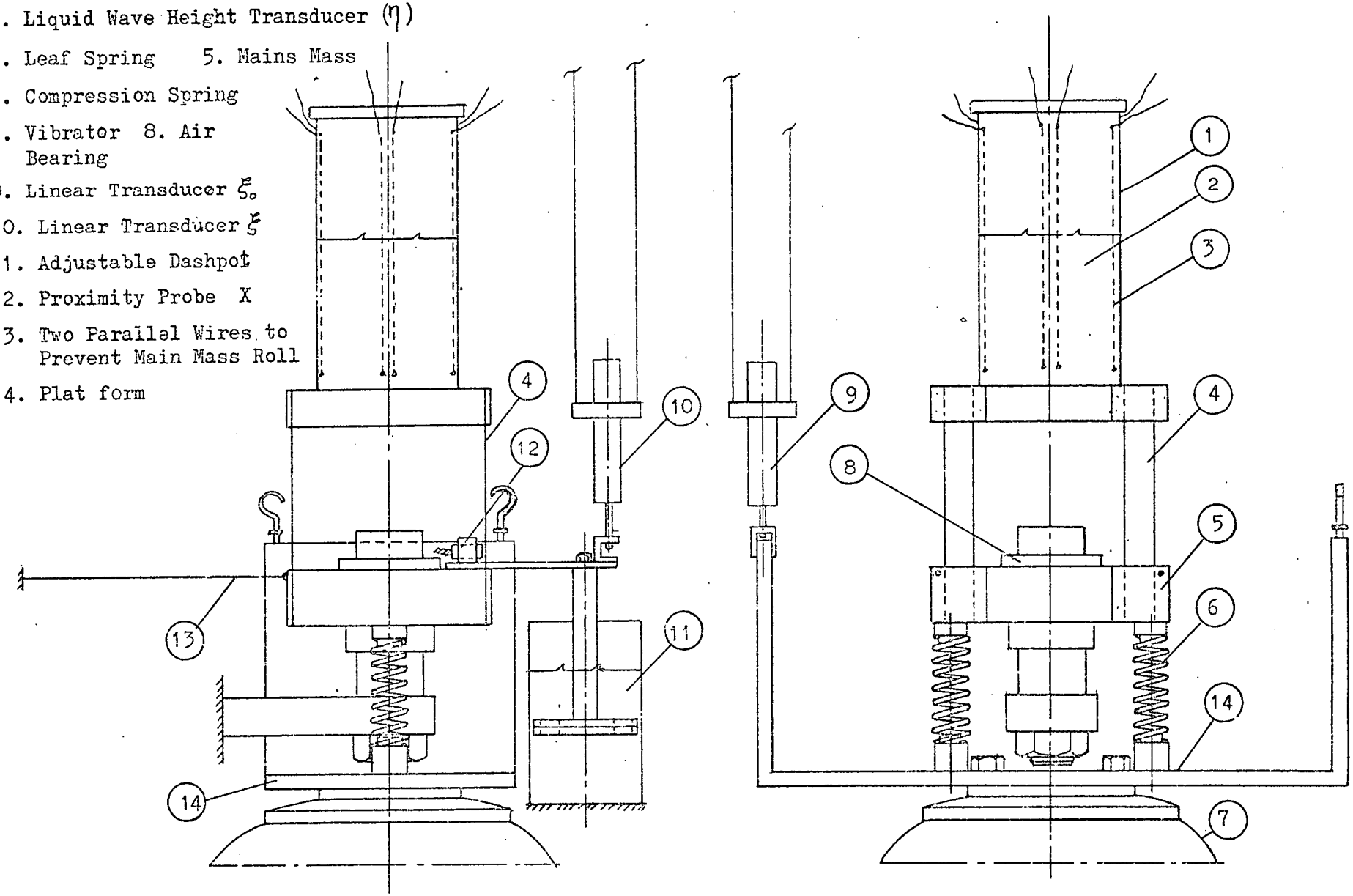


Fig. (VI. 3 ) Experimental Apparatus

damping to the motion of the main mass. Any torsional or roll oscillations created by torsion in the compression springs is prevented by two long parallel wires extending (under slight tension) from the main mass to a fixed stand.

The design of the air bearing, compression springs and leaf springs will be discussed briefly in the following sections.

VI.1.1 Design of the Air Bearing

For the design of an externally pressurised air lubricated journal bearing which is inherently compensated (i.e. the air feeder holes are not furnished with orifices) there are four governing dimensionless parameters, namely [M11],

1) The length-to-diameter ratio : $(L/D)$
2) The supply pressure ratio : $(P_s/P_a)$
3) The eccentricity ratio : $(\varepsilon)$
4) The restrictor coefficient : $\Lambda_s = \frac{6\mu n d \sqrt{\mathcal{R}T}}{P_s C^2}$

where

$L$ = the overall bearing length

$D$ = the bearing diameter

$P_s$ = the supply pressure

$P_a$ = the ambient pressure

$\mu$ = viscosity of air

$n$ = total number of feeding holes

$d$ = diameter of feeding holes

$\mathcal{R}$ = gas constant

$T$ = absolute temperature

$C$ = radial clearance

With suitable values of the first three dimensionless parameters there is an optimum value of $\Lambda_s$ for maximum stiffness.

In the present application it is important that the response of the main mass due to lateral motion of the tank should be as small as possible. The angular stiffness of the bearing was designed to give a resonant frequency of the main mass/bearing system alone of the order 100 Hz, (well above the experimental frequency range of 0 - 10 Hz). A check was also made to ensure that the maximum pitching movement of the tank about the bearing centre would not cause contact between the bearing surfaces.

The selection of the bearing geometry was made using the information of reference [M11]. Fig. 5.5.13 of this reference shows a plot of dimensionless angular stiffness against $\Lambda_s$, for various values of $P_s/P_a$ with L/D = 1.0 and $\varepsilon \to 0$. For the maximum available pressure ratio of about 6.0, the optimum value of $\Lambda_s \approx 0.8$. The following bearing dimensions were selected in order to achieve the required angular stiffness of $4.8 \times 10^5$ lb in/rad;

L = 2.5 in. = 62.5 mm.

D = 2.0 in. = 50.0 mm.

C = 0.001 in. = 0.025 mm.

n = 10 Single admission plane (equi-spaced holes distributed circumferential in the central plane).

d = 0.0465 in = 1.17 mm.

A detailed drawing of a section through the bearing is shown in Fig. (VI.4)

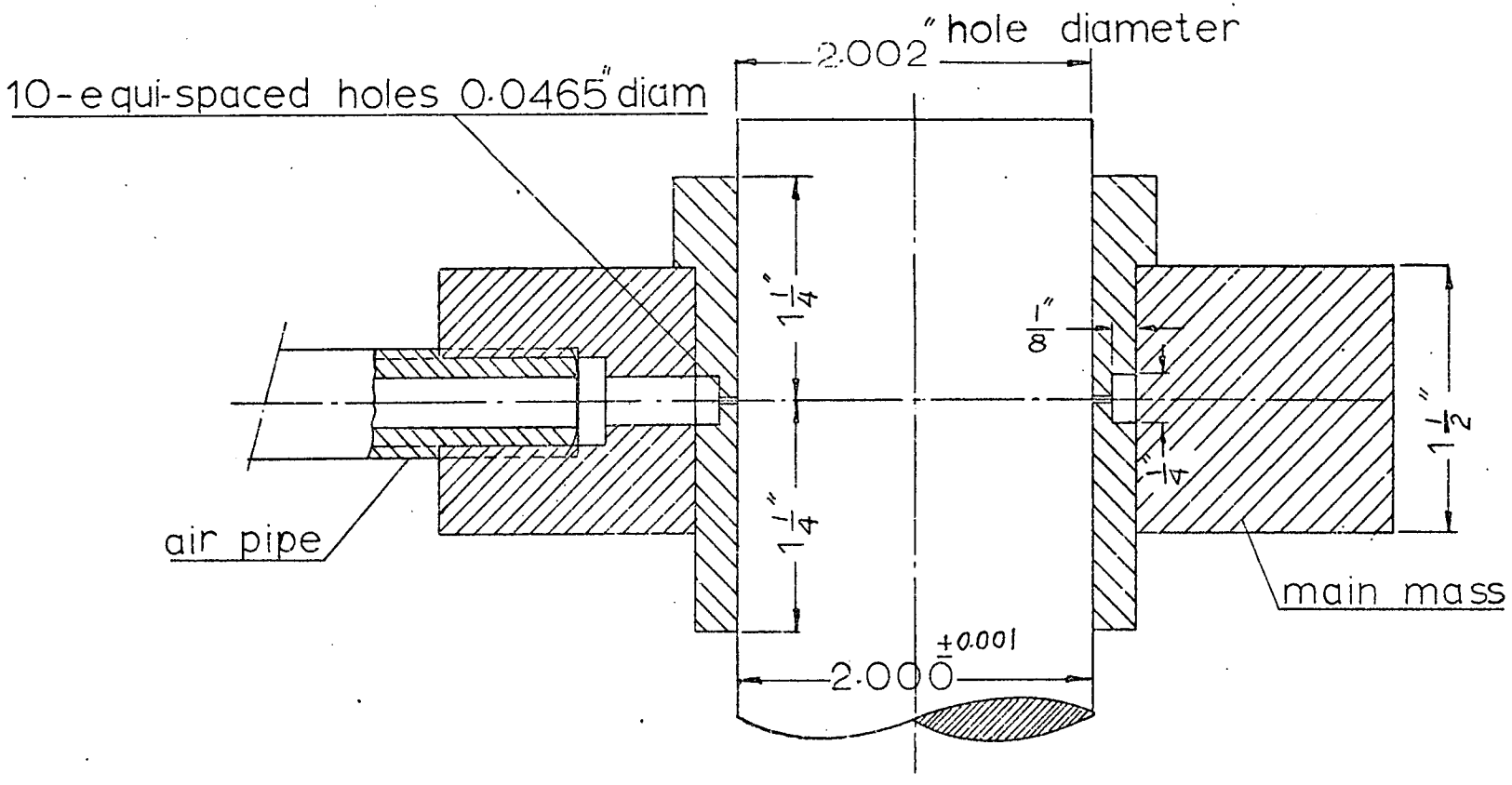


Fig(VI.4) Air Bearing Detail Drawing

VI.1.2 Design of the Compression Springs

The specifications for the compression springs are chosen so that the internal resonance conditions can be achieved. Accordingly, the dimensions can be determined by using the simple relation of the natural frequency of a spring-mass system;

$$f_{s1} = \frac{1}{2\pi}\sqrt{\frac{K_{s1}}{[M_o+m_{t1}]}} \quad \text{Hz}$$

where

$K_{s1}$ = spring stiffness

$= \frac{Gd^4}{8ND^4}$

G = modulus of rigidity [$11.5 \times 10^6$ lb/inch$^2$]

d = wire diameter

N = number of active coils [= total number-2, for closed and ground ends]

D = mean coil diameter [= outside diameter-d]

$M_o + m_{t1}$ = total mass carried by the spring

Among the available springs, it has been found that two springs of d = 0.093" and D = 0.777" are suitable. The number of active coils depends on the resonance condition and the total mass. Fig. (VI.5) shows the relationship between $f_{s1}$ and the active number of coils n for two values of $M_o + m_{t1}$ = 13.11 and 13.85 lb. Table (VI.1) gives the required number of active coils for each autoparametric resonance condition.

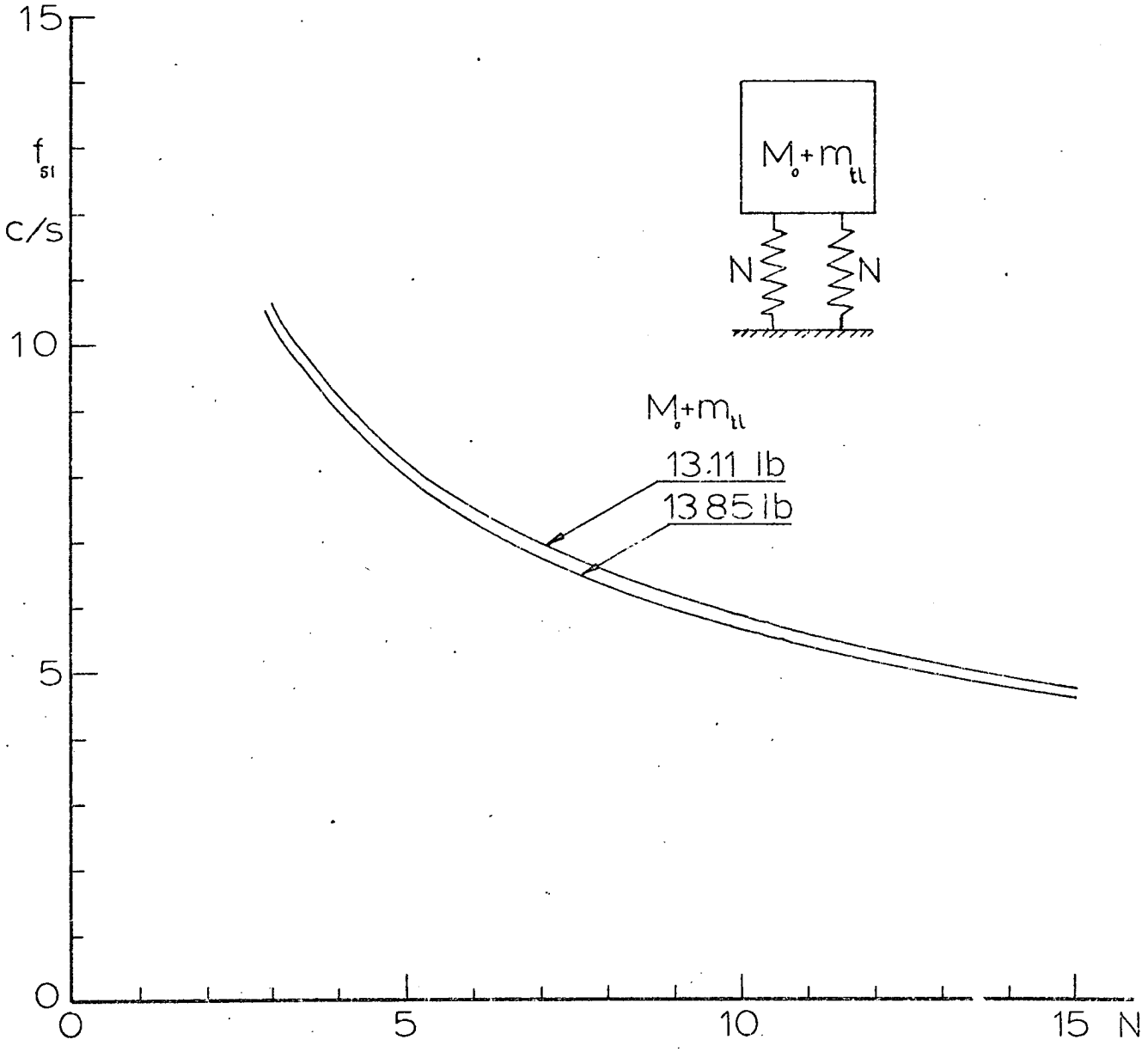


Fig(VI.5) Natural Frequency $f_{s1}$ vs. Effective Number of Coils of Compression Spring.

TABLE (VI.1)

| Resonance Conditions | h/a | $f_{11}$ (Hz) | $r_1$ | $r_2$ | $r_3=r_{s1}$ | $f_{s1}$ (Hz) | $r_{s2}$ | $\ell$ (cm)* | N |
|---|---|---|---|---|---|---|---|---|---|
| $r_{s1} = 2$ | 1 | 3.05 | - | - | 2.0 | 6.1 | - | - | 9 |
| | 2 | 3.11 | - | - | 2.0 | 6.22 | - | - | 9 |
| $r_3 = r_1+r_2$ | 1 | 3.05 | 1.15 | 0.85 | 2.0 | 6.1 | 0.96 | 12<br>10.7 | 9 |
| $= n\nu$ | 2 | 3.11 | 1.12 | 0.90 | 2.0 | 6.22 | 0.95 | 11.4<br>10 | 9 |
| $r_3 = r_1-r_2$ | 1 | 3.05 | 3.0 | 0.99 | 2.01 | 6.13 | 2.9 | 5.9<br>4.8 | 9 |
| $= n\nu$ | 2 | 3.11 | 3.0 | 0.99 | 2.01 | 6.25 | 2.9 | 5.7<br>4.7 | 9 |
| $r_3 = 2r_1$ | 1.0 | 3.05 | 1.33 | - | 2.66 | 8.113 | 0.95 | 12.06<br>10.3 | 6 |
| $= n\nu$ | 2.0 | 3.11 | 1.211 | - | 2.42 | 7.53 | 0.95 | 11.4<br>9.9 | 6 |
| $r_3 = 2r_2$ | 1.0 | 3.05 | - | 0.805 | 1.61 | 4.91 | 0.85 | 12.9<br>10.6 | 12 |
| $= n\nu$ | 2.0 | 3.11 | - | 0.843 | 1.68 | 5.23 | 0.90 | 11.9<br>10.1 | 12 |
| $r_3 = r_1+r_2$ | 1.0 | 3.05 | 1.04 | 0.43 | 1.47 | 4.48 | 0.45 | 19.7<br>15 | 15 |
| $= r_{01}$<br>$= n\nu$ | 2.0 | 3.11 | 1.05 | 0.40 | 1.45 | 4.51 | 0.42 | 20.0<br>15.3 | 15 |
| $r_3 = r_1+r_2$ | 1.0 | 3.05 | 1.05 | 0.30 | 1.35 | 4.12 | 0.30 | $>20$ | $>18$ |
| $= r_{21}$<br>$= n\nu$ | 2.0 | 3.11 | 1.04 | 0.25 | 1.29 | 4.01 | 0.26 | $>20$ | $>18$ |
| $r_3 = 2r_2$ | 1.0 | 3.05 | - | 0.73 | 1.46 | 4.45 | 0.82 | 13.3<br>11.1 | 16 |
| $= r_{01}$<br>$= n\nu$ | 2.0 | 3.11 | - | 0.72 | 1.44 | 4.48 | 0.73 | 13.5<br>11.4 | 16 |
| $r_3 = 2r_2$ | 1.0 | 3.05 | - | 0.67 | 1.35 | 4.12 | 0.70 | 14.75<br>12.0 | $>18$ |
| $= r_{21}$<br>$= n\nu$ | 2.0 | 3.11 | - | 0.64 | 1.29 | 4.01 | 0.65 | 14.75<br>12.0 | $>18$ |
| $r_3 = r_1-r_2$ | 1.0 | 3.05 | 2.49 | 0.99 | 1.5 | 4.58 | 2.35 | 5.7 | 16 |
| $= r_{01}$<br>$= n\nu$ | 2.0 | 3.11 | 2.45 | 0.99 | 1.46 | 4.54 | 2.35 | 5.4 | 16 |
| $r_3 = r_1-r_2$ | 1.0 | 3.05 | 2.3 | 0.99 | 1.31 | 3.99 | 2.2 | 5.9 | $>18$ |
| $= r_{21}$<br>$= n\nu$ | 2.0 | 3.11 | 2.27 | 0.99 | 1.28 | 4.08 | 2.2 | 5.8 | $>18$ |

* two values given for $\ell$, the first is theoretical, Fig. (VI.6) and the second is experimental Fig. (VI.15a)

VI.1.3 Design of the Leaf Springs

Applying the same procedure as for the compression springs;

$$f_{s2} = \frac{1}{2\pi}\sqrt{\frac{K_{s2}}{m_{tl}}}$$

where:

$K_{s2}$ = spring stiffness

= $12\ nEI/\ell^3$

n = total number of leaf springs = 4

E = Young's Modulus ($30 \times 10^6$ lb/in$^2$)

I = Area moment of inertia of the leaf spring cross-section about the bending axis.

$\ell$ = length of the leaf spring

$m_{tl}$ = total mass carried by the springs.

For the elastic beam of width 0.75" and thickness 0.02", the relationship between the natural frequency $f_{s2}$ and the length $\ell$ is shown in Fig. (VI.6) for various values of $m_{tl}$.

With the help of the relationships between the normal mode frequencies $r_1$ and $r_2$ and $r_{s2}$ shown in Figs. (IV.1-3) the required value of $f_{s2}$ corresponding to the relevant internal resonance conditions can be defined. Having obtained $f_{s2}$, the length $\ell$ can be determined, see table (VI.1).

VI.2.0 Instrumentation

The response of the system when it is being excited parametrically needs to be measured. The response of each degree of freedom of the apparatus has its own measuring device as shown in Figs. (VI.3, 9 and 10). The measuring instruments are:

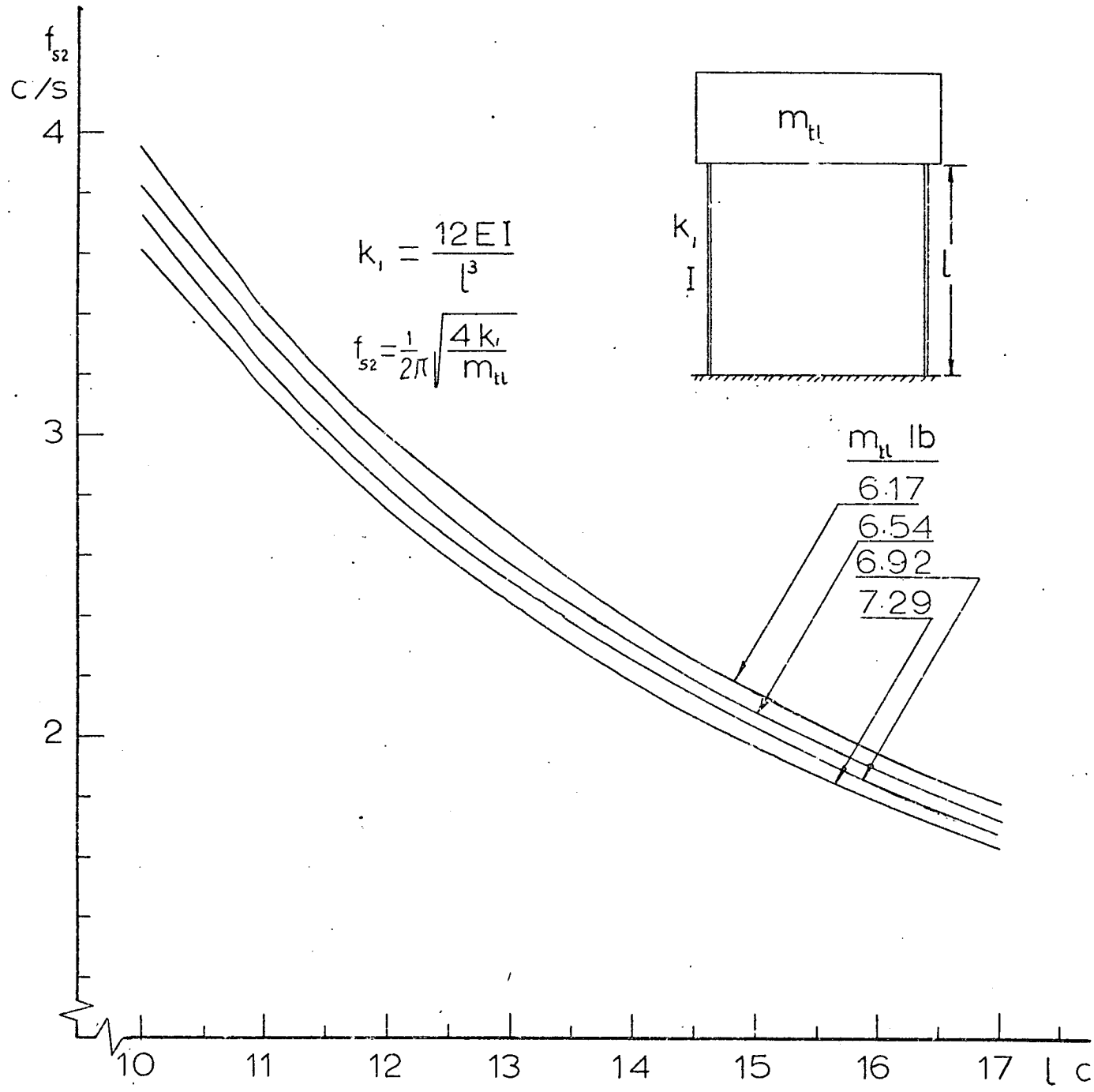


Fig.(VI.6) Natural Frequency of Upper Structure $f_{s2}$ vis. Length of Leaf Spring l.

VI.2.1 Liquid Surface Amplitude Transducer

The electrical methods of detecting liquid displacements are based on the variation of one parameter in an electrical sensing circuit, caused by a variation of the liquid depth. Lion [L2], classified these methods as resistive, inductive and capacitive. For the purpose of the present experimental investigation it has been found that the resistive type is the simplest.

The device, shown schematically in Fig. (VI.7), consists basically of two uniformly spaced ($\frac{1}{8}$" apart) electrical resistance wires (Gilby-Brunton, No. A-g, 0.0124" diam, 5.74 ohm/yrd). Each pair of these wires is stretched between the tank bottom and its top, a sufficient space being left between the wires and the tank wall to avoid any fluid being trapped. At each $45^{o}$ angle around the inside wall of the tank there is a pair of wire detectors to monitor the fluid surface displacement at these positions.

An A.C. carrier signal of 8.4 KHz at 5V r.m.s. is applied across R1 and the fluid transducer in series. This signal is modulated according to the wave height across the probe. To block any d.c. signal an a.c. coupling capacitor C1 is provided through which the modulated signal passes to the amplifier, A1, R2, R3 and R4. The ratio R4/R2 determines the gain of the amplifier. RV1 is the offset null control and the amplifier supply is +15V and -15V d.c. The amplified output is then applied to a diode detector (D1, C2, and R5). The original modulating signal is extracted from the carrier and this signal directly represents the wave motion of the fluid free surface.

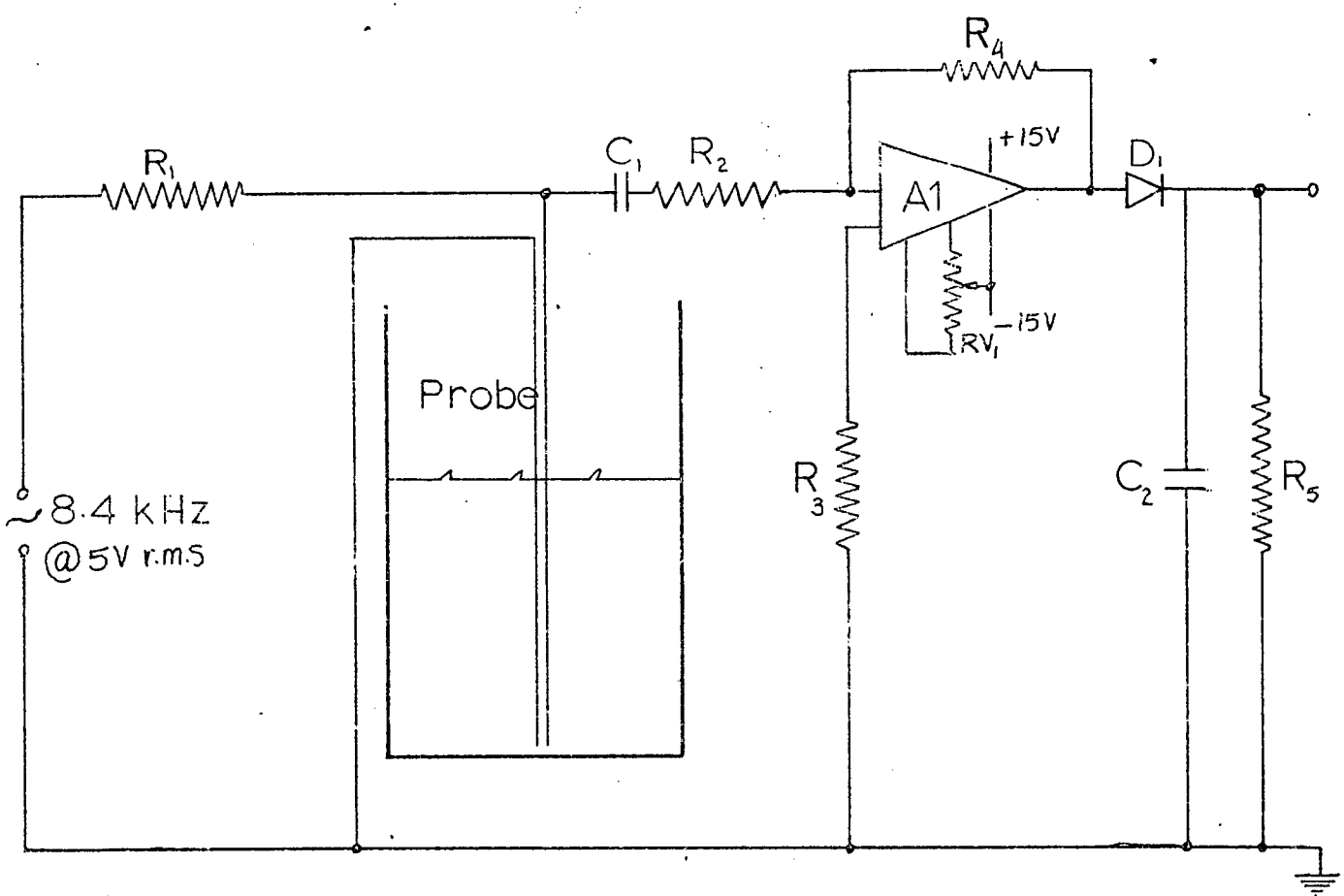


$R_1$ = 1 KΩ
$R_2$ = 2 KΩ
$R_3$ = 1 KΩ
$R_4$ = 47 KΩ
$R_5$ = 470 KΩ
$D_1$ = OA73
A1 = μA741
$C_1$ = 0.1 μF
$C_2$ = 1.0 μF
$RV_1$ = 10 KΩ

Fig(VI.7) Liquid Wave Height Transducer

VI.2.2 Input Excitation and Main Mass Response Measurements

The vibrator head amplitude $\xi_0$ and the main mass amplitude are measured by two linear displacement transducers (Hewlett-Packard Sanborn Type 7DCDT-250). This type of transducer is basically a linear variable differential transformer with a built in carrier oscillator and demodulator system. The coil assemblies of both transducers are hung by vertical strings from the stationary frame. The core of one transducer is fixed to the wall of the platform (to measure $\xi_0$) and the other is fixed on the edge of the dashpot arm of the main mass (to measure $\xi$), see Fig. (VI.1). Both transducers are energised by a 6 volt d.c. supply. When the core is displaced axially within the core of the coil assembly it produces a voltage change in the output proportional to the displacement.

VI.2.3 Tank Lateral Response Measurement

The lateral displacement of the container is monitored by a probe which is mounted on the main mass and brought into proximity with the flat surface of one of the leaf springs carrying the tank. The capacitance, formed between the probe face and the metallic surface of the leaf spring is displayed in terms of distance and peak to peak vibration amplitude on a Wayne Kerr Vibration meter B731B. The location of the proximity probe is shown in Fig. (VI.8). The displacement shown by the Wayne Kerr proximity probe represents the lateral displacement at the station where the probe is located. This displacement is proportional to the actual displacement of the tank.

VI.2.4 Recording the Results

The four transducers described previously convert the displacements into electrical signals. These signals are amplified (at the suitable sensitivity) and then fed on to highly sensitive mirror galvanometers in

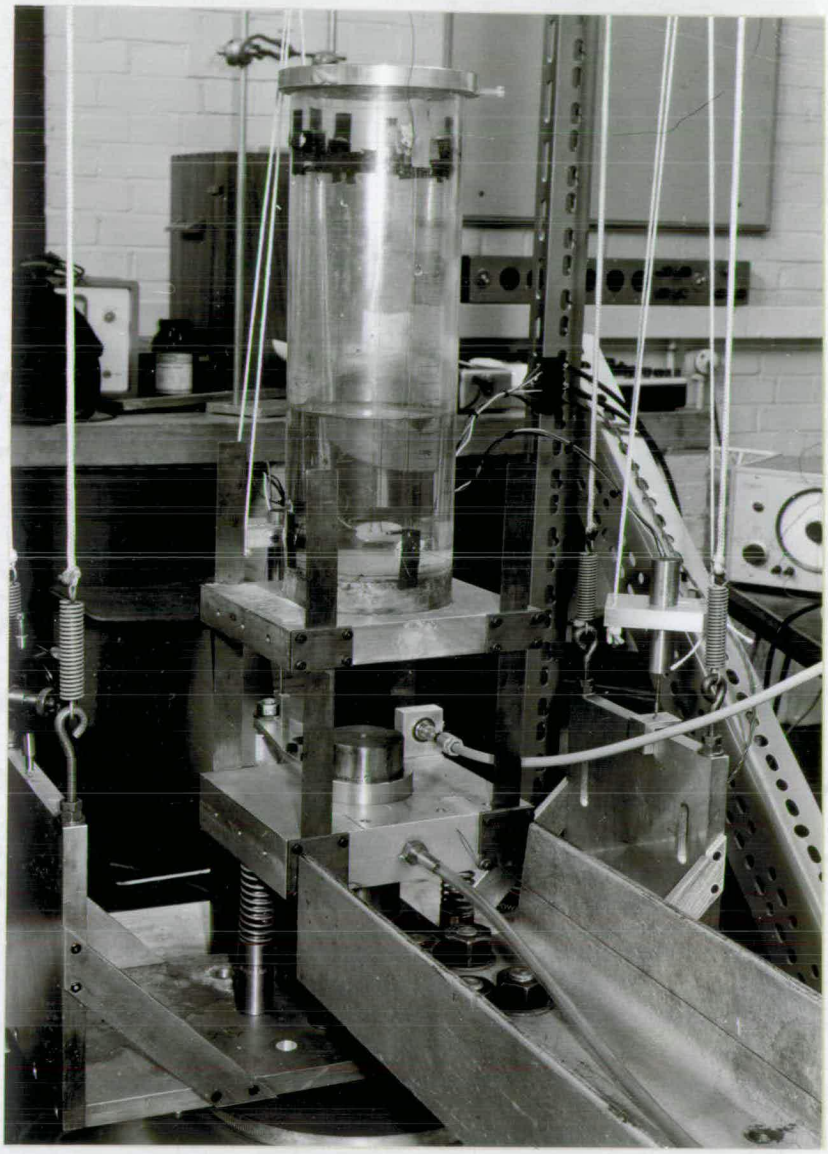

Fig(VI.8) Side View Shows the Positions of the Air Inlet and the Proximity Probe.

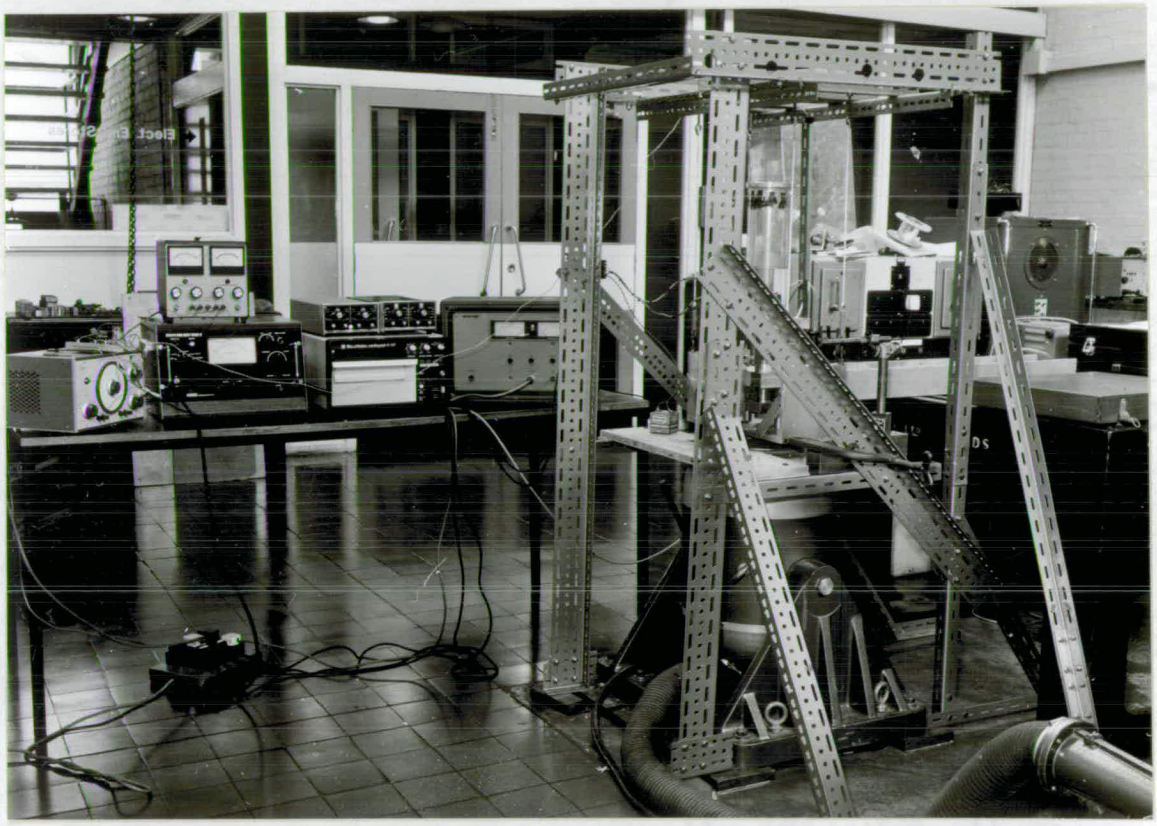

Fig(VI.9)General Set up of the Experimental Rig

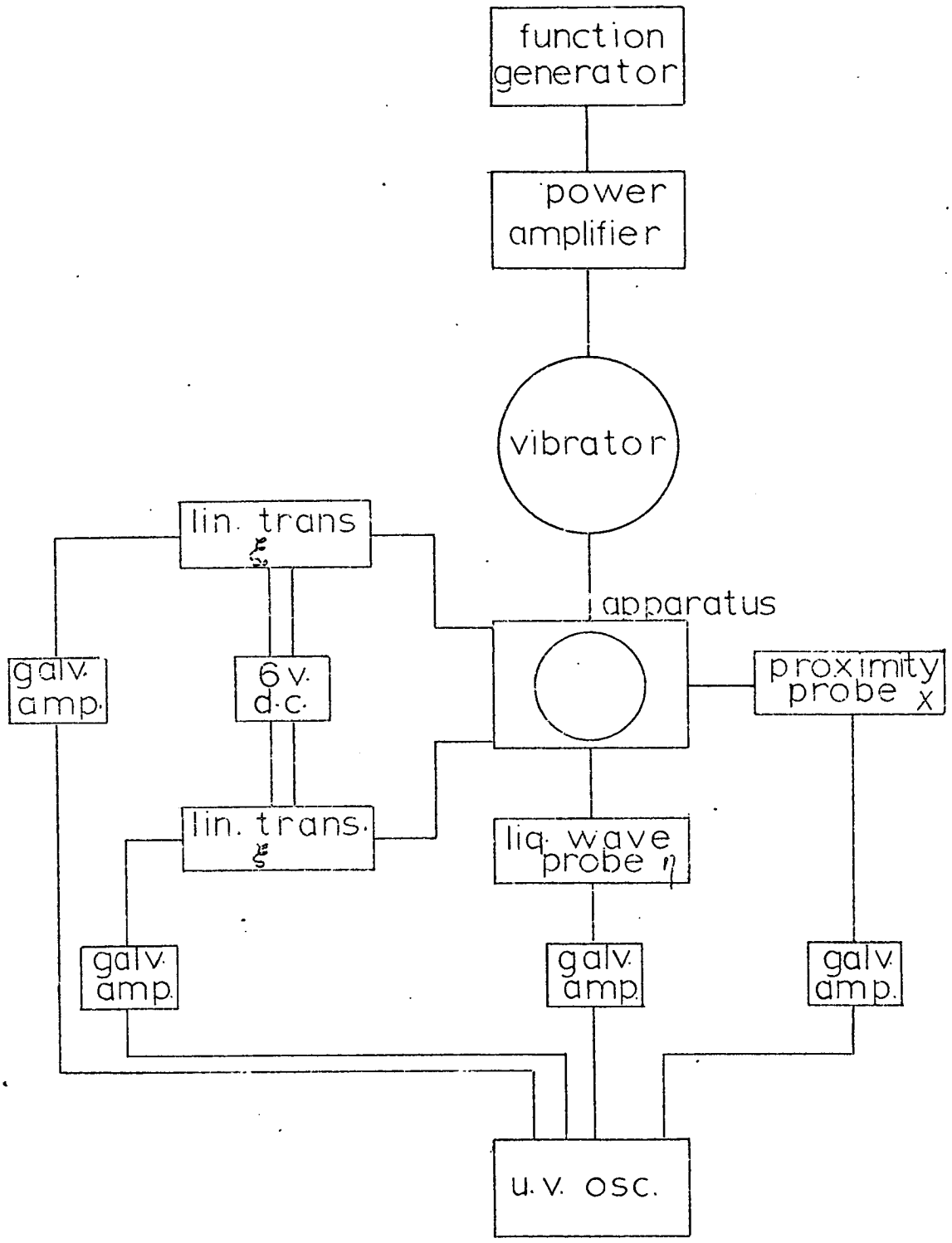


Fig(VI.10) Arrangement of Experimental Equipment

the Bell and Howell oscillograph-type S-137. The amplified signals vary the mirror positions, i.e. the galvanometers are electro-mechanical transducers which accept electrical energy and transform it into mechanical rotation. Light from a mercury arc U.V. lamp is reflected by the galvanometer mirrors through a simple optical system to focus a spot of light on a moving strip of light-sensitive paper. The trace of each signal represents the signal from the corresponding transducer in the system.

VI.3.0 Calibration

The traces obtained from the oscillograph represent the variation of the electrical signals produced by the four transducers which are in turn proportional to the displacements of the system. The ordinate of each trace can be calibrated to read directly the corresponding displacement of each transducer. The calibration curve of each transducer depends on the sensitivity of its galvanometer amplifier.

For the liquid wave height transducer the dynamic calibration was obtained by exciting the container laterally with a small vibrator (Goodmans type 390) as shown in Fig. (VI.11). The wall of the container is graduated in half centimetres so that the waveheight can be read off directly at each excitation frequency. Fig. (VI.12) gives two calibration curves corresponding to two sensitivity values V/in = 0.25 and 0.5.

The reading of the Wayne-Kerr meter does not indicate the actual displacement of the tank because the proximity probe detects only the displacement at its location. In order to calibrate the reading of the trace with the actual tank displacement, a static calibration was carried out using a dial indicator of accuracy 0.001" to indicate the actual tank displacement. Fig.(VI.13) shows two

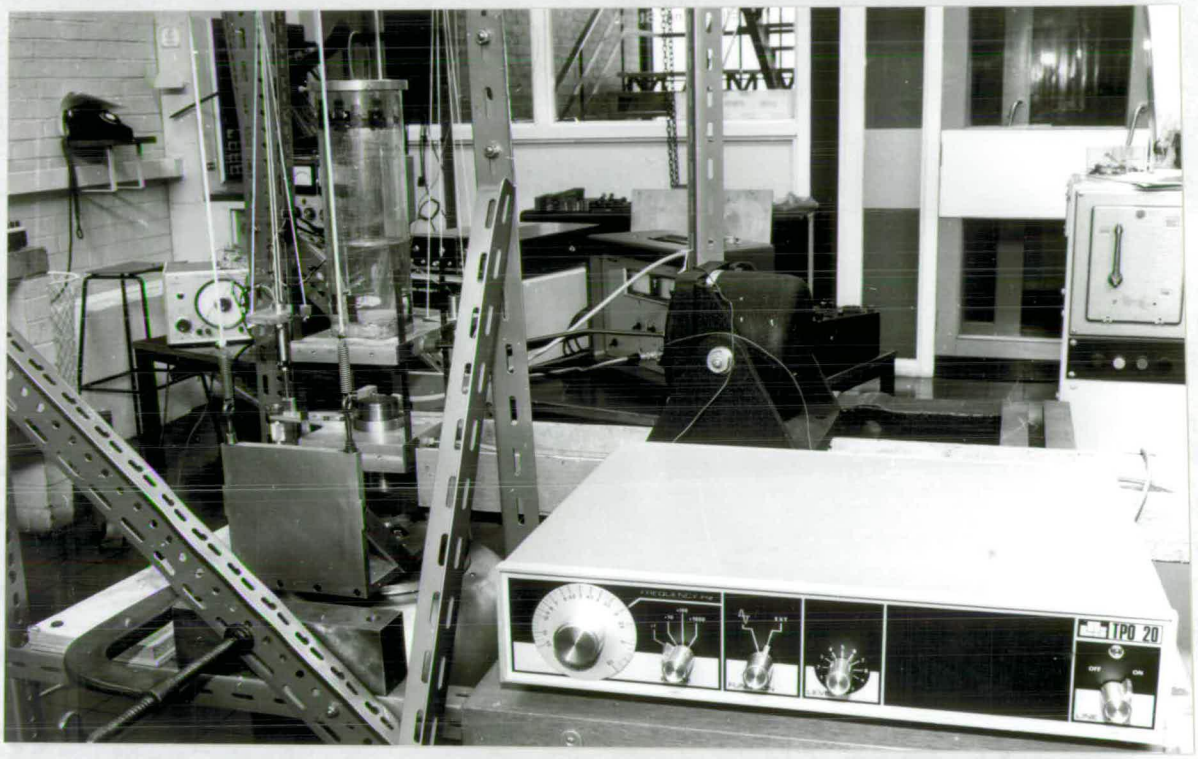


Fig(VI.11) Dynamic Calibration of the Liquid Free Surface Wave Height.

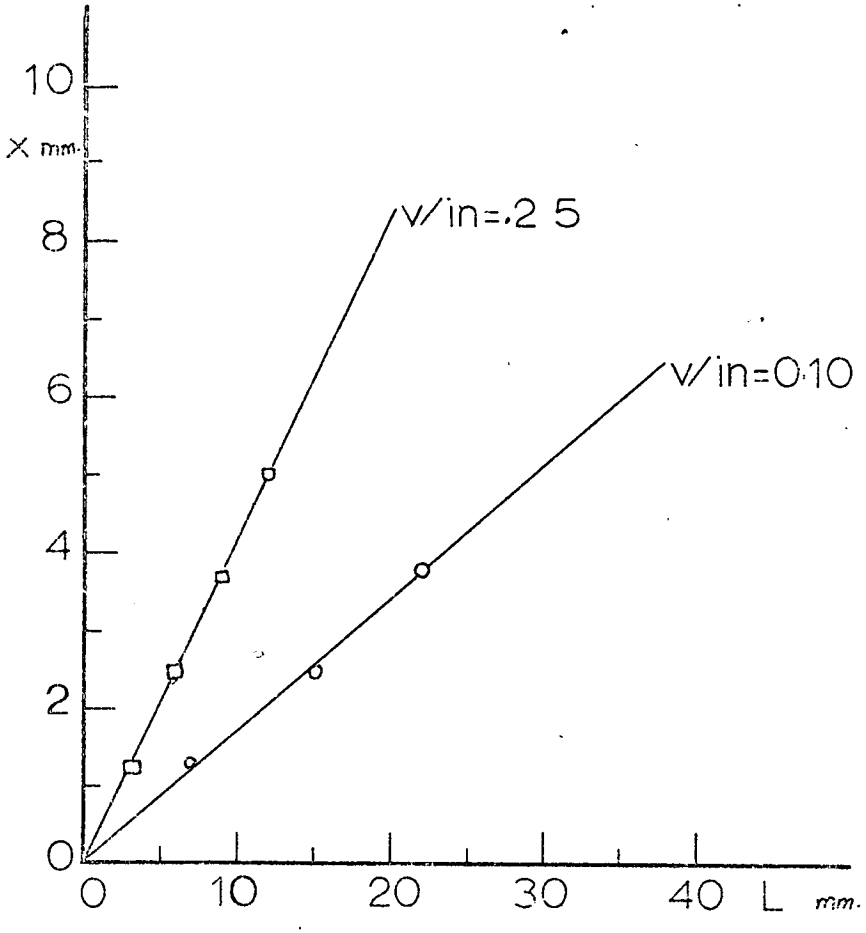


Fig.(VI·13) Static Calibration of Lateral Displacement Transducer

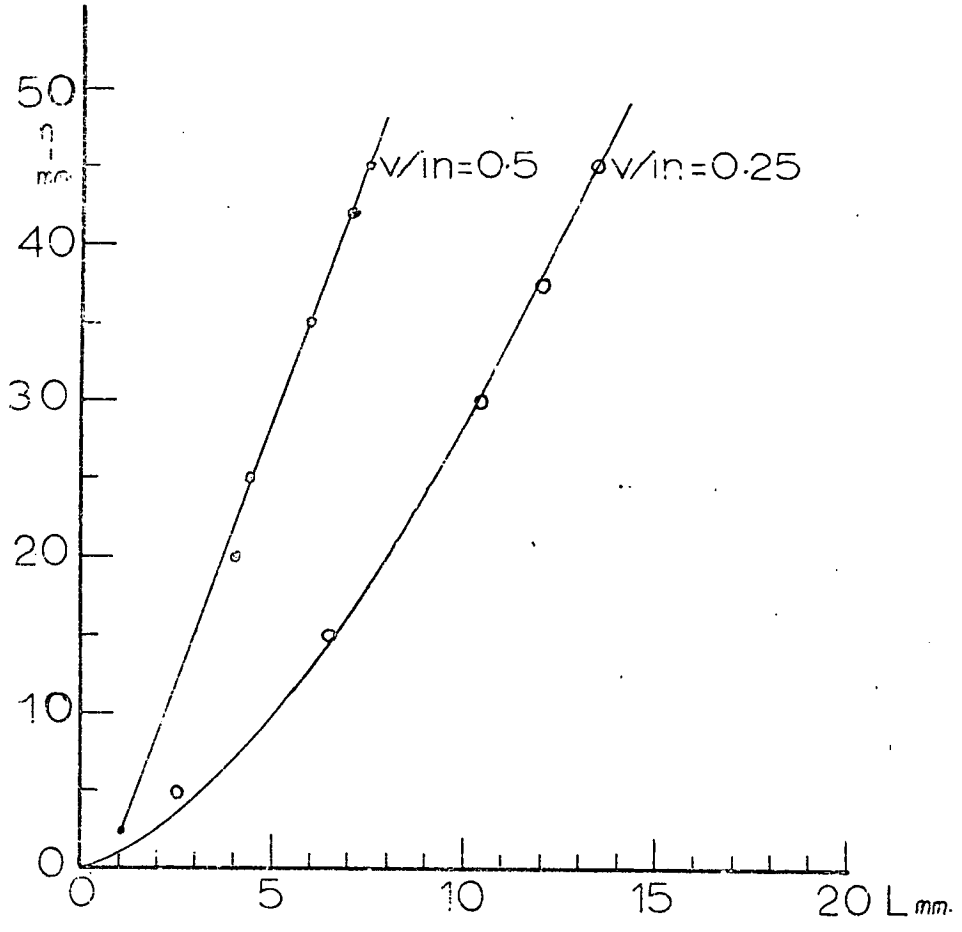


Fig(VI·12) Dynamic Calibration of Liquid Wave Transducer

calibration curves for two sensitivities V/in = 0.1 and 0.25, when the tank was at height 10 cm from the main mass upper surface. For other tank heights similar calibration curves were obtained.

Regarding the linear transducers that measure $\xi_o$ and $\xi$, the calibration was found to be linear when the sensitivity was 0.5V/in for $\xi$ transducer and 0.2V/in for $\xi_o$ transducer. It was also found that if the reading on the oscillograph is L mm., then $\xi$ = 0.264 L mm. and when the reading corresponding to the other transducer is $L_o$ mm then $\xi_o$ = 0.06 $L_o$mm.

Accuracy of Measurements

The accuracy of the measurements is estimated as follows;

| | |
|---|---|
| Driving frequency $\Omega/2\pi$ | $= \pm$ 0.05 Hz |
| Driving amplitude $\xi_o/a$ | $= \pm$ 0.0005 |
| Main mass amplitude $\xi/a$ | $= \pm$ 0.01 |
| Wave height amplitude $a_{11}/a$ | $= \pm$ 0.1 |

VI.4.0 Experimental Procedure and Results

Before conducting the forced oscillation tests it is necessary to measure the natural frequency and damping ratio of each system in the absence of any interaction from the other systems. Basically there are three systems whose natural frequencies and damping ratios are measured as follows;

VI.4.1 Measurements of the Natural Frequencies and Damping Ratios

1) First System: The first system consists of the compression springs $K_{s1}$, the dashpot $\bar{\zeta}_{s1}$ and the total mass $[M_o + m_{t1}]$. The liquid motion effects are eliminated by removing the water from the tank and replacing it by an equal solid mass. The lateral motion of the tank is prevented

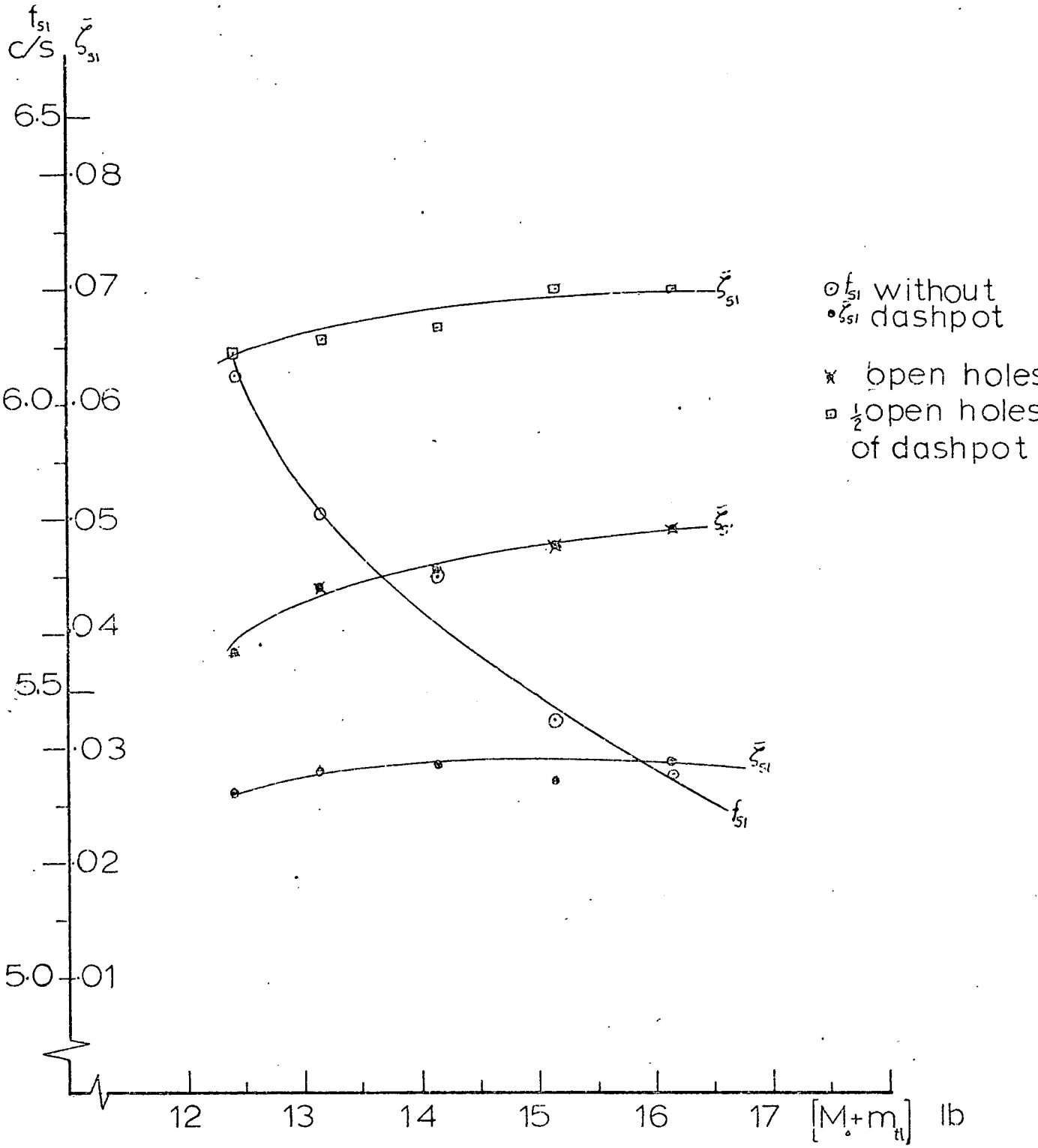


Fig (VI.14) Experimental Results of Natural Frequency and Damping Coefficient vis Mass of 1st System.

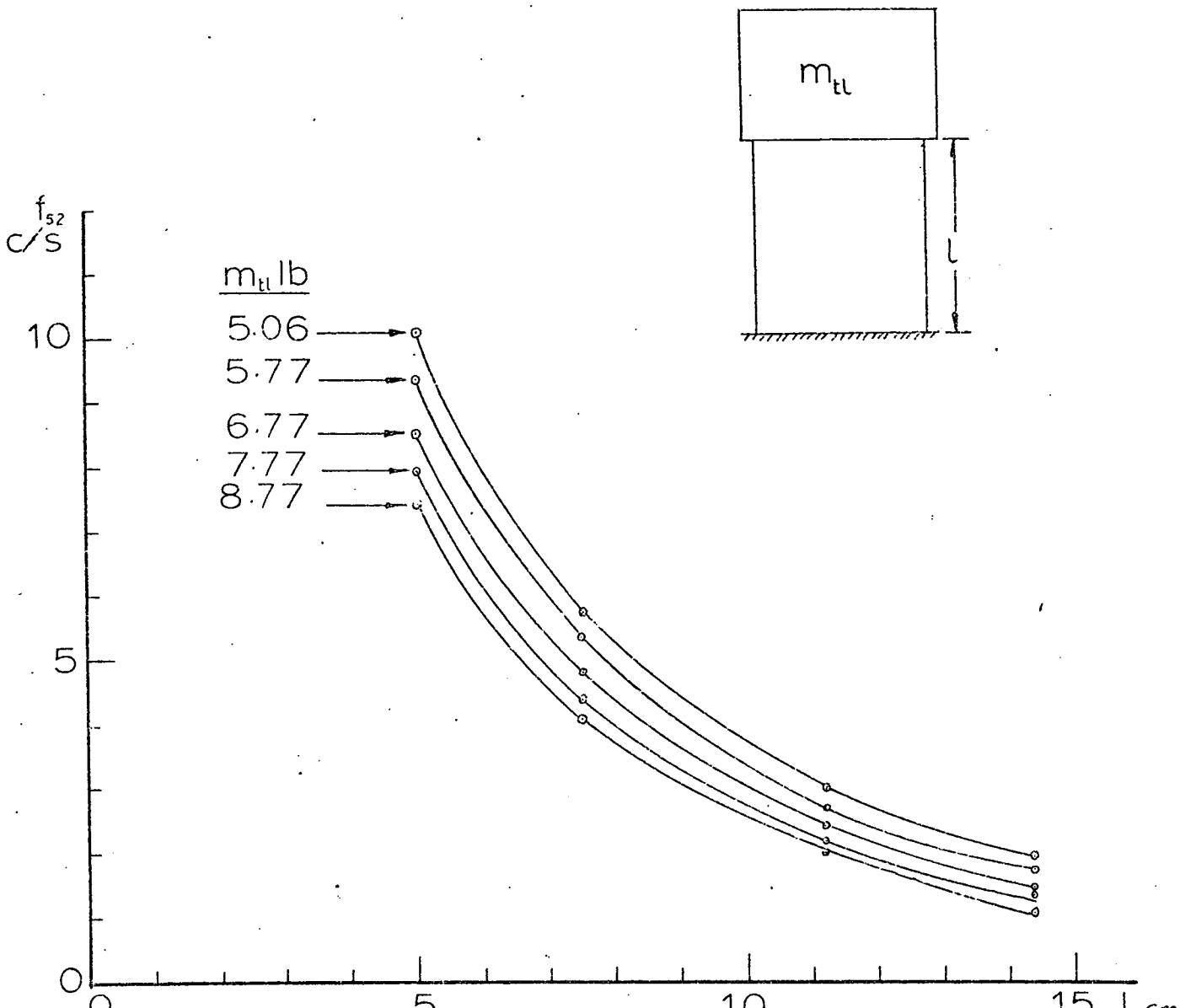


Fig(VI.15a) Experimental Results of Natural Frequency of Upper Structure.

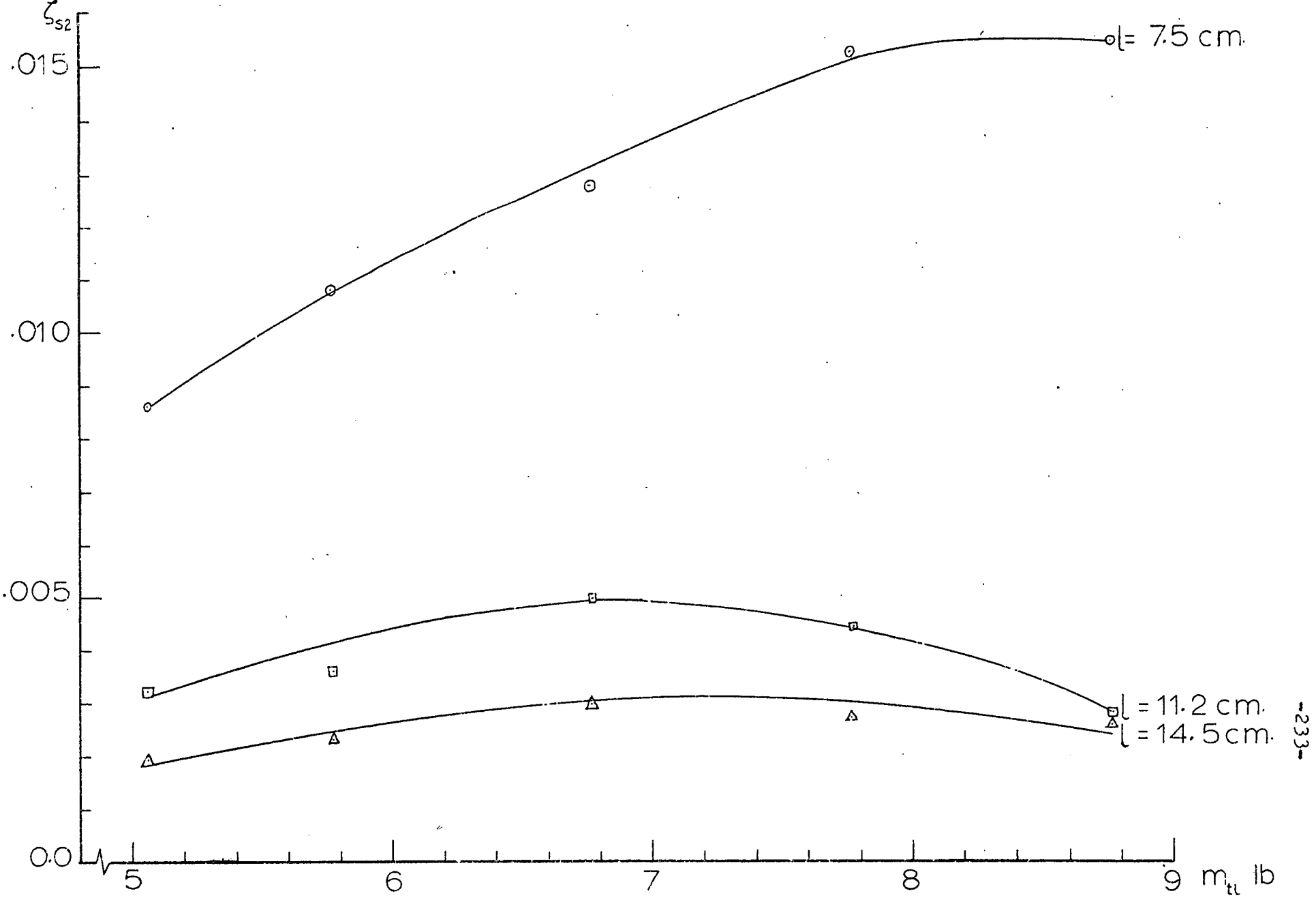


Fig(VI-15b) Experimental Results of Damping Coeff. of Upper Structure

by attaching the tank base to the main mass by two rigid panels whose combined mass is 0.326 kg. A series of free oscillation tests were conducted for different values of the solid mass, with and without the dashpot. Using the method of logarithmic decrement [T3], the damping ratio $\bar{\zeta}_{s1}$, is determined. In Fig. (VI.14) the natural frequency $f_{s1}$ and the damping ratio $\bar{\zeta}_{s1}$ are plotted against the total mass.

2) Second System: The second system comprises the leaf springs $K_{s2}$, and the upper mass $m_{t1}$. The influence of the main mass vertical motion is eliminated by fixing it to the platform by strong studs while the effect of the liquid motion is eliminated as described in the first system. A series of free oscillation tests was conducted for different values of $m_{t1}$ and the values of $\bar{\zeta}_{s2}$ and $f_{s2}$ were determined. These tests were repeated for different values of leaf springs length $\ell$ and the results are plotted in Figs. (VI.15).

3) Third System: The water inside the tank forms the third system. The damping ratio $\bar{\zeta}_{\ell}$ and the natural frequency $f_{11}$ of the water free surface were obtained by knocking the container gently and recording the subsequent response of the free surface. For two values of water depth ratios h/a, $\bar{\zeta}_{\ell}$ and $f_{11}$ were found as

$$h/a = 1.0 \quad , \quad \bar{\zeta}_{\ell} = 0.01035 \quad , \quad f_{11} = 3.0 \text{ Hz}$$
$$h/a = 2.0 \quad , \quad \bar{\zeta}_{\ell} = 0.0092 \quad , \quad f_{11} = 3.05 \text{ Hz}$$

VI.4.2 Response of the Two-Degrees-of-Freedom System

$$r_{s1} \approx 2.0$$
$$\approx 2\nu$$

There is a slight change in the natural frequency of the fluid free surface between the two liquid depth ratios h/a = 1.0 and 2.0 caused by a difference of 0.74 lb in the total mass $[M_c + m_{tl}]$. This causes a 2.69% variation in the natural frequency of the mass-spring-dashpot system. So the condition of internal resonance $\omega_{s1} = 2\omega_{11}$ is not met exactly.

To obtain the amplitude-frequency response of the system in the neighbourhood of the parametric resonance condition $r_{s1} \approx 2.0$, a series of forced oscillation tests were conducted. Keeping the amplitude of the vibrator head at a constant level, the excitation frequency was increased and decreased in a step-wise manner. Figs. (VI.16-19) show the amplitude-frequency responses for an excitation amplitude $\xi_o$ = 0.125 mm. With and without the dashpot. As the excitation frequency is increased from a value below $2\omega_{11}$ (or $\omega_{s1}$, i.e. $n<1$) the response of the system, path CD, is identical to that of a single degree of freedom system with an identically zero liquid amplitude response. As n approaches 1.0 the state of the liquid free surface begins to oscillate and achieves a steady-state. This transition in the liquid response appears as the jump DE with a considerable reduction in the main mass amplitude indicated by the drop BJ. A further increase in frequency results in a continuous decrease in the liquid amplitude, path EFG , until the free liquid surface becomes plane, while the main mass response follows a typical linear resonance response JLM. Reversing the procedure by decreasing Ω starting from a value higher than $2\omega_{11}$ gives the paths HGFEI for the liquid amplitude response with a collapse at I and MLJK for the main mass response.

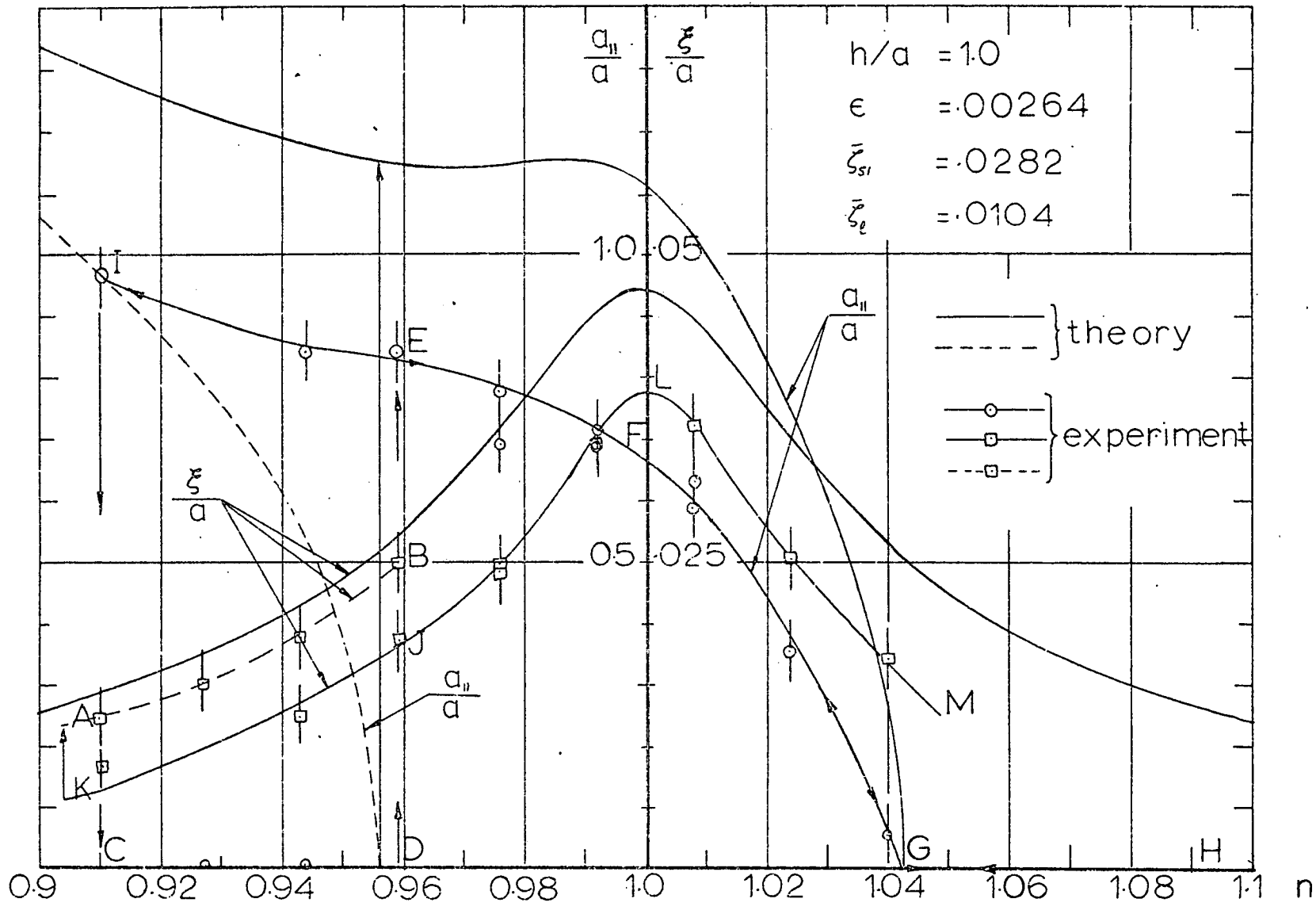


Fig(VI.16 ) Comparison of Theoretical and Experimental Response of Structure - Liquid System Under Parametric Excitation.

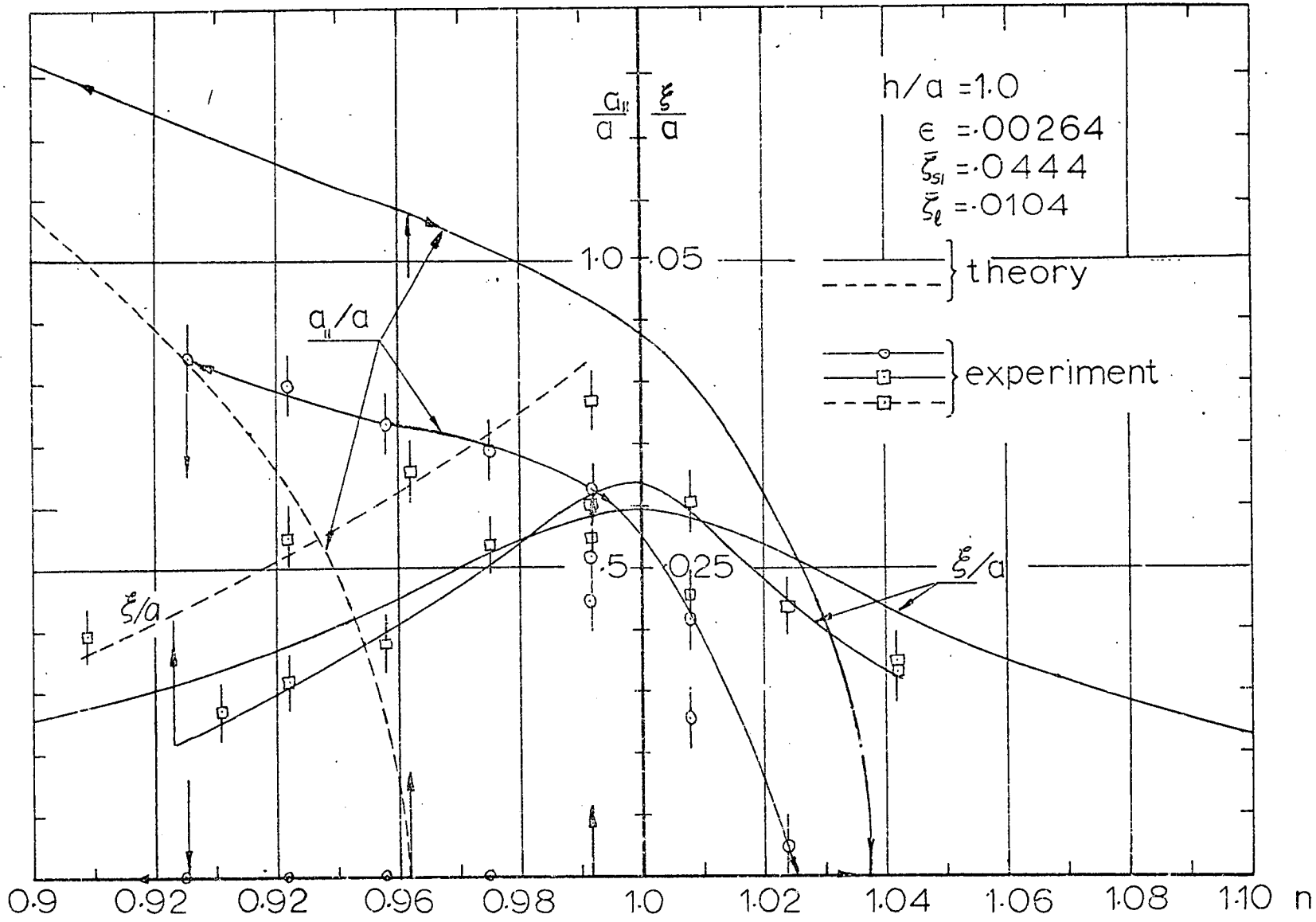


Fig(VI·17) Comparison of Theoretical and Experimental Response of Structure-Liquid System Under Parametric Excitation.

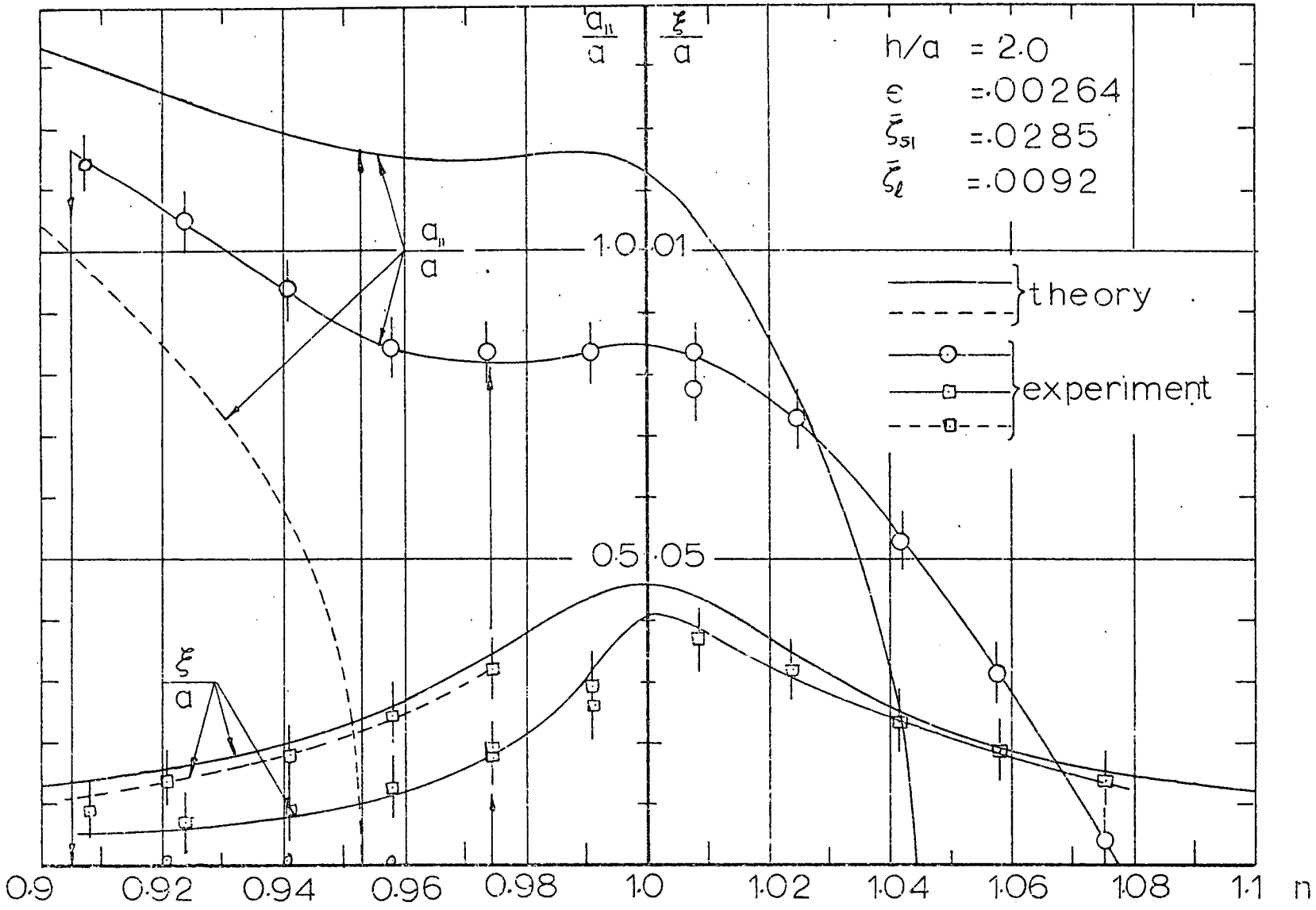


Fig (VI·18) Comparison of Theoretical and Experimental Response of Structure - Liquid System Under Parametric Excitation.

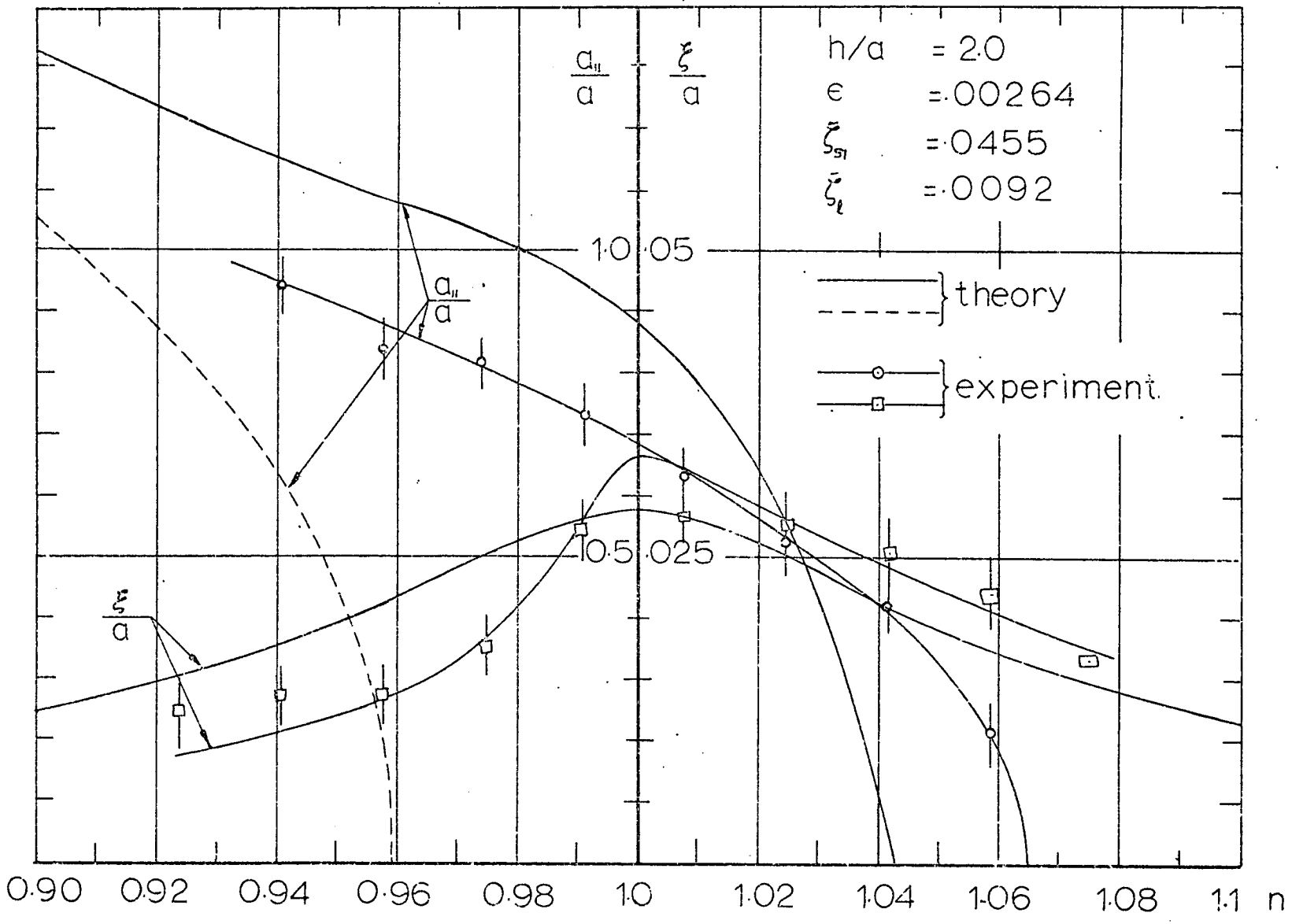


Fig(VI.19) Comparison of Theoretical and Experimental Response of Structure-Liquid System under Parametric Excitation.

Comparison with Theory

In Figs. (VI.16-19) a comparison between theoretical and experimental results is given. It can be seen that the theoretical amplitude response curves are rather higher than the experimental ones, however the overall system characteristic is the same in both results. It can be seen that when the liquid sloshing begins, the main mass response drops to the lower curve JLM, the lower curve is thought to be associated with the increased damping of the vertical oscillations of the main mass in the air bearing due to the lateral force on the bearing resulting from the liquid free surface motion. This is indicated by the unsymmetrical nature of the main mass experimental response curve about $n = 1$ (see Fig. VI.19). On the right side of $n=1$, the main mass response is rather higher than on the left side. This results from a lowering $\bar{\zeta}_{s1}$ due to the continuous decrease in the liquid free surface amplitude as n increases.

VI.4.3 Response of the Three-Degrees-of-Freedom System

Case a)

$$r_3 = r_1 + r_2$$
$$= n\nu$$

With internal resonance of the summed type, the configuration of the system is given according to the information of table (VI.1). According to the experimental observations and the time history record of the three mode response shown in Fig. (VI.20), the system does not achieve a constant amplitude steady-state and an energy exchange between the fluid and the structure takes place in a form of beating with constant maximum amplitude. It was also observed that the system did not respond to any parametric excitation - except at the exact resonance - unless an initial lateral disturbance was applied.

At exact resonance, it is a long time before the liquid free surface starts to oscillate with a very tiny amplitude. The resulting small sloshing force causes the structure to oscillate laterally. This energy flow continues with a build up in amplitude until the damping of each mode controls this growth and the system follows the response given in Fig. (VI.20). The envelopes of the liquid and upper structure responses oscillate with a long period of 1.5 sec at a constant amplitude. The transient time before the system achieves the steady beating response is about 40 sec.

If the internal resonance condition is distorted by reducing or increasing $\ell/a$, the system possesses a complete steady response. The transient and steady-state responses for $\ell/a = 1.9$ are shown in Fig. (VI.21), and it can be seen that slight beating occurs during the transient period.

The amplitude-frequency response curves are obtained by a similar procedure to the previous section. Figs. (VI.22-24) show the experimental amplitude response curves $\Xi/a$, $a_{11}/a$, and x/a respectively for two values of excitation amplitude when $\bar{\zeta}_{s1} = 0.0282$, and h/a = 2.0. For the same fluid depth ratio but with a different damping ratio $\bar{\zeta}_{s1} = 0.0444$, similar curves are given in Figs. (VI.25-27) for two excitation amplitudes. Both the liquid and upper structure amplitude curves possess instability at an excitation frequency less than $f_{s1}$, indicated by the jump and the collapse amplitudes. On the right side of n = 1, the amplitudes $a_{11}$ and x decrease gradually as n increases until they cease at an excitation frequency slightly higher than $2f_{11}$. Within the frequency range bounded by $2f_{11}(1 - 0(\epsilon)) < \Omega < 2f_{11}$, the liquid free surface oscillates about a nodal diameter perpendicular to the direction of the tank oscillations. When $\Omega$ approaches $2f_{11}$ the

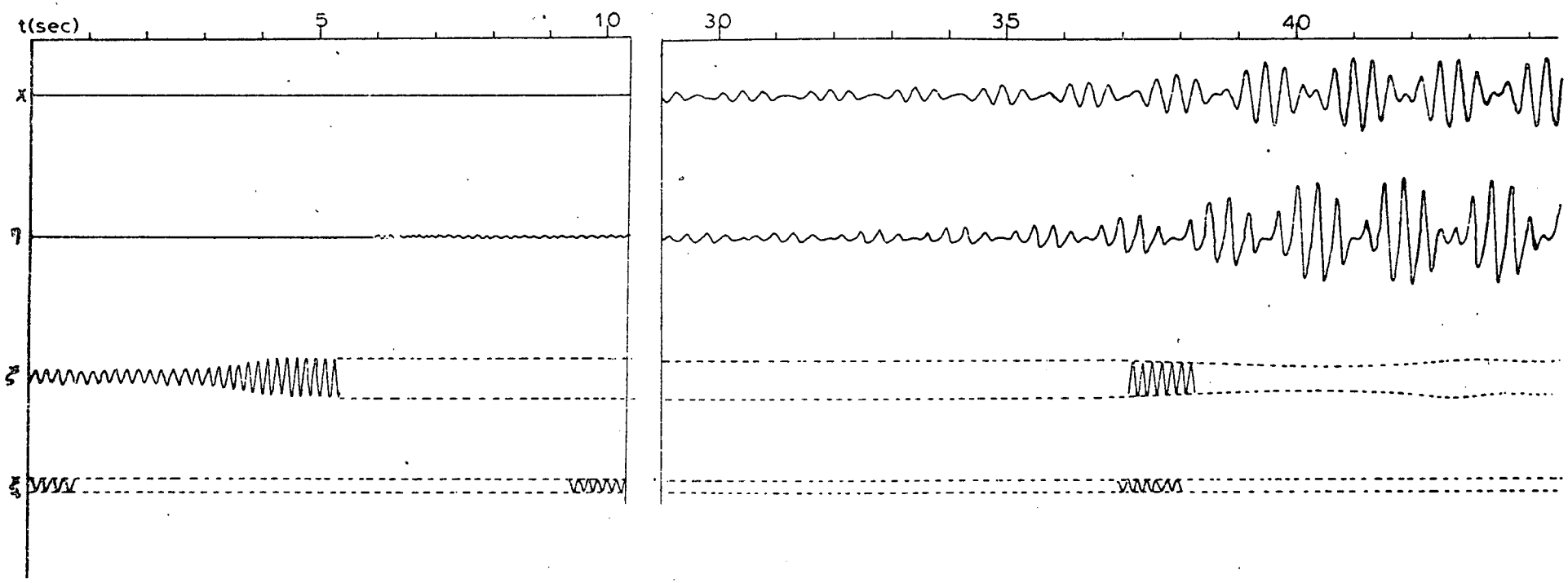


Fig(VI.20) Experimental Time History of Transient and Steady State Responses Under Nearly Internal Detuning System.

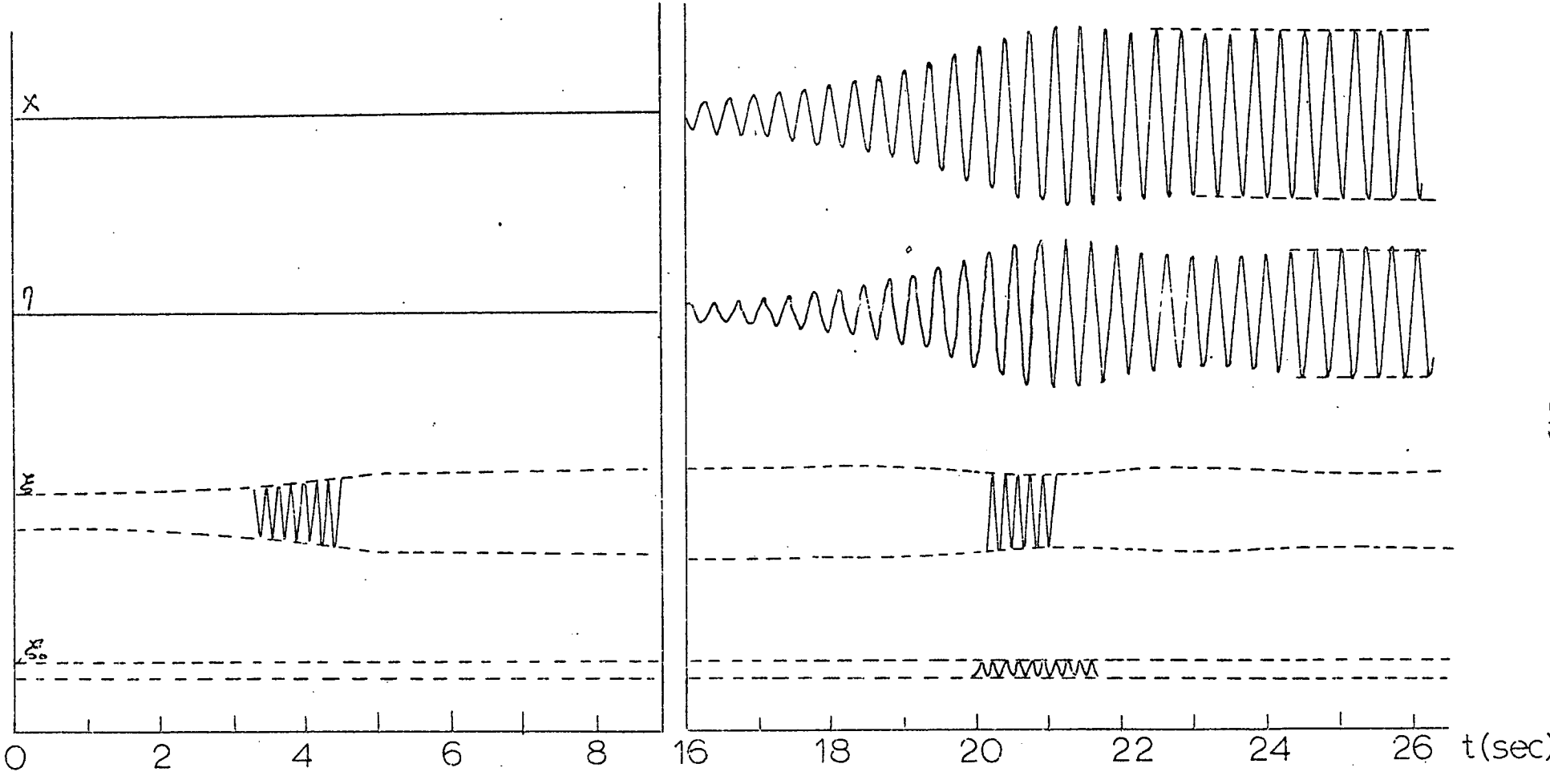


Fig(VI.21) Experimental Time History of Three Mode Interaction, $r_3 - (r_1 + r_2) \neq 0.0$

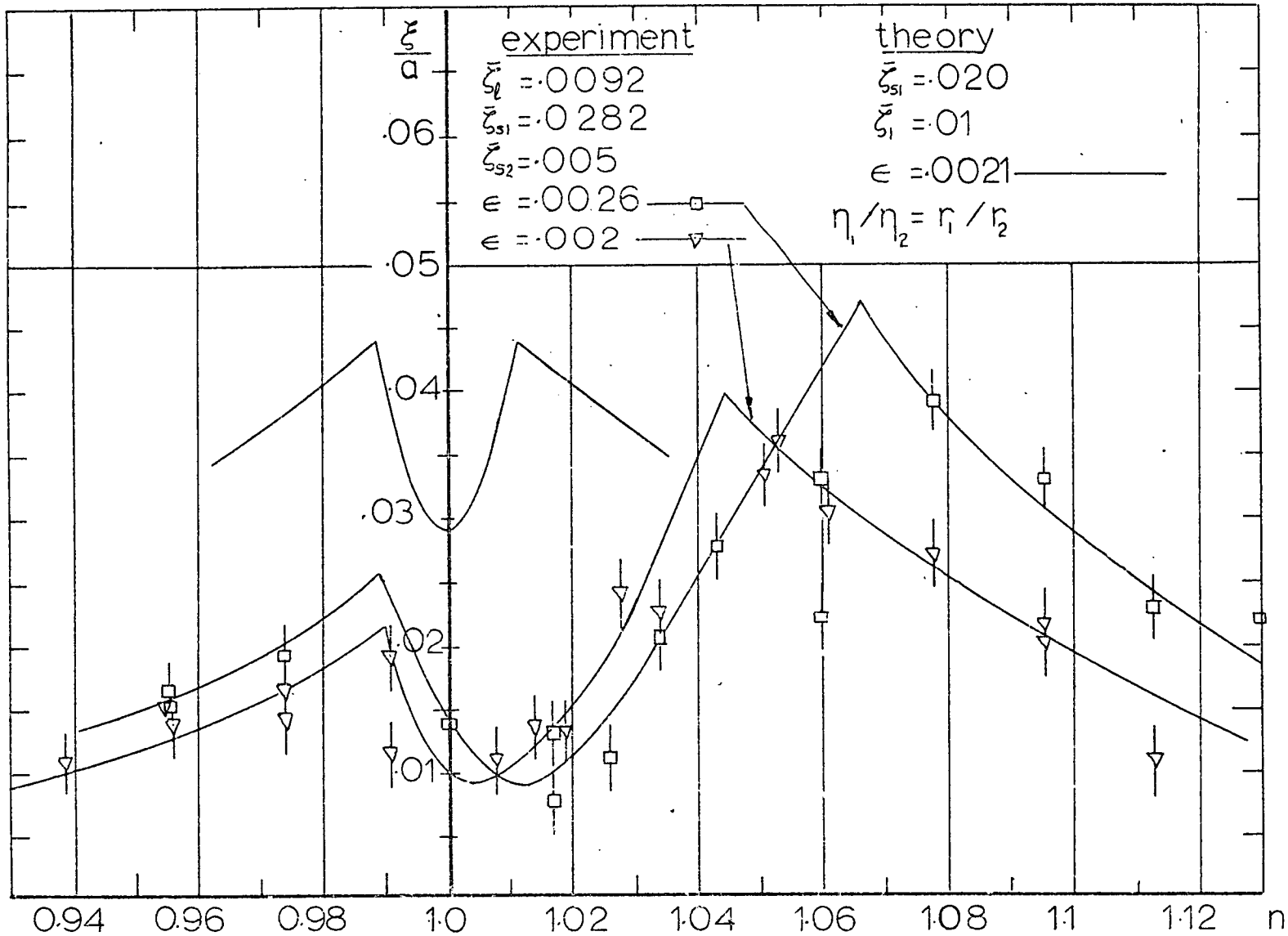


Fig(VI·22) Experimental Main Mass Response Under Frequency Summed Internal Resonance $r_3 = r_1 + r_2$, $h/a = 2.0$, $l/a = 2.1$

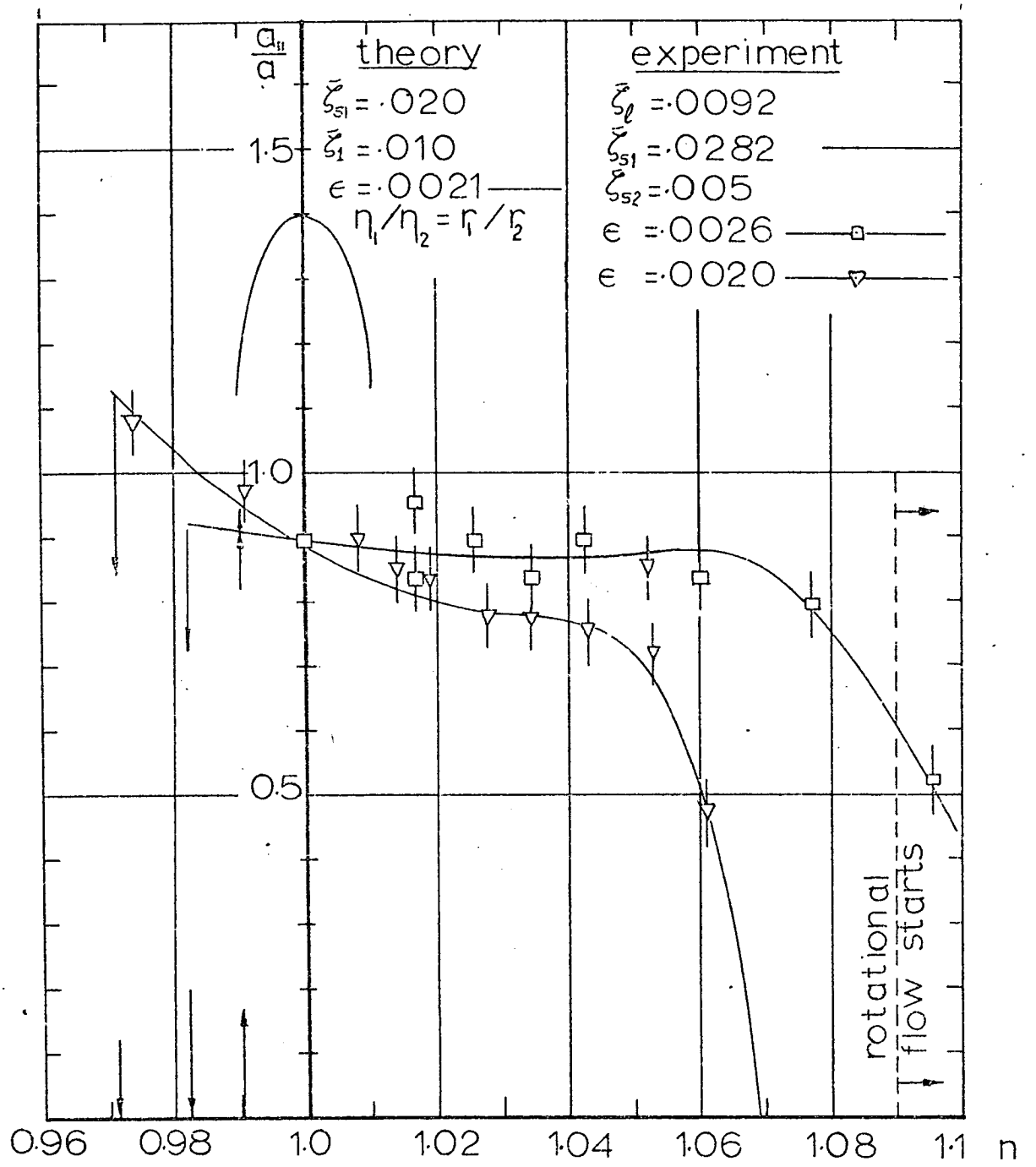


Fig(VI.23) Exprimental Liquid Response,
$r_3 = r_1 + r_2$, $h/a = 2.0$, $l/a = 2.1$

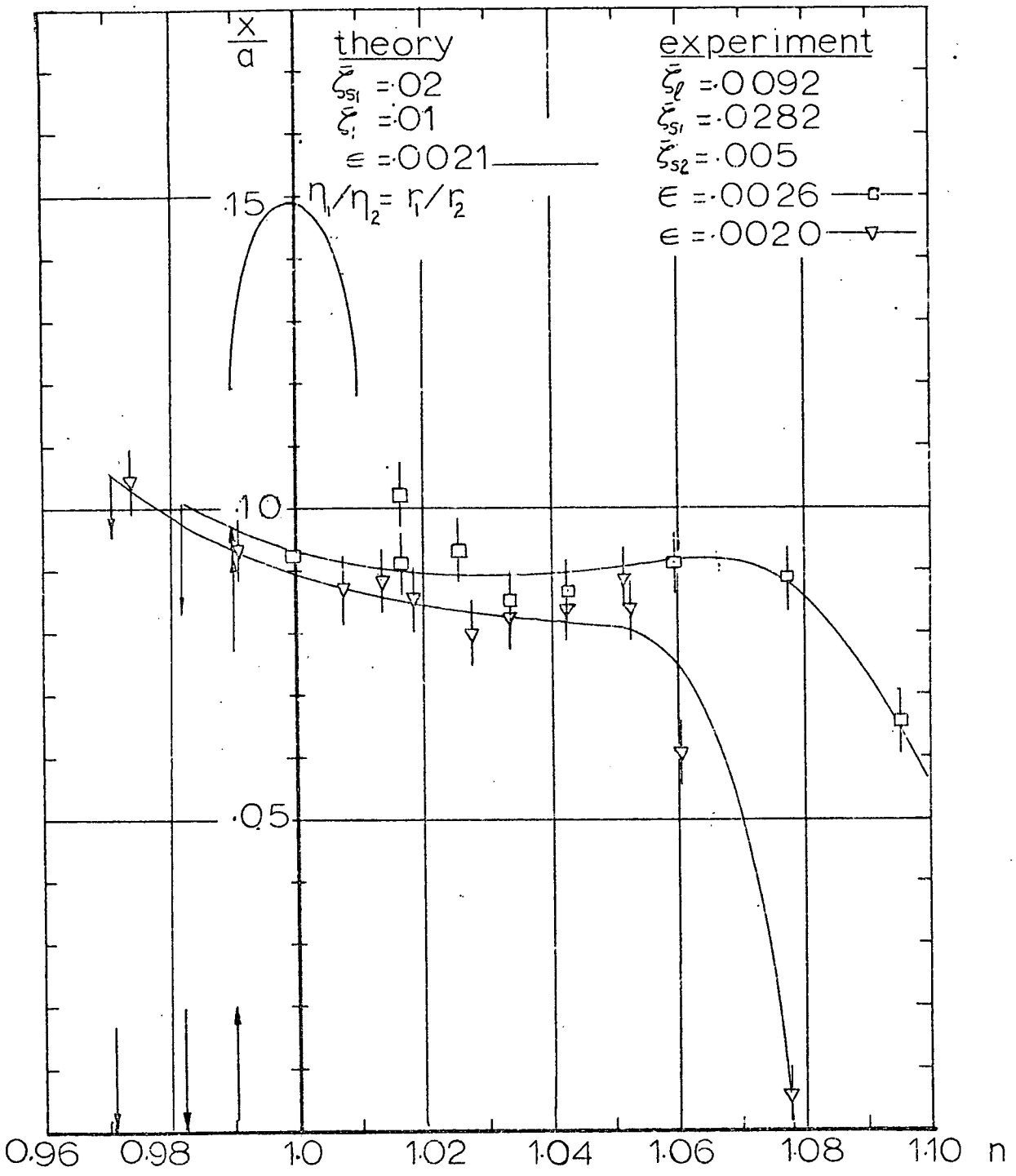


Fig(VI·24) Experimental Upper Structure Response, $r_3 = r_1 + r_2$, $h/a = 2.0$, $l/a = 2.1$

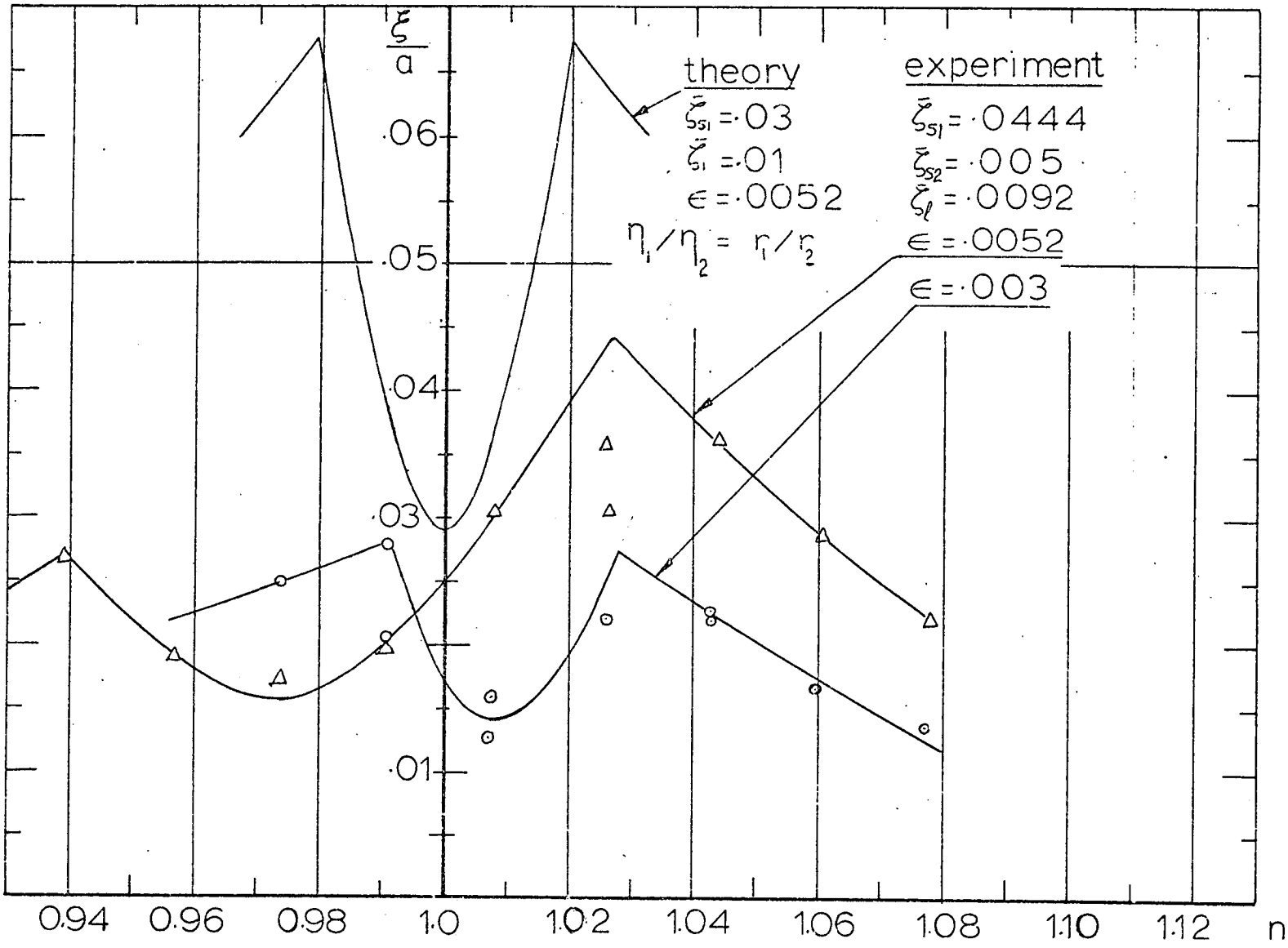


Fig(VI.25) Experimental Main Mass Response Under Frequency Summed Internal Resonance $r_3 = r_1 + r_2$, $h/a = 2.0$, $l/a = 2.1$

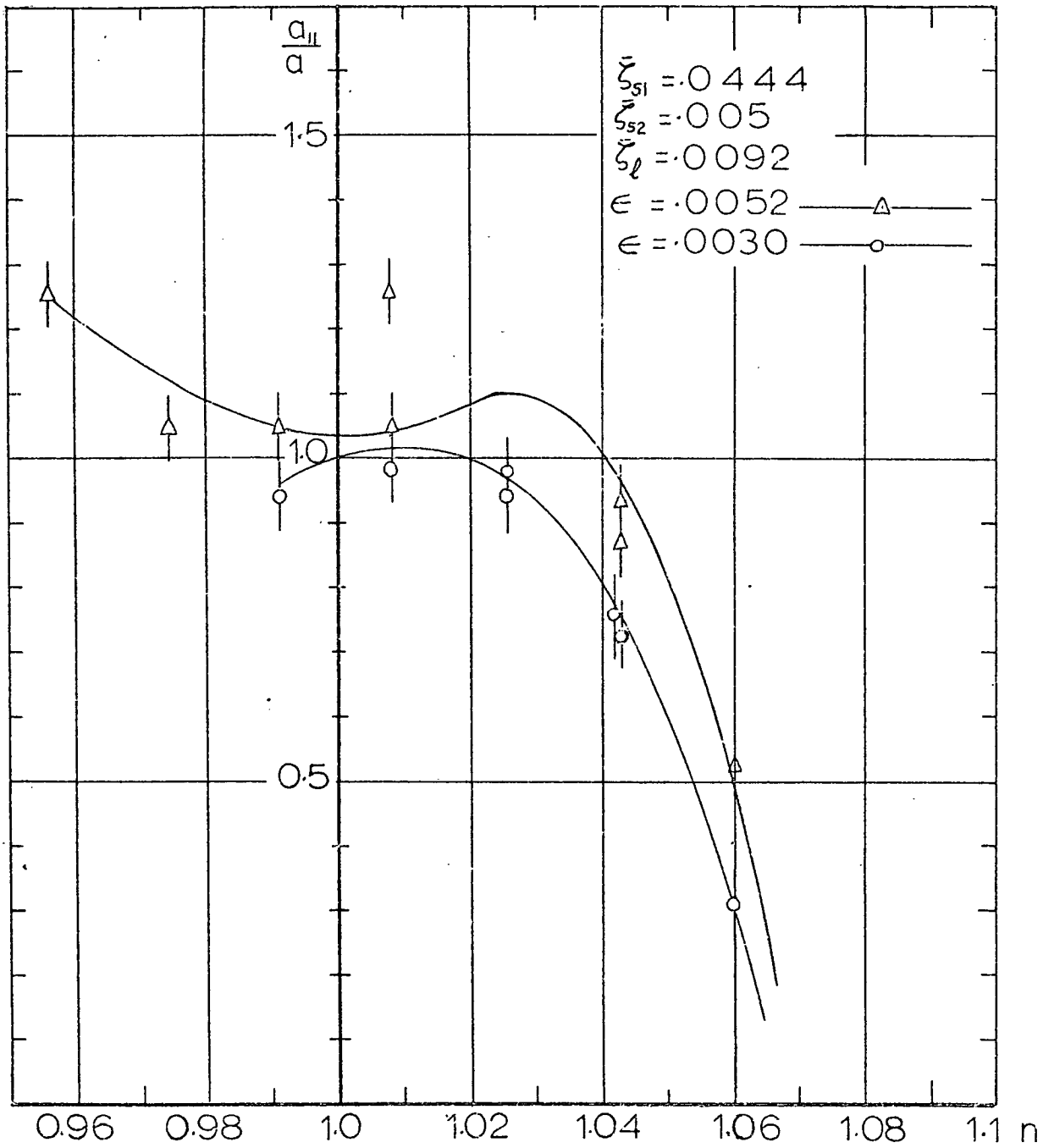


Fig(VI.26) Experimental Liquid Response

$r_3 = r_1 + r_2$ , $h/a = 2.0$ , $l/a = 2.1$

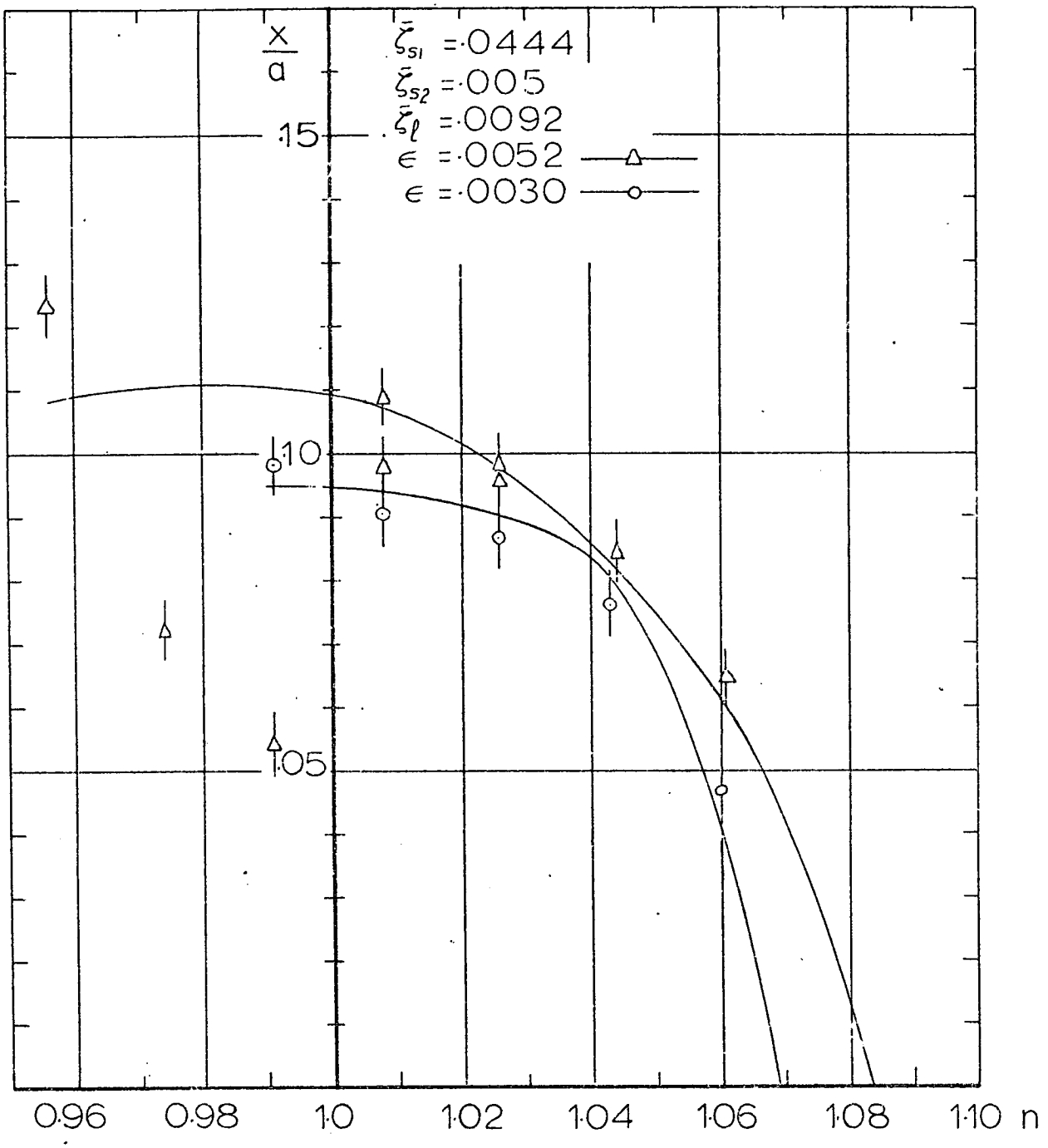


Fig(VI·27) Experimental Upper Structure Response, $r_3 = r_1 + r_2$, $h/a = 2{\cdot}0$, $l/a = 2{\cdot}1$

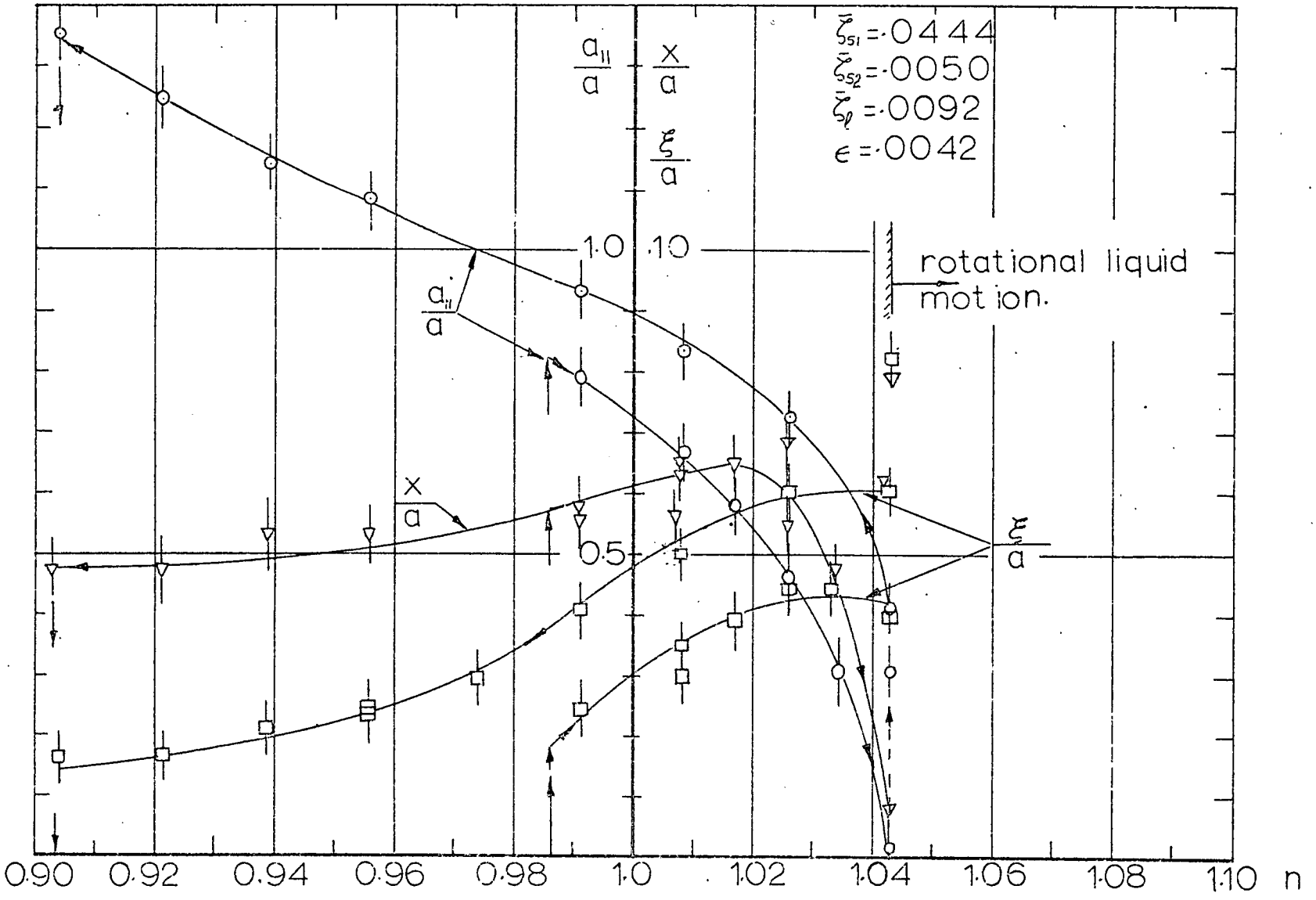


Fig(VI·28) Experimental Response of Three Mode Interaction with $r_3 - (r_1 + r_2) \neq 0.0$ $h/a = 2.0$, $l/a = 1.9078$

liquid amplitude shows a large decrease and then ceases. If $\Omega$ is then increased slightly, eventually the nodal diamter begins to rotate around the longitudinal centre line of the tank and there is a new increase in the liquid wave height. This rotation sometimes reverses its direction and sometimes continues in the same direction without achieving constant amplitude in both cases. This phenomena has been studied before [H12] and is discussed in chapter (IV). The unsymmetry in the $a_{11}/a$, and $x/a$ curves can this time be attributed to two causes viz. the nonlinear soft character of the liquid and the rotation of the nodal diameter.

The main mass response $\xi/a$ shows the characteristic of the autoparametric vibration absorber. The effect of air bearing damping vibration is also apparent in the unsymmetry of that response. The absorber effect does not occur exactly at $n=1$ because it was difficult to produce experimentally a system with an exact internal resonance condition.

More experimental results shown in Fig. (VI.28) delineate the response of the system when $\ell/a = 1.9$. It can be seen that the response of the system when $\Omega$ is increasing is different to the response when $\Omega$ is decreasing. However, the main mass response does not show any autoparametric suppression.

Case b) $$r_3 = r_1 - r_2$$
$$= n)$$

The behaviour of the system under the present condition is similar to that of case(a), however, the system now requires a strong initial condition to trigger its response. It was observed that with a small lateral disturbance, the liquid with its structure oscillate for

a few seconds and then rapidly regain their original position. With a stronger disturbance, under the same excitation frequency and amplitude, the system achieves a beating type response between the fluid and its structure, while the main mass response follows the absorber curve. This indicates that the system possesses two limit cycles; one is stable and the other is unstable. Figs. (VI.29-31) show the amplitude frequency response curves $a_{11}/a$, $x/a$ and $\xi/a$ for two values of $\bar{\zeta}_{s1}$.

Case c) $$r_3 = 2r_1 = n\nu$$

In the present case it was observed that there are two other liquid sloshing modes that can be stimulated. These two sloshing modes are the zero and the second symmetric modes. Figs.(VI.32-33) show the formation of these modes when the excitation frequency equals $2f_{01}$ and $2f_{21}$ respectively. For this reason it was difficult to isolate the first antisymmetric sloshing mode from these two modes, and no amplitude frequency response curves could be obtained.

Case d) $$r_3 = 2r_2 = n\nu$$

A complete steady-state response was observed. Fig. (VI.34) shows the steady-state time history of the two normal mode (three generalised modes) interaction. The amplitude frequency response curves $a_{11}/a$, $x/a$ and $\xi/a$ are given in Figs. (VI.35-37) for two values of $\bar{\zeta}_{s1}$. For the higher damping ratio $\bar{\zeta}_{s1}$, the system does not respond for $\in = 0.0052$ and the main mass motion follows the normal resonance curve of a single degree of freedom system as shown in Fig.(VI.37). The responses of the liquid free surface and its structure follow similar curves as in cases (a) and (b).

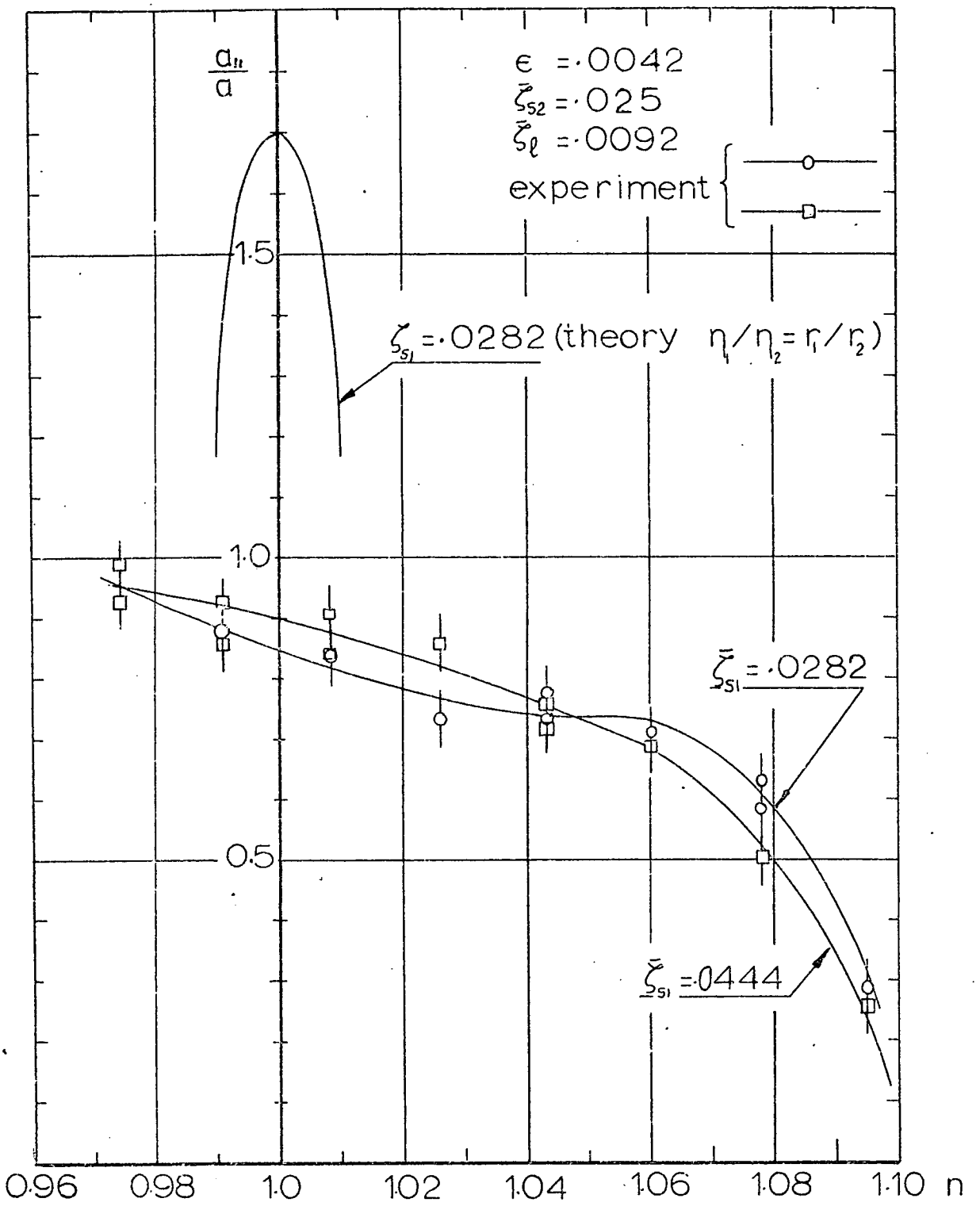


Fig(VI.29) Experimental Response of Liquid Free Surface, $r_3 = r_1 - r_2$, $h/a = 2.0$ $\ell/a = 1.05$

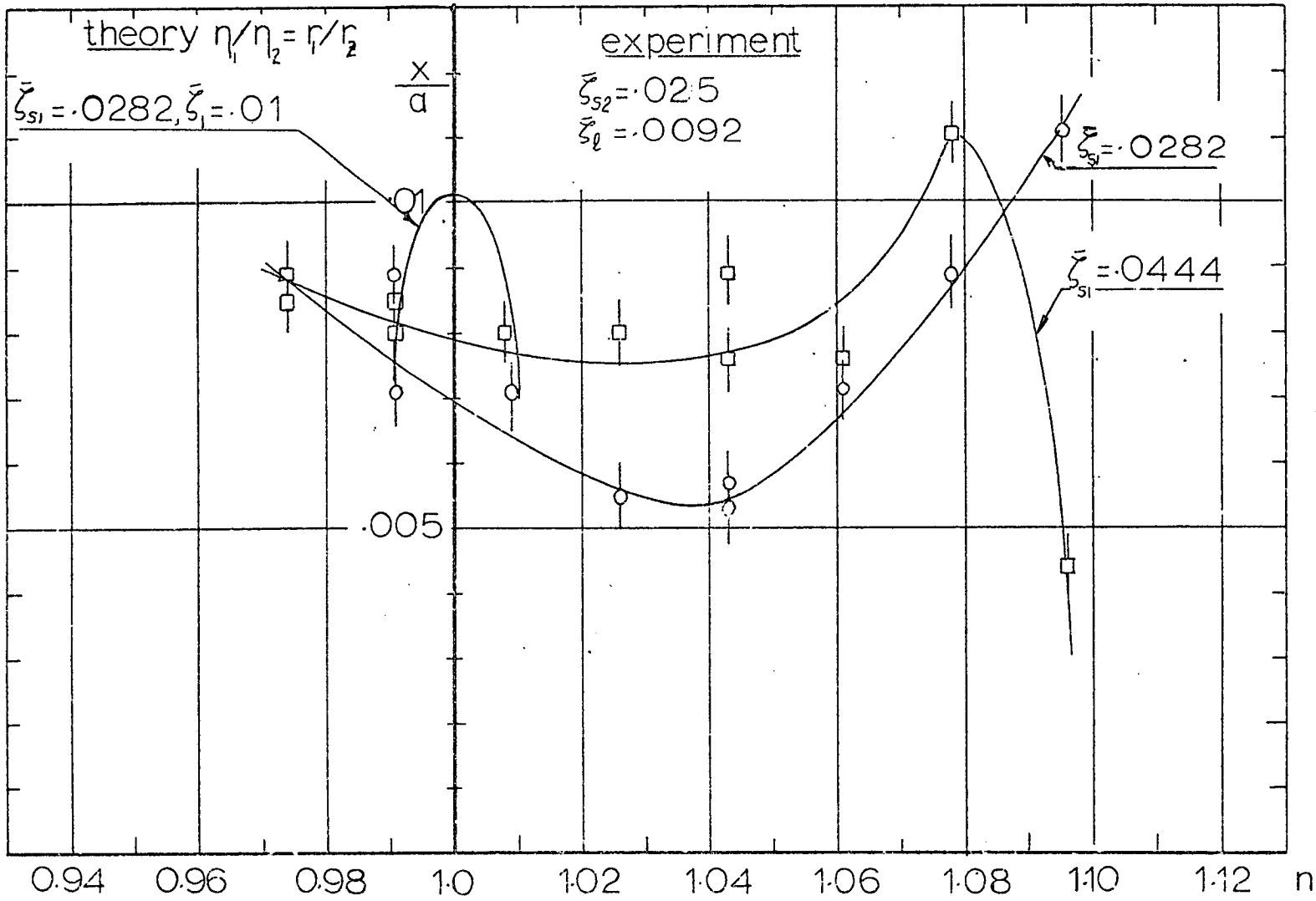


Fig.(VI30) Experimental Response of the Upper Structure.

$r_3 = r_1 - r_2$, $\epsilon = \cdot 0042$, $h/a = 2{\cdot}0$, $l/a = 1{\cdot}05$

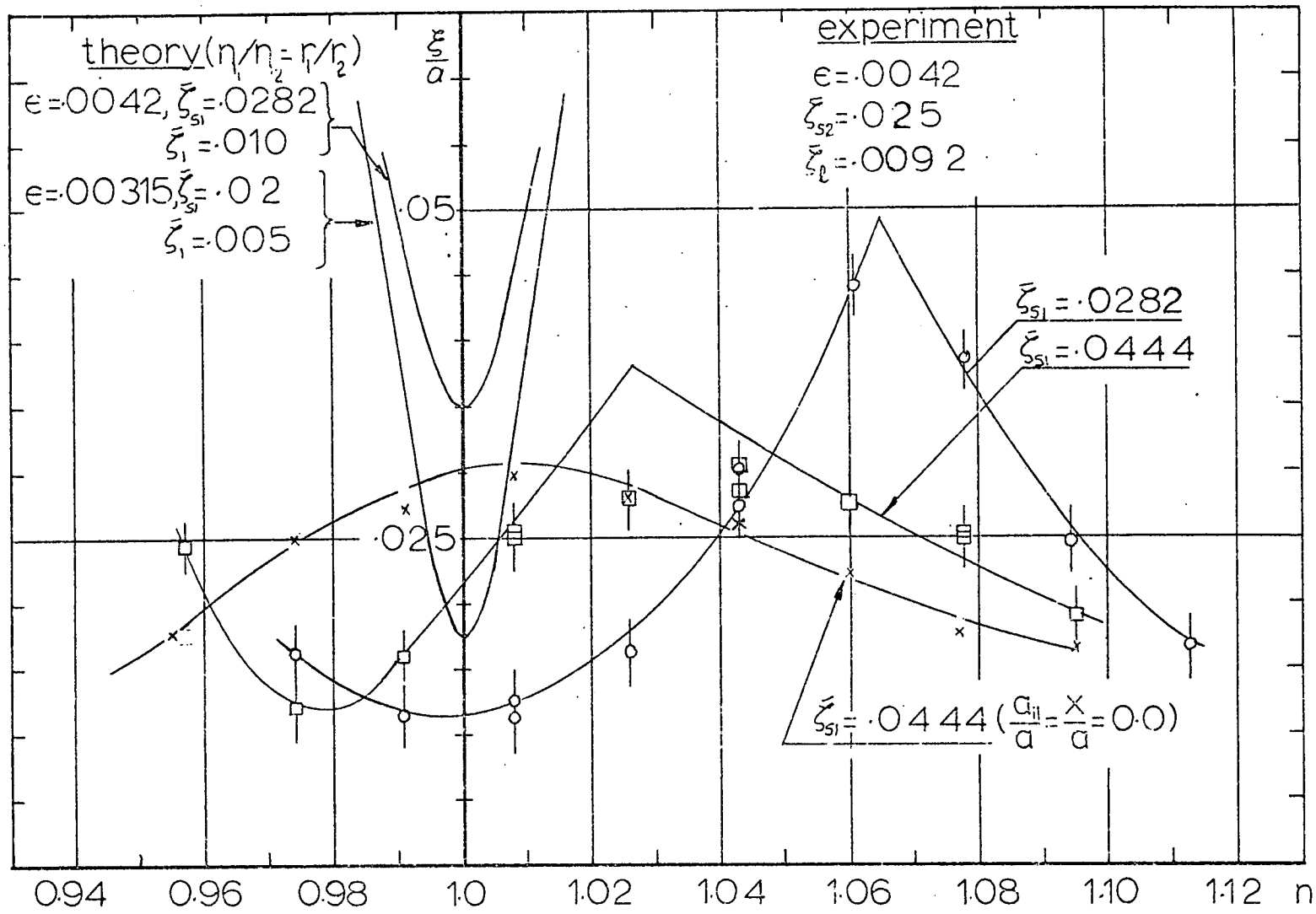


Fig(VI·31) Experimental Response of the Main Mass.

$r_3 = r_1 + r_2$, $h/a = 2·0$, $l/a = 1·05$

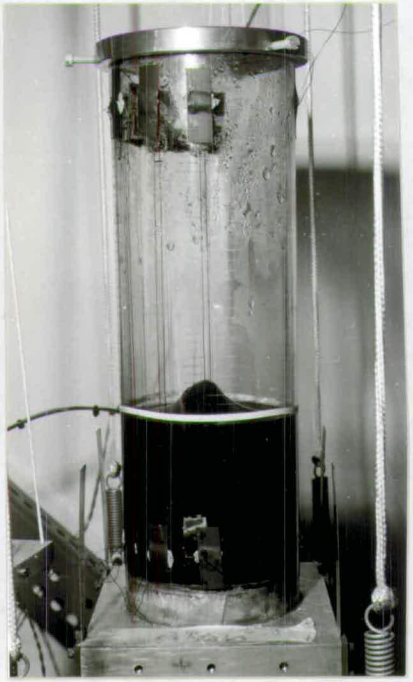

Fig(VI.32) Zeroth Sloshing Mode Formation Under a) One Internal Resonance Condition $r_3 = 2r_{01}$

b) Two Internal Resonance Conditions $r_3 = r_{01}$ , $r_3 = r_1 - r_2$

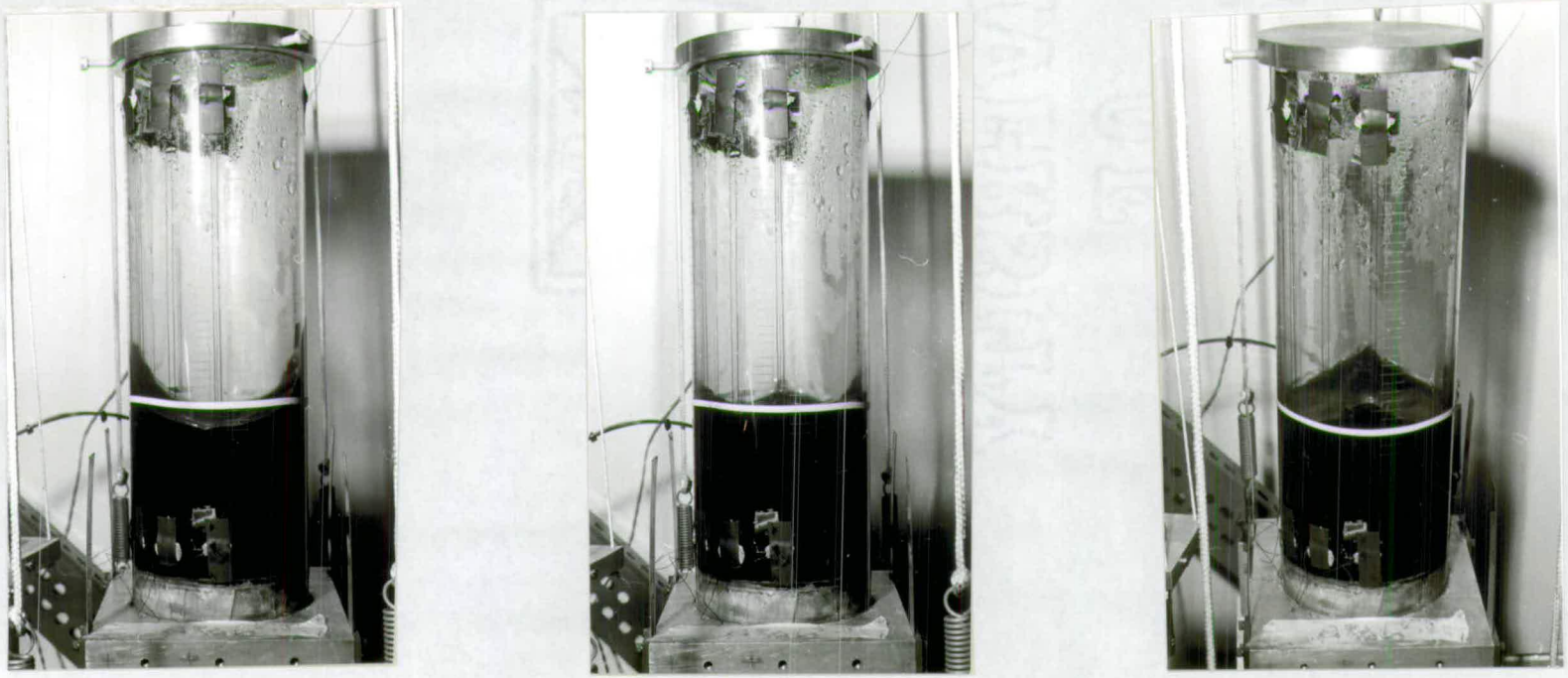

Fig(VI.33) Formation of the 2nd Symmetric Sloshing Mode Under a) One Internal Resonance Condition $r_3 = 2r_{21}$

b) Two Internal Resonance Conditions:

$$r_3 = r_{21} \quad , \quad r_3 = r_{1-2}$$

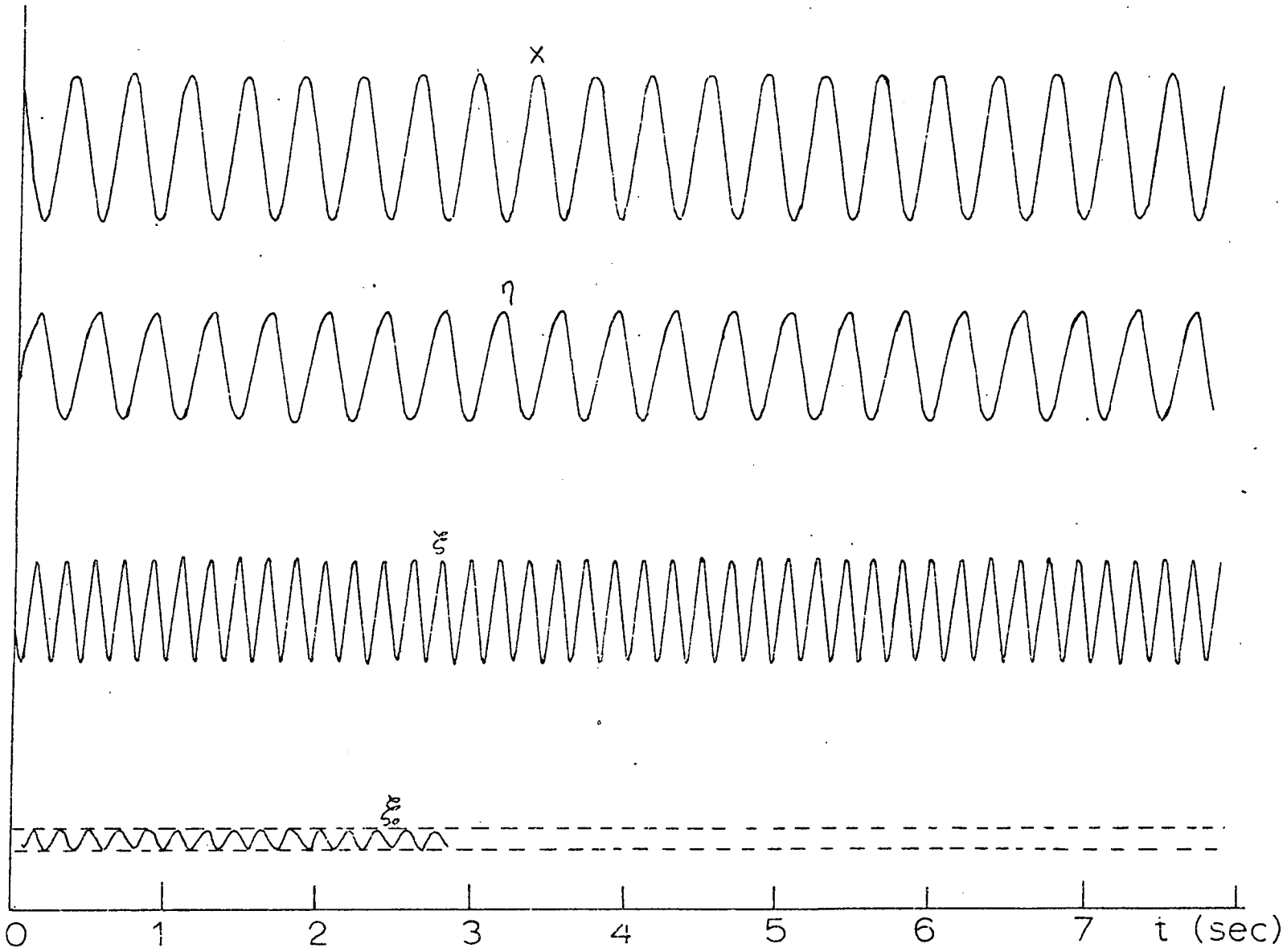


Fig(VI-34) Steady State Time History Under Principal Internal Resonance $r_3 = 2r_2$

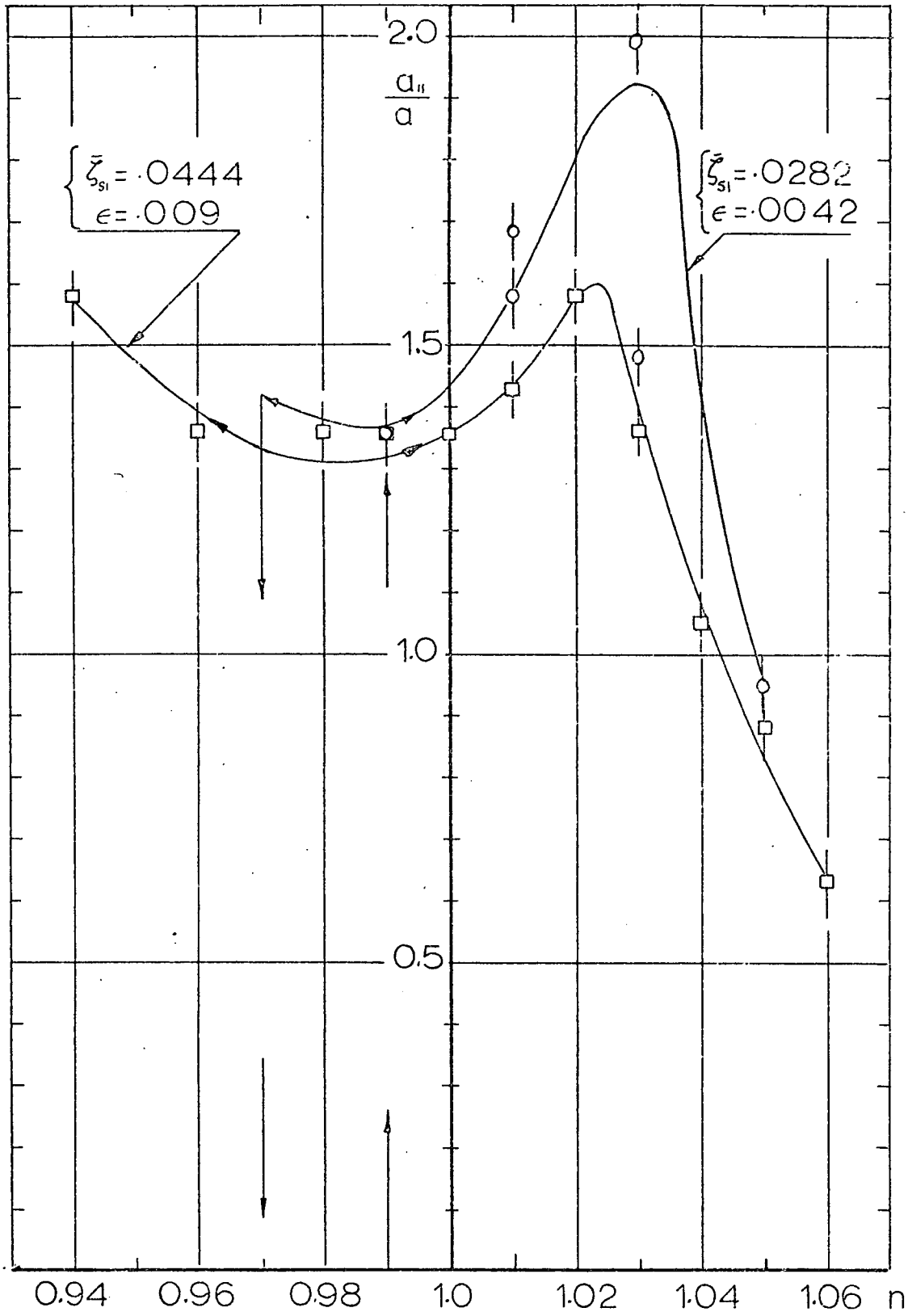


Fig(VI·35) Experimental Response of the Liquid Free Surface, $r_3 = 2r_2$ , $h/a = 2.0$, $l/a = 2.23$ $\bar{\zeta}_{s2} = ·005$, $\bar{\zeta}_{\ell} = ·0092$

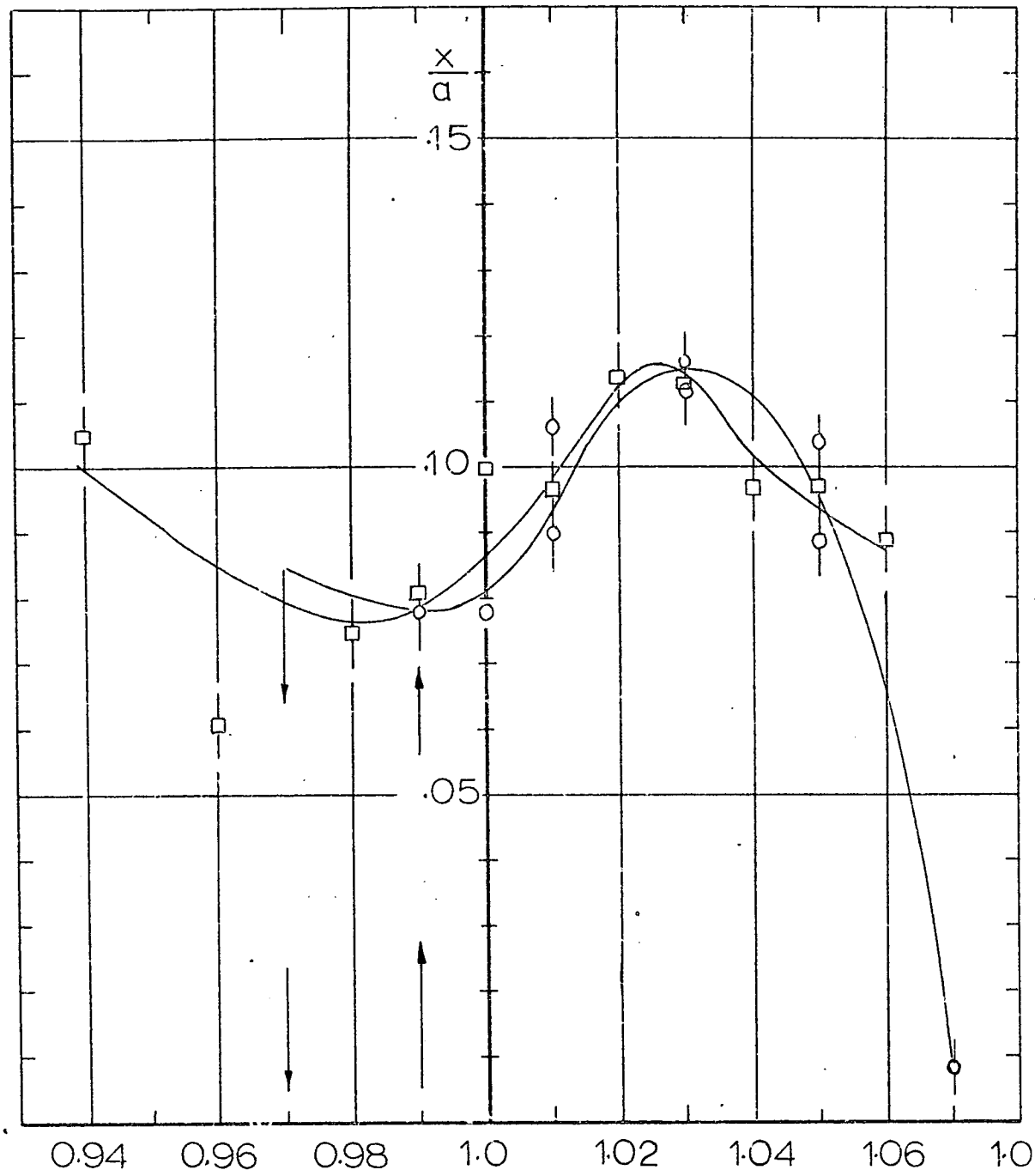


Fig(VI·36) Experimental Response of the Upper Structure, $r_3 = 2\, r_2$ , Conditions as fig(VI·35).

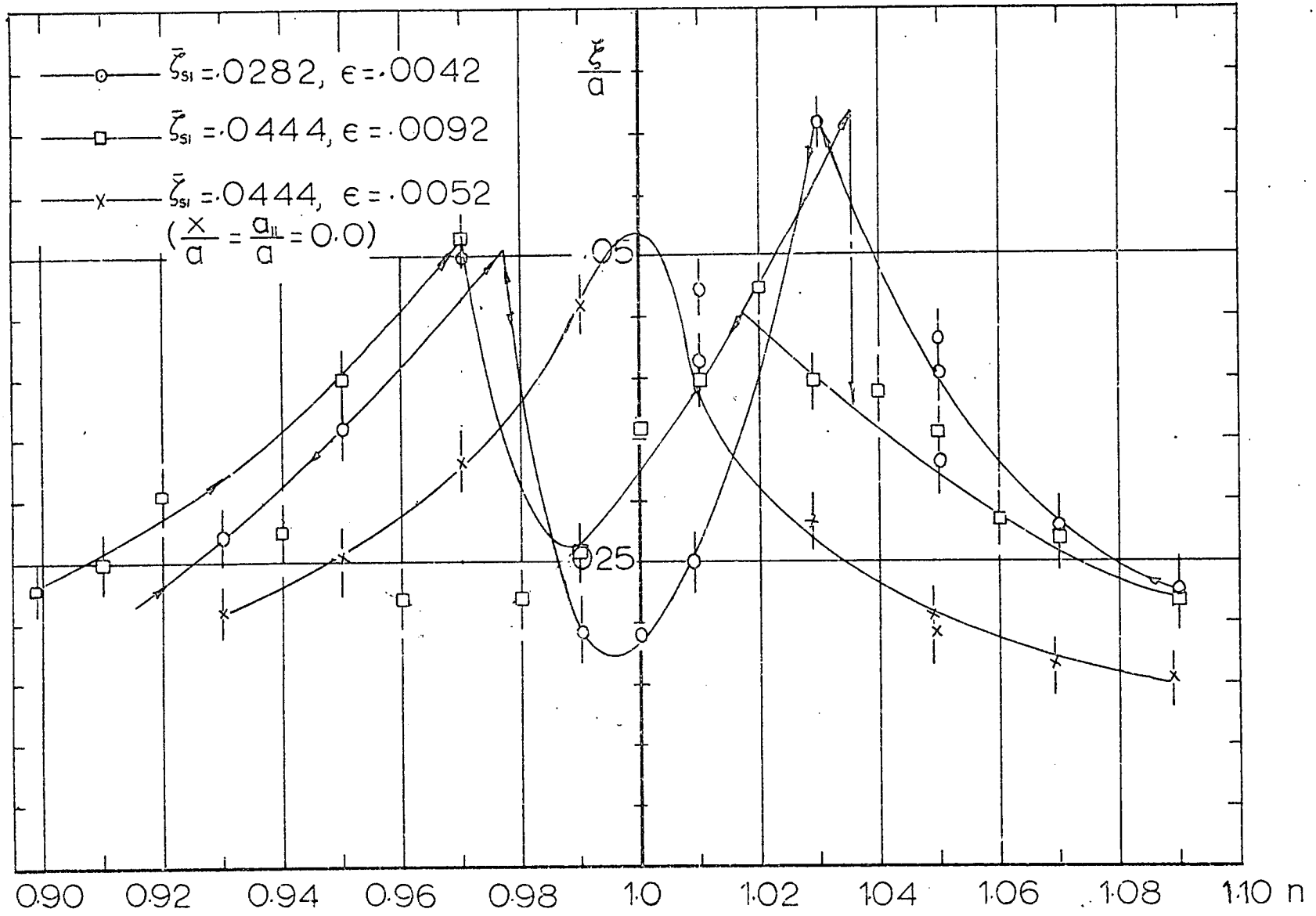


Fig(VI.37) Experimental Response of the Main Mass, $\underline{r_3 = 2r_2}$
$h/a = 2.0$, $l/a = 2.23$, $\bar{\zeta}_{s2} = \cdot005$, $\bar{\zeta}_{\ell} = \cdot0092$

Comparison with the Theory

The experimental results given in this section represent the response of the system in its generalised co-ordinates, however, the theoretical results of chapter (IV) were given in terms of the normal modes. It is necessary to transform these results into generalised modes (by using the transformation matrix IV.19) in order to make a direct comparison between the two methods.

Figs. (VI.22-24) compare in a dimensionless form the theoretical response of the system and the experimental one for the summed type internal resonance $r_3 = r_1 + r_2$, with $h/a = 2.0$ and $\ell/a = 2.1$. Because the damping ratios in the normal mode configuration are difficult to transform into the corresponding values in the generalised modes, both the excitation amplitude and the damping ratios of the theoretical curves were chosen within the practical range. While the theory agrees with the experiment in predicting the dangerous regions of autoparametric instability, there is poor agreement between the amplitude response curves. Moreover, the theoretical curves are bounded within a narrow frequency band. The response of the main mass in Fig. (VI.22) has the same features in both approaches. Unlike the theoretical response curves, shown in section (IV.3) which reveal two kinds of instability on both sides of n=1, the experimental results possess only the characteristics of a nonlinear soft system with two kinds of instability on the left side of n=1.

Figs. (VI.29-31) give also a comparison between the theoretical and experimental results for the difference type internal resonance $r_3 = r_1 - r_2$ with $h/a = 2$ and $\ell/a = 1.05$. Theoretical response curves show higher values than the experimental ones. The experimental regions of instability occur on the left side of n=1.

In the principal internal resonance condition $r_3 = 2r_2$ the theoretical results were so much higher than the experimental ones that their locations lie out of the range of the diagrams of Figs. (VI.35-37).

The discrepancies between theory and experiment can be attributed to the following factors;

i) The transformation into normal modes does not include the damping of the system before transformation, However an assumed diagonal damping matrix has been inserted. Both theory and experiment show that the damping plays a great role in defining the characteristic of the system.

ii) The theoretical results were derived from the analytical solution which assumes the condition $\eta_1/\eta_2 = r_1/r_2$. This condition is a special case. A preliminary free test was conducted on the top structure with its liquid and after transformation of the responses into the normal modes, This showed that the condition $\eta_1/\eta_2 = r_1/r_2$ did not hold.

iii) The theoretical solutions were derived up to the first order in $\epsilon$ which contains only quadratic terms and it is the third order terms which define accurately the characteristics of the system as indicated in Chapter (III).

iv) As a result of the lateral forces created by the liquid sloshing and the lateral structure motions, the damping of the air bearing is subjected to continuous change.

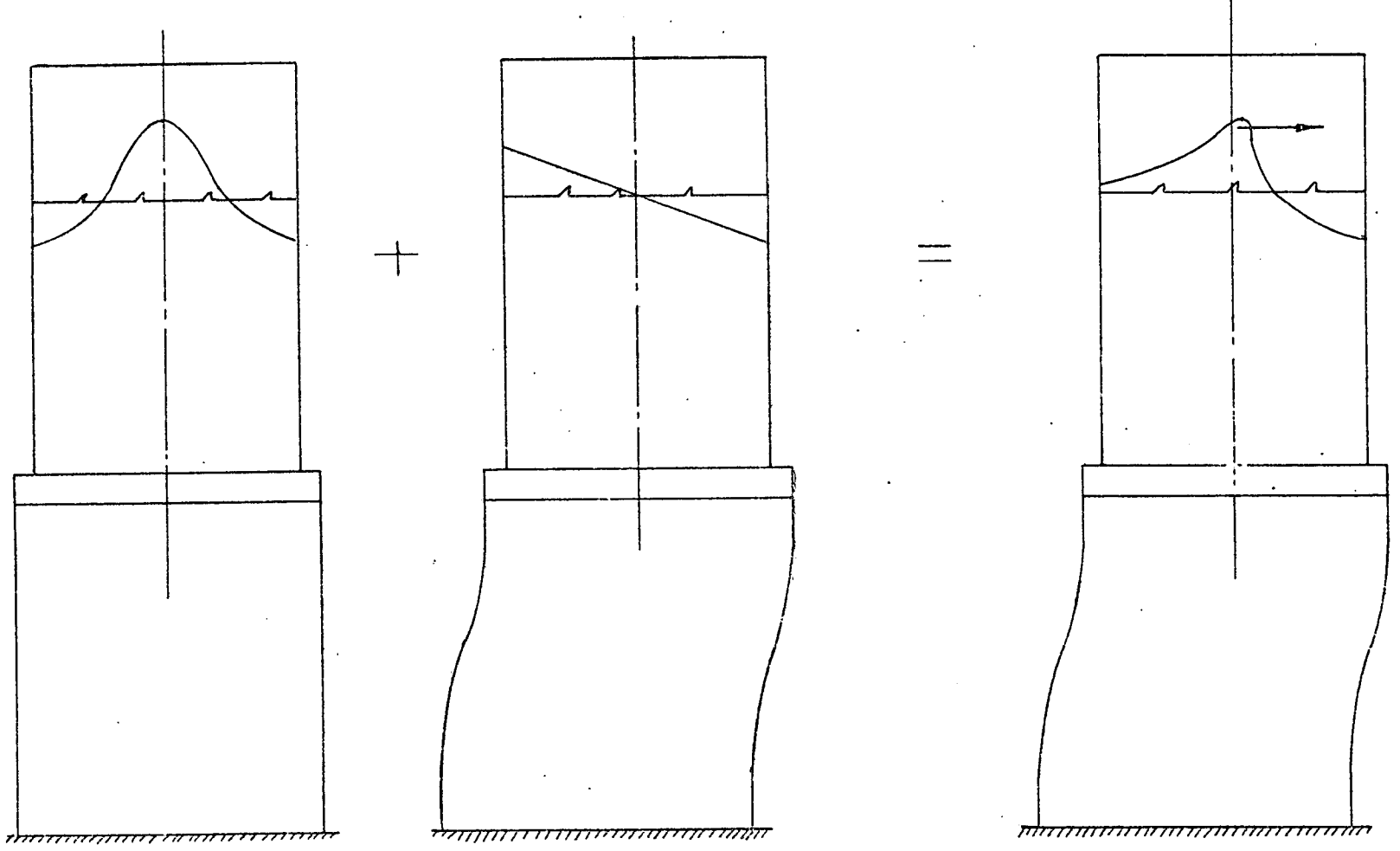


Fig(VI-39) Mode Shape of Vibrating Structure Containing a Liquid under the Resonance Conditions: $r_3 = r_1 + r_2 = r_{01}$

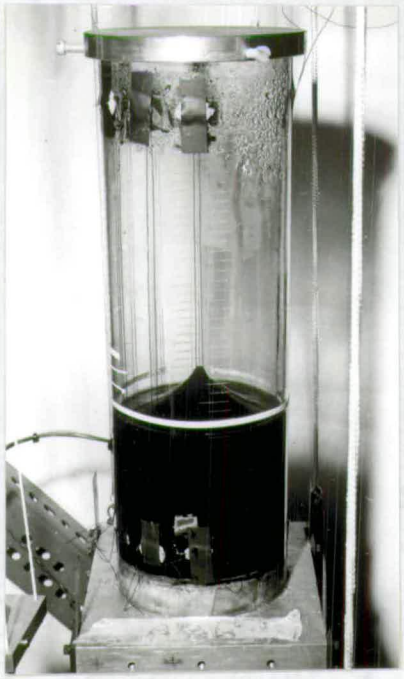

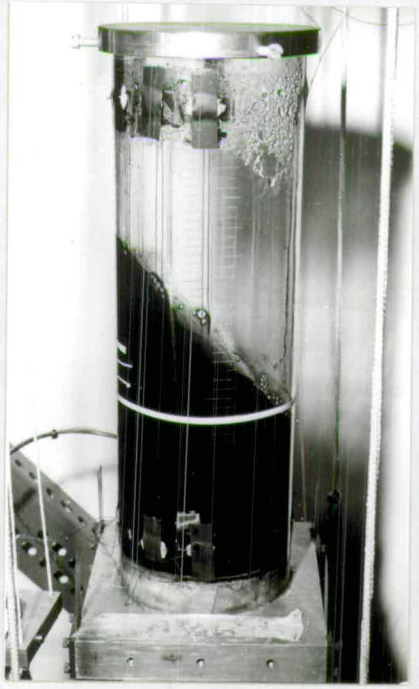

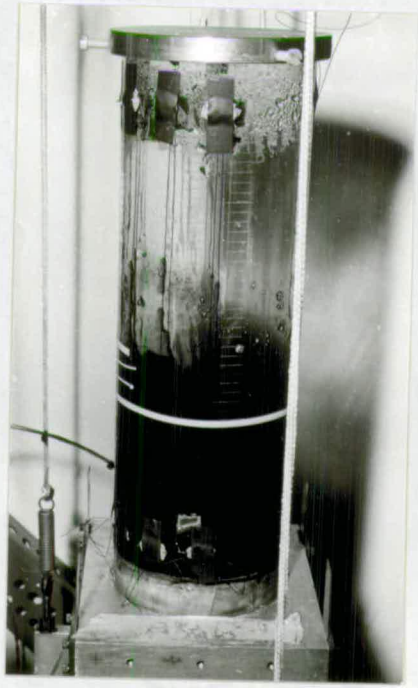

Fig(VI.39) Development of Instability Under Two Internal Resonance Conditions : $r_3 = r_1 + r_2$ , $r_3 = r_{01}$

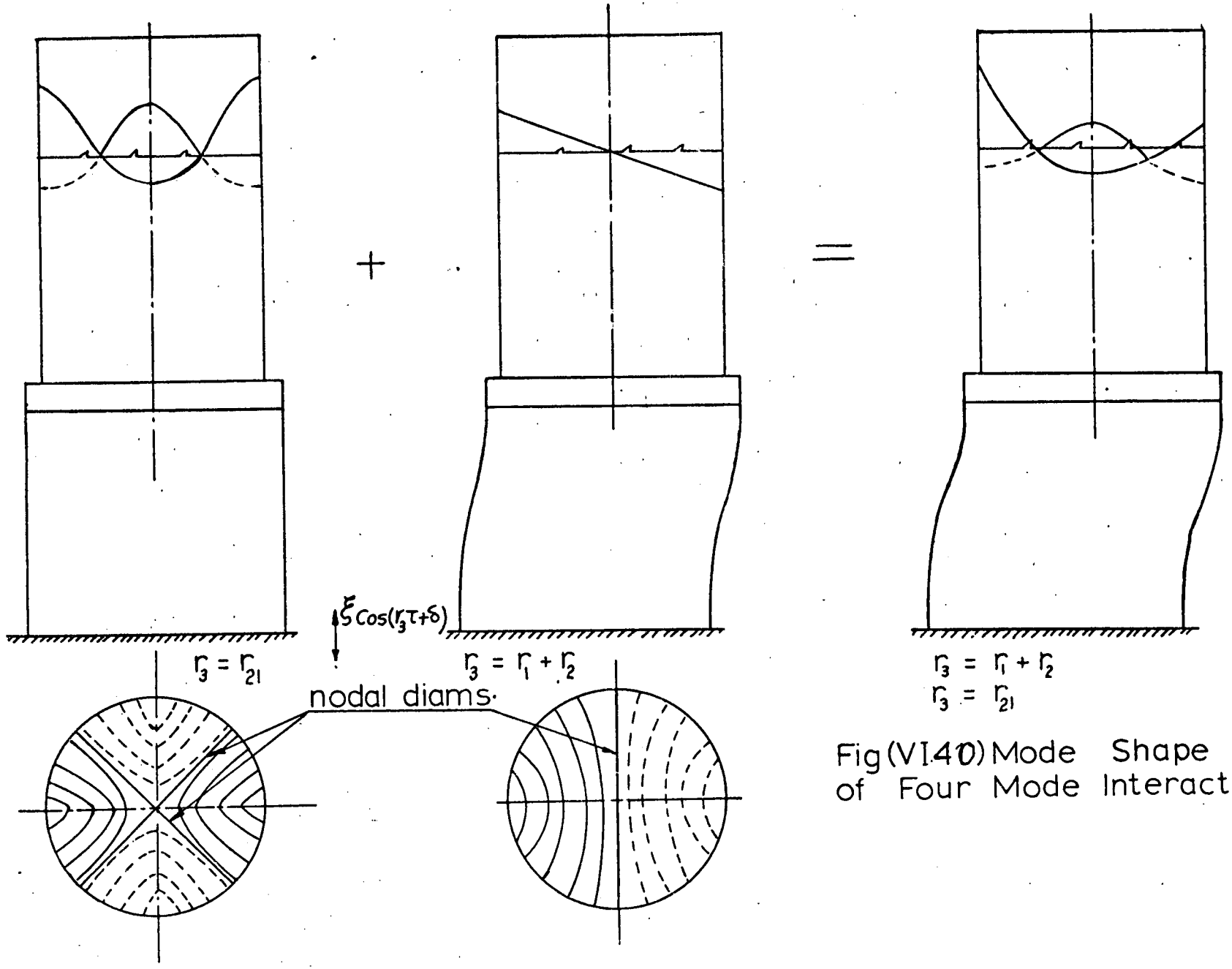


Fig (VI.40) Mode Shape of Four Mode Interaction

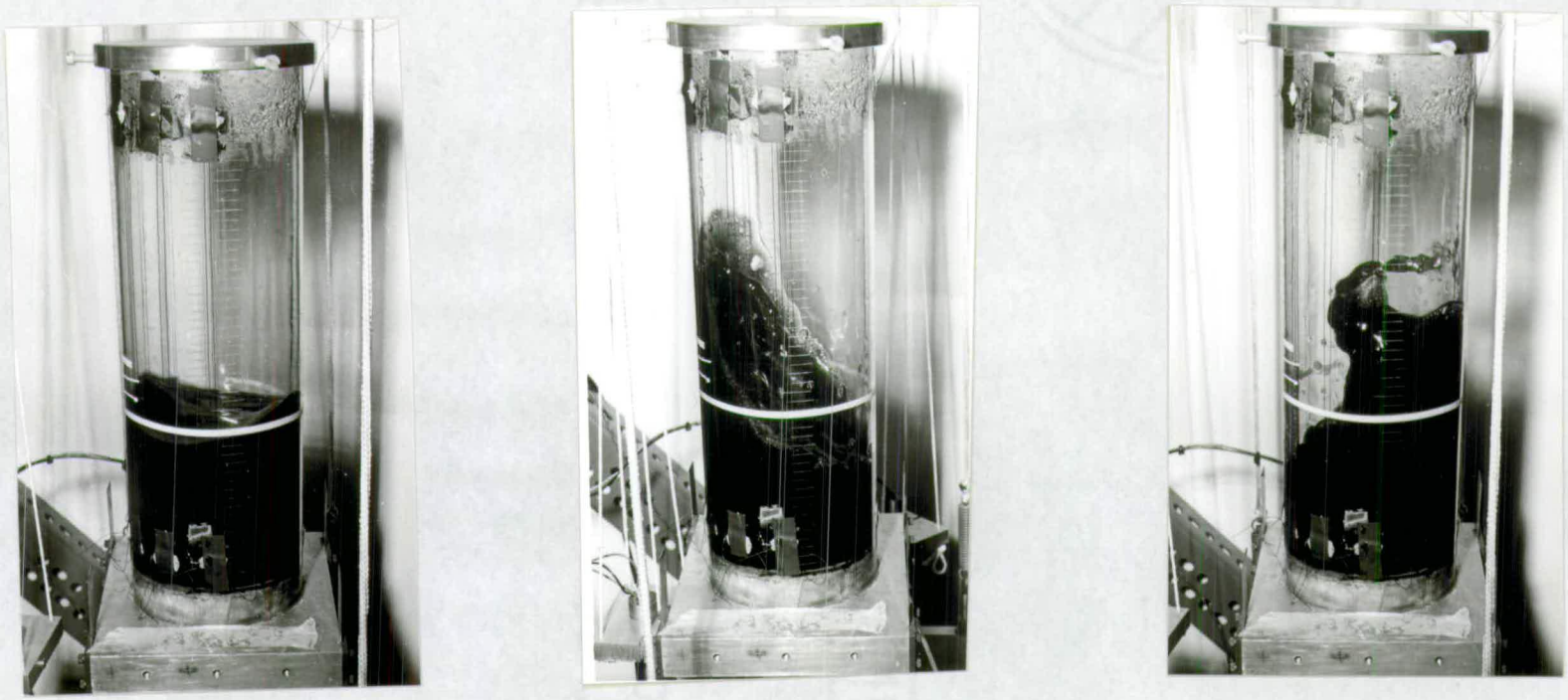

Fig(VI.41) Development of Instability Under Two Inernal Resonance Conditions: $r_3=r_1+r_2$ , $r_3=r_{21}$

VI.4.4 Response of the Two Liquid Sloshing Modes Coupled with the Structure Modes

a) Conditions of Summed Internal Resonance

i) $r_3 = r_1 + r_2$
$= r_{01}$
$= n\nu$

ii) $r_3 = r_1 + r_2$
$= r_{21}$
$= n\nu$

Experimental observations showed that when the apparatus is excited in the neighbourhood of the above relations vibrations of the structure and liquid free surface started to appear simultaneously with a continuous increase in their amplitudes. This growth could lead to structural failure if the vibrator were not stopped. The amplitudes were very large and showed no regular mode shapes.

In the earlier period of excitation, according to the first resonance relations (i) a central spike of the liquid free surface together with the first antisymmetric sloshing mode and lateral oscillations of the tank were observed simultaneously. The antisymmetric sloshing mode cause the spike to move forward and backward as shown in Fig. (VI.38). This type of interaction led to an indefinite growth of amplitudes and the development of this kind of instability is photographed as shown in Fig. (VI.39).

Regarding relations (ii), four circumferential liquid peaks with two nodal diameters were excited as well as the antisymmetric mode and the lateral structure mode. The mode shape of the resulting motion is illustrated in Fig. (VI.40). Due to the large lateral displacement of the container, the amplitudes of the modes were not maintained for a long time and a continuous increase

in the values of amplitudes led to instability of the system response. In Fig. (VI.41) a few pictures show the way in which the instability developed.

b) Conditions of Principal Resonance:

$$\text{i)} \quad r_3 = 2r_2 = r_{01} = n\nu$$

Under this type of resonance condition, experimental observations showed a steady-state response over a frequency range defined by the regions of instability. The amplitude-frequency relations of the liquid free surface amplitude at the tank wall, lateral tank displacement, and the main mass response are shown in Figs. (VI.42-44). Measurements are obtained for two excitation amplitudes ($\epsilon = .008$, and $.0116$) and two damping ratios $\bar{\zeta}_{s1} = .0282$ and $0.0444$.

The results show two regions of instability indicated by the collapse amplitudes AB (or $\acute{A}\acute{B}$) and CD (or EF). Another type of instability occurs at the collapse amplitudes on the right side of resonance is much stronger than that on the left side. The time history of the response at $\Omega/2\pi = 4.65$Hz (n = 1.045 EF) is shown in Fig. (VI.45). At that frequency the fluid free surface oscillates with a continuous increase in the amplitudes of the tank lateral oscillations and the main mass. For another few cycles the sequence is reversed. This type of energy flow appears in a form of beating until the fluid free surface oscillations and the tank lateral motion cease and the main mass response adjusts itself to that of a single degree of freedom system.

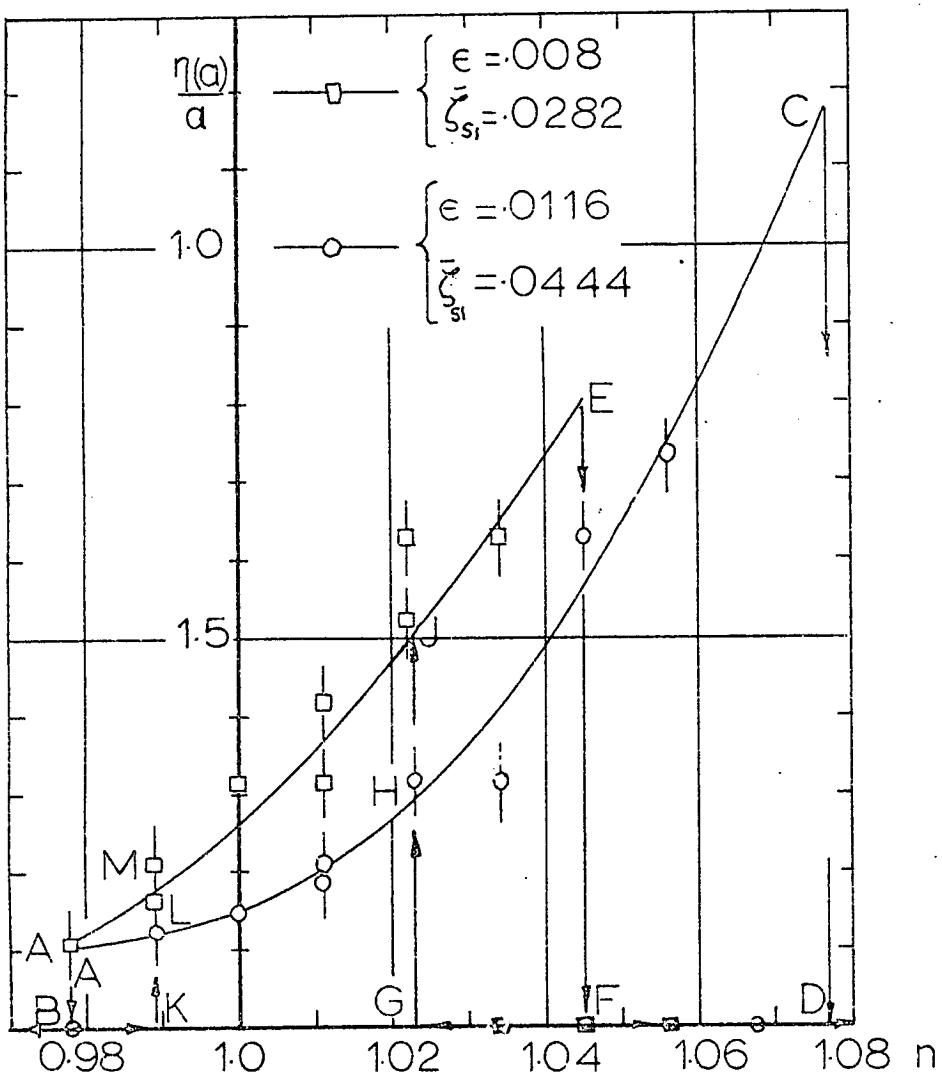


Fig(VI.42) Liquid Surface Response
$r_3 = 2\,r_2 = r_{01}$ h/a=2·0, l/a=2·35

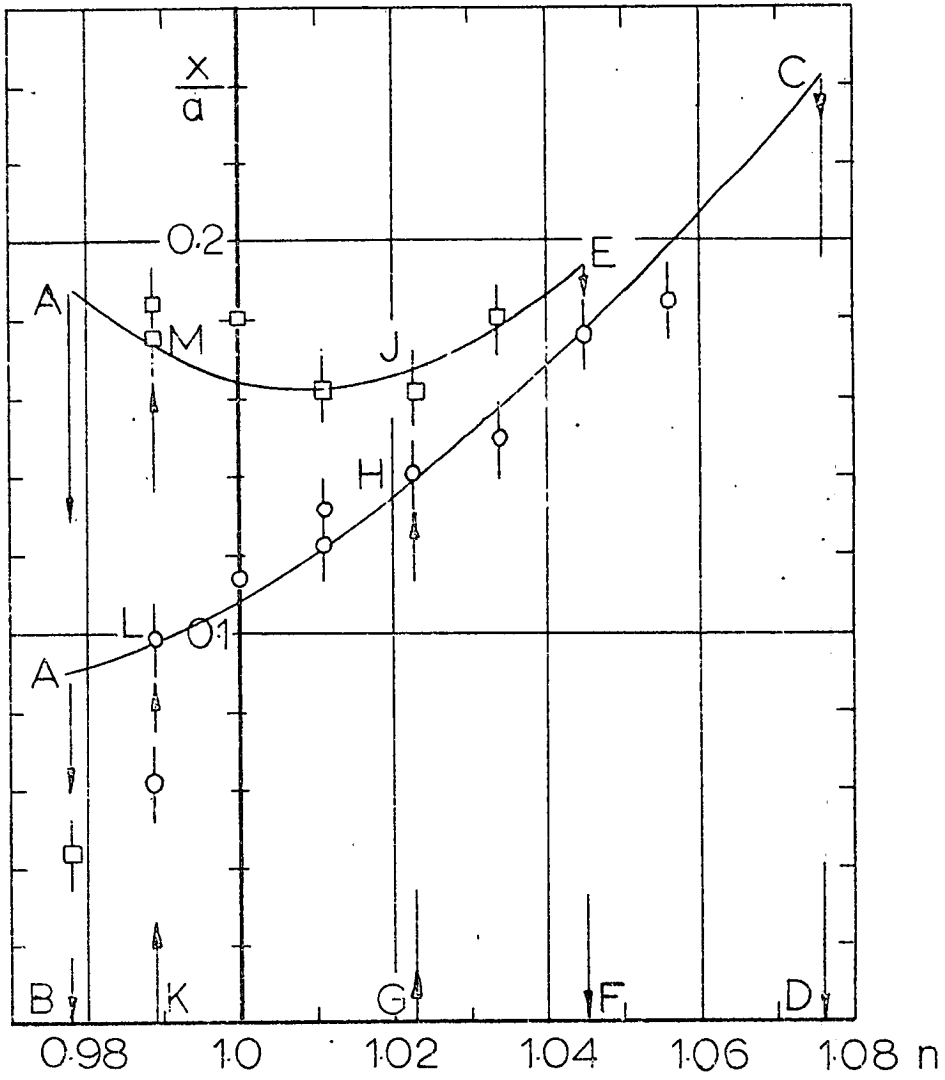


Fig(VI.43) Upper Structure Response
(conditions as in fig VI.42)

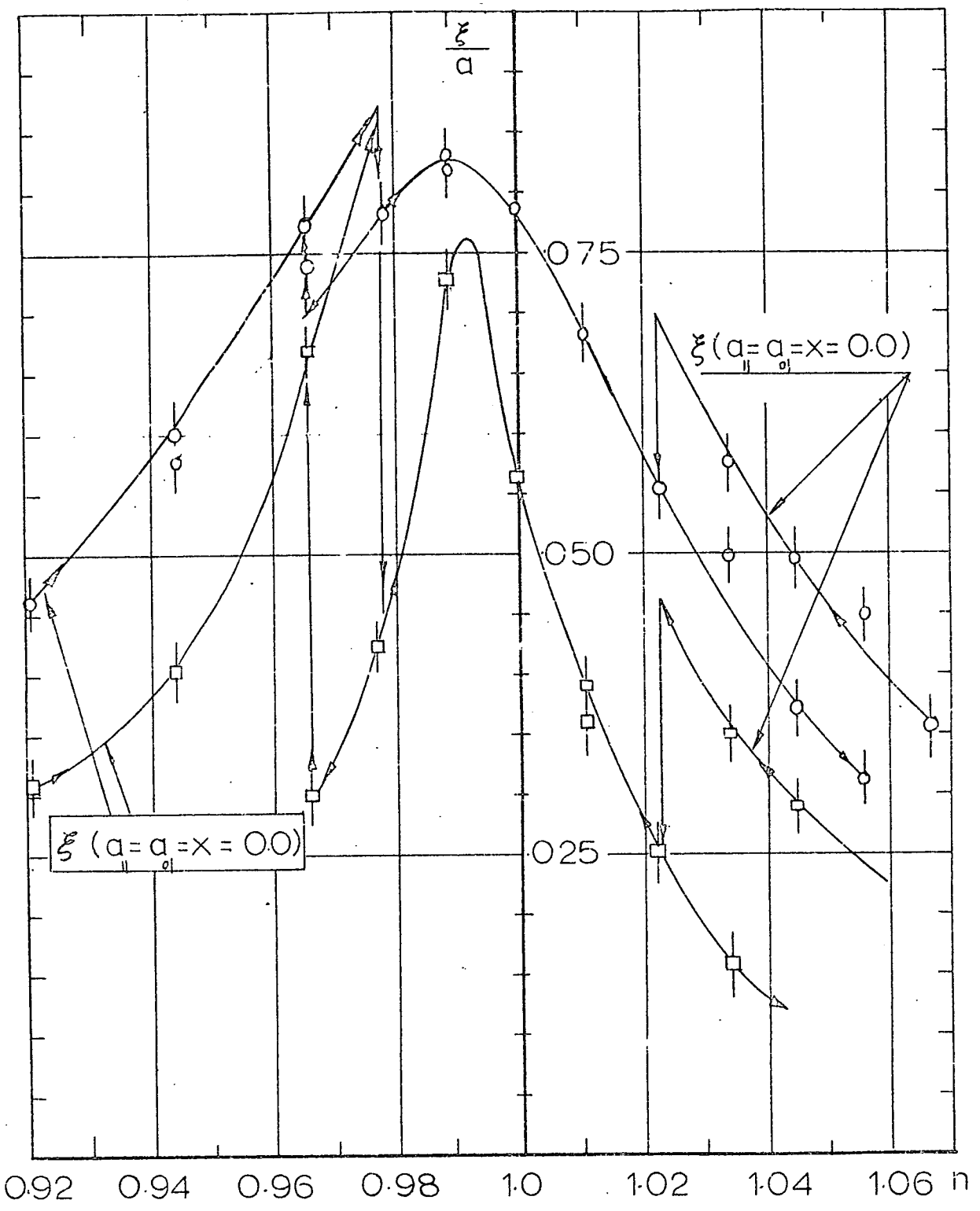


Fig(VI.44) Experimental Response of the Main Mass ——□—— $\epsilon = \cdot 008$, $\bar{\zeta}_{51} = \cdot 0282$ | $r_3 = 2\, r_2 = r_{01}$

——○—— $\epsilon = \cdot 0116$, $\bar{\zeta}_{51} = \cdot 0444$ | $h/a = 2 \cdot 0$

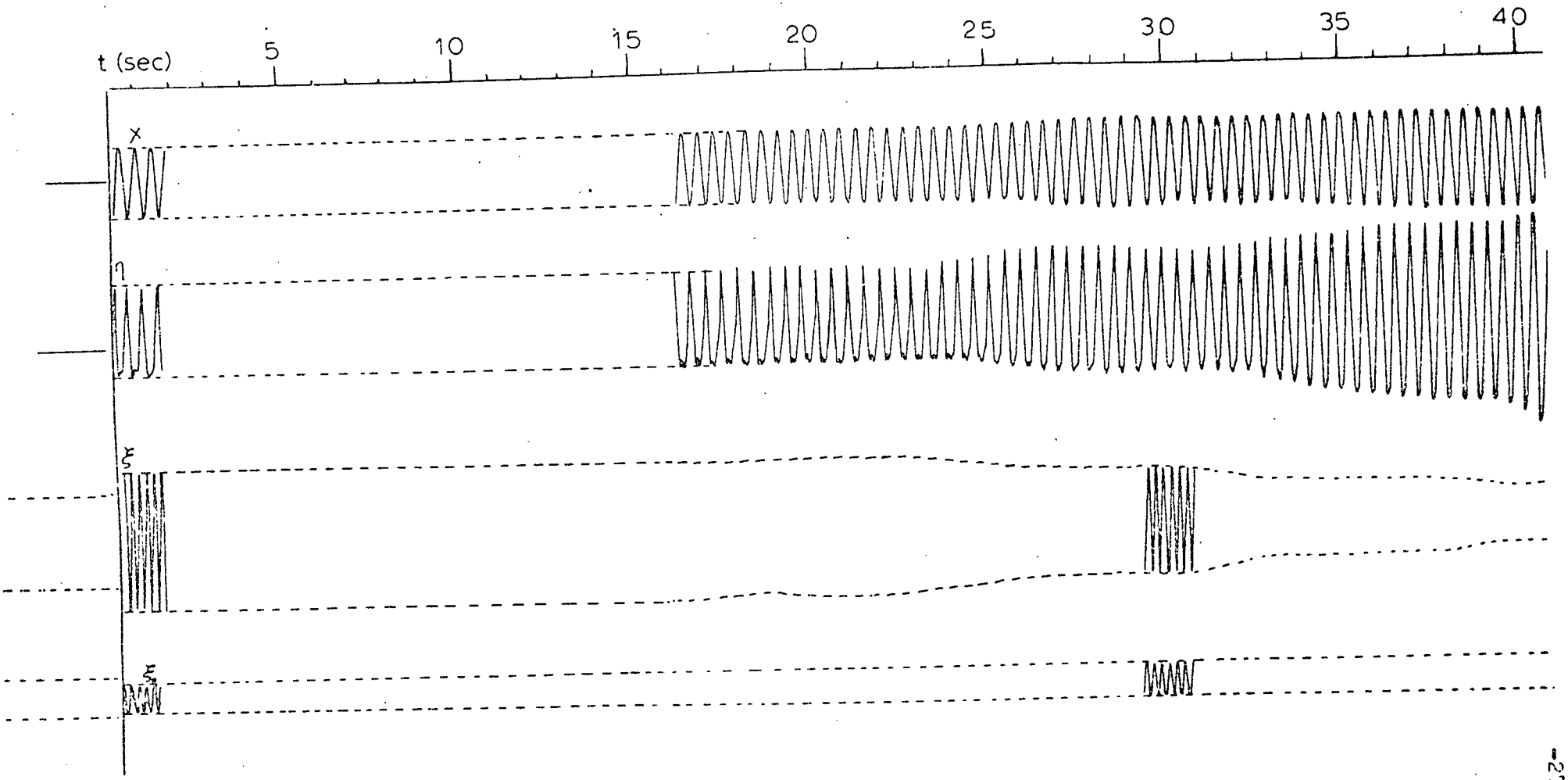


Fig(VI.45) Time History at the Collapse Frequency $\Omega/2\pi = 4.65$ Hz.

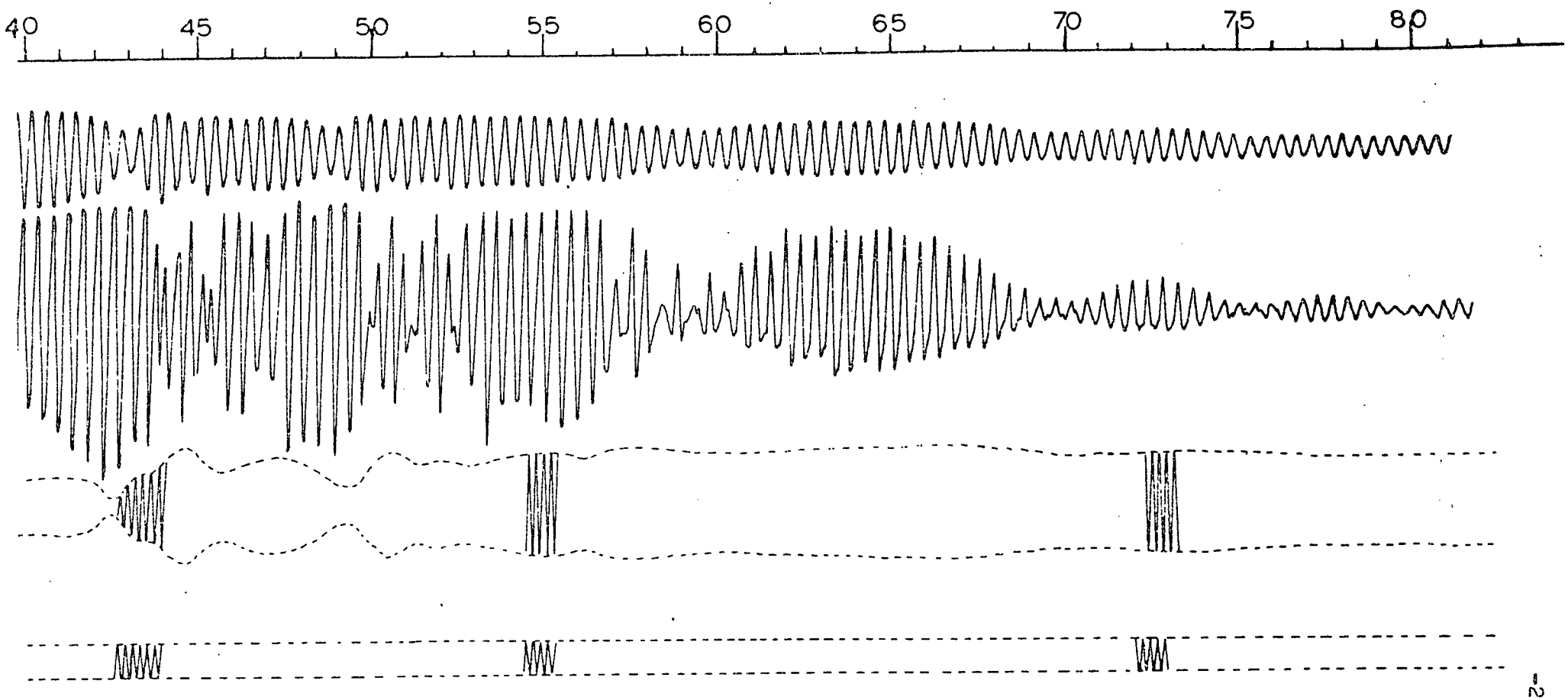


cont. of Fig(VI. 45)

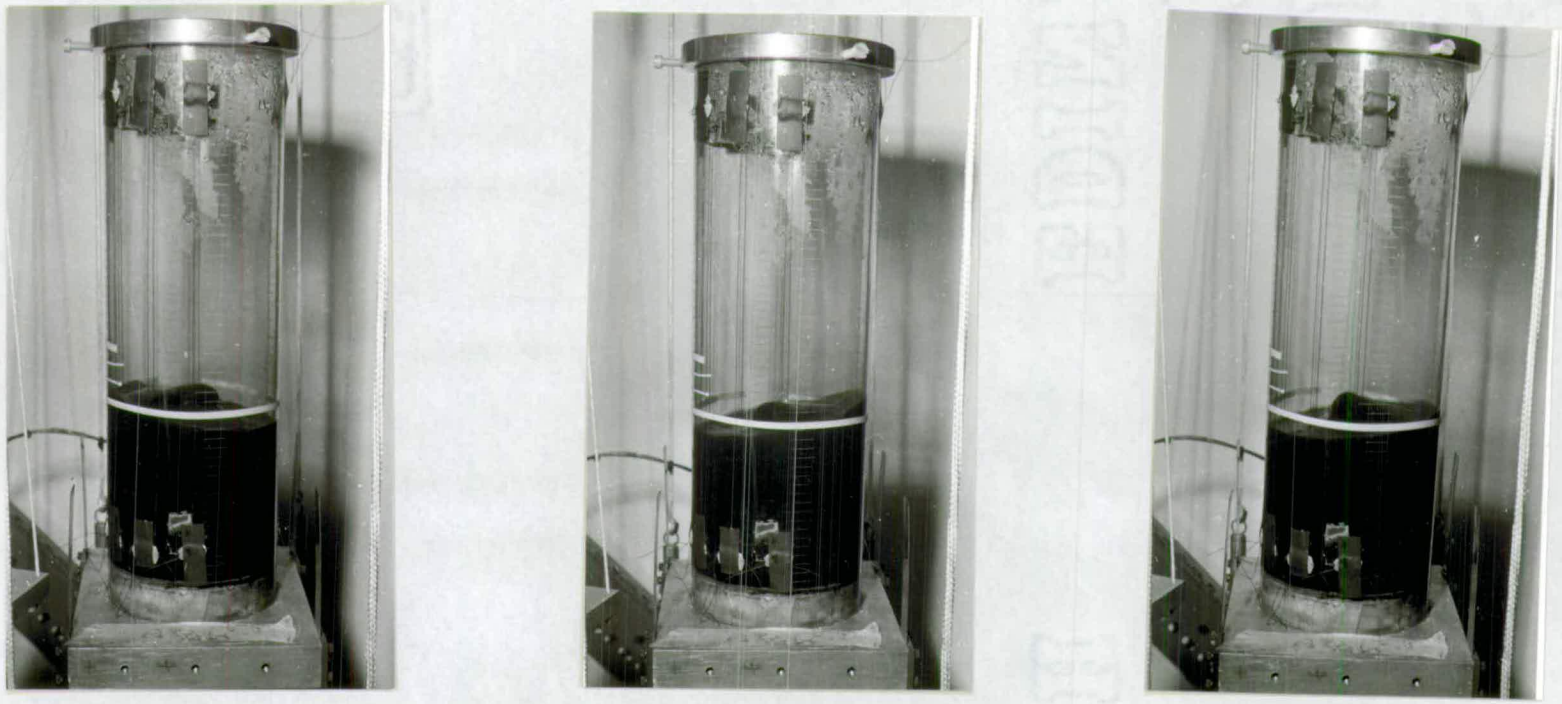

Fig(VI.46) Liquid Free Surface Mode Shapes Under Two Internal Resonance Conditions: $r_3 = 2r_2$ , $r_3 = r_{01}$

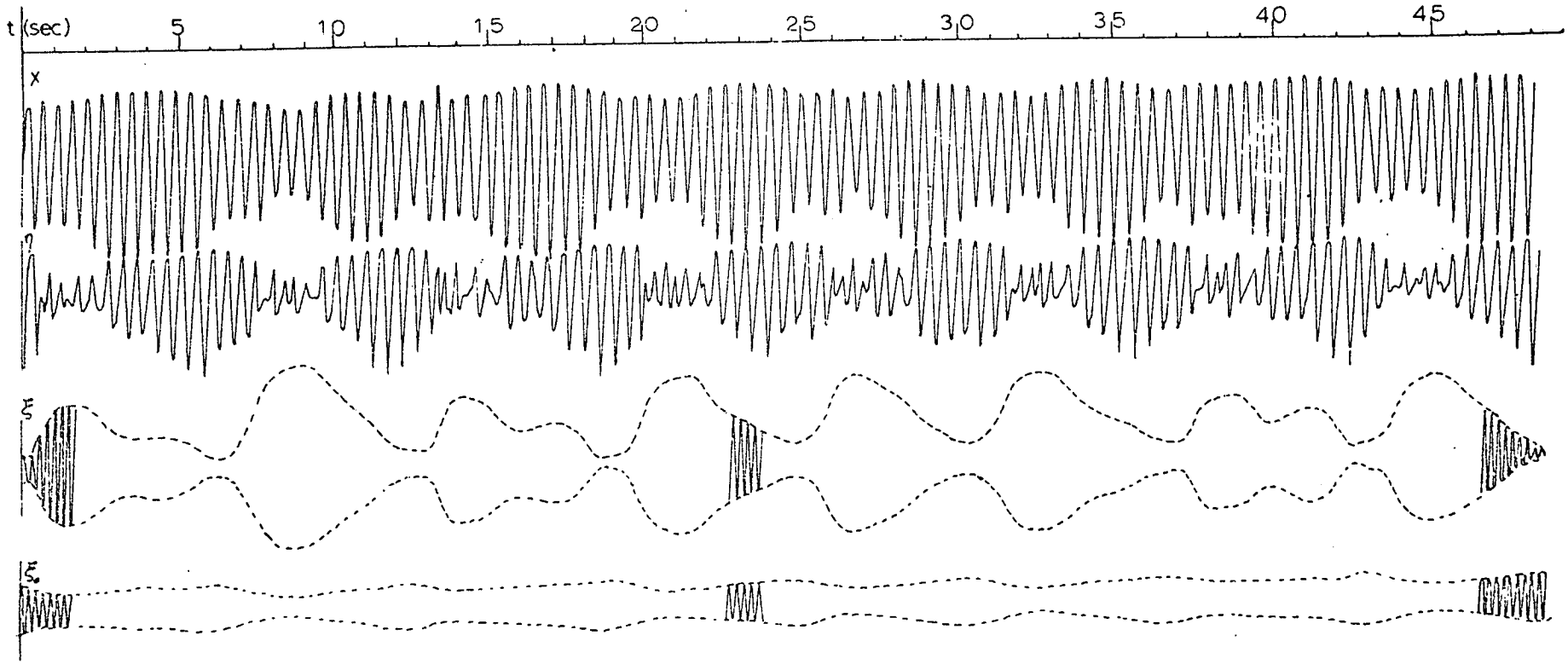


Fig(VI.47) Amplitude-Time History Under Two Simultaneous Internal Resonanse Conditions: $r_3 = 2r_2$, $r_3 = r_{21}$

The other type of instability which appears as a jump in amplitudes is formed by a weak energy flow between the fluid modes and structure modes for a few cycles. Within a few seconds the system achieves steady-state response.

The liquid amplitude response represents the resultant liquid free surface displacement at the tank wall, however it is difficult to display the two fluid amplitudes $a_{11}$ and $a_{01}$ since they are coupled.

Shown in Figs. (VI.46) are the mode shapes as photographed while the apparatus was excited

$$\text{ii)}\quad r_3 = 2r_2 = r_{21} = n\gamma$$

It is indicated in table (VI.1) that the critical resonance frequency occurs at 4Hz. However, exciting the system at that frequency does not give any response unless a small lateral disturbance is applied to the tank. The response starts first with two nodal diamaters at the free liquid surface and four peaks distributed around the tank wall at $90^{\circ}$ apart. At the same time the tank is oscillated laterally and this is associated with the first antisymmetric liquid sloshing mode. This mode disturbs the symmetric mode in such a way that the liquid free surface motion becomes unstable. The unstable fluid motion appeared as a rotation of one peak and a change in the orientation of the others. On increasing the forcing frequency a non-uniform unsteady response of a strong beating type was obtained. The liquid amplitude at the tank

wall and the upper structure responses are exchanging their energy with the main mass response as shown in the record Fig. (VI.47). The interaction is so severe that it reflects its effect on to the platform. When the frequency is further increased to 4.3 Hz the zero symmetric sloshing mode appears with a spike moving in two dimensions till the collapse amplitude occurs at $\Omega/2\pi = 4.5$Hz.

c) Conditions of Difference Internal Resonance:

$$\text{i)}\quad r_3 = r_1 - r_2 = r_{01} = n\gamma \qquad \text{ii)}\quad r_3 = r_1 - r_2 = r_{21} = n\gamma$$

The response of the system is observed to take place only between the main mass and the zero symmetric liquid sloshing mode (for condition i) or the second symmetric sloshing mode (for condition ii). The first two normal modes are not likely to be excited experimentally even with applying a strong lateral disturbance. The shape of the liquid free surface is similar to that shown in Figs. (VI.32, 33).

## VI.5.0 Remarks on the Experimental Investigations

The results and observations discussed in this Chapter exhibited important conclusions summarised in the following points:

i) The liquid free surface oscillations, inside a container supported on an elastic structure which is subjected to parametric excitation, does not contribute any influence on the structure vertical response as long as the container is constrained from lateral motion. This means that the liquid forces in the vertical direction are secondary effects.

ii) It is the horizontal component of the liquid sloshing forces which has a significant effect when the structure is free to oscillate horizontally. The structure - liquid interaction has a feed back influence on the vertical motion of the structure. This auto-parametric coupling occurs when one of the autoparametric resonance conditions is met.

iii) The liquid free surface and the structure modes do not exhibit an ordinary steady-state response when the autoparametric resonance conditions are of the summed or difference type, i.e. when $r_3 = r_1 \pm r_2$.

iv) For more than one liquid sloshing mode, the system does not achieve either a steady-state or a stable response in most cases.

v) Observations showed that the system in general possesses two limit cycles while it is excited parametrically. If an external disturbance whose magnitude is less than a critical value is applied the system returns to its original state. If the disturbance exceeds that critical value the system achieves either a beating response of maximum constant amplitude or a steady-state response.

vi) Due to the well known phenomenon of the liquid swirling motion near the sloshing frequency of the antisymmetric mode, the system shows instability when $\Omega \geqslant 2\omega_{11}$.

# CHAPTER (VII)

## CONCLUSIONS

The interaction of the structure vibrating modes with the liquid sloshing modes under parametric harmonic excitation has been investigated theoretically and experimentally for a limited number of modes. A general mathematical model, involving two structural modes and an infinite number of liquid sloshing modes, has been formulated such that the problem can be examined for any number of modes with the required degree of nonlinearity. The interaction has been studied when the system is taken to possess two, three and four degrees of freedom. In each case there were a certain number of nonlinear internal resonance conditions which could hold, depending on the degree of nonlinearity and the number of modes involved.

In the case when the liquid container is constrained so that it can only perform vertical motion, the second order nonlinear analysis fails to predict the behaviour of the system when the internal resonance is half subharmonic $\omega_{s1} = 2\omega_{11}$. It is the third order terms which determine the response of the system as confirmed by the experiments. Coupling between one structure mode and the first antisymmetric liquid sloshing mode is very weak because the vertical liquid sloshing forces are very small and vanish as the liquid depth ratio h/a exceeds 0.5. The liquid behaviour would be governed by Mathieu's equation if the structure amplitude and frequency were taken as the forcing parameters.

The other two cases, when the system possesses three or four degrees of freedom, have been studied by considering only quadratic terms in $\epsilon$. In these cases the lateral sloshing forces are

significant and the analysis was carried out in terms of normal modes. A number of nonlinear resonance conditions such as $r_3 = r_1 \pm r_2$, $r_3 = 2r_1$, $r_3 = 2r_2$, $r_3 = r_{01} = r_1 \pm r_2$, $r_3 = r_{21} = r_1 \pm r_2$,... etc. were found. The theoretical analysis is satisfactory for determining the dangerous regions of instability, however it is not adequate to determine the response of the system as can be seen from comparison between the theoretical and experimental results. Moreover, the theory and the experiments show that there is suppression in the response of the main mass near resonance, and the system does not achieve a steady state response under the conditions $r_3 = r_1 \pm r_2$. Experimental investigations have shown that both the liquid free surface and the upper structure responses follow the behaviour of a nonlinear soft system.

Considerations of more sloshing modes lead to a rather complex response. Both the liquid free surface and the upper structure responses are unstable. The first antisymmetric mode and the zeroth (or second) symmetric sloshing modes are excited simultaneously with the amplitudes increasing up to a level which could lead to a catastrophe in the system if the excitation were allowed to continue.

The theoretical analysis would be more refined if the third order terms in $\epsilon^2$ and a proper transformation into normal modes, including the damping terms, were considered. It seems that if higher order terms were included in the analysis other resonance conditions may be obtained such as $r_3 = r_1 \pm r_2 + r_{01}$, $r_3 = r_1 \pm r_2 + r_{21}$, $r_3 = r_{21} + r_{01} + r_1$,...etc. It also appears that these conditions would be difficult to observe experimentally as they could not be isolated from the adjacent modes.

Autoparametric interaction between the modes in a vibrating system deserves more investigations. For the example the case could be studied when systems are subjected to random excitations or combinations of different harmonics. The question of stability still needs more investigation under a wide range of autoparametric resonance conditions.

"Until Here God Helped Me"

"Amen, Come My Lord Jesus"

## PRINCIPAL NOTATION

| | |
|---|---|
| $A_{11}$ | Nondimensional liquid wave height parameter |
| $a_m$ | Maximum liquid surface wave height of the mth mode (eq. I.7) |
| a | Tank inside radius |
| $a_n$, $b_n$, $d_n$, $u_n$, $v_n$ | perturbed solutions of the nth order |
| $b_i$ | amplitude parameter of the ith mode |
| C | damping coefficient |
| C(t) | arbitrary function of time |
| D | dissipation function (eq. II.18) |
| E | Young's Modulus |
| F | Excitation amplitude parameter |
| $F_n$ | coefficients of the Dini Series |
| $F_x$ | liquid sloshing force in x direction |
| f | time function in equation (I.11) |
| g | gravitational acceleration |
| H | function of nonlinear terms in equation (eq. II.34) |
| h | expansion parameter of Fourier-Bessel Series (eq. II.35, 36) |
| h | liquid depth inside the tank |
| J | Area moment of inertia |
| $J_m(\ )$ | Bessel series of the 1st kind of the order m |
| K | Elastic stiffness |
| L | the Lagrangian |
| $\ell$ | total length of the leaf spring (or the beam) |
| $M_o$ | the mass of the first structure in the system of Fig. (II.1 ) |

| | |
|---|---|
| $m_\ell$ | total mass of the liquid inside the tank |
| $m_{t\ell}$ | total mass of the top structure with its liquid |
| OXYZ | moving Cartesian co-ordinates |
| $O' X' Y' Z'$ | inertial Cartesian co-ordinates |
| $P_m$, $q_m$ | characteristic numbers of Mathieu's equation (I.7) for the mth mode |
| P | hydrodynamic pressure |
| $P_i$ | Normal modes |
| $P_1^*$ | Euler buckling load of the first mode |
| $Q_i$ | generalised forces |
| q | liquid velocity |
| $q_{rel}$ | relative velocity of the liquid particle w.r.t. the moving co-ordinates |
| $q_i$ | generalised co-ordinates |
| $r_i$ | normal mode frequencies |
| r | frequency parameter |
| r,θ,Z | cylindrical co-ordinates |
| S | function of nonlinear terms in equation (II.31) |
| $S_m$ | expansion parameter of Fourier-Bessel series equation (II.32, 33) |
| $S_i$ | frequency ratio parameter $(r_i / r_3)$ |
| T | non-dimensional time parameter |
| T | kinetic energy |
| t | time |
| V | potential energy |
| $V_o$ | tank velocity |
| $X_d$ | lateral displacement of the main mass |

| | |
|---|---|
| $X_o$, $Z_o$ | horizontal and vertical acceleration components of the tank |
| $X_o$ | excitation amplitude in Mathieu's equation |
| $\alpha_{mn}$ | generalised co-ordinates of the liquid velocity potential function of the mode mn |
| $\delta_o$ | the excitation amplitude (eq. I.3) |
| $\delta$ | the Croneker |
| $\eta_i$ | damping parameter |
| $\eta(r,\theta)$ | free surface wave height at a point r,θ on the liquid free surface |
| $\bar{\zeta}$ | damping ratio |
| $\sigma$ | non-dimensional forcing frequency parameter |
| $\xi_{mn}$ | zeros of the first derivative of the Bessel function of the first kind $J'_m(\xi_{mn}) = 0$ |
| $\xi$ | vertical displacement of the main mass |
| $\xi_o$ | vertical excitation amplitude |
| $\lambda_{mn}$ | $\xi_{mn}/a$ |
| $\lambda$ | wavenumber (eq. I.8) |
| $\Phi$ | velocity potential function |
| $\Psi_i$ | phase parameter |
| $\Psi_1(f)$, $\Psi_2(f,f',f'')$ | nonlinear functions in equation (I.11) |
| $\varphi,\theta,\gamma,\alpha,\delta$ | phases of the fundamental harmonic solution |
| $\gamma$ | detuning parameter |
| $\nu$ | kinematic viscosity (eq. I.8) |
| $\mu$ | excitation parameter (eq. I.11) |
| $\mu_1,\mu_2,\mu_3$ | mass ratios |
| $\rho$ | liquid density |

| | |
|---|---|
| $\acute{\Delta}$ | the vertical drop of the tank due to its lateral displacement |
| $\tau$ | non-dimensional time parameter (IV.8) |
| $\epsilon$ | perturbation parameter |
| $\omega$ | natural frequency |
| $\Omega$ | excitation frequency |

Subscripts

| | |
|---|---|
| s1 | first structure |
| s2 | upper structure |
| 11 | first antisymmetric liquid sloshing mode |
| $\ell$ | liquid |

## BIBLIOGRAPHY

A1) ABRAMSON, H.N., "Amazing Motions of Liquid Propellents" Astronautics, Vol. 6 March 1961, pp.35-37.

A2) ABRAMSON, H.N., "The Dynamic Behaviour of Liquids in Moving Containers", NASA SP 106, 1966.

A3) ABRAMOWITZ, M., and SEGUN, I.A., "Handbook of Mathematical Functions" Dover Pub. New York, 5th edition 1968.

A4) ARMSTRONG, G.L., and KACHIGAN, K., "Propellent Sloshing" Handbook of Astronautical Engineering, ed. by Koelle, H.H., Chapter 14, 1961, pp. 14.14-14.27.

A5) ASMIS, K.G., and TSO, W.K., "Combination and Internal Resonance in a Nonlinear Two-Degrees-of-Freedom System" J. Appl. Mech., Trans. ASME, Series E, Vol. 39, Sept. 1972, pp.832-834.

B1) BARR, A.D.S., and McWHANNELL, D.C., "Parametric Instability in Structures under Support Motion" J. Sound and Vibrations Vol. 14, No. 4,22 November 1971, pp.491-509.

B2) BARR, A.D.S., and DONE, G.T.S., "Parametric Oscillations in Aircraft Structures" Aeronautical Journal Vol. 75, Technical Note, Sept. 1971, pp.654-658.

B3) BARR, A.D.S., "Dynamic Instabilities in Moving Beams and Beam System", Second Int. Cong. on "Theory of Mechanics and Mechanisms", Zakopan, Poland 1, 1969, pp. 365-374.

B4) BARR, A.D.S., and NELSON, D.J., "Autoparametric Interaction in Structures", Symposium on Nonlinear Dynamics, Loughborough Univ. of Tech., 27-28 March 1972.

B5) BAUER, H.F., and CHANG, S.S. and WANG, J.T.S., "Nonlinear Liquid Motion in a Longitudinally Excited Container with Elastic Bottom" AIAA Journal Vol. 9, No. 12 December 1971, pp. 2333-2339.

B6) BENJAMIN, T.B., and URSELL, F., "The Stability of a Plane Free Surface of a Liquid in Vertical Periodic Motion", Proc. Royal Soc. (London), A-225, 1954, pp.505-515.

B7) BISHOP, R.E.D., and JOHNSON, D.C., "The Mechanics of Vibration" Cambridge Univ. Press, 1960.

B8) BISHOP, R.E.D., and GLADWELL, G.M.L. "An Investigation into the Theory of Resonance Testing" Phil. Trans. of the Royal Society of London, Series E., Math and Phys. Sci., No. 1055, Vol. 255. 17 Jan. 1963, pp.241-280.

B9) BISPLINGHOFF, R.L., and DOUGLAS, M., "Some Structural Dynamic Problems of Space Vehicles", Japan Society of Aeronautical and Space Sciences. Tokyo, Nov. 1963.

B10) BOGOLIUBOFF, N.M., and MITROPOLISKY, Yu.A., "Asymptotic Methods in the Theory of Nonlinear Oscillations" Gordon Breach Science Publishers, New York, 1962.

B11) BOLOTIN, V.V., "On the Motion of a Fluid in an Oscillating Vessel" PMM, 20, 2, 1956, pp. 293-294.

B12) BOLOTIN, V.V., "Dynamic Stability of Elastic Systems" Holden-Day, Inc., San Francisco, 1964.

B13) BRAND, R.P., and NYBORG, W.L., "Parametrically Excited Surface Waves" J. Acoust. Soc. Amer. Vol. 37, No. 3, March 1965, pp. 509-515.

B14) BRISKMAN, V.A., and SHAIDUROV, G.F., "Parametric Instability of a Fluid Surface in an Alternating Electric Field" Soviet Physics-Doklady, Vol. 13, No. 6, Dec. 1968, pp.540-542.

C1) CAUGHEY, T.K., "Classical Normal Modes in Damped Linear Dynamic Systems" J. Appl. Mech., Trans. ASME, Series E. Vol. 27, No. 2., June 1960, pp. 269-271.

C2) CESARI, L., "Sulla Stabilita delle Soluzioni dei Sistemi de Equazion Differenzialli Lineari a Coefficienti Periodici" Mem. Acad. Italia, Vol. 11, 1941, p.633.

C3) CESARI, L., "Asymptotic Behaviour and Stability Problems in Ordinary Differential Equations" Academic Press, New York, 1963, p.55.

C4) CHANG, S.S., "Longitudinally Excited Nonlinear Liquid Motion in a Circular Cylindrical Tank with Elastic Bottom" Ph.D. Thesis, Georgia Institute of Technology, Atlanta, Dec. 1969.

C5) CHEN CHZHEN - CHEN., "On the Hydrodynamic Pressure on a Dam caused by its Aperiodic or Impulsive Vibrations and Vertical Vibrations on the Earth Surface", J. Appl. Mech. (PMM) Vol. 25, No. 4, 1961, pp.1060-1076.

C6) CHEN, Yu., "Vibrations" Addison-Wesely, Mass. 1966.

C7) CHESHANOV, B.I., "Resonance Oscillations of a Spherical Double Pendulum". PMM, 33, 6, 1969, pp. 1075-1082.

C8) CHOPRA, A.K., "Hydrodynamic Pressures on Dams During Earthquakes". Journal of the Engineering Mechanics Division, Proc. ASCE, Vol. 93 (EM6) 1967, pp. 205-223.

C9) CHU, W.H., "Subharmonic Oscillations in Arbitrary Axisymmetric Tank Resulting from Axial Excitation" J. Appl. Mech. ASME Series E, Vol. 35, No.1, March 1968, pp.148-150.

C10) COOPER, R.M., "Dynamics of Liquids in Moving Containers" Journal of American Rocket Society, Vol. 30, No. 8 August 1960, pp. 725-729.

D1) DEVITT, E.B., and MELCHER, J.R., "Surface Electrodynamics with High-Frequency Fluids" The Physics of Fluids, Vol. 8, No. 6, June 1965, pp.1193-1195.

D2) DODGE, F.T., KANA, D.D. and ABRAMSON, H.N., "Liquid Surface Oscillations in Longitudinally Excited Rigid Cylindrical Containers" Southwest Research Institute, T.R.2. 30th April 1964, also AIAA Journal, 30, 4, April 1965, pp. 685-695.

E1) EULITZ, W.R. and GLASER, R.F., "Comparative Experimental and Theoretical Considerations on the Mechanics of Fluid Oscillations in Cylindrical Containers" Report MJP-M-S and M-61, Army Ballistic Missile Agency, Huntsville, Ala., 29 May, 1961.

E2) EVAN-IWANOWSKI, R.M., "On the Parametric Response of Structures" Appl. Mech. Rev. 18, 9, Sept. 1965, pp. 699-702.

F1) FARADAY, M., "On the Forms and States Assumed by Fluids in Contact with Vibrating Elastic Surfaces", Philosophical Transactions of the Royal Society, Vol. 121, 1831, pp. 319-346.

F2) FU, F.L. and NEMAT-NASSER, S., "On the Stability of Steady-State Response of Certain Nonlinear Dynamics Systems Subjected to Harmonic Excitations" Ingeneur-Archiv. Vol. 41, 1972, pp. 407-420.

G1) GELFAND, I.M. and LIDSKII, V.B., "Uspehi Mat" Nauk (N.S.) 10,63, 1955 [English Translation A.M.S. Translation Series 8, 143, (1958)].

G2) GOLDMAN, R.L., "Elimination of POGO Instability from Gimini Launch Vehicle" Proc. Int. Conference "Dynamic Stability of Structures" ed. by Hermann, G., Pergamon Press, 1965, pp.157-166.

G3) GRAHAM, E.W. and RODRIGUEZ, A.M., "The Characteristics of Fuel Motion which Affect Airplane Dynamics" J. Appl. Mech. ASME Trans. Series E, Vol. 74, Sept. 1952, pp.381-388.

G4) GRAHAM, E.W., "The Forces Produced by Fuel Oscillations in a Rectangular Tank" Douglas Aircraft Comp. SM-13748, April 1951.

G5) GOLD, H., McARDLE, J.G. and PETRASH, D.A., "Slosh Dynamics Study in Near Zero Gravity" NASA TN D-3985, May 1967.

H1) HAGEDORN, P., "Kombinations resonanz und Instabilitatsbereich Zweiter Art bei Parametererregten Schwingungen mit nicht linearer Dampfung" Ingeneur-Archiv, Vol. 38, 1969, pp. 80-96.

H2) HAHN, W., "Stability of Motion" Berlin-Gottingen-Heidelberg Springer 1967.

H3) HALE, J.K., "Ordinary Differential Equations" Wiley, Interscience 1969.

H4) HASSELMAN, T.K., "Method for Constructing a Full Modal Damping Matrix from Experimental Measurements" AIAA Journal Vol. 10, No. 4, April 1972, pp.526-527.

H5) HAXTON, R.S. and BARR, A.D.S., "The Autoparametric Vibration Absorber" J. Engineering for Industry 94, 1, Feb. 1972, pp. 119-125.

H6) HERMANN, G., "Stability of Equilibrium of Elastic Systems Subjected to Nonconservative Forces" Appl. Mech. Rev. 20, 2, 1967, pp.103-108.

H7) HERMANN, G. and HAUGER, W., "On the Interrelation of Divergence, Flutter and Auto-Parametric Resonance", Ingeneur Archiv, 42, 1973, pp. 81-88.

H8) HOUSNER, G.W., "The Dynamic Behaviour of Water Tanks" Bull. Seismol. Soc. Amer. 53, 2, Feb. 1963, pp.381-387.

H9) HSU, C.S., "On the Parametric Excitation of a Dynamic System Having Multiple Degree of Freedom" J. Appl. Mech. 30, 1963, pp. 367-372.

H10) HSU, C.S., "Further Results on Parametric Excitation of a Dynamic System", J. Appl. Mech., 32, 1965, pp.373-377.

H11) HSU, C.S., "Impulsive Parametric Excitation : Theory" J. Appl. Mech, 39, June 1972, pp. 551-558.

H12) HUTTON, R.E., "An Investigation of Resonant, Nonlinear and Non-Planar Free Surface Oscillations of Fluid" Ph.D. thesis, University of California, 1962, Also NASA TN D-1870, 1963.

J1) JAEGER, L.G. and BARR, A.D.S., "Parametric Instabilities in Structures Subjected to Prescribed Periodic Support Motion", Proc. Symposium on Design for Earthquake Loadings, VII-1 McGill Univ. of Canada, 1966.

K1) KANA, D.D., "An Experimental Study of Liquid Surface Oscillations in Longitudinally Excited Compartmented Cylindrical and Spherical Tanks" NASA CR-545, Aug. 1966.

K2) KANE, T.R. and KAHN, M.E., "On a Class of Two-Degree-of-Freedom Oscillations" J. Appl. Mech. 35, Sept. 1968, pp.547-552.

K3) KENNEDY, C.C. and PANCU, C.D., "Use of Vectors in Vibration Measurement and Analysis", J. Aeronautical Sciences, 14, 11, Nov. 1947, pp. 603-625.

L1) LAMB, H., "Hydrodynamics"Cambridge Univ. Press, 6th ed. 1945.

L2) LION, K.S., "Instrumentation in Scientific Research" McGraw-Hill Book Company, Inc., 1969.

M1) MASSA, E., "On the Instability of Parametrically Excited Two Degrees of Freedom Vibrating Systems with Viscous Damping" Meccanica, Vol. 2, Dec. 1967, pp.243-255.

M2) MATHIESSEN, L., "Akustische Versuche, die Kleinsten Transversalivellen der Flussigkeiten betreffend," Annalen der Physik, 134, 1868, pp.107-117.

M2a) MATHIESSEN, L., "Uber die Transversalsch Wingungen tonender Tropfharer und Elastisher Flussigkeiten" Annalen der Physik, 141, 1870, pp. 375-393.

M3) McLACLAN, N.W., "Theory and Application of Mathieu Functions" Oxford University Press, 1947.

M4) MEI, C.C., and LIU, L.F., "The Damping of Surface Gravity Waves in a Bounded Liquid", J. Fluid Mechanics, 59, 2, 1973, pp. 239-258.

M5) MERRITT, R.G. and WILLEMS, N., "Parametric Resonance of Skew Stiffened Plates" J. Appl. Mech. 40, June 1973, pp.439-444.

M6) METTLER, E., "Stability and Vibration Problems of Mechanical Systems Under Harmonic Excitation" Proc. Int. Conf. on Dynamic Stability of Structures (1965), editor Hermann, G., Pergamon Press 1967, pp. 169-188.

M7) METTLER, E., "Combination Resonances in Mechanical Systems Under Harmonic Excitation" 4th Conf. on Nonlinear Oscillations, Prague, 1967, pp. 51-70.

M8) MILES, J.W., "Surface Wave Damping in Closed Basins" Proc. Roy. Soc. A297, 1967.

M9) MINORSKY, N., "Nonlinear Oscillations" Van Nostrand Co., New York 1962.

M10) MOISEEV, N.N., "On the Theory of Nonlinear Vibration of a Liquid of Finite Volume", Prikl. Mati. Mekh. Vol. 22.

M11) MTI (Mechanical Technology Incorporated), "Design of Gas Bearing" Vol. 1, Sec. 5, 1969.

N1) NAYFEH, A.H., "Perturbation Methods", Wiley-Interscience Pub., 1973.

N2) NEWMARK, N.M., and ROSENBLUETH, E., "Fundamentals of Earthquake Engineering" Prentice Hall, Inc. Englewood Cliffs, 1971.

O1) OSGOOD, W.F., "Mechanics" Dover Pub. New York 1965.

P1) PENNEY, W.G., and PRICE, A.T., "Finite Periodic Stationary Gravity Waves in a Perfect Liquid: Part II " Phil. Trans. Royal Soc. (London) A244, 1952, pp.254-284.

P2) POPELAR, C.H., "Dynamic Stability of Thin-Walled Column" J. Engineering Mech. Div. ASCE (EM3) June, 1972, pp. 657-577.

R1) RAYLEIGH, L., "On the Crispations of Fluid Resting Upon a Vibrating Support" Phil. Mag. 15, April 1883, pp. 229-235.

R2) RAYLEIGH, L., "On the Maintenance of Vibrations by Forces of Double Frequency and on the Propagation of Waves through a Medium Endowed with a Periodic Structure" Phil. Mag. 24, Aug. 1887, pp. 145-159.

R3) RAYLEIGH, L., "On the Instability of Cylindrical Fluid Surfaces", Collected papers Cambridge Univ. Press, Vol. 3, 1892, p.594.

R4) RAYLEIGH, L., "Theory of Sound" Vol. 1, Dover Publ. New York, N.Y., 1945.

R5) REYNOLDS, J.M., "Stability of an Electrostatically Supported Fluid Column" The Physics of Fluids, 8, 1 Jan. 1965, pp. 161-170.

R6) RAVEN, F.H., "Automatic Control Engineering" McGraw-hill, New York, 1967.

S1) SALYER, R.A., "Hybrid Techniques for Modal Survey Control and Data Appraisal" The shock and vibration bulletin, No. 14, Pt. 3, Dec. 1970, pp.25-42.

S2) SCHMIDT, G., "On the Nonlinear Vibration Problems" Proc. of the Fourth Conference on Nonlinear Oscillations. Prague 1967, pp.459-466.

S3) SCHOENHALS, R.S., WINTER, E.R.F. and GRIGGS, E.I., "Effects of Longitudinal Vibration on Discharge of Liquids from Propellent Tanks" Proc. of the 1967 Heat Transfer and Fluid Mechanics Institute, San Diego, Calif. June 19-21, 1967, pp. 277-297.

S4) SEN GUPTA, N.D., "Notes on the Effect of Periodic Perturbation at Resonance" Acta Mechanica, Vol. 14, 1972, pp.59-63.

S5) SETHNA, P.R., "Transients in Certain Autonomous Multiple-Degree-of-Freedom Nonlinear Vibrating Systems", J. Appl. Mech., Vol. 30, March 1963, pp. 44-50.

S6) SETHNA, P.R., "Vibrations of Dynamical Systems with Quadratic Nonlinearities", J. Appl. Mech, 32, 1965, pp. 576-582.

S7) SETHNA, P.R., "Coupling in Certain Classes of Weakly Nonlinear Vibrating Systems" Int. Symposium on Nonlinear Differential Equations and Nonlinear Mechanics, Academic Press, New York, 1963, pp.58-70.

S8) SEVIN, E., "On the Parametric Excitation of a Pendulum-Type Vibration Absorber", J. Appl. Mech., 28, 1961, pp.330-334.

S9) SKALAK, R. and YARYMOVYCH, M.I., "Subharmonic Oscillations of a Pendulum", J. Appl. Mech., 27, 1960, pp. 159-164.

S10) SKALAK, R. and YARYMOVYCH, M.I., "Forced Large Amplitude Surface Waves", Proc. of the Fourth U.S. National Congress on Applied Mech., 1962, pp.1411-1418.

S11) SOROKIN, V.I., "The Effect of Fountain Formation at the Surface of a Vertically Oscillating Liquid" Soviet Physics - Acoustics, 3, 3, July-Sept. 1957, A translation of the J. Acoustics of the Academy of Science of the USSR, pp. 281-291.

S12) STEINBRUGGE, K.V. and MORAN, D.F., "Engineering Aspects of the Dixie Valley-Fairview Peak Earthquake", Bulletin of the Seismological Society of America, 47, 1957, pp. 335-349.

S13) STOKER, J.J., "Nonlinear Vibrations", Interscience Pub. New York, 1950.

S14) STRUBLE, R.A., and FLETCHER, J.E., "General Perturbational Solution of the Harmonically Forced Van der Pol Equation", J. Math. Phys. 2, 1961, pp. 880-891.

S15) STRUBLE, R.A., "Nonlinear Differential Equations" McGraw-hill, 1962.

S16) STRUBLE, R.A., "Oscillations of a Pendulum Under Parametric Excitation", Quarterly Appl. Math. 2, 1963, pp.121-131.

S17) STRUBLE, R.A., "On the Oscillations of a Pendulum Under Parametric Excitation" Quartely Appl. Math. 22, 1964, pp.157-159.

S18) STRUBLE, R.A., and HEINBOCKEL, J.H., "Energy Transfer in a Beam-Pendulum System" J. Appl. Mech., 29, 1962, pp.590-592.

S19) STRUBLE, R.A. and HEINBOCKEL, J.H., "Resonant Oscillations of a Beam Pendulum System", J. Appl. Mech., 30, 1963, pp. 181-188.

T1) THOMSON, M.M., "Theoretical Hydrodynamics", MacMillan, New York, 4th ed., 1965.

T2) TOMÁŠ, J., "The Contribution to the Problem of Internal Resonance in a Nonlinear System with Two-Degrees-of-Freedom", Proc. of the 4th Conference on Nonlinear Oscillations, Prague, 1967, pp. 503-508.

T3) THOMSON, W.T., "Vibration Theory and Applications" London, George Allen and Unwin Ltd., 1966.

V1) VALEEV, K.G., "On the Danger of Combination Resonance" PMM, 27, 1963, pp.1745-1759.

W1) WOODWARD, J.H., "Fluid Motion in a Circular Tank of Sector-Annular Cross Section when Subjected to a Longitudinal Excitation", Ph.D. thesis, Georgia Institute of Technology, Dec. 1966.

W2) WOODWARD, J.W. and BAUER, H.F., "Fluid Behaviour in a Longitudinally Excited Cylindrical Tank of Arbitrary Sector-Annular Cross-Section", AIAA Journal, 8, 4, April, 1970, pp.713-719.

Y1) YAMAMOTO, T., and SAITO, A., "On the Vibrations of Summed and Differential Types Under Parametric Excitation", Memoirs of the Faculty of Engineering, Nagoya University, Japan, May 1970, pp. 54-123.

Z1) ZIEGLER, H., "Die Stabilitatskriterien der Elasto-Mechanik", Ingenieur Archiv, 20, 1, 1951, pp.49-56.